AN ABSTRACT OF THE THESIS OF

Chris Goldfinger for the degree of Doctor of Philosophy in Geology presented on January 31, 1994.

Title: Active Deformation of the Cascadia Forearc: Implications for Great Earthquake Potential in Oregon and Washington

Redacted for Privacy

Abstract approved: _____
Robert S. Yeats

Nine west-northwest-trending faults on the continental margin of Oregon and Washington, between 43° 05'N and 47° 20'N latitude, have been mapped using seismic reflection, sidescan sonar, submersibles, and swath bathymetry. Five of these oblique faults are found on both the Juan de Fuca and North American plates, and offset abyssal plain sedimentary units left-laterally from 2.0 to 5.5 km. These five faults extend 8-18 km northwestward from the deformation front. The remaining four faults, found only on the North American plate, are also inferred to have a left-lateral slip sense. The age of the Wecoma fault on the abyssal plain is 600±50 ka, and has an average slip rate of 7-10 mm/year. Slip rates of the other four abyssal plain faults are 5.5 ± 2 - 6.7 ± 3 mm/yr. These faults are active, as indicated by offset of the youngest sedimentary units, surficial fault scarps, offsets of surficial channels, and deep fluid venting. All nine faults have been surveyed on the continental slope using SeaMARC 1A sidescan sonar, and three of them were surveyed with a high-resolution AMS 150 sidescan sonar on the continental shelf off central Oregon. On the continental slope, the faults are expressed as linear, high-angle WNW trending scarps, and WNW trending fault-parallel folds that we interpret as flower structures. Active structures on the shelf include folds trending from NNE to WNW and associated flexural slip thrust faulting; NNW to N trending right-lateral strike-slip faults; and WNW trending left-lateral strike-slip faults. Some of these structures intersect the coast and can be correlated

with onshore Quaternary faults and folds, and others are suspected to be deforming the coastal region. These structures may be contributing to the coastal marsh stratigraphic record of co-seismic subsidence events in the Holocene.

We postulate that the set of nine WNW trending left-lateral strike-slip faults extend and rotate the forearc clockwise, absorbing most or all of the arc parallel component of plate convergence. The high rate of forearc deformation implies that the Cascadia forearc may lack the rigidity to generate $M > 8.2$ earthquakes. From a comparison of Cascadia seismogenic zone geometry to data from circum-Pacific great earthquakes of this century, the maximum Cascadia rupture is estimated to be 500 to 600 km in length, with a 150-400 km rupture length in best agreement with historical data.

Active Deformation of the Cascadia Forearc: Implications for Great Earthquake Potential in Oregon and Washington

By

Chris Goldfinger

A THESIS

submitted to

Oregon State University

in partial fulfillment of
the requirements for the
degree of

Doctor of Philosophy

Completed January 31, 1994

Commencement June 1994

APPROVED:

Redacted for Privacy

Professor of Geology in charge of major

Redacted for Privacy

Head of Department of Geosciences

Redacted for Privacy

Dean of Graduate School

Date thesis is presented January 31,1994

Typed by Chris Goldfinger for Chris Goldfinger

TABLE OF CONTENTS

CHAPTER 1: INTRODUCTION 1

CHAPTER 2: TRANSVERSE STRUCTURAL TRENDS ALONG THE OREGON CONVERGENT MARGIN: IMPLICATIONS FOR CASCADIA EARTHQUAKE POTENTIAL AND CRUSTAL ROTATIONS 3
Abstract 4
Introduction 5
Active Transverse Structures of the Central and Northern Oregon Continental Margin 6
Abyssal Plain 6
Continental Slope and Shelf 10
Implications for Cascadia Seismicity 12
Plate Coupling and Rotations 13
Conclusions 15
References Cited 16
Acknowledgments 18

CHAPTER 3: ACTIVE STRIKE-SLIP FAULTING AND FOLDING OF THE CASCADIA PLATE BOUNDARY AND FOREARC IN CENTRAL AND NORTHERN OREGON 19
Abstract 20
Introduction 22
Methods of Study 25
Strike Slip Faults on the Juan de Fuca Plate 29
Characteristics of the Wecoma Fault 33
Age, Net Slip, and Average Slip Rate of the Wecoma Fault 42
Abyssal-Plain Stratigraphy 42
Timing Constraints 43
Fault Restoration 47
Late Pleistocene-Holocene Slip Rate 51
Intersection of the Wecoma Fault and the Accretionary Wedge 53
Influence of the Wecoma Fault on the Accretionary Wedge 56
Fault Orientation and the Regional Tectonic Setting 69
Strike-Slip Faults and the Accretionary Wedge 70
Kinematics of Oblique Fault - Accretionary Wedge Interaction 73
Conclusions 76
References 77
Acknowledgments 82

CHAPTER 4: CASCADIA SUBDUCTION ZONE: ACTIVE DEFORMATION OF THE OREGON CONTINENTAL SHELF 83
Abstract 84
Introduction 85
Methods 86
Age Constraints on Late Quaternary Structures 88
Active Structures on the Oregon Continental Shelf 90
Folding and Flexural-Slip Faulting 90
Strike-Slip Faulting 92
Oblique Strike-Slip Faults 92
Wecoma Fault 93
Daisy Bank Fault 94
Heceta South Fault 100
Arc Parallel Strike-Slip Faults 100
Nehalem Bank Fault 102
Fulmar Fault 103
Coquille Fault 103
Oregon's Submarine Banks 106
Vertical Tectonics of Heceta Bank 108
Relationship of Active Shelf Structures to Coastal Deformation 110
Discussion 113
Local Structures and the Coastal Marsh Record 113
Oregon Submarine Banks as Asperities 115
Conclusions 118
References Cited 119

CHAPTER 5: FOREARC DEFORMATION AND THE PROBABILITY OF GREAT EARTHQUAKES ON THE CASCADIA SUBDUCTION ZONE 124
Abstract 125
Introduction 127
Oblique Strike-slip Faulting in Cascadia 129
Washington Margin Faults 130
North Nitinat Fault 130
South Nitinat Fault 135
Quinault Canyon Fault 135
Oregon Margin Faults 136
Wecoma Fault 136
Daisy Bank and Alvin Canyon Faults 138
Heceta South, Coos Basin, and Thompson Ridge Faults 140
Discussion 145
Forearc Deformation and Great Earthquakes 145
Heterogeneity of Modern and Late Quaternary Forearc Deformation 149
Comparison of Rupture Zone Geometry for Recent Great Earthquakes to Possible Cascadia Earthquakes 152
Estimate of the Extent of the Locked Zone in Cascadia 152

Potential Rupture Length of Cascadia Interplate Earthquakes 156
Conclusions 160
References Cited 161
Acknowledgments 166

BIBLIOGRAPHY 167

APPENDIX A: TEXT ACCOMPANYING OREGON NEOTECTONIC MAP 180

APPENDIX B: SLIP-RATE CALCULATIONS FOR OREGON AND WASHINGTON MARGIN STRIKE-SLIP FAULTS 198

LIST OF FIGURES

CHAPTER 2

Figure 2.1. Structure map of northern and central Oregon margin. 7

Figure 2.2. Composite block diagram of intersection between fault A and deformation front. 8

Figure 2.3. Development of left-lateral R' faults within dextral setting driven by oblique plate convergence. 14

CHAPTER 3

Figure 3.1. Index map showing tectonics of the Cascadia subduction zone. 23

Figure 3.2. Trackline map showing the location of all seismic-reflection profiles used in this study. 25

Figure 3.3. Map showing seismic-reflection tracklines and bathymetry in the Ocean Drilling Program (ODP) site survey area. 27

Figure 3.4. Structure of the central Oregon continental margin. 30

Figure 3.5. Perspective mesh plot of SeaBeam swath bathymetry data off central and northern Oregon. 33

Figure 3.6. Mosaic of SeaMARC 1A 5 km swaths near the Wecoma fault off the central Oregon coast. 34

Figure 3.7. Structure map of the western part of the Wecoma fault, adjacent abyssal plain, and frontal accretionary wedge off the central Oregon coast. 35

Figure 3.8. Migrated MCS line 37 crossing of the Wecoma fault between the pressure ridge and the deformation front off the Oregon coast. 37

Figure 3.9. Part of MCS line 45 showing the Wecoma fault and the pressure-ridge anticline off the central Oregon coast. 38

Figure 3.10. Composite block diagram of the pressure-ridge area and intersection of the Wecoma fault and the deformation front as viewed from the southwest. 41

Figure 3.11. Line drawing of a single-channel reflection profile (Oregon State University cruise YALOC 70, Leg 5) linking Deep Sea Drilling Project drill site 174A to the pressure ridge anticline and the Wecoma fault, off the Oregon coast. 45

Figure 3.12. Lithology and coiling directions of *Globigerina pachyderma* in cores from Deep Sea Drilling Project site 174A. 46

Figure 3.13. Cartoon illustrating the method used in retrodeformation of the Wecoma fault, off the Oregon coast. 48

Figure 3.14. Pseudo-isopach plot of abyssal-plain unit 2. 50

Figure 3.15. High-resolution SeaMARC 1A sidescan image of the Wecoma fault offsetting the west bank of a late Pleistocene distributary channel on the southeastern Astoria submarine fan. 52

Figure 3.16. Structural interpretation of the intersection zone and pop-up structure at the intersection of the Wecoma fault and the deformation front. 54

Figure 3.17. Block diagram illustrating structure of the pop-up at the intersection of the Wecoma fault and the deformation front. 56

Figure 3.18. Bathymetry and ALVIN submersible tracklines near the intersection of the Wecoma fault and the deformation front. 58

Figure 3.19. SeaMARC 1A sidescan image of the Wecoma fault crossing the accretionary wedge. 59

Figure 3.20. Unmigrated 24-channel seismic profile of the Wecoma fault on the lower continental slope, 26 km landward of the deformation front. 62

Figure 3.21. Shaded relief plot of SeaBeam bathymetry and structure of a part of the central continental slope crossed by the Wecoma fault. 64

Figure 3.22. Seismic profiles showing the Wecoma fault and deformation zone off the Oregon coast. 67

Figure 3.23. SeaBeam bathymetry perspective view along the strike of the Wecoma fault as it crosses from the abyssal plain into the accretionary wedge. 71

Figure 3.24. Vector diagram of the inferred local effect of Wecoma fault slip on the plate convergence vector. 72

CHAPTER 4

Figure 4.1. Color change across the Holocene/Pleistocene boundary. 89

Figure 4.2. Single channel airgun seismic record (OSU line SP-118) showing an active syncline and flexural-slip faults. 90

Figure 4.3. DELTA video image of encrusting methane-derived carbonate slabs along the Daisy Bank fault zone, 5 km northwest of Daisy Bank, central Oregon. 96

Figure 4.4. Active scarp within the Daisy Bank fault zone. 98

Figure 4.5. AMS 150 sonar swath over Stonewall Bank, Oregon continental shelf. 99

Figure 4.6. Shaded relief perspective plot of NOAA BS^3 swath bathymetry, Heceta Bank, Oregon continental shelf. 101

Figure 4.7. Klein 50 kHz sidescan record of the Coquille fault zone off Bandon, Oregon. 105

Figure 4.8. Physiography and bathymetry of the Oregon continental margin showing the three major submarine banks. 107

Figure 4.9. Elevation of the Pleistocene low-stand shoreline angle at Heceta Bank, Oregon. 109

CHAPTER 5

Figure 5.1. Preliminary tectonic map of central Washington continental slope and abyssal plain. 131

Figure 5.2. Interpretation of a part of Plate 2. 133

Figure 5.3. Portion of SeaMARC 5 km swath showing the Wecoma fault zone on the upper continental slope. 137

Figure 5.4. Alvin Canyon fault, shown cutting the sedimentary section and basaltic basement of the Juan de Fuca plate. 139

Figure 5.5. Locations of nine strike-slip faults mapped on the Oregon and Washington continental margin. 141

Figure 5.6. Shaded relief plot of NOAA SeaBeam swath bathymetric data in the vicinity of the Thompson Ridge fault. 142

Figure 5.7. Plot of slip vector residual vs. Ms magnitude of major earthquakes this century, from the data of McCaffrey (1993). 148

Figure 5.8. Map showing locked (hatched) and transition (shaded) zones on the Cascadia plate interface, projected to the surface. 150

Figure 5.9. Effective rupture width vs. rupture length for great circum-Pacific earthquakes this century. 155

LIST OF TABLES

Table 5.1. Earthquake and subduction parameter data used in Figure 5.9. 157

Table A.1. Data sources used in this study and approximate navigational accuracy. 184

Table B.1. Sum of arc parallel component of slip from strike-slip faulting, Oregon and Washington. 202

LIST OF PLATES

Plate 1. Neotectonic map of the Oregon continental margin and adjacent abyssal plain.

Plate 2. Trackline map of Cascadia seismic reflection surveys.

Plate 3. SeaMARC 5 km swath along the Daisy Bank segment of the Daisy Bank fault.

Plate 4. 2 km SeaMARC sonar swath of the N. Nitinat fault on the Washington abyssal plain.

CONTRIBUTION OF AUTHORS

The four main chapters of this thesis are manuscripts that have been published or are presently being reviewed by co-authors for submission. LaVerne D. Kulm and Robert S. Yeats were the Principal Investigators on the NOAA, NSF, and USGS sponsored research programs detailed herein, and are closely involved with each of the investigations presented here. Specific contributions to these manuscripts by other co-authors are listed below.

Chapter 2: Mary MacKay processed the 1989 Digicon multichannel seismic data under the direction of Greg Moore at the University of Hawaii. Bruce Appelgate collected and processed the 1989 SeaMARC 1A data on the central Oregon margin at the NOAA Pacific Marine Environmental Laboratory at Newport, Oregon.

Chapter 3: Mary MacKay and Guy Cochrane processed the 1989 Digicon multichannel seismic data under the direction of Greg Moore at the University of Hawaii. Bruce Appelgate collected and processed the 1989 SeaMARC 1A data on the central Oregon margin at the NOAA Pacific Marine Environmental Laboratory at Newport, Oregon.

Chapter 4: Lisa McNeill, Cheryl Hummon, Gary Huftile, Craig Schneider, Alan Niem, Hiroyuki Tsutsumi, and John Chen participated in 2 NOAA/NURP cruises in 1992 and 1993, and one NSF cruise in 1993 as members of the Scientific Party, and contributed to preliminary geologic interpretations presented here. Lisa McNeill did reconnaissance mapping of Quaternary structures deforming marine terraces on the central Oregon coast in the Siletz Bay area.

Chapter 5: Robert McCaffrey investigated the relationship of various subduction parameters and great earthquakes. These results are published in (McCaffrey, 1992; 1993). Cheryl Hummon participated in the 1993 NSF cruise on which data discussed in this chapter were collected, and contributed to preliminary geologic interpretations presented here.

ACTIVE DEFORMATION OF THE CASCADIA FOREARC: IMPLICATIONS FOR GREAT EARTHQUAKE POTENTIAL IN OREGON AND WASHINGTON

CHAPTER 1: INTRODUCTION

This thesis is composed of four main chapters, each of which is a journal manuscript that is either published or ready for submission as of this writing. Chapter 2 was published in *Geology* in February, 1992. Chapter 3 was published as U.S. Geological Survey Open File Report 92-441-s in 1992, in advance of publication as a chapter in U.S. Geological Survey Professional Paper 1560, *Assessing and Reducing Earthquake Hazards in the Pacific Northwest,* edited by A. M. Rogers, W. J. Kockelman, G. Priest, and T. J. Walsh. This book has been in press since 1991. Chapter 4 is intended for publication in *Tectonics*, and Chapter 5 is intended for the *Journal of Geophysical Research*. Plate 1 and Appendix A were published by the State of Oregon Department of Geology and Mineral Industries, Open-File Report OG-92-4, entitled Neotectonic Map of the Oregon Continental Margin and Adjacent Abyssal Plain.

Chapters 4 and 5 are not the actual submission versions of these manuscripts, as I have taken the opportunity to include material that could not fit into the intended publications. Thus, these chapters are too long for submission, but contain many details that would otherwise remain "unpublished data".

The unifying theme of this research is active tectonics of the Cascadia subduction zone. As originally conceived, we intended to "map active structures and determine the timing of deformational events" in the submarine forearc. The Principal Investigators (LaVerne D. Kulm and Robert S. Yeats), and I were not sure initially what direction this work would take, but we shared the impression that study of the submarine forearc in Cascadia was a necessary step toward understanding the structure and seismic potential of this unusually quiescent subduction zone. Fortuitously, an unusual strike-slip

fault was discovered in 1986 using SeaMARC 1A sidescan sonar (L.D. Kulm, C. Fox, R. Embley unpublished data). This fault, named the Wecoma fault for the R.V. Wecoma of Oregon State University, proved to be the first of nine unusual oblique structures discovered from 1989 to 1993, in the course of this project. These structures extend across much of the submarine forearc in Oregon and Washington. Five of the nine have demonstrable left-lateral strike slip displacements, and cut the sedimentary section of the subducting Juan de Fuca plate. The Wecoma fault probably also cuts the basaltic crust of the Juan de Fuca plate. To our knowledge, these are the first reported structures of this type that cross a subduction boundary.

Much of our subsequent research has focused on the unusual strike slip faults and their implications for forearc deformation in an oblique subduction setting. An important aspect of this work is the possible implications for great earthquakes in Cascadia. Until the late 1980's, Cascadia was assumed to be an example of an aseismic subduction zone, based mostly on the absence of large historical earthquakes. But Cascadia is too quiet, having less seismicity even than traditional "aseismic" subduction zones like the Marianas, and less than most circum-Pacific "seismic gaps". The Cascadia paradigm changed in the late 1980's with the discovery of sudden submergence of buried marshes in most of the bays and estuaries of the Cascadia coastline. These marshes may signify the occurrence of paleoearthquakes, and suggest that the quiescence in Cascadia is not due to aseismic subduction, but simply to long recurrence intervals. While the subsided marshes are evidence for large earthquakes, the issues of just how large the earthquakes are and how often they occur are less clear.

In Chapters 2 through 5 we present evidence of significant rotation and extension of the Oregon and Washington forearcs by strike-slip faulting and folding. We then investigate the implications of this deformation in light of other subduction zones that do generate great earthquakes. We examine whether our observations can shed any light on the remaining questions about Cascadia seismicity.

CHAPTER 2: TRANSVERSE STRUCTURAL TRENDS ALONG THE OREGON CONVERGENT MARGIN: IMPLICATIONS FOR CASCADIA EARTHQUAKE POTENTIAL AND CRUSTAL ROTATIONS

Chris Goldfinger
Department of Geosciences, Oregon State University, Corvallis Oregon 97331

LaVerne D. Kulm
College of Oceanography, Oregon State University, Corvallis Oregon 97331

Robert S. Yeats
Department of Geosciences, Oregon State University, Corvallis Oregon 97331

Bruce Appelgate, Mary E. MacKay, Gregory F. Moore
School of Ocean and Earth Science and Technology, University of Hawaii, Honolulu Hawaii 96822

ABSTRACT

A remarkable set of WNW trending left-lateral strike-slip faults intersect the Cascadia subduction zone. Three of these faults have been mapped off northern and central Oregon by using seismic reflection, SeaMARC-1A sidescan sonar, and SeaBeam bathymetry. These faults are highly oblique to the north-south structural grain of the active accretionary wedge. One of them has 6 km of horizontal slip, with an average slip rate of 7-10 mm/yr. The faults cut the subducting Juan de Fuca plate, and can be traced into the North American plate. Folds that deform late Pleistocene and Holocene sediments on the upper continental slope and shelf strike north-northwest to west-northwest. Some of the WNW-trending folds are associated with the throughgoing strike-slip faults, whereas other NW-trending folds are approximately normal to the plate convergence direction. Many of these folds are mapped across the shelf, and several active shelf synclines project toward Oregon's coastal bays, where marsh subsidence events are inferred to be the result of great subduction-zone earthquakes. These subsidence events may actually record the growth of local synclines, possibly as secondary effects of slip on the megathrust. We postulate that shortening of the forearc region by clockwise tectonic rotation, associated with movement of the left-lateral faults and folding of the upper plate, may accommodate a significant amount of plate convergence.

INTRODUCTION

The Cascadia subduction zone off Oregon and Washington should be capable of generating great earthquakes. The convergence rate is fast enough (4.0 cm/yr; DeMets and others, 1990) and the subducting Juan de Fuca plate is young (10 Ma) and buoyant enough to characterize Cascadia as a Chilean-type margin (Heaton and Hartzell, 1987) capable of generating earthquakes with M >8.0. The first geologic evidence for great earthquakes was found in buried marsh deposits of the coastal bays of Washington (Atwater, 1987). Peat layers overlain abruptly by marine sands are perhaps best explained by rapid coseismic submergence accompanied by tsunamis (Atwater, 1987; Darienzo and Peterson, 1990). The absence of historic great earthquakes in Cascadia is explained by long recurrence intervals; the problem is that Cascadia has the lowest incidence of instrumental plate-boundary seismicity of any subduction zone. The unusual lack of seismicity raises the question: can modern convergence be accommodated by means other than slip on the megathrust? We present new structural data from the Oregon continental margin and subducting Juan de Fuca plate that bear on the response of both plates to oblique convergence and on the development of repeated coseismic marsh burial deposits along the Oregon and Washington coasts.

ACTIVE TRANSVERSE STRUCTURES OF THE CENTRAL AND NORTHERN OREGON CONTINENTAL MARGIN

ABYSSAL PLAIN

On the abyssal plain, three west-northwest (WNW)-trending left-lateral strike-slip faults (A, B, and C in Fig. 2.1) extend from the abyssal plain across the plate boundary. First discovered in 1986 by SeaMARC 1A sidescan sonar, these faults were imaged extensively in a follow-up 1989 narrow-swath, high-resolution survey (Appelgate and others, 1992). In migrated multichannel seismic reflection profiles, all three faults offset the entire 3-4-km-thick sedimentary section, as well as the oceanic basement of the incoming Juan de Fuca plate (MacKay and others, 1992; this study). Magnetic modeling of fault A (Appelgate and others, 1992) and reflection profiles both indicate about 75-100 m of vertical separation of the basaltic basement, northeast block up. SeaMARC 1A sidescan imagery shows that fault A offsets left laterally a late Pleistocene channel and an older slump scar on the Astoria submarine fan. Horizontal displacements are about 120 and 350 m, respectively (Appelgate and others, 1992; this study). Isopachs (two-way time) of prefaulting sedimentary units (AP in Fig. 2.2) within the abyssal plain sequence show that these units are offset horizontally 5-6 km by fault A, which represents the net slip on this structure near the deformation front (Goldfinger and others, in press). Horizontal and vertical displacement on fault A dies to nearly zero 17-20 km seaward of the deformation front. Faults A and B both cut or have generated plunging anticlines near their intersections with the deformation front. The doubly-plunging anticline associated with fault A, 9.3 km seaward of the deformation front, appears to be the result of a compressional right step in the left-lateral fault, and is hereinafter referred to as a pressure ridge (Figs. 2.1 and 2.2). Stratigraphic correlations suggest that growth of the pressure ridge was approximately coeval with dip-slip motion on fault A. Stratigraphic thinning over the crest of the pressure ridge and thickening on the downthrown side of the fault are pronounced in the syn-faulting section (Fig. 2.2, upper part of Astoria Fan unit AF). Faulting began at about 600±50 ka, on the basis of the age of strata that separate prefaulting and synfaulting parts of the section, assuming that dip-slip and strike-slip

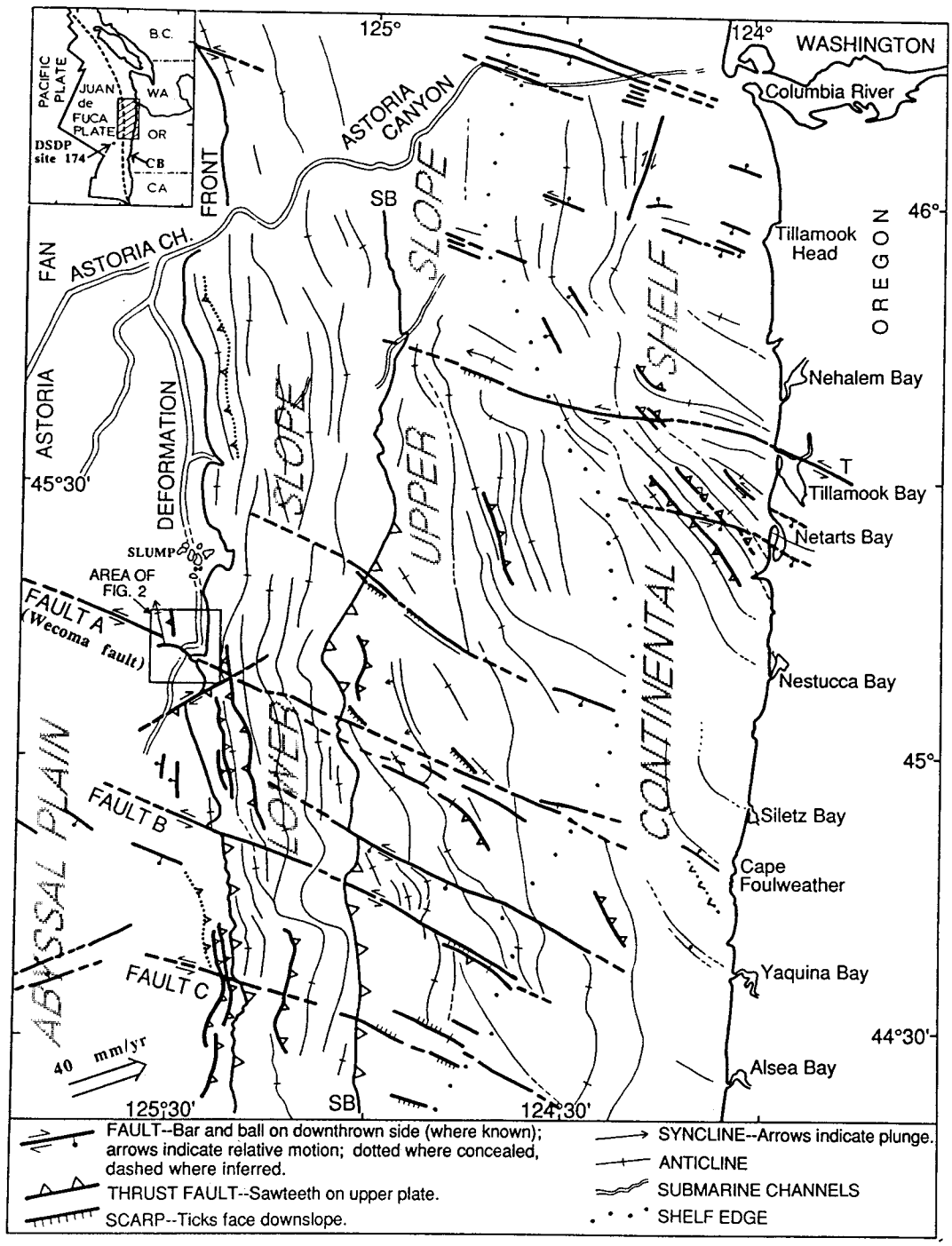

Figure 2.1. Structure map of northern and central Oregon margin. Most structures cut or deform sea floor. Deformation front is thrust fault south of fault B and base of seaward-dipping ramp north of fault B. SB = slope break; T = Tillamook Bay fault; CB = Coos Bay.

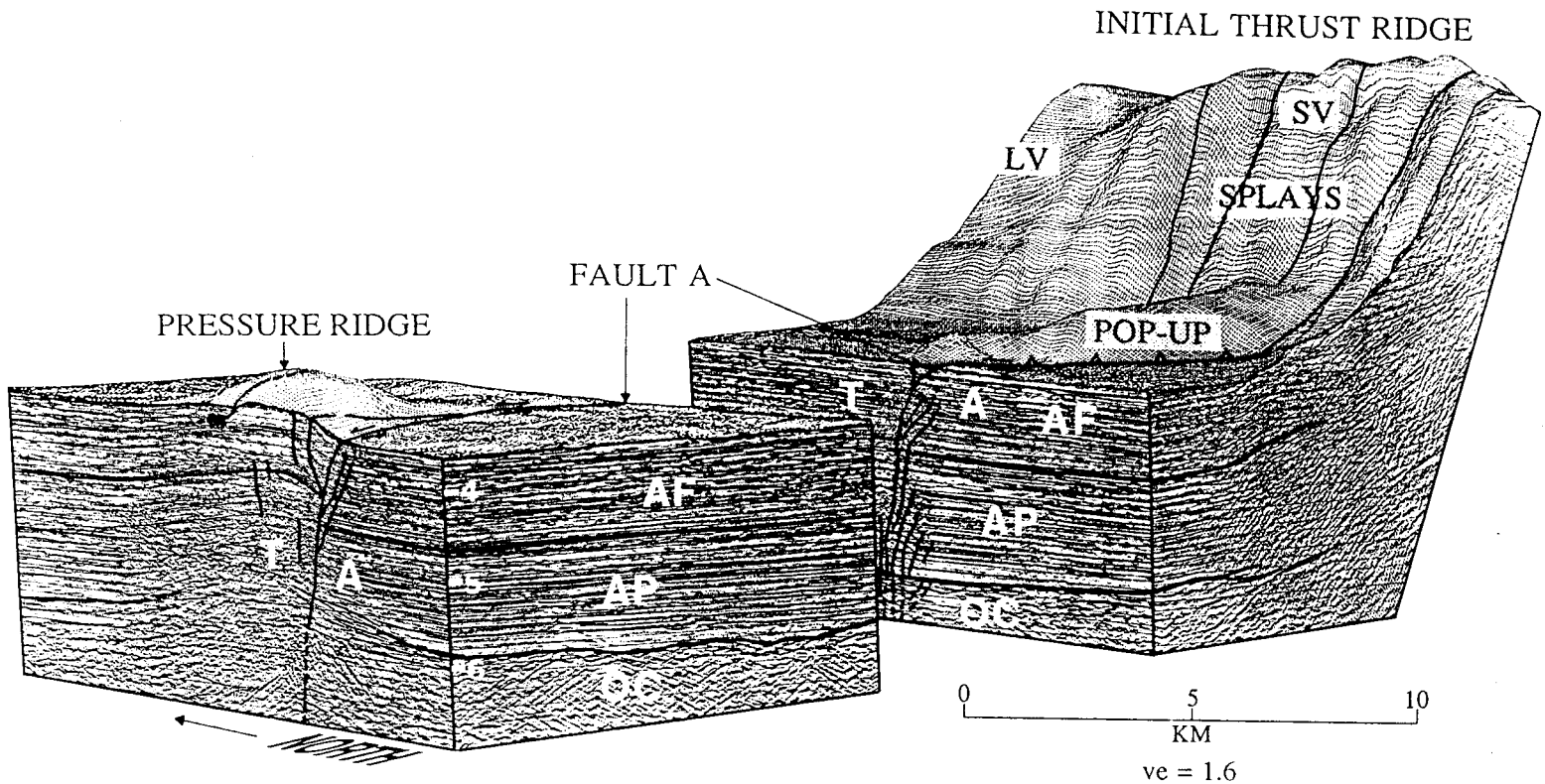

Figure 2.2. Composite block diagram of intersection between fault A and deformation front, view toward southwest. Migrated seismic sections in two-way travel time. AP = abyssal plain section; AF = Astoria fan; A = away; T = toward; SV = seaward vergence; LV = landward vergence; OC = oceanic crust. See Figure 2.1 for location.

motion began concurrently (Goldfinger and others, in press). This age is derived from sedimentation rates and correlation of the base of the Astoria submarine fan section with dated strata drilled at Deep Sea Drilling Project (DSDP) Site 174, about 70 km to the southwest (Kulm and others, 1973b; Fig. 2.1, see inset). This range of ages and net slip yield a slip rate of 7-10 mm/yr.

The offset late Pleistocene channel is blocked 18 km to the north by slump debris from a 32 km^3 bedding-plane slump off the leading accretionary thrust ridge. The age of this slump is estimated to be 10-24 ka, on the basis of a ^{14}C date from a core taken from one of the slump blocks and tied to high-resolution seismic records (Goldfinger and others, in press). Because the fault is older than either the slump or the channel, these relations can be used to infer a slip rate based on the offset. The channel wall was cut prior to blockage by the slump, setting the minimum age of the offset at about 10 ka. Because channel cutting would have ceased or been greatly reduced following the blockage, subsequent fault motion would offset the channel wall as observed, without modification by erosion. Thus, the maximum age of the offset is approximately the same as the maximum age of the slump, or 24 ka. The age of the channel wall is then approximately 10-24 ka, yielding a slip rate of 5-12 mm/yr, comparable to the 7-10 mm/yr based on offset isopachs.

In SeaMARC 1A sidescan records fault A intersects the initial thrust ridge as a complex flower structure, with blocks forced upward and westward as pop-ups as they impinge on the deformation front. Several splays cut upslope on the initial thrust ridge (Fig. 2.2) and continue into the structural basin to the east. *Alvin* submersible dives on these splays confirm they are shear zones associated with chemosynthetic biological communities, fluid flow and carbonate cementation (Tobin and others, 1991), indicating active faulting. On the initial thrust ridge, a seaward vergent thrust segment occupies the area between the splays of fault A in an overall landward vergent thrust setting, which suggests that a local reversal of vergence is induced by the interaction of the thrust and the strike-slip fault. Fault B also coincides with a reversal of thrust vergence at its intersection with the deformation front (MacKay and others, 1992). Faults B and C are also inferred to be left-lateral faults on the basis of offset sediment isopachs in the abyssal plain (Goldfinger and others, in press). Faults B and C offset the deformation front 3.7 and 2.2

km, respectively, in a left-lateral sense. The active frontal accretionary thrust, on the other hand, does not appreciably offset the traces of the strike-slip faults where they cross the plate boundary. These relations suggest that the strike-slip faults may actually be part of the plate boundary, coeval with the frontal accretionary thrusts.

CONTINENTAL SLOPE AND SHELF

We have correlated three throughgoing WNW trending, left-lateral strike-slip faults on the lower to upper slope with faults A, B, and C on the abyssal plain (Fig. 2.1) using GLORIA long-range sidescan, SeaBeam swath bathymetry, and a network of academic and U.S. Geological Survey seismic profiles. At least one of the strike-slip faults (A) on the subducting plate clearly crosses the deformation front into the accretionary wedge. The connection of faults B and C is supported by numerous crossing reflection profiles. Several other WNW trending faults on the slope have, as yet, no documented abyssal plain extensions. Crossings by individual seismic profiles are augmented by GLORIA imagery and SeaBeam bathymetry, where sigmoidal bending and offset of fold axes and linear WNW trending scarps constrain the orientation of faults observed on reflection profiles (Goldfinger and others, in press). In northern Oregon, the continental slope consists of upper and lower terraces separated by a major landward-dipping thrust fault and a coincident break in slope (SB in Fig. 2.1). Seaward of this boundary, thrusts and folds of the accretionary wedge trend north-south, subparallel to the continental margin. Landward of the boundary, folds of the upper slope and shelf, with the exception of outer-shelf submarine banks, trend mostly north-northwest to west-northwest, oblique to the margin. In the structural province traversed by faults A, B, and C, a few of the folds are subparallel to the principal strike-slip faults (Fig. 2.1). While the genetic relation between these young strike-slip faults and oblique folds is not yet documented, we postulate that they both developed in the regional stress field related to oblique Juan de Fuca subduction. Although many folds on the continental shelf and upper slope involve older rocks ranging in age from Eocene to Pliocene (Kulm and Fowler, 1974), Pleistocene and Holocene strata are also deformed. Continued activity

on older folds and faults on the shelf has resulted in scarps of probable Holocene age on the sea floor, although the continuity of the faults is difficult to document due to absence of sidescan sonar data.

Because the active structures of the inner shelf commonly project into the coast, we postulate related active deformation of the coastal region. We have correlated several offshore faults with onshore structures, notably the Tillamook Bay fault (T in Fig. 2.1) mapped onshore by Niem and Niem (1985). This structure may have as much as 19 km of left slip in rocks of Miocene age, but the age of movement is still under investigation (R. E. Wells, 1991, pers. comm.). Offsets of the uppermost units in a reflection profile 8.5 km offshore show that it is probably active in the nearshore region. Furthermore, active inner shelf synclines project toward Tillamook, Netarts, Nehalem, Nestucca, Siletz, and Yaquina bays. This relation is similar to that noted in the Coos Bay area of southwestern Oregon (CB in Fig. 2.1 inset), where South Slough occupies the axis of a late Quaternary syncline that intersects the coast (McInelly and Kelsey, 1990). We propose that, like Coos Bay, many of northern Oregon's bays are influenced by growth of local synclines.

IMPLICATIONS FOR CASCADIA SEISMICITY

The structural features mapped off central and northern Oregon suggest a mechanism for the rapid, periodic submergence of marshes as documented by other investigators in Oregon's coastal bays. Co-seismic downwarping along a coastal strip with simultaneous uplift offshore, similar to the vertical response noted by Plafker (1972) for the 1960 M_W = 9.5 Chilean and 1964 M_W = 9.2 Alaskan events (Heaton and Kanamori, 1984), has been invoked as the mechanism for sudden submergence of coastal salt marshes in Oregon and Washington (Atwater, 1987; Darienzo and Peterson, 1990). However, these two margins differ significantly from the Cascadia margin in that convergence is approximately normal to the margins of Chile and Alaska, whereas convergence is oblique to the Oregon part of the Cascadia margin (DeMets and others, 1990). If active synclines are associated with bays in northern and central Oregon, then growth of local folds may influence or control the burial of marsh surfaces during earthquakes in Oregon. We speculate that both co-seismic plate flexure and growth of folds may simultaneously account for the downwarping of the bays, but their relative importance is unknown.

The question remains as to whether the transverse folds and faults described on the slope and shelf are activated in sympathy with movement on the megathrust, or whether they act independently. The very low seismicity of the upper plate offshore northern and central Oregon shows that the structures we have mapped are relatively quiescent at present. Independent activity on the structures we have mapped would probably call for a higher incidence of instrumental seismicity than observed, if the convergence rate is accurate. Given the evidence for late Pleistocene to Holocene activity on these faults and folds, and the evidence for large Cascadia earthquakes, their present quiescence circumstantially supports their role as structures secondary to the megathrust.

PLATE COUPLING AND ROTATIONS

Several lines of evidence suggest that the Juan de Fuca and North American plates are well coupled. The strike-slip faults discovered on the subducting plate also cut the overriding North American plate, which strongly suggests coupling between the two plates. We do not know whether the faults originate within the upper or lower plate, or in which direction they propagate. However, the presence of these faults in both plates indicates that interplate shear stress must be high enough at the plate boundary for them to propagate from one plate to the other. The dominant NNW to WNW trending structural grain of the upper slope and shelf also indicates strong plate coupling. The active folds are generally orthogonal to the inferred plate convergence direction and direction of crustal shortening (062° at 45° N; DeMets and others, 1990), which suggests that a broad coupled zone extends from the mid-slope region to the vicinity of the coast. The sharp division of structural domains in the mid-continental slope (Fig. 2.1, SB) may correspond to the seismic front of Byrne and others (1988). We speculate that seaward of this boundary, basal shear stress is less than that needed to form structures normal to the maximum principal stress (σ_1), and that a "backstop" effect at or near the slope break (SB) dominates the margin-parallel orientation of the youngest structures. Landward of this boundary, folds that are oblique to the continental margin but close to normal to the inferred plate convergence direction dominate structural orientations, suggesting strong coupling eastward to the coastal region.

A set of parallel strike-slip faults of the same sense of motion requires that the intervening segments and the faults themselves must rotate with time (Freund, 1974). Such rotations are documented for the Transverse Ranges of southern California (Jackson and Molnar, 1990), and for the Oregon and Washington Coast Ranges (Wells and Coe, 1985) on the basis of paleomagnetics. In fact, Wells and Heller (1988) reported clockwise rotations of 16°-22° in 12-15 Ma Columbia River Basalt at coastal sites in western Oregon and Washington. They attribute these rotations to dextral shear distributed across the forearc region, with a monotonic westward increase in rotation. We speculate that the left-lateral faults we have mapped may be R' (secondary) shears within an overall dextral shear couple driven by oblique

convergence, similar to the model proposed by Wells and Coe (1985) for southwestern Washington (Fig. 2.3) and to a block rotation model proposed by Geist and others (1988) for the Aleutian Ridge. If this model is correct, upper-plate shortening due to growth of the submarine fold belt and clockwise rotation may account for a significant part of convergence between the Juan de Fuca and North American plates. Some additional shortening due to a thrust component on these transverse faults may also occur. If this is the case, nonelastic deformation of the upper plate may be a significant process acting to absorb some of the plate convergence, and thus the rate of accumulation of elastic strain energy. At present, quantitative data are insufficient to calculate rotation rates and shortening due to these mechanisms, but additional marine field studies of these transverse structures should shed new light on the problem of very low plate-boundary seismicity in Cascadia.

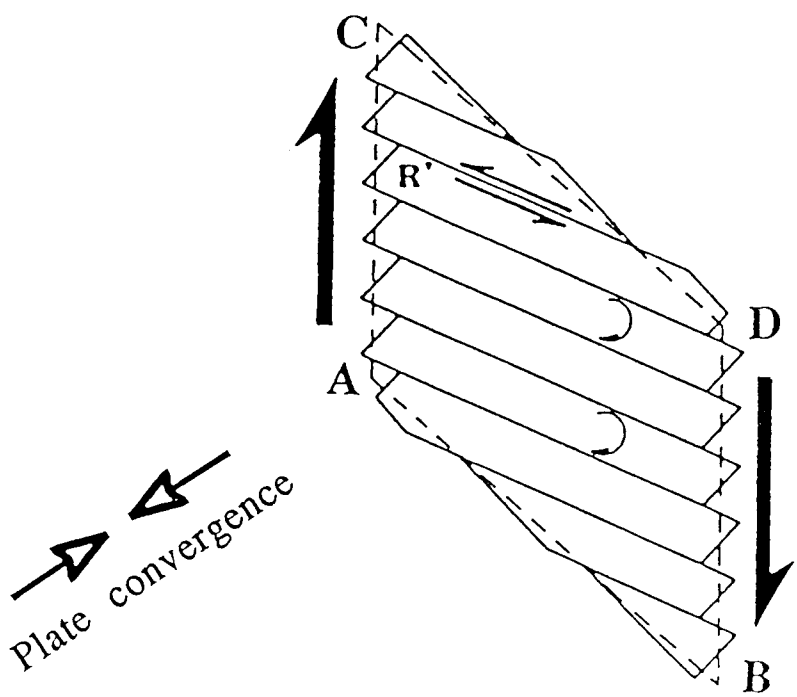

Figure 2.3. Development of left-lateral R' faults within dextral setting driven by oblique plate convergence. As clockwise rotation occurs, line perpendicular to sites A-B and C-D of parallelogram shortens in direction of plate convergence. After Wells and Coe (1985).

CONCLUSIONS

Three left-lateral strike-slip faults in the Cascadia subduction zone that offset both the Juan de Fuca and North American plates, as well as folds in the upper continental slope and shelf, trend obliquely to the continental margin. These transverse structures suggest that the two plates are well coupled. Furthermore, a considerable amount of plate convergence may be accommodated by folding and clockwise rotation of the forearc region in northern and central Oregon. We propose that Holocene subsidence events in the Oregon-Washington coastal bays are, at least in part, a response to the growth of active synclines that trend obliquely to the coastline. This style of deformation does not support either arguments for great earthquakes or earthquakes of more moderate magnitude. It does, however, offer an alternative mechanism for the sudden submergence of salt marshes that does not *require* a great earthquake. Nevertheless, we suspect that growth of these structures is triggered by movement on the megathrust because of their low modern seismicity and because geodetic evidence suggests that elastic strain accumulation and uplift on the adjacent coast are occurring at the same time.

REFERENCES CITED

Appelgate, T.B., Goldfinger, C., MacKay, M., Kulm, L.D., Fox, C.G., Embley, R.W., and Meis, P.J., 1992, A left-lateral strike-slip fault seaward of the central Oregon convergent margin: Tectonics, v. 9, p. 465-477.

Atwater, B.F., 1987, Evidence for great Holocene earthquakes along the outer coast of Washington State: Science, v. 236, p. 942-944.

Byrne, D.E., Davis, D.M., and Sykes, L.R., 1988, Loci and maximum size of thrust earthquakes and the mechanics of the shallow region of subduction zones: Tectonics, v. 7, p. 833-857.

Darienzo, M.E., and Peterson, C.D., 1990, Episodic tectonic subsidence of late Holocene salt marshes, northern Oregon central Cascadia margin: Tectonics, v. 9, p. 1-22.

DeMets, C., Gordon, R.G., Argus, D.F., and Stein, S., 1990, Current plate motions: Geophysical Journal International, v. 101, p. 425-478.

Freund, R., 1974, Kinematics of transform and transcurrent faults: Tectonophysics, v. 21, p. 93-134.

Geist, E.L., Childs, J.R., and Scholl, D.W., 1988, The origin of summit basins of the Aleutian Ridge: Implications for block rotation of an arc massif: Tectonics, v. 7, p. 327-341.

Goldfinger, C., Kulm, L.D., Yeats, R.S., Appelgate, T.B., MacKay, M.E., and Cochrane, G., in press, Active strike-slip faulting and folding of the Cascadia plate boundary and forearc in central and northern Oregon, *in* Rogers, A.M., Kockelman, W.J., Priest, G., and Walsh, T.J., eds., Assessing and reducing earthquake hazards in the Pacific Northwest, U.S. Geological Survey Professional Paper 1560.

Heaton, T.H., and Hartzell, S.H., 1987, Earthquake hazards on the Cascadia subduction zone: Nature, v. 236, p. 162-168.

Heaton, T.H., and Kanamori, H., 1984, Seismic potential associated with subduction in the northwestern United States: Seismological Society of America Bulletin, v. 74, p. 933-941.

Jackson, J., and Molnar, P., 1990, Active faulting and block rotations in the western Transverse Ranges, California: Journal of Geophysical Research, v. 95, p. 22,073-22,087.

Kulm, L.D., and Fowler, G.A., 1974, Oregon continental margin structure and stratigraphy: a test of the imbricate thrust model, *in* Burke, C. A., and Drake, C. L., eds., The geology of continental margins: New York, Springer-Verlag, p. 261-284.

Kulm, L.D., Von Huene, R., and scientific party, 1973b, Initial reports of the Deep Sea Drilling Project, Volume 18: Washington, D.C., U. S. Government Printing Office, p. 97-168.

MacKay, M. E., Moore, G.F., Cochrane, G.R., Moore, J.C., and Kulm, L.D., 1992, Landward vergence, oblique structural trends, and tectonic segmentation in the Oregon margin accretionary prism: Earth and Planetary Science Letters, v. 109, p. 477-491.

McInelly, G.W., and Kelsey, H.M., 1990, Late Quaternary tectonic deformation in the Cape Arago-Bandon region of coastal Oregon as deduced from wave cut platforms: Journal of Geophysical Research, v. 95, p. 6699-6713.

Niem, A.R., and Niem, W.A., 1985, Oil and gas investigations of the Astoria Basin, Clatsop and northernmost Tillamook Counties, northwestern Oregon: Oregon Department of Geology and Mineral Industries, Oil and Gas Investigation 14, scale 1:250,000.

Plafker, G., 1972, Alaskan earthquake of 1964 and Chilean earthquake of 1960: implications for arc tectonics: Journal of Geophysical Research, v. 77, p. 901-925.

Tobin, H.J., Moore, J.C., MacKay, M.E., Cochrane, G.R., Orange, D.L., Moore, G.F., and Kulm, L.D., 1991, Generation of fracture permeability along a vertical fault at the Oregon accretionary margin and implications for wedge thrust vergence: Geological Society America Abstracts with Programs, v. 23, p. A366.

Wells, R.E., and Coe, R.S., 1985, Paleomagnetism and geology of Eocene volcanic rocks of southwest Washington, implications for mechanisms of tectonic rotation: Journal of Geophysical Research, v. 90, p. 1925-1947.

Wells, R.E., and Heller, P., 1988, The relative contribution of accretion, shear, and extension to Cenozoic tectonic rotation in the Pacific Northwest: Geological Society of America Bulletin, v. 100, p. 325-338.

ACKNOWLEDGMENTS

Supported by National Science Foundation Grants OCE-8812731 and OCE-8821577 and by the National Earthquake Hazards Reduction Program, U.S. Geological Survey, Department of Interior, under award 14-08-001-G1800.

CHAPTER 3: ACTIVE STRIKE-SLIP FAULTING AND FOLDING OF THE CASCADIA PLATE BOUNDARY AND FOREARC IN CENTRAL AND NORTHERN OREGON

Chris Goldfinger
Department of Geosciences, Oregon State University, Corvallis, Oregon 97331

LaVerne D. Kulm
College of Oceanography, Oregon State University, Corvallis, Oregon 97331

Robert S. Yeats
Department of Geosciences, Oregon State University, Corvallis, Oregon 97331

Bruce Appelgate and Mary E. MacKay
School of Ocean and Earth Science and Technology, University of Hawaii, Honolulu, Hawaii 96822

Guy R. Cochrane
Earth Sciences, University of California at Santa Cruz, California 95064

ABSTRACT

Three west-northwest-trending left-lateral strike-slip faults on the abyssal plain off northern and central Oregon between 44° 40'N and 45° 12'N. latitude have been mapped using seismic reflection, sidescan sonar, data from ALVIN submersible dives, and SeaBeam bathymetry. These oblique faults, the Wecoma fault and faults B and C, intersect the north-south striking structures of the active accretionary wedge. The faults cut the oceanic lithosphere of the subducting Juan de Fuca plate and appear to cross the plate boundary. The best studied of these, the Wecoma fault, extends 18 km (kilometers) northwestward across the abyssal plain from the deformation front. Displacement on this fault is 5.5± 0.8 km at the deformation front, decreasing to zero at the northwestern fault tip based upon piercing-point offset. The Wecoma fault has been active for about 600±50 thousand years, and has an average slip rate of 7-10 mm/year (millimeters per year). The latest Pleistocene-Holocene slip rate is 5-12 mm/year. These faults are active, as indicated by the offset of the youngest sedimentary units, the presence of surficial fault scarps, and the venting of deep source fluids. The Wecoma fault intersects the deformation front in a complex structural zone consisting of fault-bounded pop-ups (uplifted asymmetrical triangular plateaus), an embayment in the deformation front, and a local reversal of vergence in the basal thrust of the accretionary wedge. Fault B also is associated with an abrupt change in vergence direction of the basal accretionary thrust.

Linear gullies and scarps in the Wecoma fault zone extend into the first several thrust ridges of the continental slope, suggesting that this fault remains active beneath the accretionary wedge. Changes in fold orientation and amount of shortening in the initial three to four thrust ridges of the accretionary wedge suggest that the strike-slip faults have influenced the development of coeval accretionary-wedge structures through differential slip of the downgoing plate.

Several west-northwest-trending deformation zones have been mapped on the continental slope off northern and central Oregon. The deformation zones are composed of west-northwest-trending linear scarps, en-echelon northwest to west-northwest-trending folds, and left-stepping and sigmoidally bent folds. Oblique folds are commonly fault-propagation and

fault-bend folds developed above high-angle faults. Some of these active faults and folds striking north-northwest to west-northwest are refolding somewhat older north and north-northeast-trending folds. Deformation in these zones is consistent with a left-lateral sense of shear. Three of these deformation zones adjoin the three abyssal-plain strike-slip faults, whereas at least one zone and possibly several others are restricted to the continental slope. We postulate that the deformation zones are shear zones developed in the upper plate above the subducted strike-slip faults, or alternatively, that strike-slip faulting in the upper plate has propagated seaward into the subducting plate.

INTRODUCTION

The Cascadia subduction zone (Fig. 3.1) off Oregon and Washington may be one of the best studied subduction zones in the world. Its proximity to major United States ports and three decades of study by oceanographic institutions, government agencies, and industry have produced an extensive data set for use in geological and geophysical investigations. In recent years, attention has been focused on the anomalous seismic quiescence of much of the Cascadia subduction zone in comparison to other subduction zones. The moderate plate convergence rate of 40 mm/year directed 062° (calculated from JDF-NAM (Juan de Fuca-North America) Euler vector of DeMets and others, 1990) and the relative youth of the subducting lithosphere (9-10 Ma (mega-annum) according to Wilson and others, 1984) should characterize the Cascadia subduction zone as a Chilean-type convergent margin (Heaton and Kanamori, 1984). Because most Chilean-type margins have had great (M>8.4) earthquakes in historic times, the Juan de Fuca-North America plate boundary should also be capable of generating great earthquakes. Geological evidence for great earthquakes has been inferred from buried marsh deposits of the coastal bays of Washington (Atwater, 1987; Atwater and Yamaguchi, 1991), Oregon (Darienzo and Peterson, 1990), and northern California (Carver and others, 1989; Clarke and Carver, 1989; Vick, 1988). Rapid coseismic submergence in the bays accompanied by tsunamis is inferred from peat layers overlain by marine sands (Atwater, 1987). Presently, the Oregon Cascadia convergent margin may have the lowest incidence of plate-boundary seismicity of any subduction zone. Although earthquakes in the upper and lower plates are well monitored by the University of Washington seismic network, no thrust-type earthquakes at any magnitude level have been located on the plate interface (Ludwin and others, 1991). The absence of historic great earthquakes on the Cascadia plate boundary can be explained by long recurrence intervals of 300 to 1,000 years or more (Adams, 1990; Atwater, 1987; Darienzo and Peterson, 1990; Atwater and Yamaguchi, 1991; Carver and others, 1989), yet the Cascadia plate interface nonetheless remains singularly quiet among the world's convergent margins.

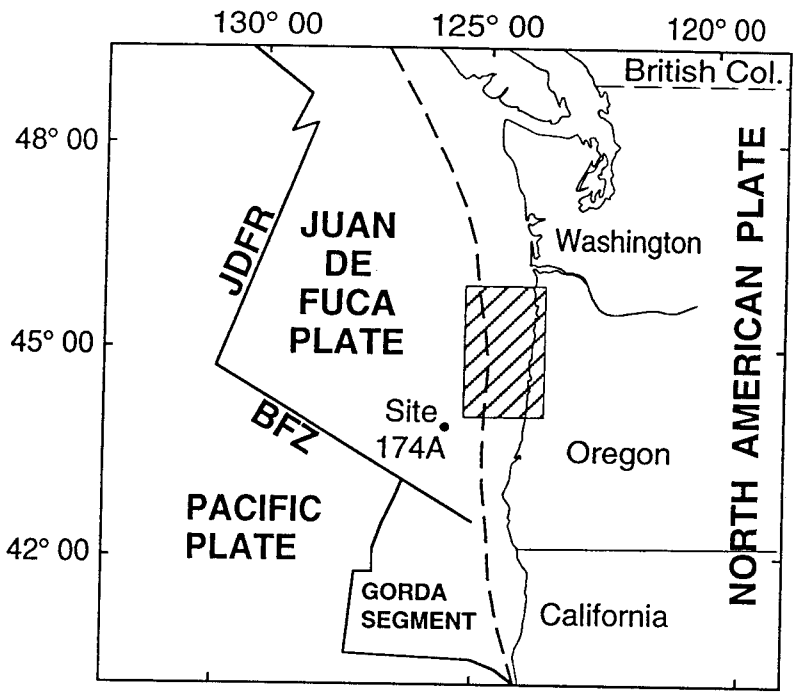

Figure 3.1. Index map showing tectonics of the Cascadia subduction zone. Heavy dashed line, Plate convergence boundary; lined box, study area of this chapter; site 174A, Deep Sea Drilling Project site 174A; BFZ, Blanco fracture zone; JDFR, Juan De Fuca ridge; GORDA SEGMENT, Gorda segment of the Juan de Fuca plate.

The low seismicity of the Cascadia subduction zone has led investigators to explore a variety of hypotheses to explain the apparent seismic gap along the Cascadia margin (Ando and Balasz, 1979; Sykes, 1989; West and McCrumb, 1988). Our investigation of the structure of the plate boundary and forearc off the Oregon coast arose in part from the discovery of several oblique strike-slip faults in the abyssal plain off north-central Oregon. These faults cut the downgoing Juan de Fuca plate and cross the plate boundary, extending some distance into the overriding North America plate. To our knowledge, faults of this type have not previously been described from other subduction zones around the world, although strike-slip faulting restricted to the upper plate has been described in both orthogonal and oblique convergent settings (Lewis and others, 1988, and references therein; Geist and others, 1988). This discovery is almost certainly the result of the increased resolution in sea-floor mapping tools in recent years, but these faults may also represent something unique about the Cascadia convergent margin. The discovery of these faults suggests that detailed structural investigations may offer new information about oblique subduction in general and the Cascadia subduction zone in particular.

The purpose of this chapter is to document the structural characteristics of the Wecoma fault, the largest and best known of three strike-slip faults discovered on the abyssal plain off Oregon, and to discuss the relationship of this fault to new mapping of active tectonic features of the continental slope. The long-term goal of this study is to better define the active tectonics of the Cascadia subduction zone and thereby develop a better understanding of the regional tectonics and seismic hazards of the Pacific Northwest. The chapter concludes with a discussion of possible origins for the oblique faults, and the implications of the oblique faults and folds we have mapped for plate-boundary processes within the Cascadia convergent margin.

METHODS OF STUDY

We are studying the submerged plate boundary and forearc region off Oregon and Washington (Fig. 3.1) using SeaMARC 1A and GLORIA sidescan sonar imagery, SeaBeam swath bathymetry, ALVIN submersible observations, and a dense network of single-channel and multichannel seismic (MCS) surveys. We are mapping the Oregon-Washington plate boundary and submarine forearc at a scale of 1:500,000. We have used about 30,000 km of seismic-reflection profiles collected by Oregon State University, University of California at Santa Cruz, University of Hawaii, University of Washington, Scripps Institution of Oceanography, U.S. Geological Survey, U.S. National Oceanic and Atmospheric Administration, and the oil industry (Fig. 3.2).

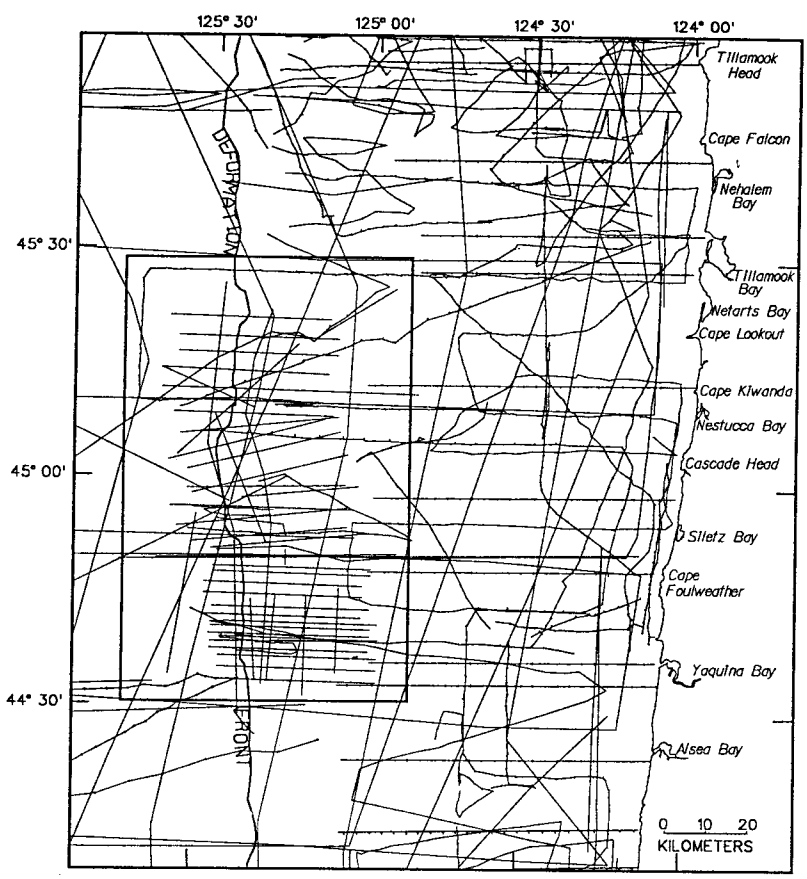

Figure 3.2. Trackline map showing the location of all seismic-reflection profiles used in this study. Tick marks are hourly or quarter-hourly ship positions. Deformation Front, deformation front of the accretionary prism. Box shows area of Figure 3.3.

The seismic-reflection profiles vary widely in quality, depth of penetration, and navigational accuracy, and range from single-channel sparker records navigated with Loran A to 144-channel digital profiles navigated with GPS (Global Positioning System). Partly in preparation for Ocean Drilling Program (ODP) Leg 146, a site survey consisting of closely spaced, high-resolution multichannel seismic lines, SeaMARC 1A sidescan mapping, SeaBeam swath bathymetry, and ALVIN submersible dives focused on the plate boundary and accretionary wedge at the proposed drilling sites near 45° N. latitude (Fig. 3.3). Within this 6,000-km^2 (square kilometers) area we were able to map submarine structures in considerable detail.

Within the ODP site survey area (Fig. 3.3), the 144-channel reflection profiles were navigated with GPS, and position information from these lines was used as the datum for mapping that portion of the larger study area. Processing through time migration was carried out at the University of Hawaii. Several other U.S. Geological Survey 24-channel and Oregon State University single-channel lines also constrain the structural interpretations. The sidescan and bathymetric surveys were navigated with a combination of GPS and Transit satellite navigation, with Loran C tracking used between satellite fixes. Navigation of the deep-towed sidescan towfish was by the method described by Appelgate (1988). Where spatial misfits occurred, we adjusted the sidescan data to best fit the GPS navigated MCS lines or the SeaBeam bathymetry where appropriate. SeaMARC 1A sidescan data were collected with a deep-towed 30-kHz (kiloHertz) system capable of imaging a 2-km or a 5-km swath width, with spatial resolutions of 1 and 2.5 m (meters), respectively. A magnetometer attached to the towfish recorded total field intensity over the sidescan tracks. Our technique with sidescan surveys was to cover the study area at the wider 5-km swath width, then return to areas of interest and conduct detailed surveys using the higher resolution 2-km swath. Sidescan processing, which included geometrical and speed corrections, correction for towfish position, georeferencing of image pixels to a latitude-longitude grid, and image enhancement (as described in Appelgate, 1988) was done at the U.S. National Oceanic and Atmospheric Administration image processing facility in Newport, Ore. Outside the ODP site survey area, navigational accuracy was more variable. Loran A navigated profiles have maximum errors on the order of 1-3 km, Loran C errors are about 0-1.5 km,

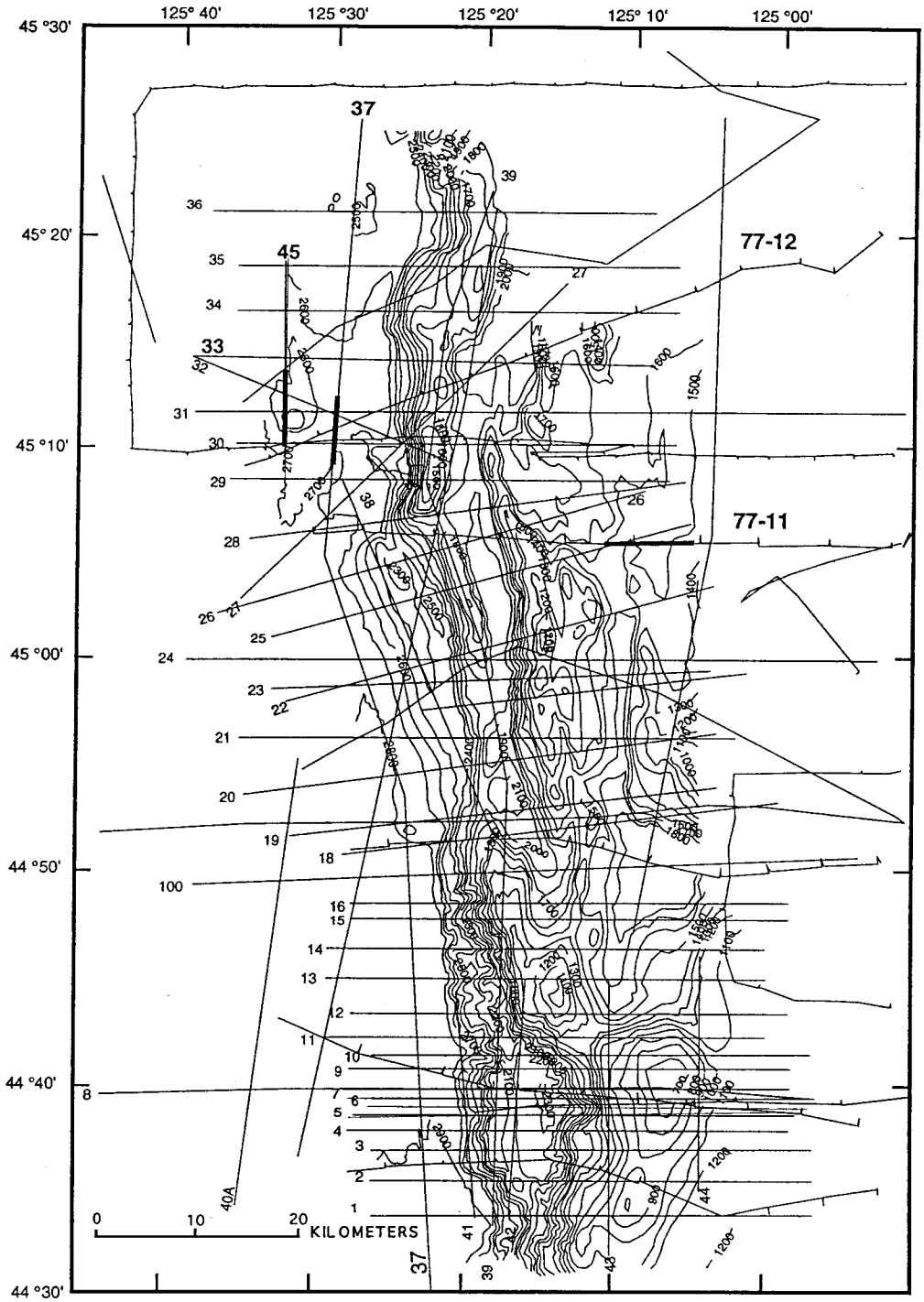

Figure 3.3. Map showing seismic-reflection tracklines and bathymetry in the Ocean Drilling Program (ODP) site survey area. Location of this map shown on Figure 3.2. Contour interval 100 meters. Bold numbered lines are referred to in text. Bold segments of profiles 37, 45, and 77-11 are sections of profiles shown in Figures 3.8, 3.9, & 3.20 respectively.

and Transit satellite errors range from near zero up hundreds of meters. The dense coverage of reflection profiles allowed adjustment of older lines where crossed by satellite-navigated lines.

STRIKE-SLIP FAULTS ON THE JUAN DE FUCA PLATE

Along the central and northern Oregon convergent margin, three west-northwest-trending left-lateral strike-slip faults (Wecoma fault and faults B and C, Fig. 3.4) extend from the base of the continental slope 10-18 km northwestward across the abyssal plain. First imaged using SeaMARC 1A sidescan sonar in 1986, these faults were surveyed in detail in 1989 using a narrow-swath, high-resolution survey (Appelgate and others, 1992) and were crossed several times by multichannel seismic (MCS) profiles made in 1989. In reflection profiles on the abyssal plain, the three faults show vertical separation of both the oceanic basement and the 2-3-km-thick overlying sedimentary section (Appelgate and others, 1992; MacKay and others, 1992; this study). The three faults strike 290° to 295°, and all three are primarily strike-slip with a minor up-to-the-north component of displacement as evidenced by offset surface and subsurface features. In this paper we discuss primarily the Wecoma fault, because this fault is better covered by seismic and sidescan surveys. Faults B and C appear to be similar in structural style to the Wecoma fault, but the more sparse data available on these faults presently precludes as detailed an assessment of them.

CHARACTERISTICS OF THE WECOMA FAULT

The Wecoma fault is the longest and best developed of the three strike-slip faults on the abyssal plain (Fig. 3.4). The general physiography of the Wecoma fault, its associated structures, and the adjacent abyssal plain and accretionary wedge are shown on Figure 3.5. The surface trace and morphologic features associated with the Wecoma fault and the complex intersection of the fault with the deformation front are shown on Figure 3.6. We have integrated all of the available geophysical data in a geologic structure map of the Wecoma fault on the abyssal plain and adjacent frontal accretionary wedge (Fig. 3.7). Migrated multichannel seismic profiles of the Wecoma fault reveal that it is nearly vertical, in some places consisting of a main strand with little other deformation (Figs. 3.8*A*, *B*), and in other places characterized by an upward-branching positive flower structure (Fig. 3.9), as

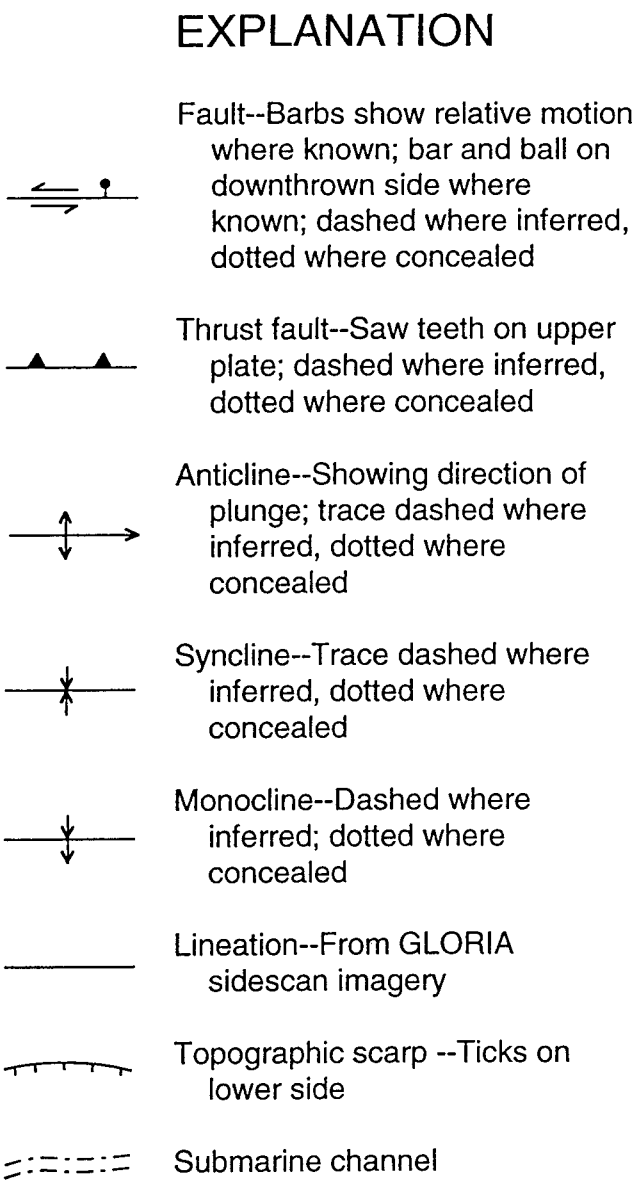

Figure 3.4. Structure of the central Oregon continental margin. This map emphasizes active features; most structures shown cut or deform the sea floor. The deformation front is a thrust fault south of Fault B, and is the base of a seaward-dipping thrust ramp north of fault B. Structure offsets along faults shown only where known. No offsets across faults may indicate 1) insufficient data, 2) no horizontal separation, or 3) horizontal separation not visible at this scale. Areas showing sets of structures intersecting and crossing other structures result from large age differences in the two structural sets.

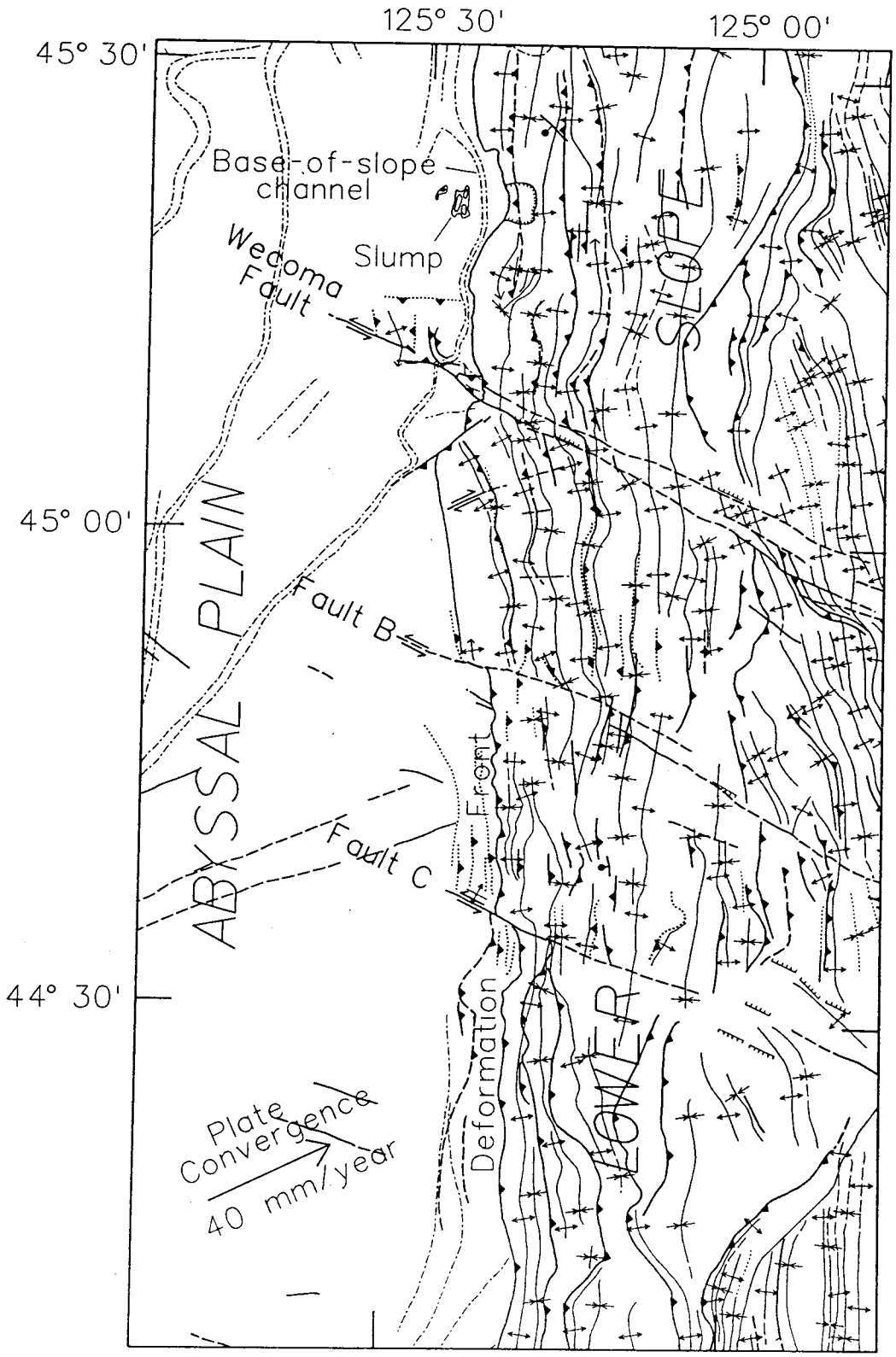

Figure 3.4, Continued.

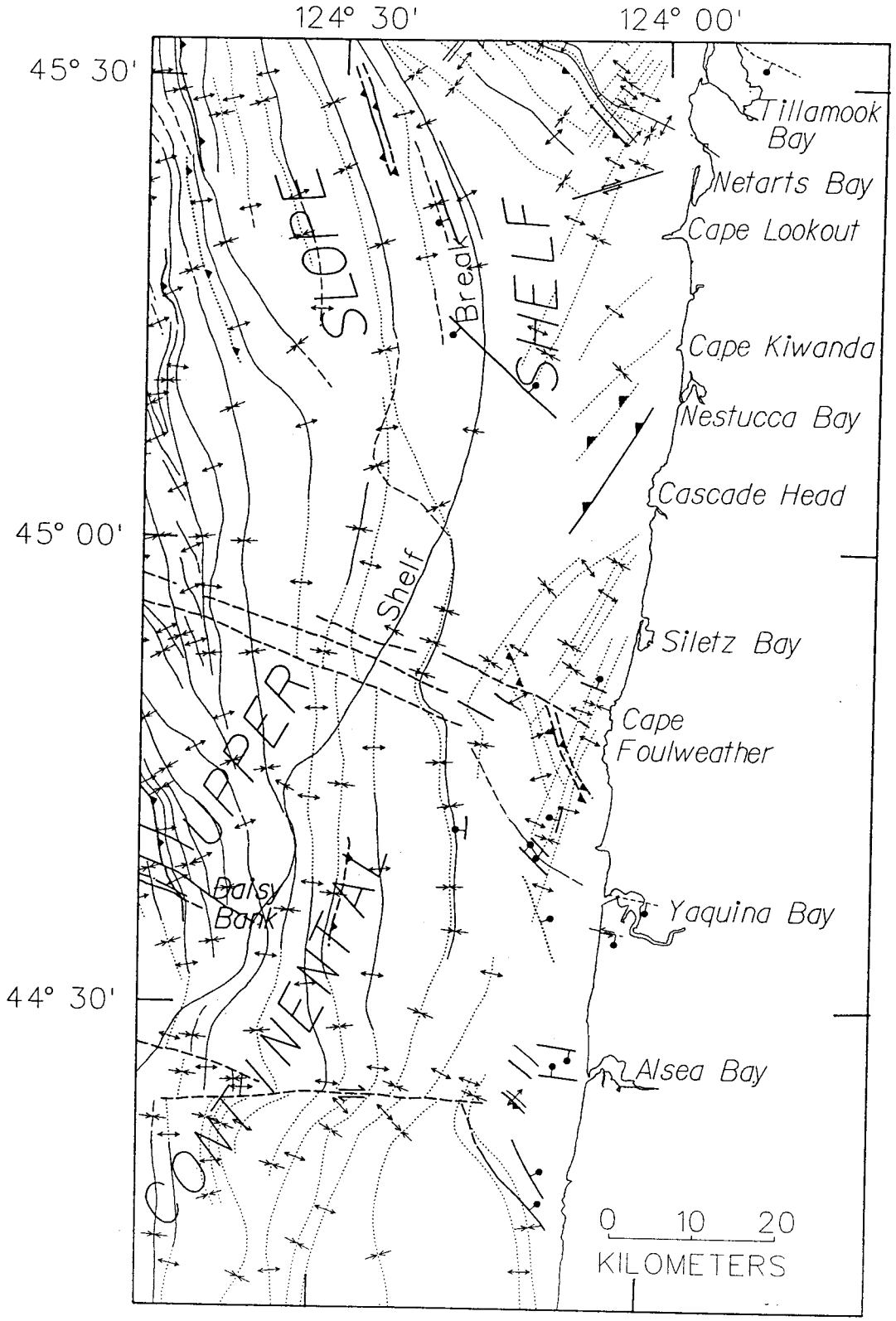

Figure 3.4, Continued.

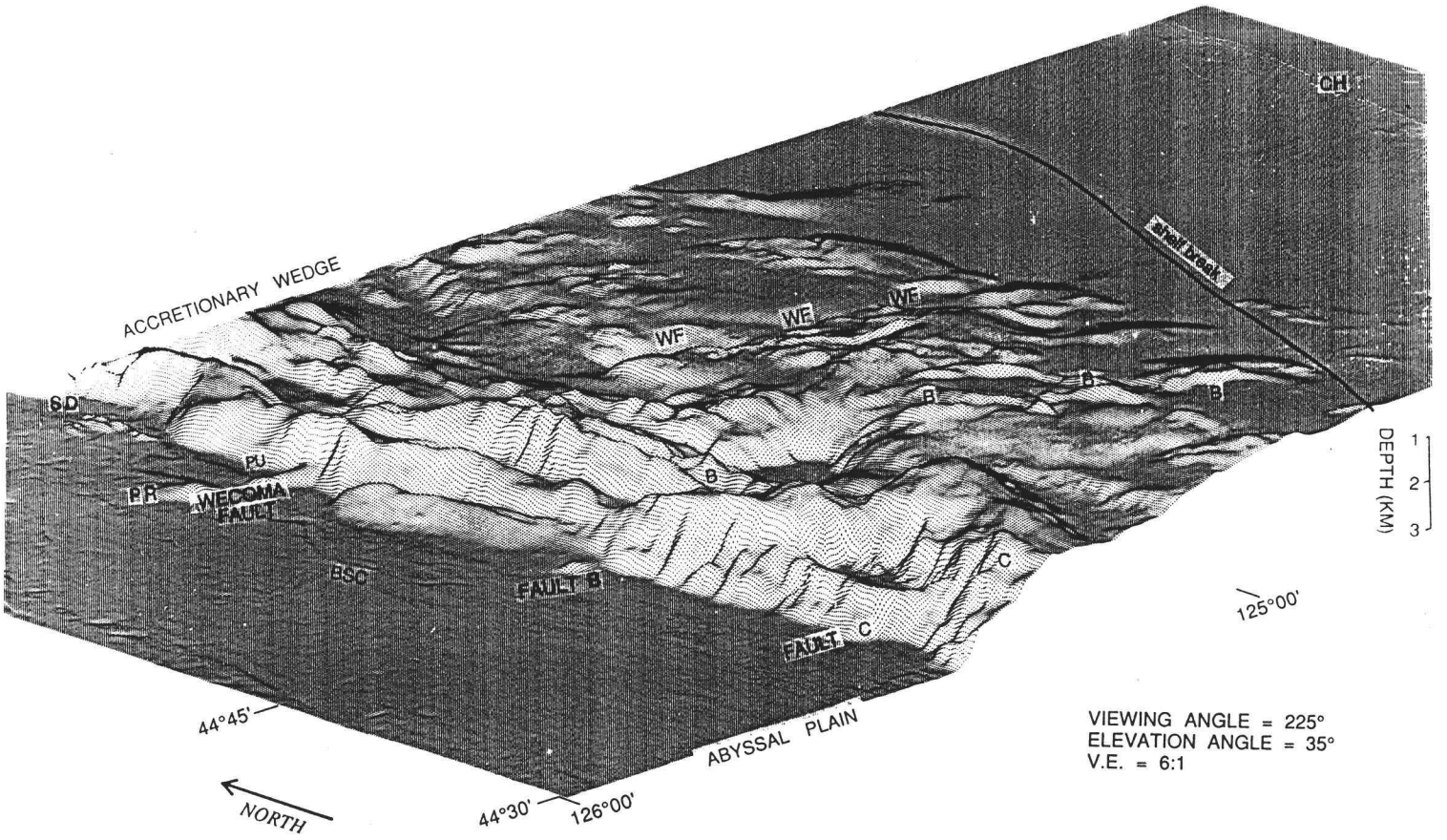

Figure 3.5. Perspective mesh plot of SeaBeam swath bathymetry data off central and northern Oregon. View from the southwest showing the physiography of the abyssal plain and accretionary wedge near the Wecoma fault (WF) and faults B (B) and C (C). Figure 3.4 shows map location of faults. BSC, base-of-slope channel; PR, pressure ridge; PU, pop-up plateau; SD, slump debris; CH, Cascade Head on the Oregon coast. Arrow shows location of Figure 3.21. Diagram provided by National Oceanic and Atmospheric Administration/National Ocean Survey.

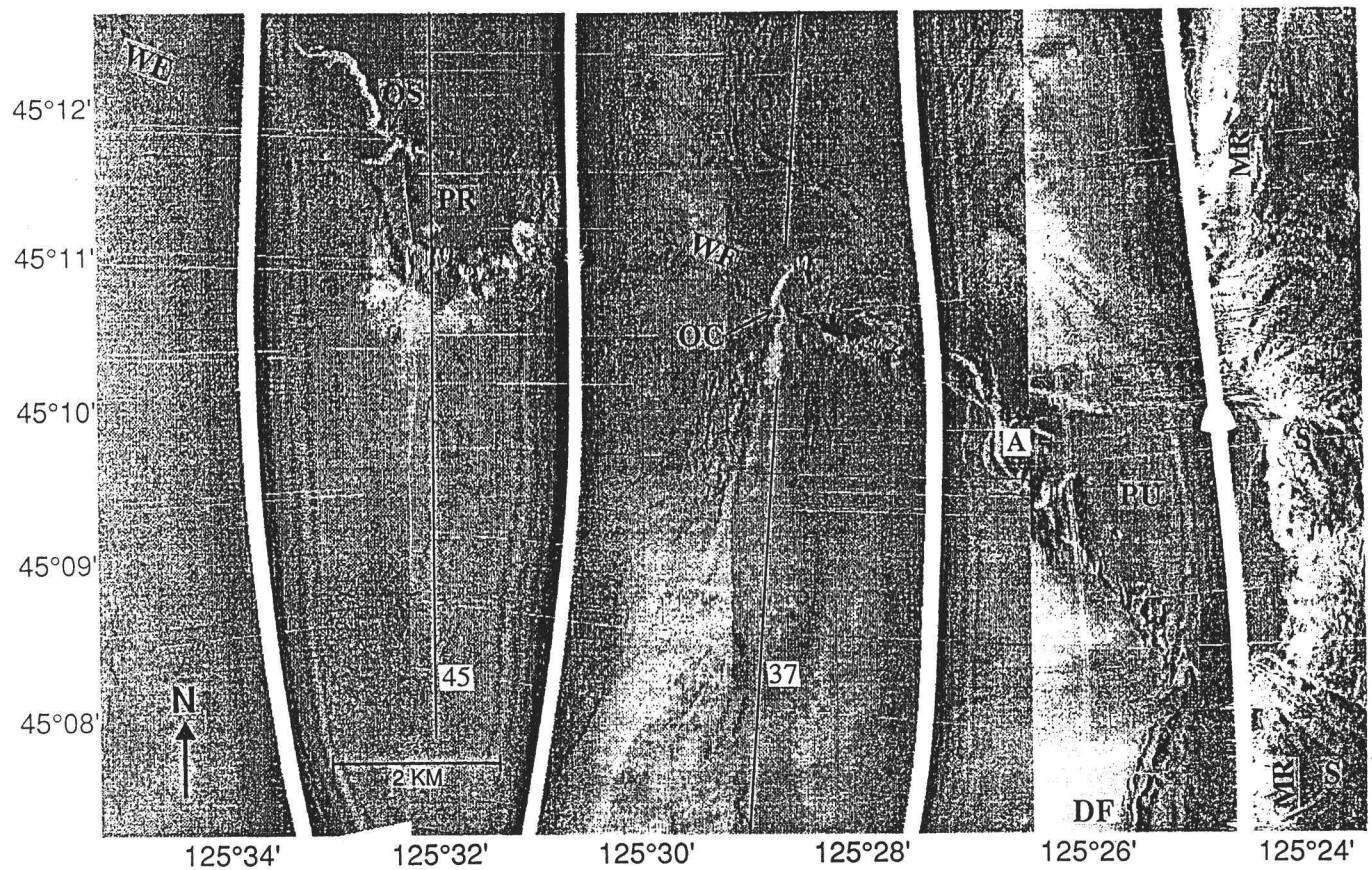

Figure 3.6. Mosaic of SeaMARC 1A 5 km swaths near the Wecoma fault off the central Oregon coast. PR, pressure ridge; WF, Wecoma fault; PU, the pop-up structure that marks the intersection of the Wecoma fault with the deformation front (DF); A, apex of pop-up, corresponds to point A in Figure 3.17; OC, offset channel; OS, offset slump scar; S, fault splays that occupy gullies on the seaward flank of the marginal ridge (MR). Embayment in the deformation front (discussed in text) is just east of the pop-up (PU). Numbered lines show location of MCS lines 37 and 45.

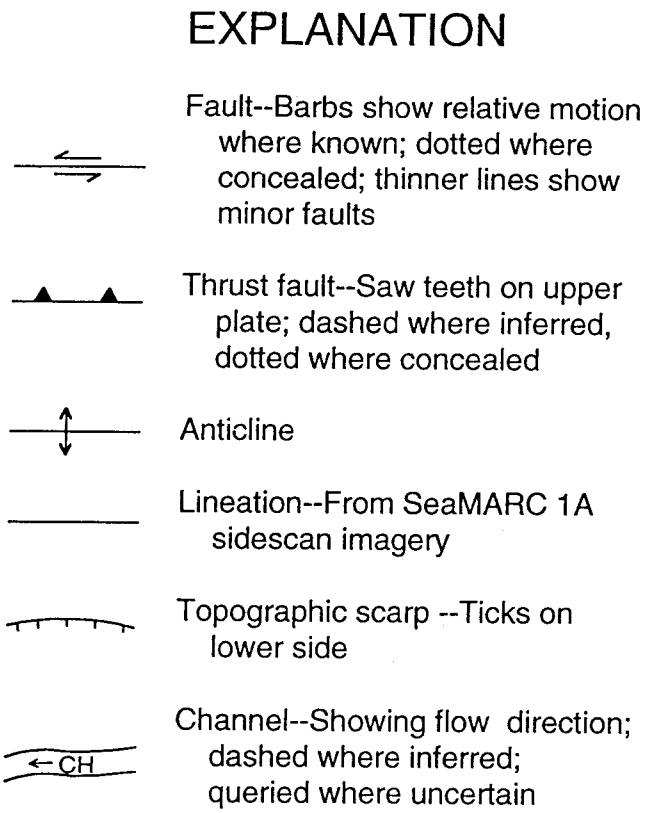

Figure 3.7. Structure map of the western part of the Wecoma fault, adjacent abyssal plain, and frontal accretionary wedge off the central Oregon coast. Structure compiled from migrated and unmigrated seismic-reflection profiles, SeaBeam bathymetry, and SeaMARC 1A sidescan imagery. A, apex of pop-up, corresponds to point A in Figure 3.17. Structures shown as offset only where known.

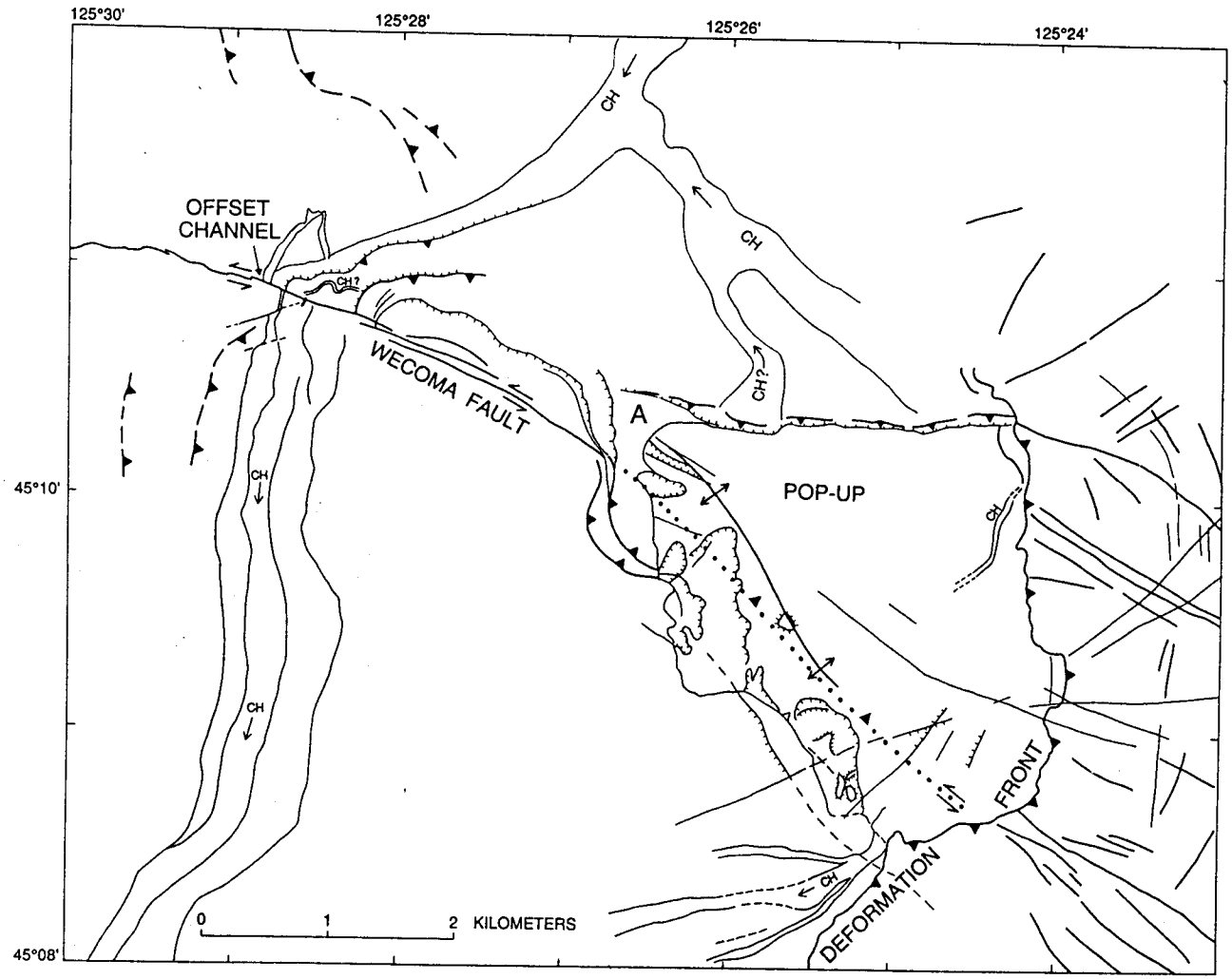

Figure 3.7, Continued.

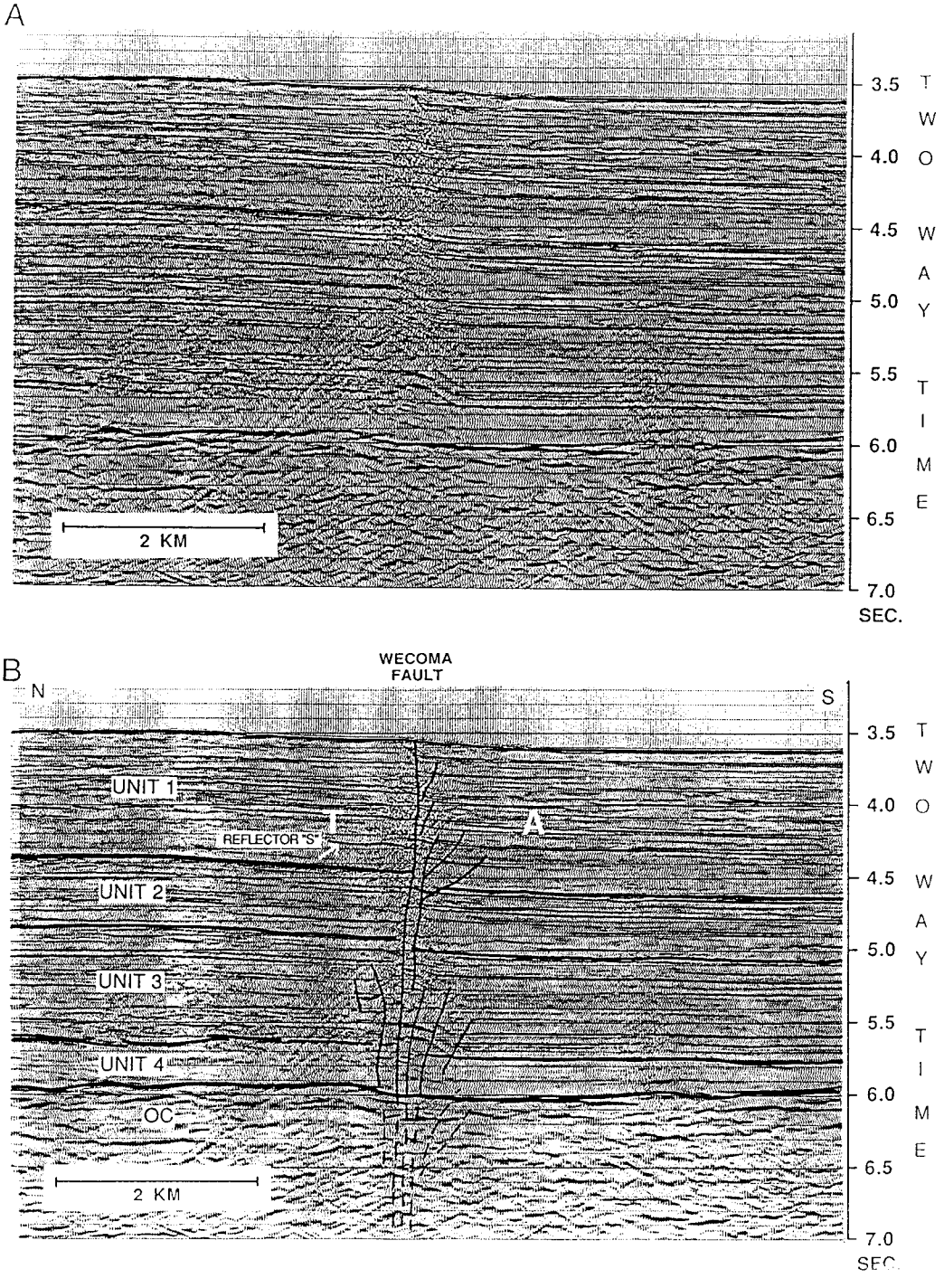

Figure 3.8. Migrated MCS line 37 crossing of the Wecoma fault between the pressure ridge and the deformation front off the Oregon coast. Location of line 37 is shown on Figure 3.3. *A,* uninterpreted section; *B,* interpreted section. Note thickening of unit 1 and thinning of units 2 and 3 on the downthrown (right) block. OC, oceanic crust; T , block moving toward the viewer; A, block moving away from viewer.

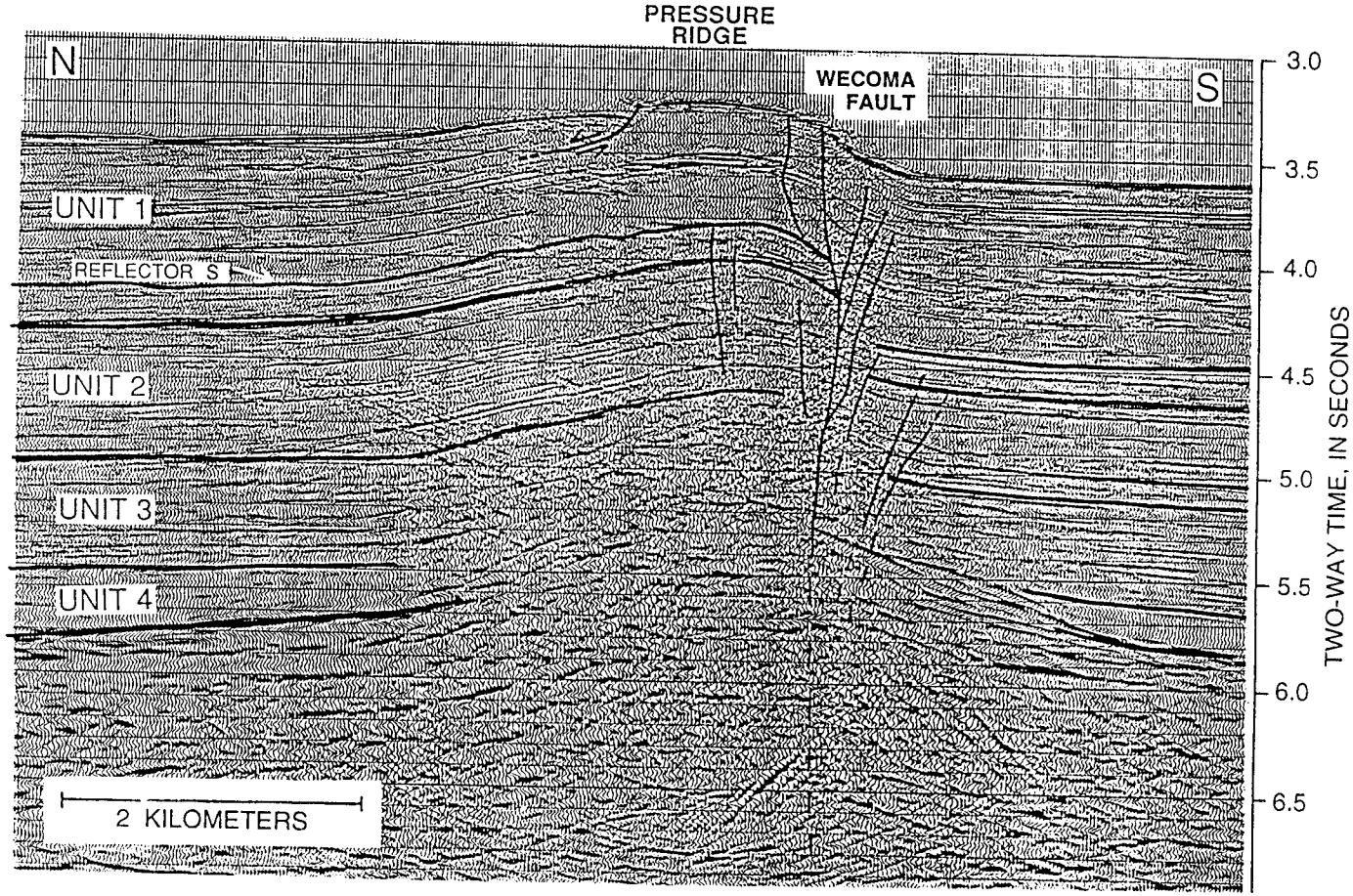

Figure 3.9. Part of MCS line 45 showing the Wecoma fault and the pressure-ridge anticline off the central Oregon coast. Location of line 45 is shown on Figure 3.3. Reflector S marks the stratigraphic point in the section above which seismic stratigraphic units thin over the ridge crest. Below reflector S the stratigraphy does not show the influence of ridge growth. This profile crossed the fault just east of the eastern terminus of the northern strand of the Wecoma fault . A small normal fault is located just north of the Wecoma fault; barbs show direction of movement.

defined by Harding (1985). Blocks within the flower structure mostly show minor reverse motion. In both seismic and sidescan records on the abyssal plain the displacement and surface expression of the Wecoma fault diminish toward the northwest. On the high-resolution 2-km sidescan swath, the trace of the fault was lost about 18 km west-northwest of the deformation front. An MCS profile (line 33, Fig. 3.3) crosses the along-strike projection of the fault 7 km west-northwest of the point at which the scarp disappeared on the 2-km sidescan record. At the projected location, only minor deformation was seen, suggesting that this profile crosses near the fault tip. Two other crossing reflection profiles, located 3.7 and 5.5 km west of the line 33 crossing of the fault, show that the fault does not extend west of longitude 125° 41' W (Fig. 3.3).

Seismic-reflection profiles indicate that the Wecoma fault is a structural break in the downgoing Juan de Fuca plate. On MCS line 37 near the deformation front (Fig. 3.8*A, B*) vertical separation of the basaltic oceanic crust is apparent, the northeast block upthrown (Appelgate and others, 1992; this study). Although the vertical separation of the basement seen in Figure 3.8 is not large, identical vertical separation also occurs in the overlying stratigraphic units. A corresponding basement offset is required to produce the vertical separation of the sediments, thus the observed basement offset cannot be a hummock on the basement surface.

The overall strike of the Wecoma fault from the base of the continental slope to its northwestern terminus is 293°, and it extends 18-km across the abyssal plain from the deformation front. The trace bends gently southward 7-km northwest of the deformation front, then abruptly terminates along the southern boundary of a structural upwarp (pressure ridge, PR, Figs. 3.6 and 3.9). Displacement is taken up by a second northwest-trending right-stepping segment that originates on the northern flank of the upwarp and strikes northwest to its terminus (Fig. 3.6; see also Appelgate and others, 1992). This upwarp was initially thought to be a mud volcano, but deep-towed seismic-reflection data showed internally coherent reflectors, suggesting a structural origin (Cochrane and Lewis, 1988). The upwarp gives much information about the timing and development of the Wecoma fault and is therefore discussed here in some detail. It is a complex structure that is bounded on the south by the southern strand of the Wecoma fault and on the other three sides

by minor reverse faults, but it is best described as a doubly plunging north-northwest-trending anticline (pressure ridge, Figs. 3.9 and 3.10). The three-dimensional structure of the upwarp is shown in Figure 3.10.

Magnetic modeling of the upwarp and Wecoma fault indicates that basaltic basement is upwarped beneath the fold in the sedimentary section and is vertically offset about 100 m by the fault, north block up (Appelgate and others, 1992). Based on the involvement of the basement and the right step in the fault, we interpret the upwarp as a restraining-bend anticline (Sylvester, 1988) formed by compression across the right step in the Wecoma fault. We here refer to the upwarp as a pressure ridge. Alternatively, the ridge may be a truncated early formed anticline of the type described by Wilcox and others (1973). If so, the anticline may have formed in the sedimentary section in response to left-lateral displacement of the underlying Juan de Fuca plate and then was partly truncated by two en echelon segments of the fault as they propagated upward with increasing fault motion. If this model is correct, the lack of a single throughgoing trace implies that the fault has not completed its final stage of development into a throughgoing single strand as modeled in clay experiments and observed in nature (Wilcox and others, 1973). A second alternative explanation of the ridge is that the upwarp is related to the growth of the accretionary wedge (Cochrane and Lewis, 1988). If so, the ridge would be linked to the master décollement by an undetected basal fault. However, analysis of the growth history of the ridge, discussed below, indicates that the ridge is roughly twice the age of the first ridge of the accretionary wedge, and began its growth when it was 28-32 km west of the longitude of the present deformation front, using the 40 mm/year Juan de Fuca-North America plate convergence rate of DeMets and others (1990). The relative longevity of the ridge and the evidence for a basement upwarp suggest that the ridge's formation was unrelated to growth of the frontal thrusts of the accretionary wedge. However, recent growth probably has been augmented by horizontal compression due to the proximity of the plate boundary.

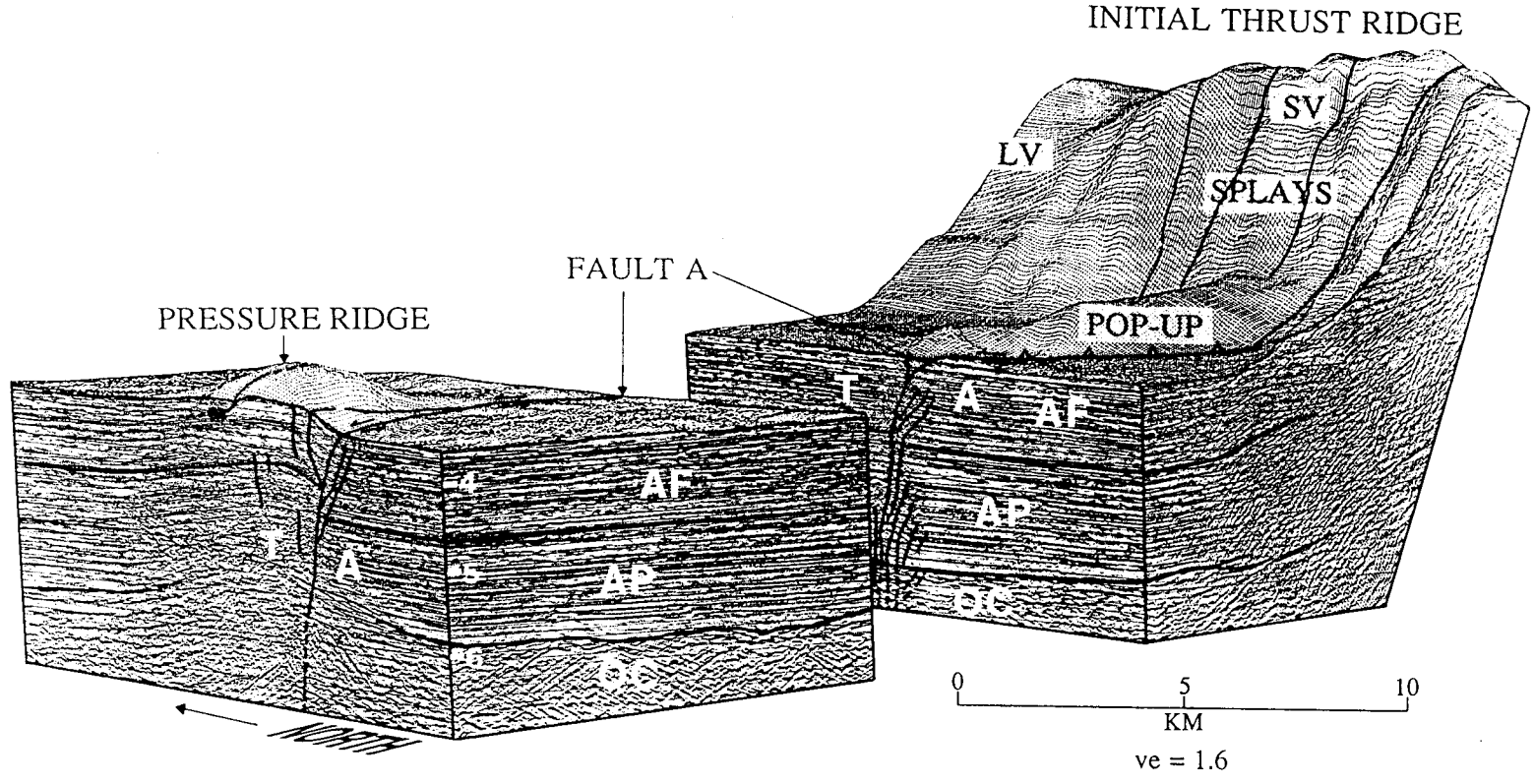

Figure 3.10. Composite block diagram of the pressure-ridge area and intersection of the Wecoma fault and the deformation front as viewed from the southwest. Other faults are also shown. Migrated seismic sections (two-way time) shown with selected reflectors enhanced. Vertical scale is two-way travel time. AP, abyssal plain section; AF, Astoria fan (note thickening across the fault and thinning over the pressure ridge); OC, oceanic crust; A, motion away from viewer; T, motion toward viewer; SV, seaward vergence; LV, landward vergence; DF, deformation front.

Age, Net Slip, and Average Slip Rate of the Wecoma Fault

Stratigraphic relationships within the abyssal-plain sedimentary section near the Wecoma fault and the pressure ridge can be used to infer the growth history of the pressure ridge as well as the slip rate and horizontal separation on the Wecoma fault.

Abyssal-Plain Stratigraphy

We have informally divided the abyssal-plain sedimentary section into four seismic-stratigraphic units on the basis of reflection character and stratigraphic coherence, using the 1989 MCS data (Fig. 3.8*B*). The lowest unit (unit 4) is a weakly reflecting seismic unit that directly overlies the basaltic rocks of oceanic layer 2. The poor reflectivity of this unit is probably due to its lithologic homogeneity, consisting of poorly stratified carbonate oozes, calcareous mudstone, and silt turbidites at Deep Sea Drilling Project (DSDP) drill site 174A on Astoria Fan (Kulm and others, 1973b). Thickness of this unit is variable because it fills in the rough basement topography, but it averages about 300 m near the pressure ridge. Units 2 and 3 (Fig. 3.8*B*) are defined somewhat arbitrarily on the basis of prominent reflectors and consist primarily of distal thin-bedded silty clay turbidites interbedded with hemipelagic clay (Kulm and others, 1973b). Units 2 and 3 are an abyssal-plain sequence that is thought to have either a Klamath Mountain or Vancouver Island source (Kulm and Fowler, 1974). Units 2 and 3 both thicken uniformly eastward in response to increasing rates of sedimentation and the eastward slope of the 9-11 Ma crust presently being subducted (Wilson and others, 1984). The uppermost unit (unit 1) is composed of overlapping lobes of the middle to late Pleistocene Astoria submarine fan (Kulm and others, 1973b). The lithology of unit 1 is dominated by thin- to thick-bedded medium- to very fine grained sand intervals with sharp lower contacts, grading upward into silts and silty clays (Kulm and others, 1973b). A capping fifth unit consists of 1-2 m of Holocene hemipelagic silt and clay (not visible on Figure 3.8*B*) (Nelson, 1976; this study).

Timing Constraints

Seismic profiles are notoriously poor at resolving stratigraphic and timing relationships in strike-slip fault zones. However, the closely spaced MCS lines near the Wecoma fault and the fortuitous presence of critical timing indicators allowed us to bracket the interval in the stratigraphic section at which vertical motion of both the fault and the pressure ridge began. On MCS line 37 (Fig. 3.8*B*) unit 1 clearly shows thickening as a whole and of individual acoustic intervals on the downthrown (south) side of the fault, indicating that the Wecoma fault has been active for most of the depositional history of the Astoria Fan. On line 45 (Fig. 3.9), the same units thin across the pressure ridge, indicating that vertical development of the ridge occurred during the same time interval. Thickness trends in units lower in the section on both lines are unaffected by the presence of the fault, indicating that they predate the Wecoma fault. Alternatively, Appelgate and others (1992) have interpreted apparent stratigraphic pinchouts against the pressure ridge as suggesting an early history for the basement upwarp, inferring that ridge formation occurred shortly after the formation of the crust at the spreading ridge (see unit 4 on Fig. 3.9). However, the morphology of the basement upwarp as determined from magnetic modeling and MCS profiles matches that of the folded sedimentary section, indicating that folding occurred following deposition of most of the sedimentary section. Additionally, the pinchout of unit 4 only is observed on some reflection profiles of the upwarp, whereas on others is clearly an artifact. We therefore now interpret this apparent pinchout as a side echo of the upwarped basement superimposed on unit 4. Oregon State University MCS line 30 and U.S. Geological Survey line 77-12, neither of which cross the upwarp, show this superimposed side echo clearly (see Fig. 3.3 for location of these lines).

On close inspection, the division between prefaulting units and synfaulting units (reflector S, Figs. 3.8*B* and 3.9) can be identified at a depth of 4.30 seconds on line 37 (Fig. 3.8*B*; abyssal plain, upthrown side), and 3.82 seconds on line 45 (Fig. 3.9; top of the pressure ridge). Reflector S was identified by examining the thickness of each stratigraphic subunit on these two lines and picking the reflector that separated units showing fault-related thickness trends from those that did not. Units 2 and 3 show just the reverse thickness relationship, with thinner units on the downthrown side of the fault

(Fig. 3.8*B*). This relationship is maintained along the length of the fault, suggesting that the fault was not active in a vertical sense during unit 2 and 3 deposition or that the sense of vertical motion was south block up. Because reflectors consistently show a south-block-down separation, we can attribute these thickness changes across the fault to left-lateral strike-slip displacement of the eastward thickening wedges of sediment (that is, left slip moves thinner wedges of sediment eastward on the south side of the fault relative to the north side). Note that not all reflectors need show any vertical separation on seismic profiles of strike slip faults, and in fact some on Figure 3.9 do not, even though other evidence discussed below demonstrates 5-6 km of net slip on the fault. Growth of the pressure-ridge anticline appears to have been coeval with slip on the Wecoma fault, as the seismic reflectors in both lines 37 and 45 (reflector S) that separate prefaulting and synfaulting sediments can be correlated over the intervening distance on MCS line 32. The high quality of the data allows correlation over tens of kilometers with a high degree of confidence.

In order to establish the time at which fault motion began, we have correlated a prominent seismic reflector at the base of the Astoria Fan with the same interval drilled at DSDP site 174A, 70 km southwest of the pressure ridge (Figs. 3.1 and 3.11). Fortuitously, during the initial survey for site 174, a seismic-reflection profile was made that connects the drill site to the pressure-ridge anticline (Kulm and others, 1973a, Fig. 3.2, line A-C). This profile allows a direct tie between the anticline and the drill site. The change in reflection character above this reflector (Fig. 3.8*B*, base of unit 1) can also be traced from the pressure ridge to the drill site. At the drill site, the profound lithologic change between the sand turbidites of the fan and the silt turbidites of the abyssal plain sequence was observed at the depth of this reflector in the cores (Fig. 3.11). Matching reflectors with their respective lithologic changes in the cores also allows accurate calculation of seismic interval velocities at the drill site.

Ingle (1973) plotted the coiling directions of the planktonic foraminifer *Globigerina pachyderma* in the cores from site 174A (Fig. 3.12). Notable are three dextral coiling events at depths below the surface of 0-40 m, 125-135 m, and 238-295 m. The earliest of these three events brackets the depth at which the base of the Astoria Fan section was found in the hole (284 m). Ingle (J. C.

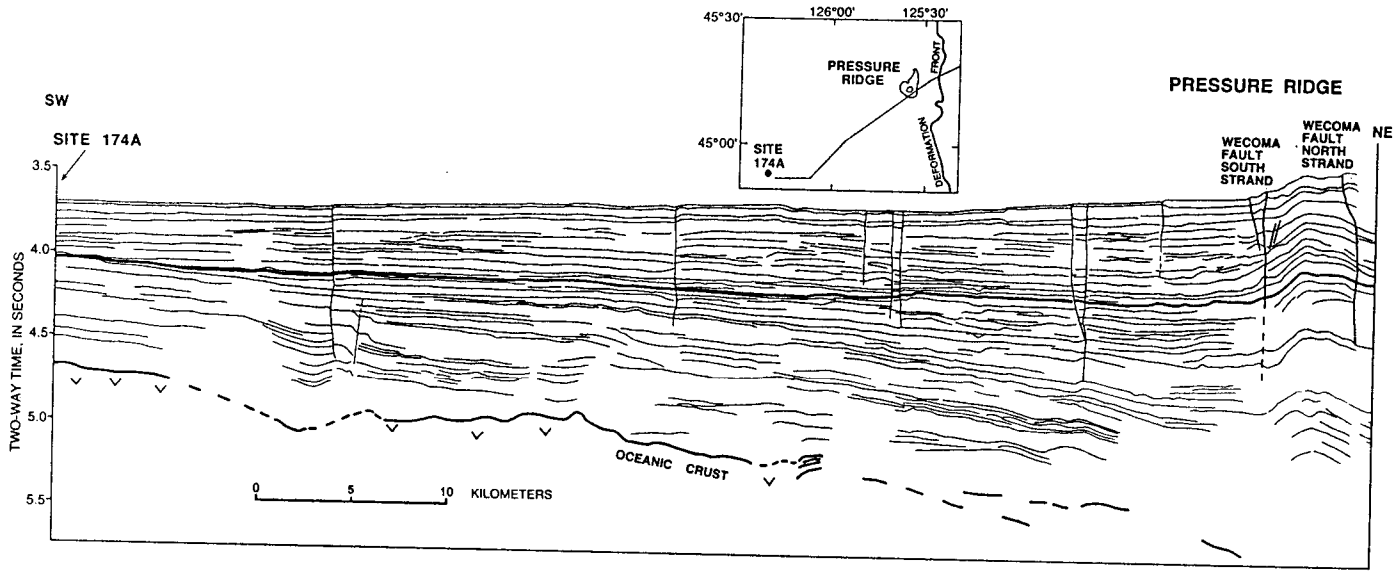

Figure 3.11. Line drawing of a single-channel reflection profile (Oregon State University cruise YALOC 70, Leg 5) linking Deep Sea Drilling Project drill site 174A to the pressure ridge anticline and the Wecoma fault, off the Oregon coast. Upper heavy line marks the base of the Astoria submarine fan at DSDP site 174. Lower heavy line with v symbols is the top of the basaltic crust. This horizon is dated by micropaleontologic techniques at 760 ± 50 ka. Inset: Trackline map showing location of the seismic profile linking the drill site with the pressure ridge.

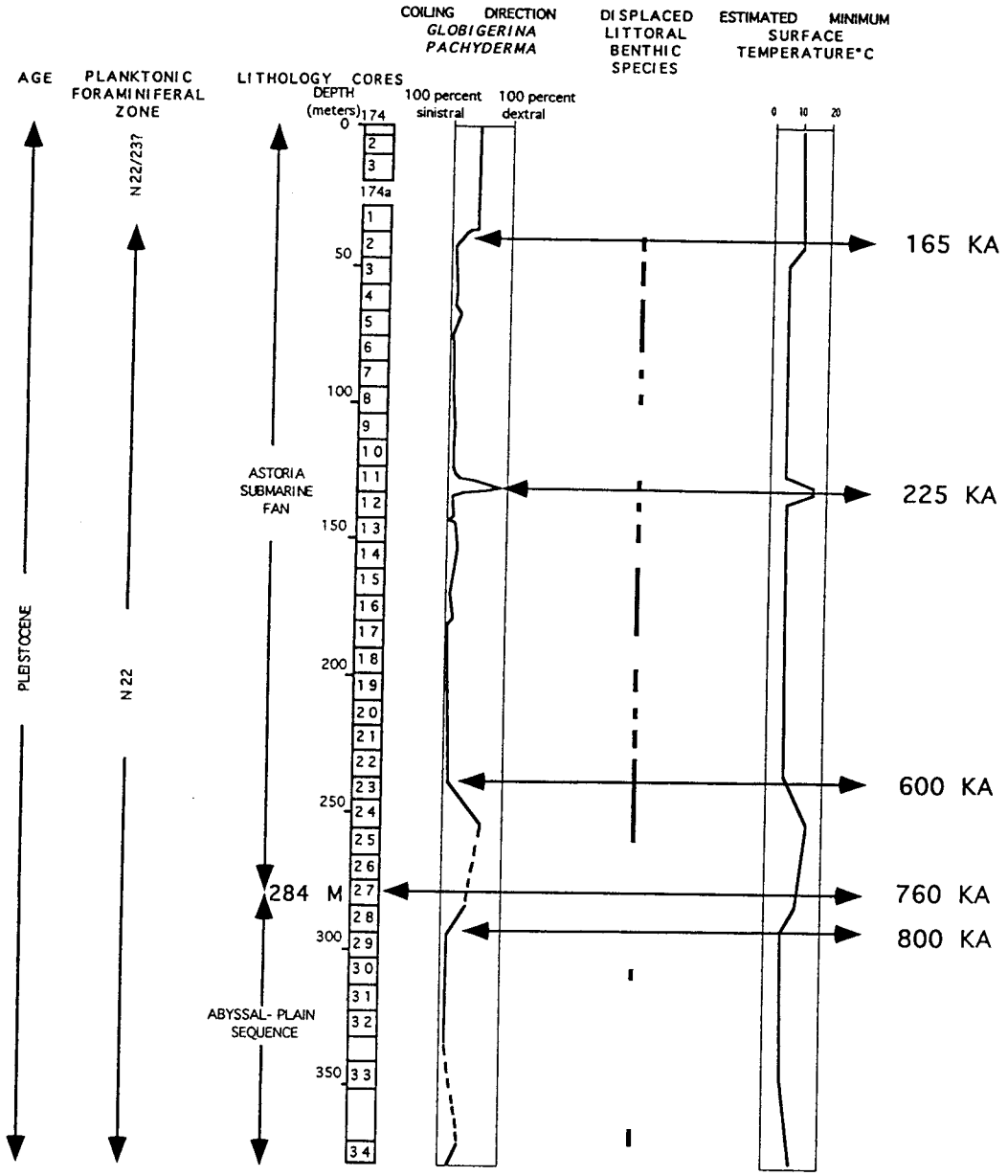

Figure 3.12. Lithology and coiling directions of *Globigerina pachyderma* in cores from Deep Sea Drilling Project site 174A. Lowermost dextral coiling event is dated by tephrochronology. Plot is dashed where inferred. Modified from Ingle (1973, Fig. 3.4).

Ingle, Stanford University, written comm., 1991) has related these dextral coiling events to regional northeast Pacific paleooceanographic events, which are dated with magnetostratigraphy and tephrochronology. By this method the upper and lower bounds of the lowest coiling event are dated as 600 ka and 800 ka, respectively (Fig. 3.12). Interpolating from these bracketing ages with sedimentation rates, the age of the base of the Astoria Fan section at site 174A is 760 ± 50 ka, with the margin of error reflecting uncertainties in using uniform sedimentation rates and in the precision of determining the age of the coiling events.

To estimate the age of this same reflector near the Wecoma fault, we infer that there is no significant time transgression between site 174A and the pressure ridge. We make this inference because no significant onlap or offlap relationships were observed within several hundred vertical meters of the base of the fan (Fig. 3.11); the reflector is nearly horizontal, and the trend of the seismic section is about perpendicular to the sediment transport direction. Using an average sedimentation rate of 110 cm/1000 years (centimeters per 1,000 years) calculated from the age, thickness, and seismic velocity of the fan section at the Wecoma fault, the age of reflector S, and thus the age of vertical motion on the Wecoma fault, is estimated to be 600 ± 50 ka. Although additional uncertainties exist in sedimentation rates, age correlation of the base of the fan, and seismic velocities, we use the same margin of error here because we are unable to quantify them independently.

Fault Restoration

We have taken advantage of the geometry of the abyssal-plain units in order to calculate the net slip on the Wecoma fault. Prefaulting sedimentary units strike mostly north-south and thicken uniformly eastward, resulting in eastward thickening sedimentary wedges. Slip on the Wecoma fault has cut and juxtaposed these wedges so that thickness changes across the fault are pronounced. On MCS line 37, units 2 and 3 (Fig. 3.8*B*) are thinner on the south (downthrown) side. We attribute this abrupt thinning across the fault to be the result of left-lateral translation of the eastward-thickening wedges making up these two units (we assume negligible differential loading of these units due to thickness changes in unit 1). In order to estimate the horizontal separation along the Wecoma fault, we have restored the abyssal-plain

section by reversing the left-lateral motion on the fault (Fig. 3.13). The blocks were translated right-laterally until the eastward-thickening wedges of sediment matched. Using this method, the thickness match across the fault was made simultaneously with 18 individual reflectors within units 2 and 3, reducing the error inherent in picking only a few reflectors. The horizontal motion needed to restore the section is 5.5 ± 0.8 km.

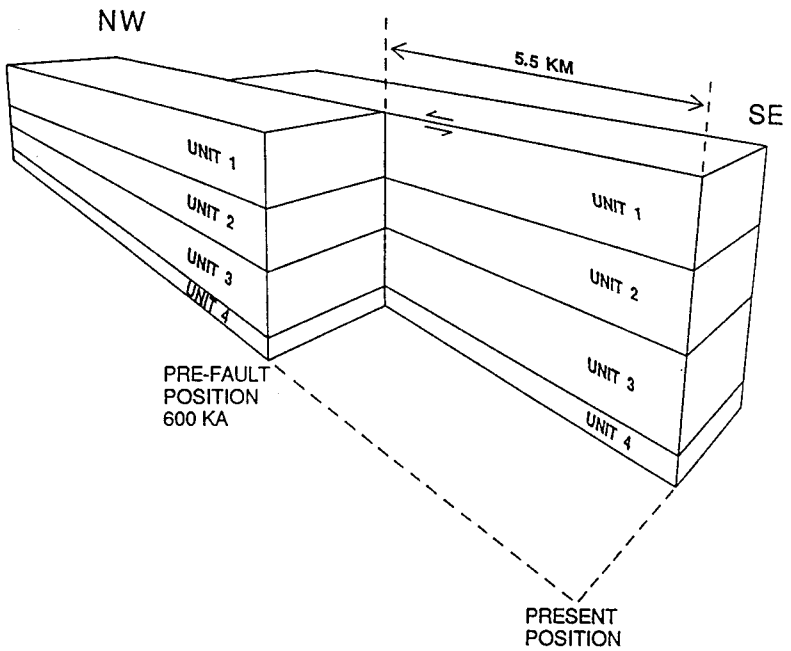

Figure 3.13. Cartoon illustrating the method used in retrodeformation of the Wecoma fault, off the Oregon coast. Fault motion was reversed graphically by moving seismic time sections on both sides of the fault until eastward-thickening sediment wedges of units 2 and 3 matched across the fault, resulting in a horizontal separation of the units of 5.5 ± 0.8 km.

We also plotted isopachs of units 2 and 3 as an alternative method for determining horizontal separation. Figure 3.14 is a pseudo-isopach plot (contours in two way travel time) of unit 2, following smoothing of the data and removal of a velocity artifact from the pressure ridge area. The pseudo-isopach plot reveals a pattern of left offsets of individual contours, decreasing northwestward to zero at the fault tip 17-20 km seaward of the deformation front. The offset of the contours near the deformation front is 3.7 ± 0.5 km, determined by averaging the three easternmost contours. We attribute this somewhat different result to poor constraint on the contours south of the fault and on disruption of thickness trends near the adjacent pop-up. Additionally, the isopach offset depends on only 3 piercing points, whereas the retrodeformation uses 18. We thus infer that the retrodeformation method is the best method of estimating horizontal separation, and we use the value 5.5 ± 0.8 km in the slip-rate calculations below. Neglecting the 100 m of vertical separation, this value represents the net slip on the Wecoma fault near the deformation front.

A potential source of error in the use of time versus thickness is the possibility of lateral velocity changes in the selected units. However, lateral velocity changes, if present, are most likely to be oriented normal to the deformation front and thus have negligible effect on restoration of the sedimentary section. Unfortunately, the youngest unit (1), (Fig. 3.8*B*) cannot be used for an independent estimate of net slip during deposition of the youngest part of the fan section because vertical movement on the Wecoma fault has influenced thickness of this unit.

Using the previously calculated age of the fault and the net-slip estimate above, we calculated that the average slip rate of the Wecoma fault since its inception 600 ± 50 thousand years ago has been 7-10 mm/year near the present deformation front. These rates depend on the estimated age of the fault, which may include a margin of error that is too small, as discussed above. Thus the calculated slip rate may have a larger error bar than calculated here.

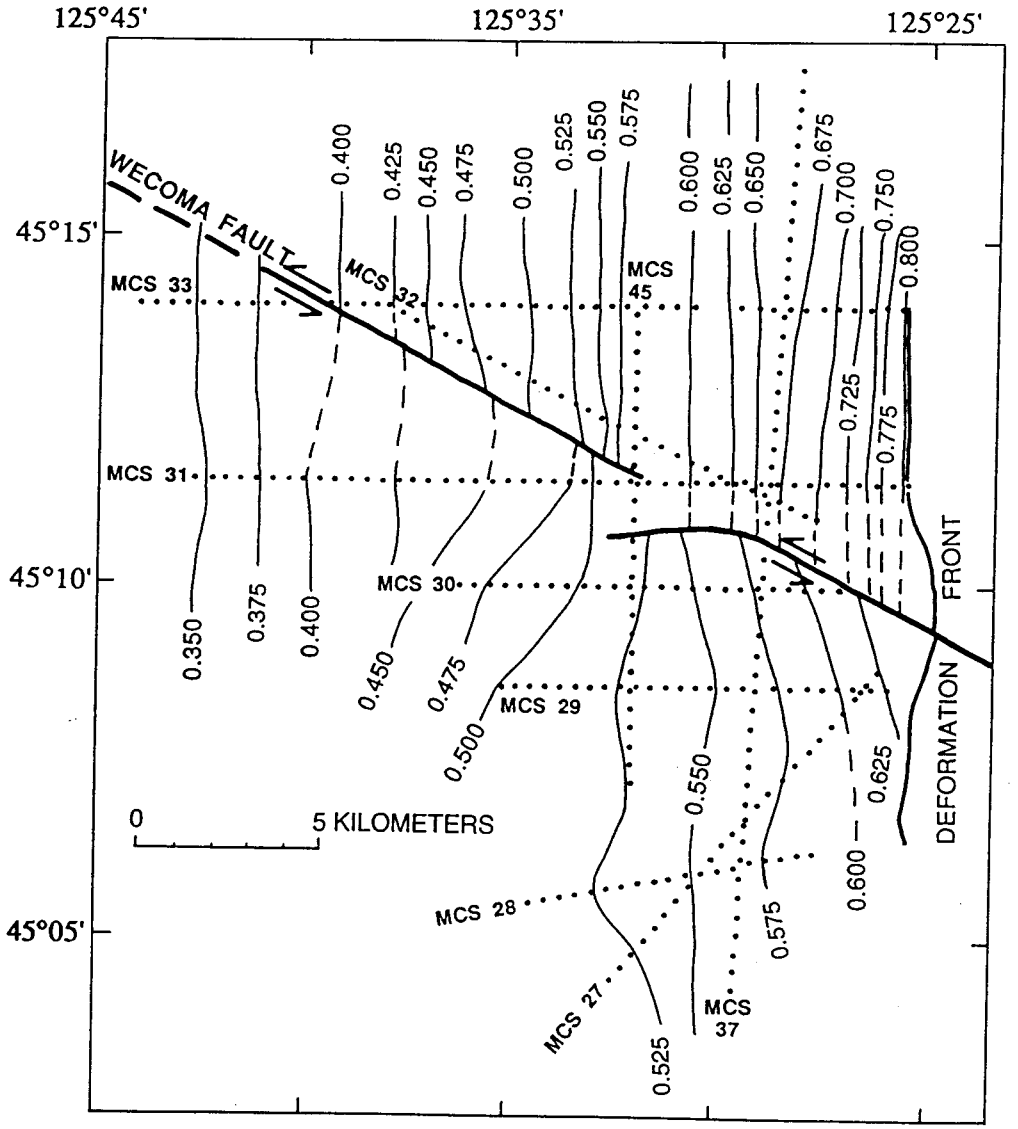

Figure 3.14. Pseudo-isopach plot of abyssal-plain unit 2. Contours are in two way time, rather than thickness; see Figure 3.8 for unit designations. Note westward-decreasing left offset of unit 2 by the Wecoma fault (barbs show direction of movement). Average offset of 0.625, 0.600, and 0.575 contours is about 4 km. Contours dashed where inferred. Solid dots are control points along MCS profiles. Line numbers correspond to the tracklines shown in Figure 3.3.

Late Pleistocene-Holocene Slip Rate

SeaMARC 1A sidescan imagery shows that the Wecoma fault offsets left laterally a late Pleistocene distributary channel and an older slump scar on the Astoria submarine fan (OC and OS, Fig. 3.6; offset channel, Fig. 3.15). Horizontal separations are about 120 ± 5 m and 350 ± 10 m, respectively (Appelgate and others, 1992; this study). These crosscutting relations can be used to obtain an independent estimate of the slip rate during latest Pleistocene and Holocene time. The offset channel, in particular, offers the best opportunity for estimating the Holocene slip rate. The channel is blocked 18 km upstream (to the north) by slump debris from a 32-km^3 (cubic kilometer) slope failure (Fig. 3.4; Fig. 3.5, labeled SD). The slump is apparently a bedding-plane slide from the western flank of the leading landward-vergent accretionary thrust ridge. We estimate the age of this slump to be 10-24 ka, based on a ^{14}C date from a gravity core taken from a sediment drape on top of one of the slump blocks and on onlapping relations observed on a high-resolution seismic record. In the reflection profile, the slump debris rests directly on the sea-floor reflector with no visible sediment onlap or ponding around the slump blocks. Using a composite late Pleistocene-Holocene sedimentation rate derived from Nelson (1968) and this study, we estimated that sediment accumulation following the slump could not continue for more than about 24,000 years without depositing a thick-enough unit to be detectable on the MCS profile, thus setting a maximum age for the slump. We derived the minimum age for the slump from the ^{14}C age of sediment at the bottom of the above-mentioned core. The core sampled only postslump hemipelagic sediment, and thus the 10,300 radio carbon years before present (R.C.Y.B.P.) date from the lowermost part of the core sets the minimum age of the slump at about 10 ka.

Because the fault is older than either the slump or the channel, a slip rate can be estimated from the channel offset shown in Figure 3.15. The channel wall must have been cut prior to blockage of the channel by the slump, establishing the minimum age at about 10 ka (that is, the minimum age of the slump). Similarly, a maximum age for the channel wall is constrained to be the same as the maximum age of the slump. Channel cutting should have ceased or been greatly reduced following the blockage; thus younger fault

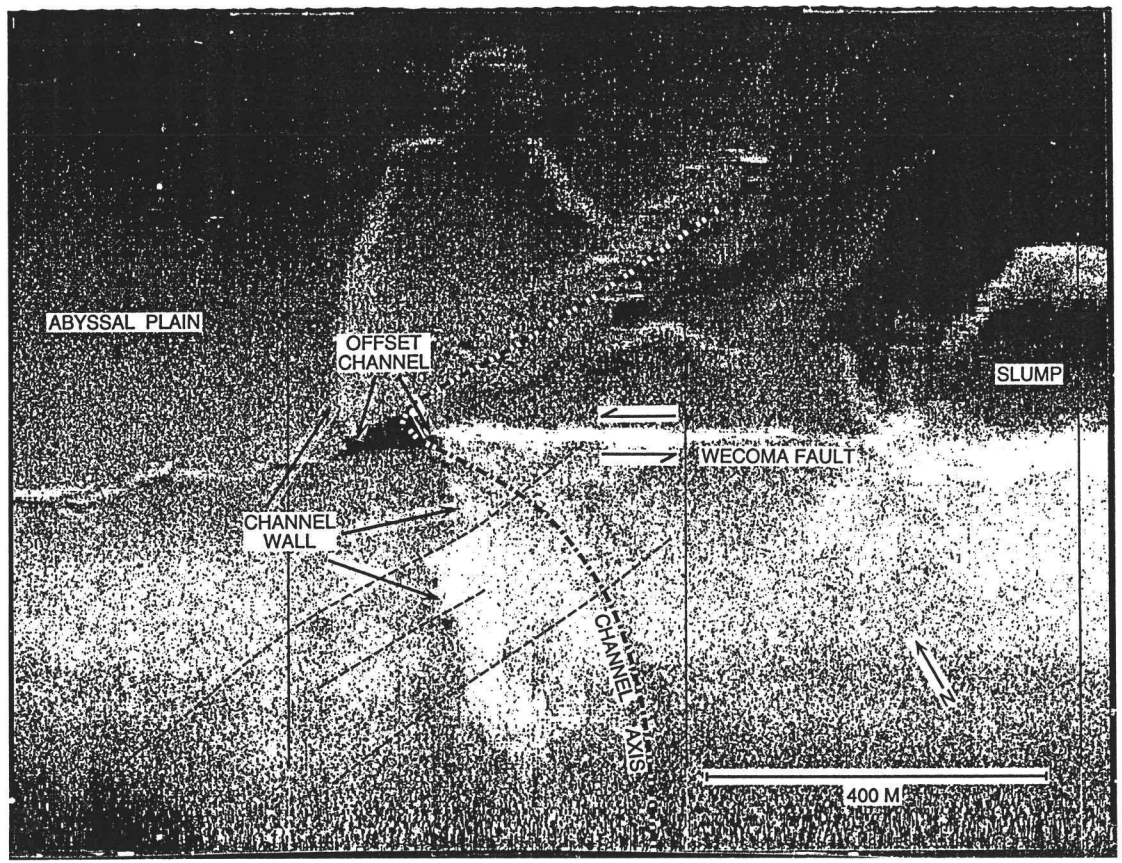

Figure 3.15. High-resolution SeaMARC 1A sidescan image of the Wecoma fault offsetting the west bank of a late Pleistocene distributary channel on the southeastern Astoria submarine fan. Horizontal separation is 120±10 m. Light tones represent high backscatter; insonification (direction of sonar illumination) is from the south. Vertical scarps (highest backscatter at right-center of image) are the result of strike-slip juxtaposition of irregular sea floor topography. Fault strike is 293°. Minor faults (dashed lines) that also offset the channel wall are interpreted as part of the surface expression of the flower structure shown in Figure 3.10.

motion would offset the channel wall, as presently observed, without modification by erosion. If channel cutting and fault motion were simultaneous, the high frequency of late Pleistocene turbidity currents carrying large quantities of sand and gravel (Duncan 1968; Nelson, 1968; Griggs and others, 1970) should have eroded the offset to something other than the crisp separation seen in sidescan images (Fig. 3.15). Seismic-reflection records showing the truncation of deep sea channel walls (Griggs and Kulm, 1973) and numerous sediment hiatuses in cores from the axial part of these channels (Griggs and Kulm, 1970) document the erosive character of the coarse-grained late Pleistocene turbidity currents in this region. Therefore, the age of the channel wall is probably 10-24 ka, consistent with incision during the last episode of high turbidity-current activity during the latest Pleistocene low stand of sea level. Using this age range, we calculated a latest Pleistocene-Holocene slip rate of 5 to 12 mm/year. These rates are comparable to the 7 to 10 mm/year average rate calculated from the net horizontal displacement since inception of the fault.

Intersection of the Wecoma Fault and the Accretionary Wedge

The complex structure of the area where the Wecoma fault intersects the initial thrust ridge indicates that this fault is not simply overridden by the accretionary prism. High-resolution SeaMARC 1A sidescan records of the intersection zone on the abyssal plain show that this area is dominated by a nested series of uplifted asymmetrical triangular plateaus, called pop-ups, bounded by reverse faults (Figs. 3.6, 3.7, and 3.16). The single trace of the Wecoma fault separates into several diverging splays at the western tip of the largest of the pop-ups (A, Figs. 3.6, 3.16, and 3.17), and the largest of these splays is the southern bounding fault of the pop-up. Sidescan and MCS records suggest that the main trace is buried by slump debris along much of its length in this area (Appelgate and others, 1992). The pop-up plateaus appear to be the result of a complex interaction between the strike-slip fault and the evolving deformation front. The model we prefer to explain their development is shown in Figure 3.17. The plateaus were uplifted between divergent splays of the main strike-slip fault and possibly were driven

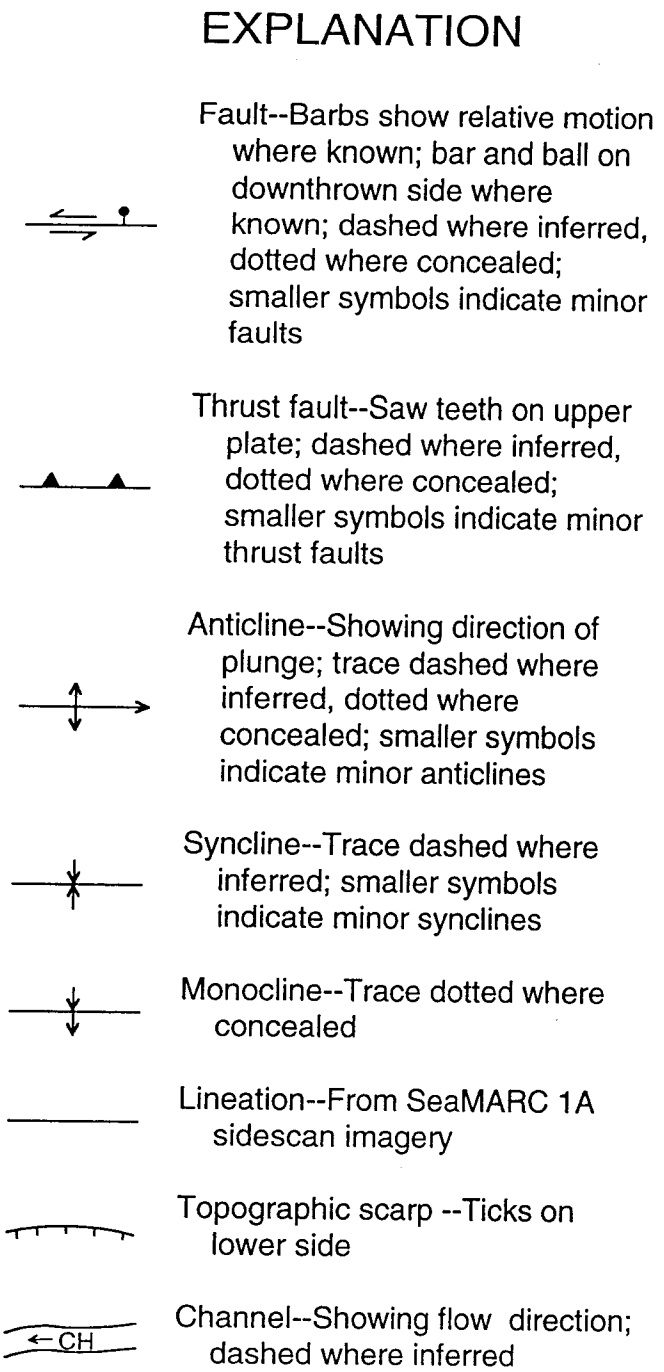

Figure 3.16. Structural interpretation of the intersection zone and pop-up structure at the intersection of the Wecoma fault and the deformation front. OS, offset scarp; PR, pressure ridge; OC, offset channel; PU, pop-up; A, apex of pop-up, corresponds to point A in Figure 3.17.

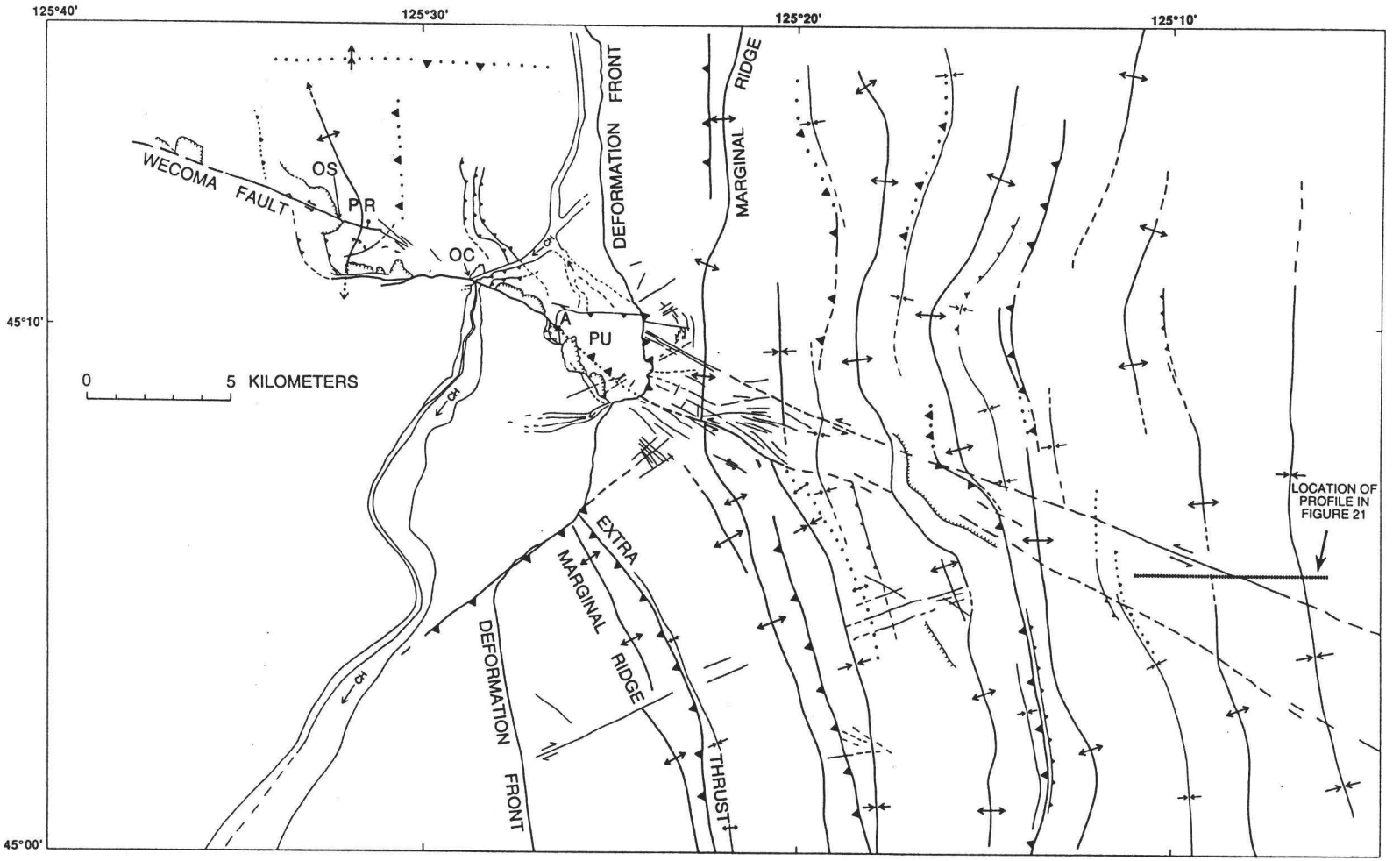

Figure 3.16, Continued.

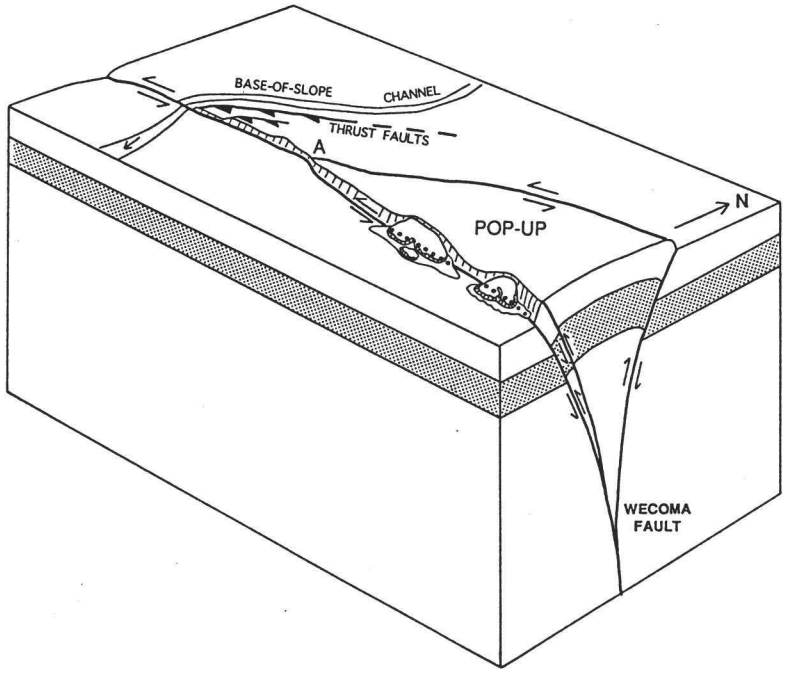

Figure 3.17. Block diagram illustrating structure of the pop-up at the intersection of the Wecoma fault and the deformation front. Blocks within the flower structure of the Wecoma fault are forced upward and westward by increasing horizontal compression as subduction progresses. Point A corresponds to point A on Figure 3.6. Modified from Sylvester (1988, Fig. 3.21*C*). Arrow in channel show flow direction. Barbs show relative motion on faults. Sawteeth on upper plates of thrust faults; faults dashed where inferred, dotted where concealed.

westward by horizontal compression because of their proximity to the plate boundary. Appelgate and others (1992) suggested that the high vertical scarps between the offset channel and the western tip of the pop-up (Fig. 3.6) are the result of 2.5 km of left-lateral displacement of a part of the pop-up.

INFLUENCE OF THE WECOMA FAULT ON THE ACCRETIONARY WEDGE

The eastern end of the above-described pop-up directly abuts the western flank of the first accretionary ridge of the North America plate (MR, Fig.

3.6). On the west side of the initial thrust ridge, the plate boundary forms an embayment corresponding to the width of the adjacent pop-up on the abyssal plain (Appelgate and others, 1992). A seaward-vergent thrust segment occupies the area of the embayment in an overall landward-vergent thrust setting described by MacKay and others (1992). This configuration suggests that a local reversal of vergence in the leading accretionary ridge may be related to the effects of the strike-slip fault subducting beneath the wedge. The mechanism for this vergence reversal may be a local reduction in pore fluid pressure due to fluid venting by the Wecoma fault. Such a pressure loss would increase the basal shear stress along the decollement, promoting development of the seaward-vergent segment (Tobin and others, 1993). The ridge formed less than about 300,000 years ago, based upon microfossil evidence from rocks dredged from the ridge (Carson, 1977). The embayment is bounded by linear gullies that cut upslope into the initial thrust ridge, and other such gullies lie within the embayment (Fig. 3.6). We interpret these linear gullies as fault splays related to slip on the Wecoma fault. Observations and samples from the submersible ALVIN confirm that the linear gullies visible in sidescan records are zones of active oblique faulting. Several dives (Fig. 3.18) showed that bedding is extensively sheared, with multidirectional slickensided surfaces and mullions. Shear planes striking west-northwest, roughly parallel to the Wecoma fault, were observed in these gullies. Linear west-northwest-trending scarps along the strike of the Wecoma fault are also present on the eastern flank of the initial thrust ridge, the crest of which has a small left-lateral offset (Fig. 3.19). These lineations follow the Wecoma fault trend and are interpreted as fault scarps because (1) they lack the dendritic drainage pattern commonly observed in nearby erosional gullies, (2) they strike at an angle to the bathymetric contours, and (3) because they originate at the highest point on the marginal ridge. MCS line 29 crosses the area of these scarps and shows a strong vertical disruption of the marginal ridge that we interpret as the cause of the sea-floor scarps.

Rocks collected with the ALVIN submersible from the gully sites on the seaward flank of the marginal ridge consist of sheared siltstone, sandstone and pebble-to-cobble conglomerate (Sample and others, 1993; Tobin and others, 1993) that probably originated on the Astoria Fan and were re-

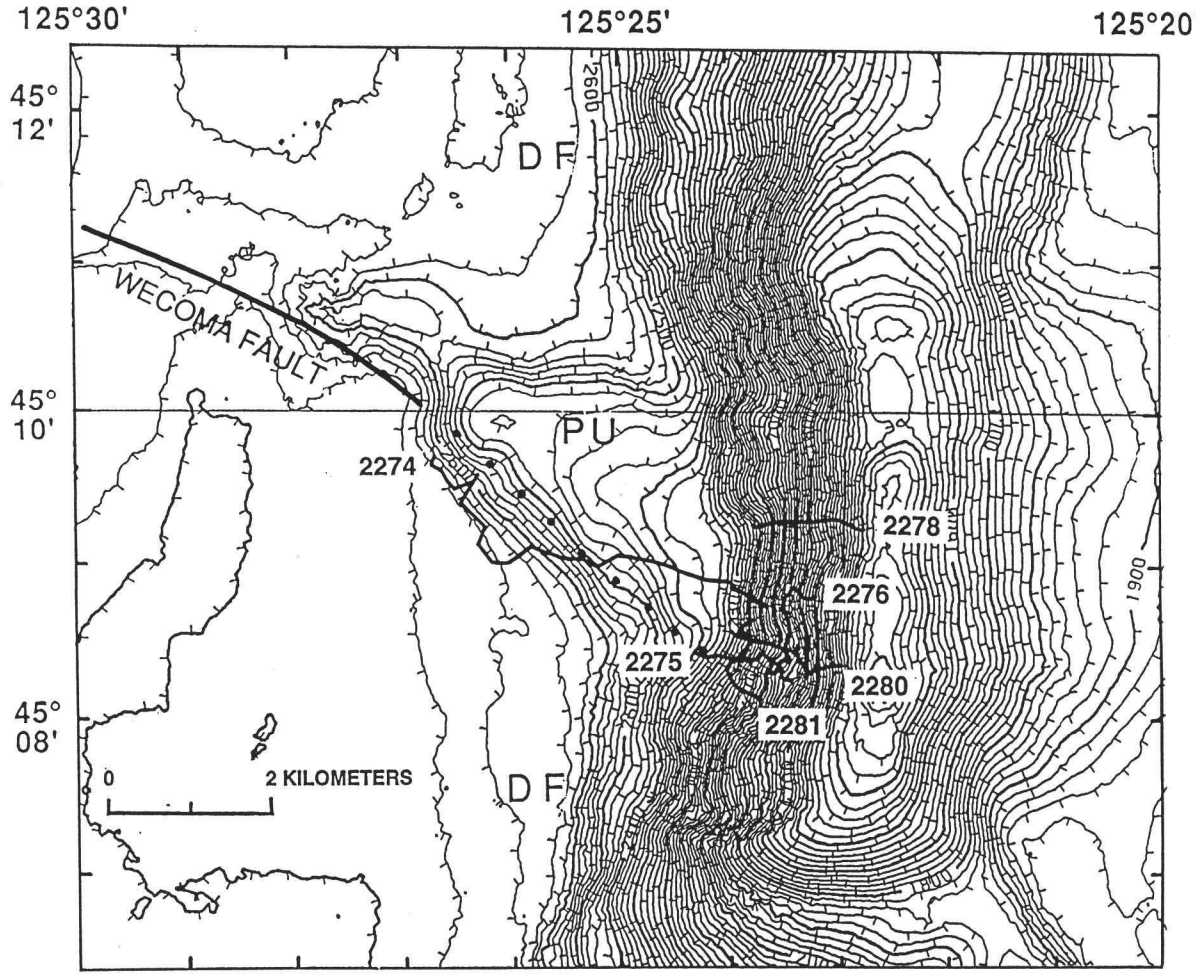

Figure 3.18. Bathymetry and ALVIN submersible tracklines near the intersection of the Wecoma fault and the deformation front. Several dives focused on the gullies visible on the SeaBeam bathymetry and SeaMARC 1A sidescan images (see also Fig. 3.6). PU, pop-up; DF, deformation front. Contour interval 20 m. Ticks face downslope. Tracklines show dive numbers. Wecoma fault dotted where concealed.

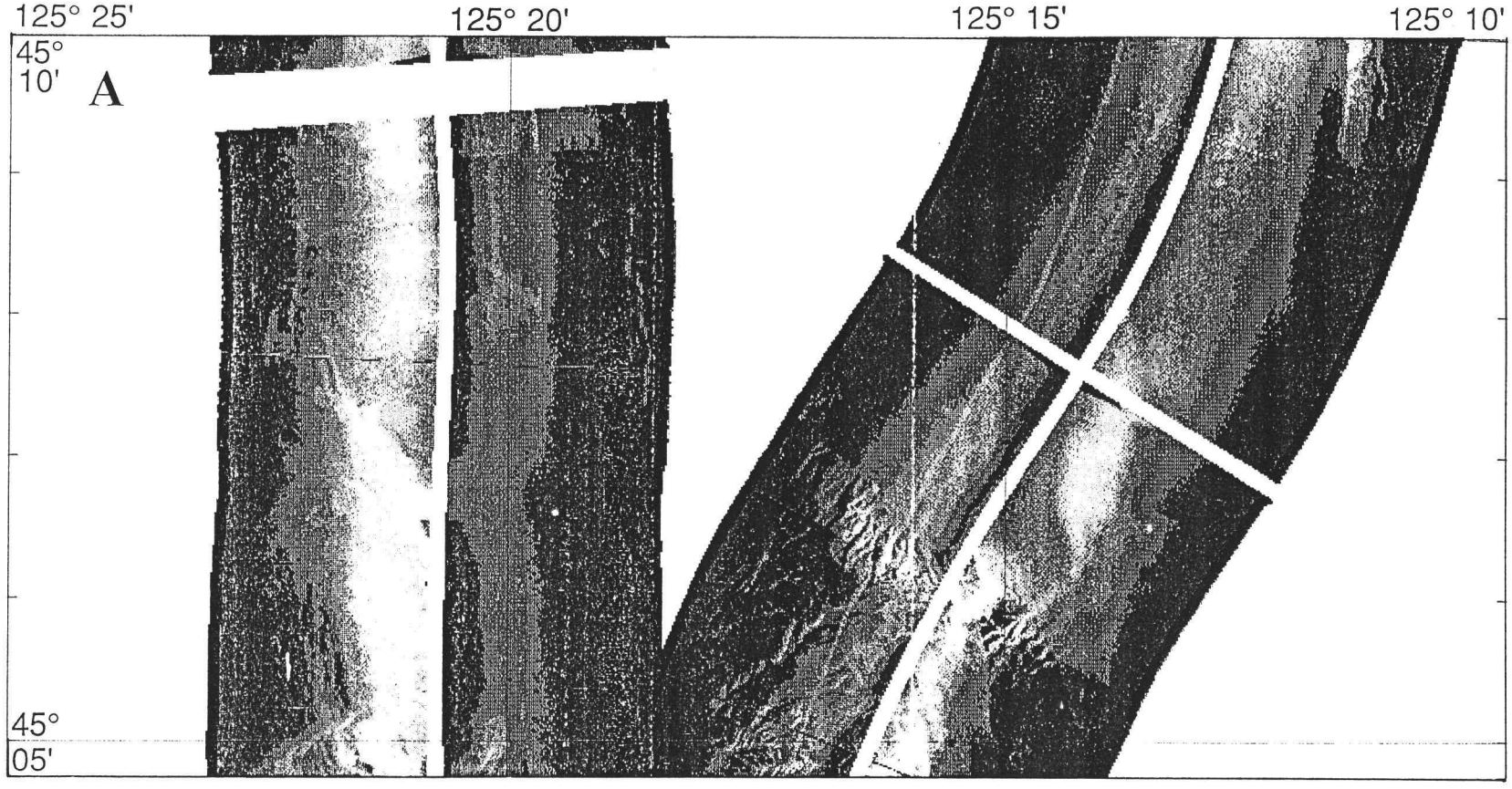

Figure 3.19. SeaMARC 1A sidescan image of the Wecoma fault crossing the accretionary wedge. *A*, Wecoma fault splays cutting the eastern flank of the first accretionary ridge are dimly visible at upper left. At lower right, the linear scarp marking the surface position of the fault is clearly visible.

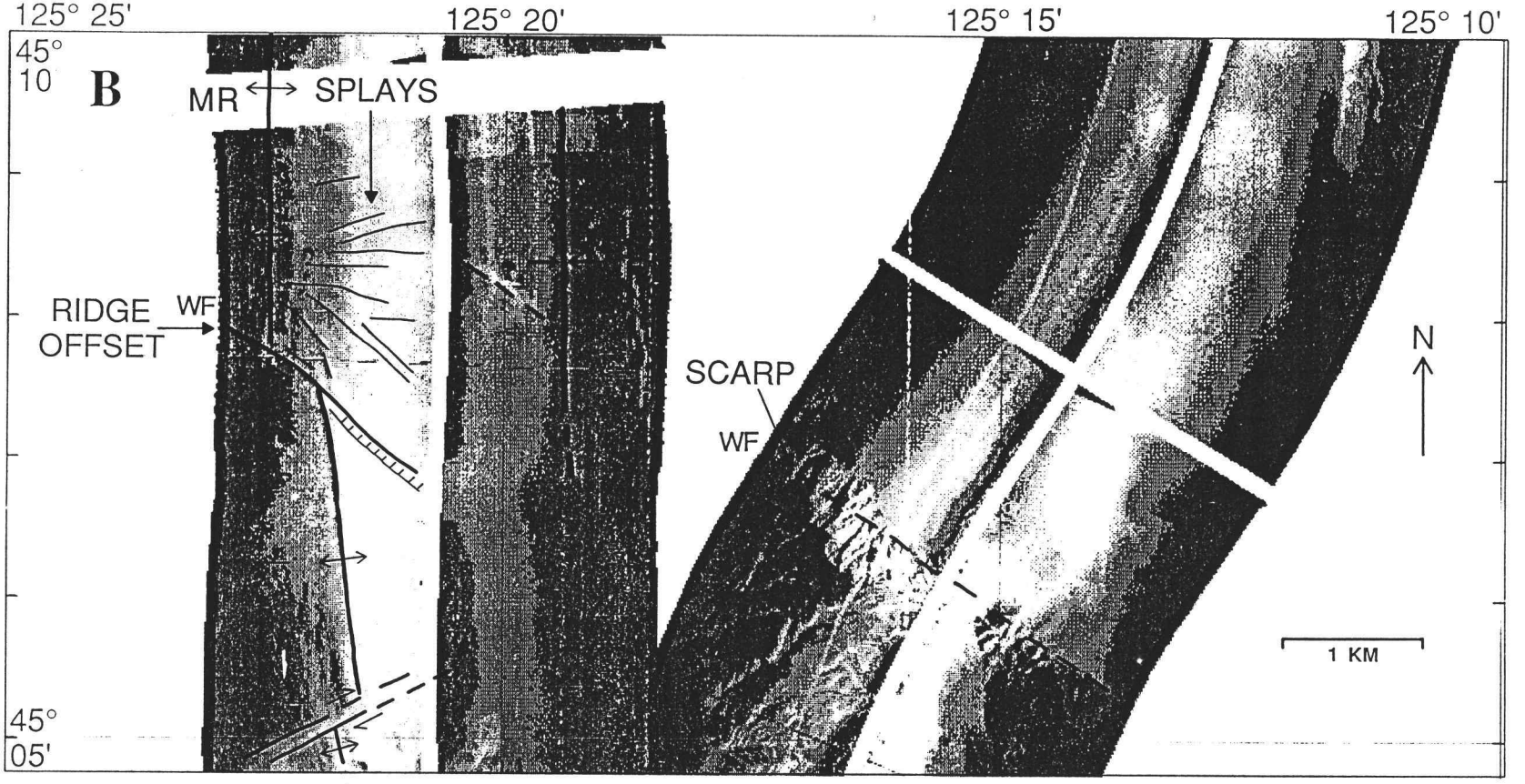

Figure 3.19. *B*, Interpretation showing offset of anticlinal axis (marginal ridge, MR). Smaller offset by a right-lateral fault shown at lower left. See Figure 3.23 for location of image. WF, Wecoma fault, dashed where inferred; Line with hachures, fault scarp; SPLAYS, minor splays of the Wecoma fault.

cemented with a secondary carbonate cement (Kulm and Suess, 1990). The carbonate cement, derived from fluids venting from the shear zones, bonds the sheared sedimentary fragments into an angular breccia that fills the bottoms of the gullies. Isotopic analyses of these pore-fluid-derived carbonate cements show that cements in the fault zone differ significantly from those elsewhere in the young accretionary wedge. Fault-zone cements from the Wecoma fault have $\delta^{18}O$ values ranging from -4.27 to -12.66‰ (permil) standard mean ocean water (SMOW) and $\delta^{13}C$ values of -1.12 to -25.01‰ Peedee Belemnite (PDB). Cements from an accretionary-wedge thrust fault on the second thrust ridge 38 km to the south have $\delta^{18}O$ values of +4.37 to +6.70‰ and $\delta^{13}C$ values of -38.47 to -54.23‰. Sample and others (1993) attributed these isotopic ratios within the Wecoma fault zone to (1) higher fluid temperatures near the Wecoma fault, perhaps as high as 100 °C, and (2) a seawater-dominated carbon reservoir derived from deeply buried sediments or oceanic crust. In contrast, isotopic ratios from the site distant from the strike-slip faults are best explained by oxygen ratios dominated by ambient seawater and carbon from an oxidized thermogenic methane source or from biogenic methane and seawater (Sample and others, 1993).

The evidence from fluid chemistry, sidescan images, and seismic profiles indicates that the leading edge of the accretionary wedge is disrupted and offset by the Wecoma fault. We have studied sidescan images, SeaBeam bathymetry, and seismic profiles of the frontal accretionary wedge in order to determine the extent to which these effects can be observed on the continental slope. In high-resolution SeaMARC 1A sidescan images, a steep west-northwest-trending scarp is observed to terminate the bathymetric expression of several thrust ridges 8-15 km landward of the deformation front (Fig. 3.19, labeled "scarp"). This scarp is subparallel to the Wecoma fault and lies along the projected trend of the fault into the accretionary wedge. Using image-enhancement techniques, we observed that, in detail, this scarp is composed of several subparallel west-northwest-trending linear scarps that also parallel the trend of the main scarp and the Wecoma fault. These linear features are clearly fault scarps as they cut across the erosional spurs and gullies of the main escarpment at nearly right angles. The seawardmost synclinal axis of the accretionary wedge lies between the northwest end of this scarp and the fault splays that cut the marginal ridge. Near the center of this

basin is a west-northwest-trending linear feature that also lies on the projection of the Wecoma fault (Fig. 3.19). Eight kilometers southeast of this scarp and 22 km southeast of the deformation front, the projected trend of the Wecoma fault is crossed by U.S. Geological Survey line 77-11 (Figs. 3.3 and 3.20). This reflection record shows a near-vertical fault at the western edge of a bathymetric bench near the projected position of the Wecoma fault. A

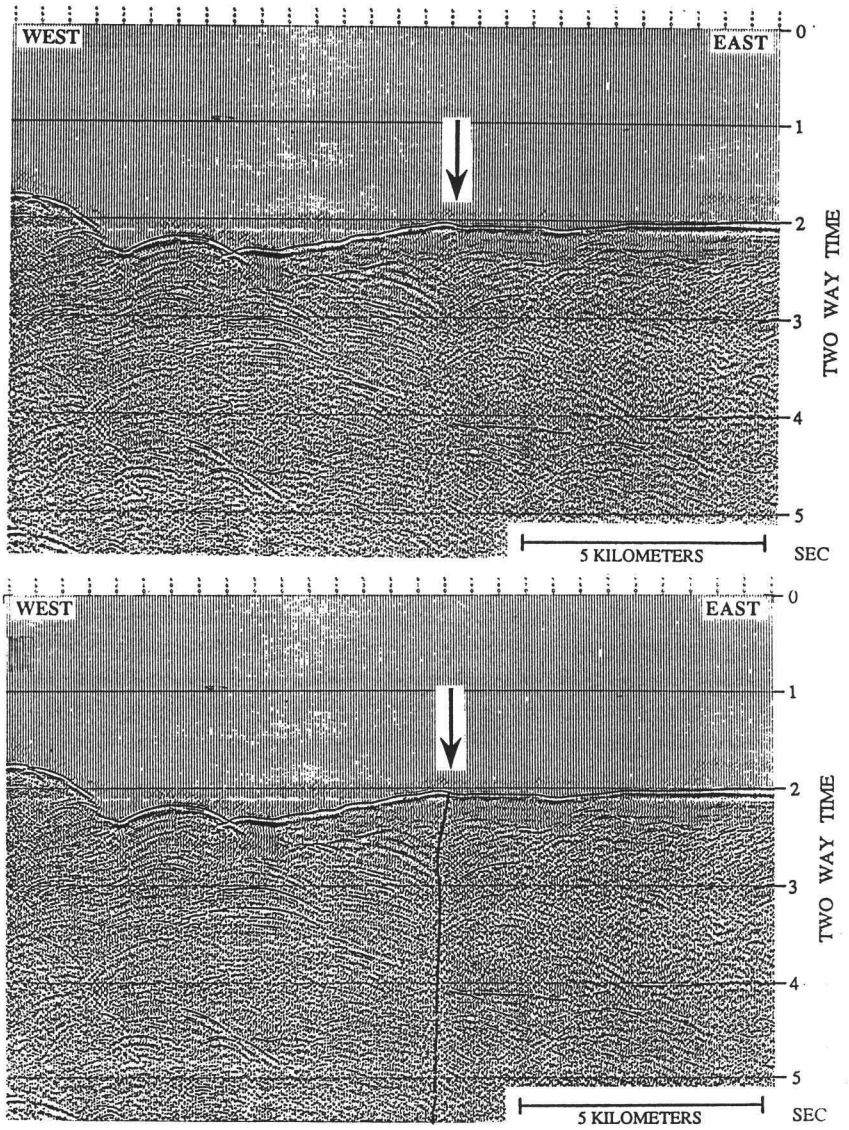

Figure 3.20. Unmigrated 24-channel seismic profile of the Wecoma fault on the lower continental slope, 26 km landward of the deformation front. Arrow shows fault location. *A*, Uninterpreted section. *B*, Interpreted section. Note near-vertical trace, the sharp dip reversals across the fault, and the up-to the-west (north block up) surface expression. Vertical exaggeration = 2.7:1. See Figure 3.22*A* and Figure 3.7 for location. (U.S.G.S. Open-File Report 87-607, Snavely and McClellan (1987), line 77-11).

surficial bump or scarp overlies the fault, which affects the uppermost flat-lying sediments of a broad basin. Reflectors deeper in the section show a sharp dip reversal and loss of coherence. The dip reversal might be resolved as a basin if the line were migrated, but we think it is too abrupt and the radius of curvature of the beds too short for this interpretation. Thus we interpret this feature as a vertical fault, possibly the landward extension of the Wecoma fault.

Having found possible evidence for an upper plate continuation of the Wecoma fault some 10-20 km southeastward into the accretionary wedge, we searched for evidence of termination or continuation of the fault, as well as faults B and C, higher on the continental slope. We used academic, U.S. Geological Survey and U.S. National Oceanic and Atmospheric Administration, and industry seismic-reflection profiles, as well as GLORIA long-range sidescan images and U.S. National Oceanic and Atmospheric Administration SeaBeam high-resolution bathymetry, now available from the abyssal plain landward to about the continental shelf break in northern Oregon.

We observed that several prominent west-northwest-east-southeast bathymetric trends cross the continental slope off central Oregon (Fig. 3.5). These trends are composed of north-northwest- to west-northwest-trending folds and scarps of 5-40 km in length. They appear prominently on the slope because they cross obliquely the north- to northwest-trending grain of the accretionary wedge and because the deformation within these zones is more intense than in the surrounding wedge. In several places the oblique folds are accretionary-wedge folds whose axes have been sigmoidally bent to the northwest, whereas others are fault-bend and fault-propagation folds overlying steeply dipping oblique faults. In map view, SeaBeam bathymetry and GLORIA images show left-stepping sigmoidal bending of fold axes along these trends, left offsets of fold axes, and linear west-northwest-trending scarps (Fig. 3.21). These features were mapped using continuous GLORIA long-range sidescan on the continental slope and continuous SeaBeam bathymetry on the slope and outermost shelf. The deformation of accretionary-wedge structures observed in the perspective SeaBeam mesh plot (Fig. 3.5) and in map view (Fig. 3.21) has a variety of forms, but older structures are systematically disrupted and younger structures developed

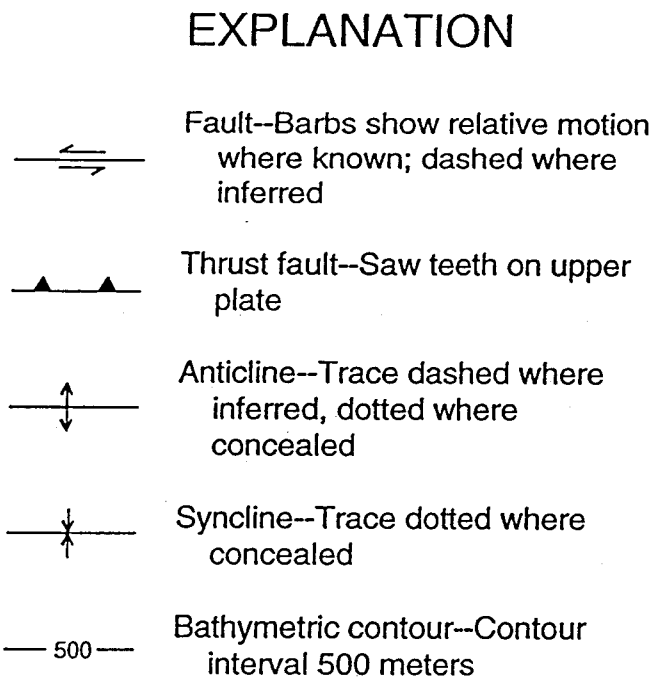

Figure 3.21. Shaded relief plot of SeaBeam bathymetry and structure of a part of the central continental slope crossed by the Wecoma fault. The fault is expressed as a wide zone consisting of several fault strands and intervening fault related folds. The sigmoidal pattern and offset of fold axes indicate left-lateral offset on the Wecoma fault. Location of Shell line 7380 (Fig. 3.22*B*) shown by dotted line, bold segment is the part shown in Figure 3.22*B*. Figure is located at the arrow on Figure 3.5.

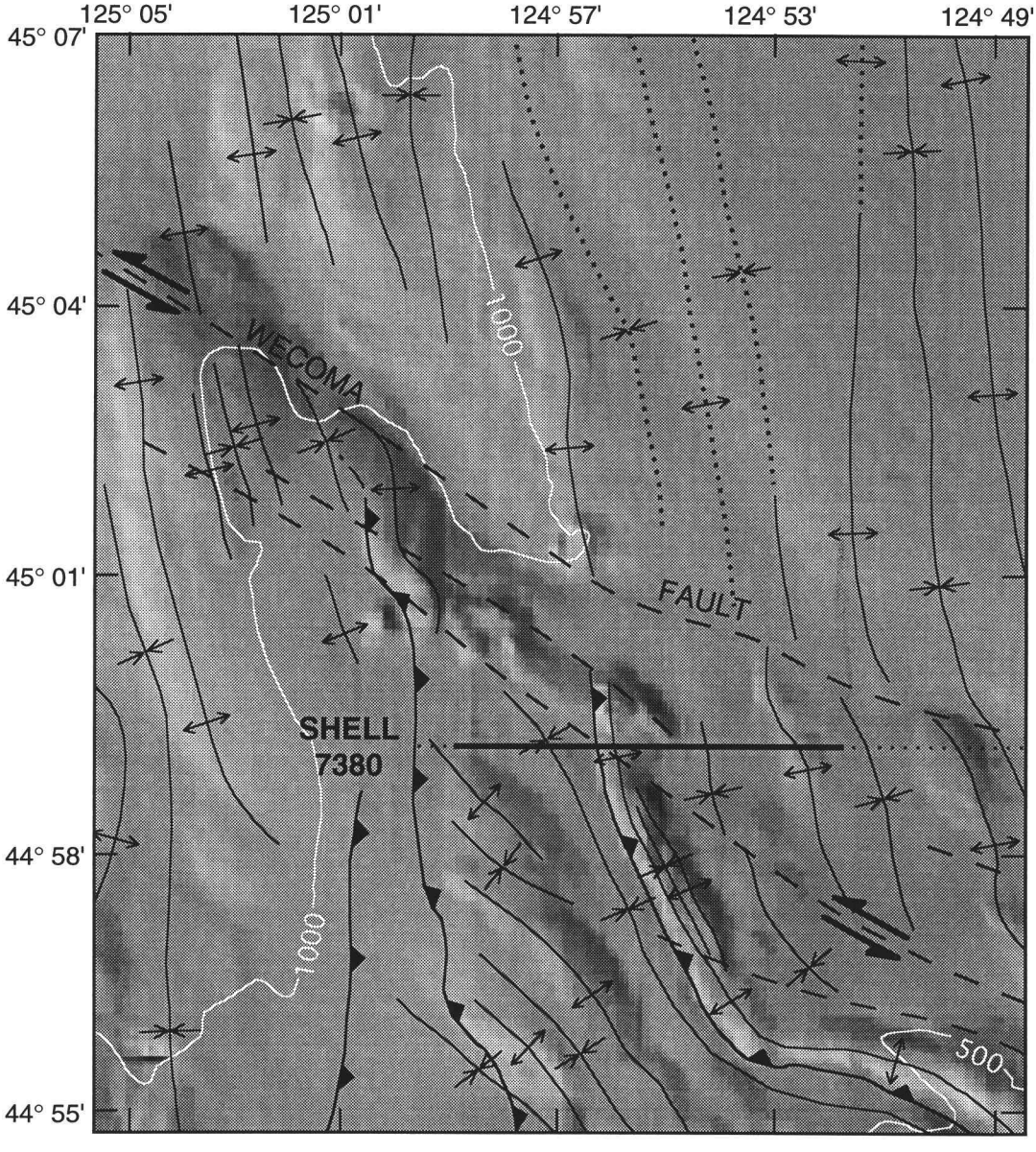

Figure 3.21, Continued.

along these throughgoing zones to the extent that they are well expressed in the bathymetry.

Three of the west-northwest-trending slope deformation zones (WF, B, and C, Fig. 3.5) adjoin the Wecoma fault and faults B and C, respectively, and have similar trends to the abyssal-plain faults. The zones begin on the middle to lowermost slope and continue southeastward to the shelf break, where bathymetric expression dies out (Figs. 3.4 and 3.5). Zone WF on Figure 3.5 extends southeastward from the area where scarps and offsets related to the Wecoma fault were mapped with sidescan imagery (Fig. 3.19). This deformation zone is crossed by several seismic-reflection lines, including four Oregon State University lines, two U.S. Geological Survey lines, and two industry lines in our data set. These profiles clearly show the oblique folds observed on the SeaBeam bathymetry, and most also show that the deformation zone includes several major and many minor high-angle faults. Several profiles reveal that the oblique folds that define the bathymetric deformation zone are fault-bend and fault-propagation folds, both landward and seaward vergent, developed above high-angle faults. Detailed mapping suggests that some of these oblique folds are superimposed on somewhat older northwest-to north-northwest-trending folds. Those that overlie high-angle faults show, by their trends, that the underlying faults also trend northwest to west-northwest. In reflection crossings, the high-angle faults are expressed as a nearly vertical main trace, commonly with attendant flower structures of varying degrees of development (Fig. 3.22 *A-D*). Development of oblique folds and faults decreases or becomes more distributed southeastward (landward) toward the upper slope and outermost shelf within the deformation zone.

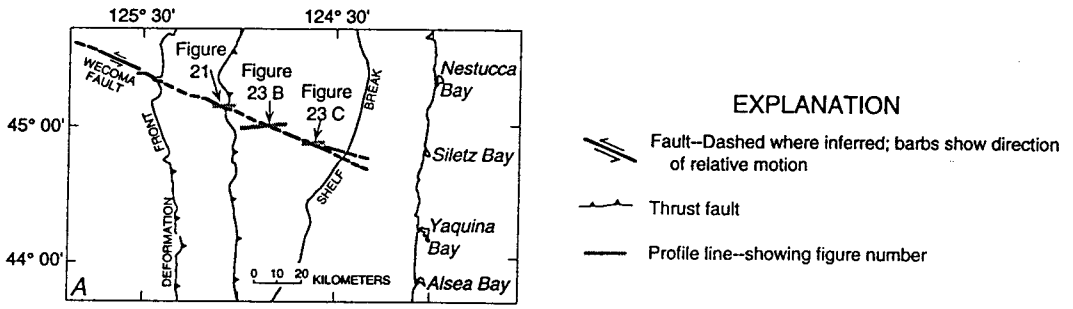

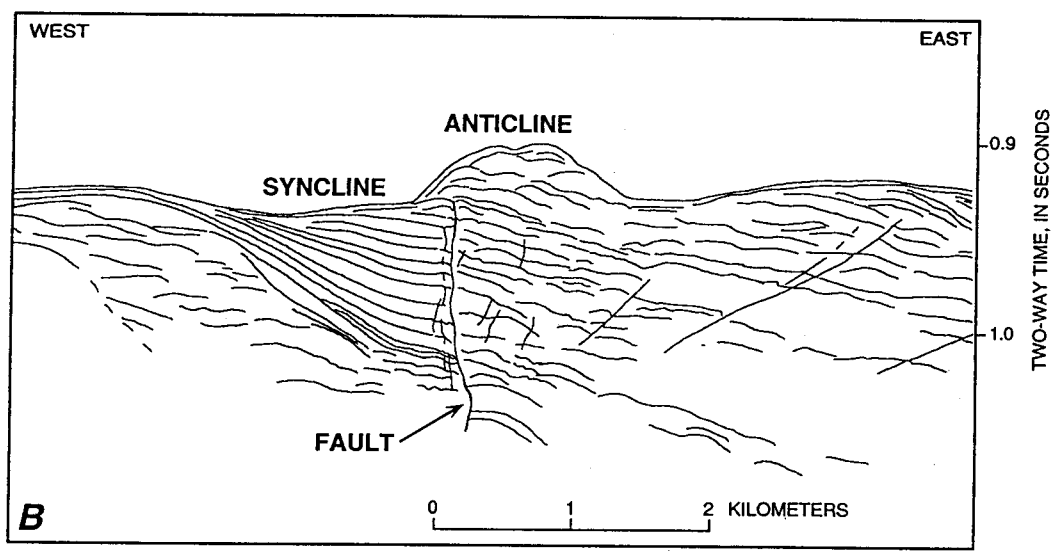

Figure 3.22. Seismic profiles showing the Wecoma fault and deformation zone off the Oregon coast. *A*, Location of seismic profiles shown on Figures 3.20 and 3.22 *B-D*. *B*, Line drawing of part of Shell line 7380. This single-channel sparker record crosses the Wecoma fault and deformation zone and shows a northwest-trending anticline and a truncated syncline separated by a high-angle fault, the central of three mapped strands of the Wecoma fault. Other dipping faults may be minor splays. The anticline is typical of young oblique structures in the deformation zone.

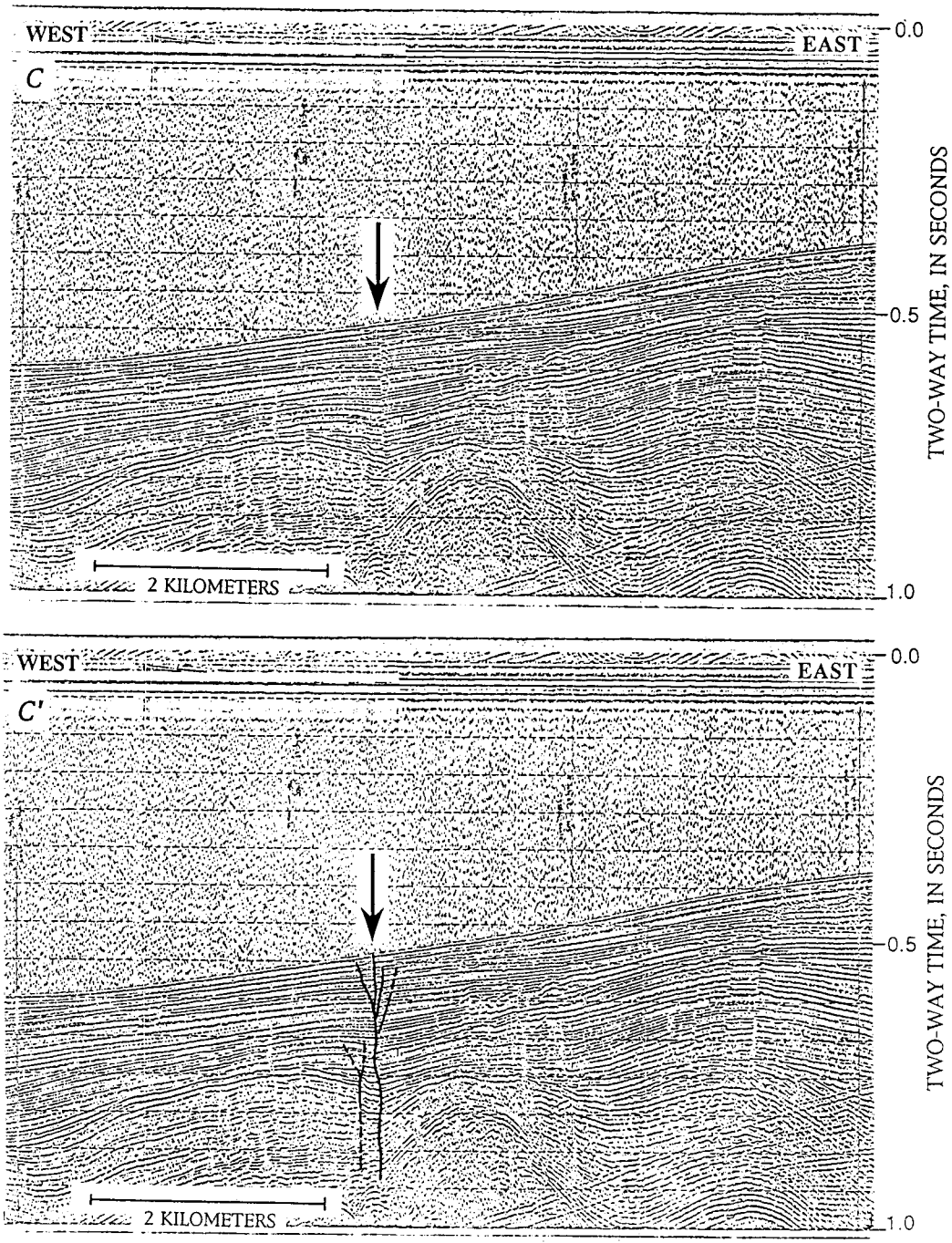

Figure 3.22. Seismic profiles showing the Wecoma fault and deformation zone off the Oregon coast. *C*, Unmigrated single-channel seismic profile of a strike-slip fault within the Wecoma fault deformation zone on the upper continental slope. *D*, Interpreted profile. Note near-vertical fault and sharp dip reversals of reflectors. Arrow shows fault location. Oregon State University line SP-56. Vertical exaggeration = 3:1.

FAULT ORIENTATION AND THE REGIONAL TECTONIC SETTING

The Wecoma fault strikes 293° on the abyssal plain, the same as the strikes of faults B and C (Fig. 3.4). This orientation is virtually the same as the 295° strike of the Blanco Fracture Zone, the transform fault that separates the Juan de Fuca and Pacific plates and forms the boundary between the Gorda segment and the main segment of the Juan de Fuca plate (Fig. 3.1). Detailed mapping of the continental slope off Washington and Oregon has also documented an additional six oblique deformation zones with similar strikes, three of which adjoin abyssal-plain strike-slip faults (Goldfinger and Kulm, unpublished data). Thus, the Wecoma fault, the eight other oblique faults, and the Blanco Fracture Zone are oriented along small circles of rotation of the Juan de Fuca plate with respect to the Pacific plate. It is presently unknown if this orientation is coincidental or if there is a fundamental relationship between plate motion and the orientation of the strike-slip faults. An attractive explanation for this similarity might be that the strike-slip faults are reactivated minor transforms formerly generated at the spreading ridge that are currently responding to the subduction-related stress field at the deformation front. Detailed reconstructions of the spreading history of the Juan de Fuca plate by Wilson and others (1984), however, indicate that the Juan de Fuca ridge (Fig. 3.1, labeled "JDFR") was oriented nearly north-south at the time the presently subducting crust was generated. Any relict transforms generated at that time should be oriented east-west, making it unlikely that reactivated faults are responsible for the observed structures. Although the reflection profiles have been interpreted to include the possibility of a long (more than 6,000,000 year) history for the Wecoma fault (Appelgate and others, 1992), our preferred interpretation suggests that the faults are on the order of 600,000 years old, eliminating a spreading-ridge origin. The youth of these faults and their proximity to and influence on the plate boundary suggest that they are a subduction-related phenomenon as opposed to relict structures or structures related to regional Juan de Fuca plate stresses. Indeed, limited seismological evidence that suggests the regional stress field may be roughly north-south in much of the Juan de Fuca plate (Spence, 1989) is incompatible with the orientation and slip direction of the abyssal-plain strike-slip faults.

STRIKE-SLIP FAULTS AND THE ACCRETIONARY WEDGE

We have shown that the Wecoma fault influences the seawardmost accretionary wedge. Seismic and sidescan records show that the intersection of the fault and the deformation front is a complex zone of interaction between the frontal thrust and the strike-slip fault. Strands of the fault extend into the seawardmost three or four thrust ridges on sidescan records, and these observations are supported by direct observation from ALVIN and analysis of carbonate material derived from venting fluids on the marginal ridge.

In addition to seismic-reflection and sidescan evidence, we observed significant differences in the style and growth history of the youngest thrust ridges near the Wecoma fault. Considerably more shortening has occurred on equivalent structures immediately south of the projection of the Wecoma fault than to the north. Both fault-bend folds and fault-propagation folds are better developed to the south, and an additional thrust ridge is present to the south that is not present to the north (Fig. 3.23). This change in fold and thrust development across the Wecoma fault is clear on reflection profiles and can also be seen in the bathymetry, which shows an abrupt bathymetric change across the fault (Fig. 3.23; see also MacKay and others, 1992). The bathymetric change corresponds to the scarp discussed above and shown in Figure 3.19. Much of the bathymetric change is due to the abrupt increase in development of the thrust ridges on the south side.

The structure map of this area (Fig. 3.7) shows that other changes in accretionary-wedge structures also occur along this bathymetric trend and escarpment (labeled scarp on Fig. 3.7). Some fold axes and thrust faults step or bend to the left, whereas others terminate altogether. The left offsets and sigmoidal bending are consistent with a left-lateral shear zone. Similar relationships between trench-parallel accretionary-wedge structures and a conjugate set of strike-slip faults have been mapped in the Shumagin segment of the Aleutian forearc (Lewis and others, 1988). The projected trend of the Wecoma fault also coincides with an abrupt change in strike of the seaward thrust ridges. North of the fault they strike about north-south; south of the fault, the strike is 340°. The differences in thrust ridge development across the projection of the Wecoma fault also support the presence of an active left-lateral shear zone. Given the plate convergence rate of 40 mm/year (DeMets

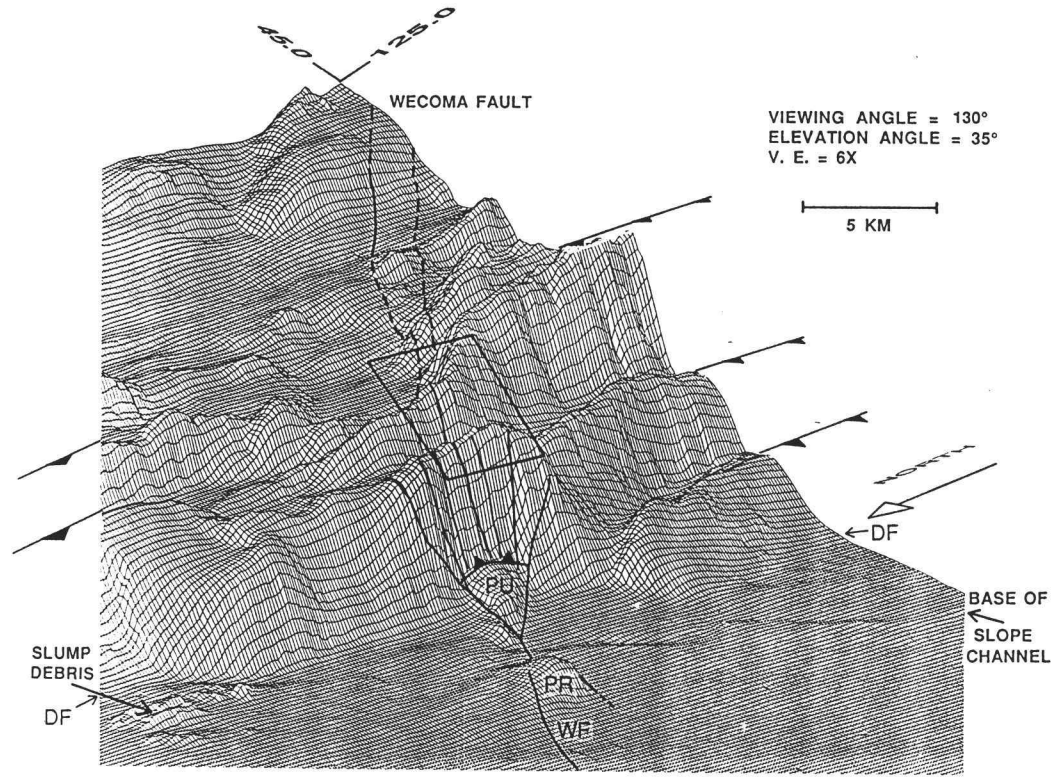

Figure 3.23. SeaBeam bathymetry perspective view along the strike of the Wecoma fault as it crosses from the abyssal plain into the accretionary wedge. Grid spacing is 250 m. Note the morphologic change in the thrust ridges from the south block to the north block of the Wecoma fault. Note also the extra thrust ridge present on the south block with no correlative to the north. Parallelogram shows location of Figure 3.19. Solid and dashed lines, faults; solid lines with sawteeth, thrust faults with sawteeth on upper plate. PR, pressure ridge; PU, pop-up; DF, deformation front; WF, Wecoma fault. percent of the 19-24 km of normal convergence that has occurred during the life span of the Wecoma fault.

and others, 1990) and a simple calculation of the shortening on these structures, we estimate that the four westernmost thrust ridges must have formed during the 600±50 thousand years that the Wecoma fault has been active. We postulate that the difference in shortening is due to a local change in the subduction rate across the fault resulting from subduction of the active Wecoma fault. Using the net slip of 5.5 ± 0.8 km and the 600 ± 50 ka age of the Wecoma fault, the difference in subduction across the fault has been 8.4-10.0 km, or 41-44 percent of the 19-24 km of normal convergence that has occurred during the life span of the Wecoma fault. Figure 3.24 illustrates this geometric result and shows that the effective local convergence rate is 28 percent greater south of the Wecoma fault than to the north. We postulate that increased convergence south of the Wecoma fault due to this difference has caused the extra shortening in the seaward thrust ridges and probably also the early development of the extra thrust ridge (Fig. 3.23).

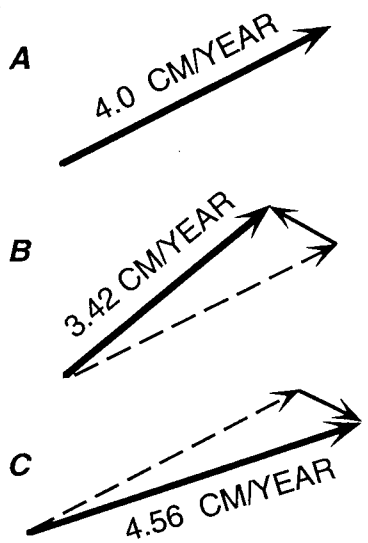

Figure 3.24. Vector diagram of the inferred local effect of Wecoma fault slip on the plate convergence vector. *A*, The regional Juan de Fuca-North America plate vector of DeMets and others (1990). *B*, JDF-NAM vector (dashed) on the north block of the Wecoma fault. Short arrow is the local vector due to motion on the Wecoma fault. New resultant and convergence rate are shown by bold arrow. *C*, JDF-NAM vector (dashed) on the south block of the Wecoma fault. Short arrow is the local vector due to motion on the fault. New resultant and convergence rate shown with bold arrow. Increased convergence south of the fault may be responsible for the greater shortening and topographic expression of the thrust faults south of the Wecoma fault. Calculated from the Euler pole of DeMets and others (1990), North America fixed.

KINEMATICS OF OBLIQUE FAULT - ACCRETIONARY WEDGE INTERACTION

We suggest three hypotheses to explain the possible interactions of the abyssal-plain faults and the accretionary wedge: 1) The strike-slip faults extend from the abyssal plain beneath the accretionary wedge and are the source of the deformation zones; 2) the strike-slip faults originate within the North America plate and propagate into the subjacent subducted slab and seaward into the abyssal plain; and 3) the deformation zones on the slope are unrelated to the abyssal-plain faults.

If the strike-slip faults originate in the Juan de Fuca plate (hypothesis 1), the deformation zones in the accretionary wedge may have developed in response to strike-slip motion of the Juan de Fuca plate beneath the accretionary wedge and thick Tertiary shelf sequence. If so, the presence of such deformation in both the overriding and downgoing plates presents a problem in reconciling strike-slip motion and oblique convergence over the last 600,000 years. Oblique convergence of about 24 km directed N.62° E. has occurred over the past 600,000 years, according to the plate vectors of DeMets and others (1990). During that time, the points at which the three strike-slip faults on the abyssal plain intersect the present deformation front should have moved some 20 km to the north (neglecting the unknown amount of advance of the deformation front), yet we observed little or no offset between the abyssal plain and accretionary-wedge segments of these faults. The discrepancy could be due to a very recent cessation or slowdown of subduction. Although cessation is unlikely given preponderance of geologic and geophysical evidence, a significant slowdown cannot be ruled out and could reduce the missing component of convergence (Riddihough, 1984). Three structural explanations might also be considered: (1) The existence of right-lateral strike-slip fault(s) in the upper plate to the east of the youngest accretionary thrusts. Such faults can decouple the seaward part of the accretionary complex and accommodate the margin-parallel component of oblique convergence (Fitch, 1972; Jarrard, 1986; Karig and others, 1986). Snavely (1987) has mapped such a fault (the Fulmar fault) on the Oregon shelf. More than 200 km of dextral slip occurred on this fault, primarily in the Eocene, but minor offsets of younger units may indicate continued or renewed

activity (Snavely, 1987; Snavely and others, 1985). (2) A right-lateral component on the accretionary thrusts themselves could accommodate the missing north-south convergence component, distributing the expected offset of the strike-slip faults over many crossing structures. The deformation zones on the continental slope do show a tendency to step or bend to the south, a requirement of this mechanism. Or (3) the subducted strike-slip faults leave progressive deformation behind in the upper plate as they pass beneath it to the northeast. Two oblique deformation zones limited to the accretionary wedge have been mapped on the continental slope and shelf, one in northern Oregon off the Tillamook Bay area, and one off southern Oregon northwest of Cape Blanco. This process might be analogous to the trail of volcanoes left on a lithospheric plate as it passes over a fixed mantle hot spot. As the Juan de Fuca plate is subducted, lower plate faults leave behind a trail of deformation in the accretionary wedge as they pass obliquely beneath the North America plate.

If the strike-slip faults originate within the upper plate (hypothesis 2), several problems with hypothesis 1 are avoided. Because not all the mapped deformation zones on the slope have abyssal-plain counterparts, an upper plate origin does not require a separate explanation for those structures. It is also more mechanically reasonable to envision faults in the thicker upper plate propagating across a locked interface into the thin, relatively warm subducting plate than the reverse. The apparent incompatibility of west-northwest-trending left-lateral faults with the focal solutions and inferred north-south principal stress of Spence (1989) for the Juan de Fuca plate is resolved if the abyssal-plain faults are only the western extensions of faults that originate within the upper plate to the east. If this is the case, the regional stress field in the oceanic plate might coexist with a somewhat different stress field within the upper plate and near the deformation front, with a transition somewhere seaward of the abyssal-plain faults. Lastly, a domain of subparallel left-lateral strike-slip faults should rotate clockwise through time (Freund, 1974; Ron and others, 1984; Scotti and others, 1991). Such rotations as a result of progressive slip on these faults were suggested by Goldfinger and others (1992b) and could resolve the question of offset across the deformation front expected in hypothesis 1, because clockwise rotation of

the upper plate could make up the missing north-south component of plate convergence.

Hypothesis 3, that there is no connection between the slope deformation zones and the abyssal-plain faults, must be considered, as data positively linking these structures is not available at present. However, the trends, shear sense, and youth of these structures all strongly suggest at least a genetic connection, if not a physical one. If these structures are not directly linked, they may be separate but similar responses by the respective plates to interplate subduction stresses.

CONCLUSIONS

Three west-northwest-trending left-lateral strike-slip faults in the Cascadia subduction zone offset both the oceanic basement and sedimentary cover of the Juan de Fuca plate. The Wecoma fault, the largest of the three faults, has a measured net slip of 5 to 6 km at the plate boundary, dying out in the Juan de Fuca plate 18 km to the northwest of its intersection with the deformation front. Two independent estimates of the slip rate on this fault during two time periods show similar rates of 5 to 12 mm/year for the most recent 24,000 to 10,000 year period, and 7 to 12 mm/year over the 600,000 year life span of the fault. The Wecoma fault intersects the deformation front in a complex area of structural pop-ups and an embayment in the deformation front. Sidescan images show that scarps and linear gullies extend along the projected strike of the subducted Wecoma fault about 15 km into the accretionary wedge. Slip on the Wecoma fault beneath the North America plate has influenced the development of the initial thrust ridges in the accretionary wedge. Three deformation zones in the accretionary wedge lie along the landward projections of the three abyssal-plain faults. These zones are composed of west-northwest-to northwest-trending folds, sigmoidally bent fold axes, and west-northwest-trending linear scarps. The style of deformation in these zones is consistent with left-lateral shear zones superimposed on the structural grain of the accretionary wedge. We postulate that these deformation zones are the result of subduction of the active strike-slip faults, or alternatively, that the shear zones originate in the upper plate and propagate across the plate boundary into the Juan de Fuca plate. The orientation of the Wecoma fault and the other strike-slip faults along small circles of rotation of the Juan de Fuca-Pacific plate system, is not yet understood.

REFERENCES CITED

Adams, J., 1990, Paleoseismicity of the Cascadia subduction zone-- Evidence from turbidites off the Oregon-Washington margin: Tectonics, v. 9, p. 569-583.

Ando, M., and Balazs, E.I., 1979, Geodetic evidence for aseismic subduction of the Juan de Fuca plate: Journal of Geophysical Research, v. 84, p. 3023-3027.

Appelgate, T.B., 1988, Tectonic and volcanic structures of the southern flank of Axial volcano, Juan de Fuca Ridge-- Results from a SeaMARC 1 sidescan sonar survey: Corvallis, Oregon State University, M.S. thesis, 161 p.

Appelgate, T.B., Goldfinger, C., MacKay, M.E., Kulm, L.D., Fox, C.G., Embley, R.W., and Meis, P.J., 1992, A left-lateral strike-slip fault seaward of the central Oregon convergent margin: Tectonics, v. 9, p. 465-477.

Atwater, B.F., 1987, Evidence for great Holocene earthquakes along the outer coast of Washington State: Science, v. 236, p. 942-944.

Atwater, B.F., and Yamaguchi, D.K., 1991, Sudden, probably coseismic submergence of Holocene trees and grass in coastal Washington State: Geology, v. 19, p. 706-709.

Carson, B., 1977, Tectonically induced deformation of deep-sea sediments off Washington and northern Oregon: Marine Geology, v. 24, p. 289-307.

Carver, G.A., Vick, G.S., and Burke, R.M., 1989, Late Holocene paleoseismicity of the Gorda segment of the Cascadia subduction zone: Geological Society of America Abstracts with Programs, v. 21, p. 64.

Clarke, S.H., Jr., and Carver, G.A., 1989, Late Cenozoic structure and seismic potential of the southern Cascadia subduction zone: EOS (Transactions, American Geophysical Union), v. 70, p. 1331-1332.

Cochrane, G.R., and Lewis, B.T.R., 1988, Deep-tow seismic reflection records from the Oregon lower slope: EOS (Transactions, American Geophysical Union), v. 69, p. 1442-1443.

Darienzo, M.E., and Peterson, C.D., 1990, Episodic tectonic subsidence of late Holocene salt marshes, northern Oregon central Cascadia margin: Tectonics, v. 9, p. 1-22.

DeMets, C., Gordon, R.G., Argus, D.F., and Stein, S., 1990, Current plate motions: Geophysical Journal International, v. 101, p. 425-478.

Duncan, J.R., 1968, Late Pleistocene and postglacial sedimentation and stratigraphy of deep-sea environments off Oregon: Corvallis, Oregon State University, Ph.D. dissertation, 222 p.

Fitch, T.J., 1972, Plate convergence, transcurrent faults, and internal deformation adjacent to southeast Asia and the western Pacific: Journal of Geophysical Research, v. 77, p. 4432-4460.

Freund, R., 1974, Kinematics of transform and transcurrent faults: Tectonophysics, v. 21, p. 93-134.

Geist, E.L., Childs, J.R., and Scholl, D.R., 1988, The origin of summit basins of the Aleutian Ridge-- Implications for block rotation of an arc massif: Tectonics, v. 7, p. 327-341.

Goldfinger, C., Kulm, L.D., Yeats, R.S., Appelgate, T.B., MacKay, M.E., and Moore, G.F., 1992b, Transverse structural trends along the Oregon convergent margin: Implications for Cascadia earthquake potential: Geology, v. 20, p. 141-144.

Griggs, G.B., and Kulm, L.D., 1970, Sedimentation in Cascadia deep-sea channel: Geological Society of America Bulletin, v. 81, p. 1361-1384.

Griggs, G.B., and Kulm, L.D., 1973, Origin and development of Cascadia deep-sea channel: Journal of Geophysical Research, v. 78, p. 6325-6339.

Griggs, G.B., Kulm, L.D., Waters, A.C., and Fowler, G.A., 1970, Deep-sea gravel from Cascadia Channel: Journal of Geology, v. 78, p. 611-619.

Harding, T.P., 1985, Seismic characteristics and identification of negative flower structures, positive flower structures, and positive structural inversion: American Association of Petroleum Geologists Bulletin, v. 69, p. 582-600.

Heaton, T.H., and Kanamori, H., 1984, Seismic potential associated with subduction in the northwestern United States: Seismological Society of America Bulletin, v. 74, p. 933-941.

Ingle, J.C., 1973, Neogene foraminifera from the northeastern Pacific ocean, Leg 18, Deep Sea Drilling Project: Initial Reports of the Deep Sea Drilling Project, v. XVIII, p. 517-567.

Jarrard, R.D., 1986, Terrane motion by strike-slip faulting of forearc slivers: Geology, v. 14, p. 780-783.

Karig, D.E., Sarewitz, D.R., and Haeck, G.D., 1986, Role of strike-slip faulting in the evolution of allochthonous terranes in the Philippines: Geology, v. 14, p. 852-855.

Kulm, L.D., and Fowler, G.A., 1974, Oregon continental margin structure and stratigraphy-- A test of the imbricate thrust model, *in* Burke, C.A., and Drake, C.L., eds., The geology of continental margins: New York, Springer-Verlag, p. 261-284.

Kulm, L.D., Prince, R.A., and Snavely, P.D., Jr., 1973a, Site survey of the northern Oregon continental margin and Astoria Fan: Initial Reports of the Deep Sea Drilling Project, v. XVIII, p. 979-987.

Kulm, L.D., and Suess, E., 1990, The relation of carbonate deposits to fluid venting processes-- Oregon accretionary prism: Journal of Geophysical Research, v. 95, p. 8899-8915.

Kulm, L.D., Von Huene, R., and scientific party, 1973b, Initial reports of the Deep Sea Drilling Project, Volume 18: Washington, D.C., U. S. Government Printing Office, p. 97-168.

Lewis, S.D., Ladd, J.W., and Bruns, T.R., 1988, Structural development of an accretionary prism by thrust and strike-slip faulting-- Shumagin region, Aleutian Trench: Geological Society of America Bulletin, v. 100, p. 767-782.

Ludwin, R.S., Weaver, C.S., and Crosson, R.S., 1991, Seismicity of Washington and Oregon, *in* Slemmons, D.B., Engdahl, E.R., Blackwell, D., and Schwartz, D., eds., Neotectonics of North America: Decade of North American Geology CSMV-1, p. 77-98.

MacKay, M.E., Moore, G.F., Cochrane, G.R., Moore, J.C., and Kulm, L.D., 1992, Landward vergence, oblique structural trends, and tectonic segmentation in the Oregon margin accretionary prism: Earth and Planetary Science Letters, v. 109, p. 477-491.

Nelson, C.H., 1968, Marine geology of Astoria deep-sea fan: Corvallis, Oregon State University, Ph.D. dissertation, 287 p.

Nelson, C.H., 1976, Late Pleistocene and Holocene depositional trends, processes and history of Astoria Deep-sea Fan: Marine Geology, v. 20, p. 129-173.

Riddihough, R., 1984, Recent movements of the Juan de Fuca plate system: Journal of Geophysical Research, v. 89, p. 6980-6994.

Ron, H., Freund, R., Garfunkel, Z., and Nur, A., 1984, Block rotation by strike-slip faulting-- Structural and paleomagnetic evidence: Journal of Geophysical Research, v. 89, p. 6256-6270.

Sample, J.C., Reid, M.R., Tobin, H.J., and Moore, J.C., 1993, Carbonate cements indicate channeled fluid flow along a zone of vertical faults at the deformation front of the Cascadia accretionary wedge (northwest U.S. coast): Geology, v. 21, p. 507-510.

Scotti, O., Nur, A., and Estevez, R., 1991, Distributed deformation and block rotation in 3D: Journal of Geophysical Research, v. 96, p. 12,225-12,243.

Snavely, P.D., Jr., 1987, Tertiary geologic framework, neotectonics, and petroleum potential of the Oregon-Washington continental margin, *in* Scholl, D.W., Grantz, A., and Vedder, J.G., eds., Geology and resource potential of the continental margin of western North America and adjacent ocean basins--Beaufort Sea to Baja California: Houston, Tex., Circum-Pacific Council for Energy and Mineral Resources, p. 305-335.

Snavely, P.D., Jr., and McClellan, P.H., 1987, Seismic data collected in June, 1976, off the Washington/Oregon coast: U.S. Geological Survey Open-File Report 87-607.

Snavely, P.D., Jr., Wagner, H.C., and Lander, D.L., 1985, Land-sea geologic cross section of the southern Oregon continental margin: U.S. Geological Survey Miscellaneous Investigations Series Map I-1463, scale 1:125,000.

Spence, W., 1989, Stress origins and earthquake potential in Cascadia: Journal of Geophysical Research, v. 94, p. 3076-3088.

Sykes, L.R., 1989, Great earthquakes of 1855 and 1931 in New Zealand: evidence for seismic slip along downgoing plate boundary and implications for seismic potential of Cascadia subduction zone: EOS (Transactions, American Geophysical Union), v. 70, p. 1331.

Sylvester, A.G., 1988, Strike-slip faults: Geological Society of America Bulletin, v. 100, p. 1666-1703.

Tobin, H.J., Moore, J.C., MacKay, M.E., Orange, D.L., and Kulm, L.D., 1993, Fluid flow along a strike-slip fault at the toe of the Oregon accretionary prism-- Implications for the geometry of frontal accretion: Geological Society America Bulletin, v. 105, p. 569-582.

Vick, G.S., 1988, Late Holocene paleoseismicity and relative sea level changes of the Mad River slough, northern Humboldt Bay, California: Arcata, California, Humboldt State University, M.S. thesis, 87 p.

West, D.O., and McCrumb, D.R., 1988, Coastline uplift in Oregon and Washington and the nature of Cascadia subduction zone tectonics: Geology, v. 16, p. 169-172.

Wilcox, R.E., Harding, T.P., and Seely, D.R., 1973, Basic wrench tectonics: American Association of Petroleum Geologists Bulletin, v. 57, p. 74-96.

Wilson, D.S., Hey, R.N., and Nishimura, C., 1984, Propagation as a mechanism of reorientation of the Juan de Fuca Ridge: Journal of Geophysical Research, v. 89, p. 9215-9225.

ACKNOWLEDGMENTS

We thank Richard Perry and Steven Mutula, U.S. National Oceanic and Atmospheric Administration, National Ocean Survey, Rockville, Md. for preliminary copies of the SeaBeam bathymetry of the Oregon continental margin. They also allowed us to publish a part of a three-dimensional-mesh diagram of the northern and central Oregon continental margin generated at their facility. We thank Sigmund Snelson and Dan Worrall of Shell Oil Company for the loan of seismic profiles on the Oregon and Washington continental shelf and for their efforts in locating these profiles in the company archives. We also thank Parke D. Snavely, Jr., Samuel H. Clarke, Jr., and Dan L. Orange for thorough reviews of the manuscript. The first two reviewers do not necessarily agree with all of our interpretations of oblique faults and folds on the upper continental slope or shelf, which are solely our responsibility. This research was supported by National Science Foundation grants OCE-8812731 (OSU) and OCE-8821577 (UH) and by the U.S. Geological Survey, National Earthquake Hazards Reduction Program under award 14-08-001-G1800 (OSU). We thank the crews of the vessels *R.V. Wecoma*, *Digicon M.V. Geotide*, and *R.V. Atlantis II* and to Margaret Mumford and Cheryl Hummon (OSU) for drafting the illustrations.

CHAPTER 4: CASCADIA SUBDUCTION ZONE: ACTIVE DEFORMATION OF THE OREGON CONTINENTAL SHELF

Chris Goldfinger
Department of Geosciences, Oregon State University, Corvallis Oregon 97331
internet: gold@oce.orst.edu

LaVerne D. Kulm
College of Oceanic and Atmospheric Sciences, Oregon State University, Corvallis Oregon 97331
internet: lkulm@oce.orst.edu

Lisa McNeill, Robert S. Yeats, Cheryl Hummon, Gary J. Huftile, Craig L. Schneider, Alan R. Niem, Hiroyuki Tsutsumi
Department of Geosciences, Oregon State University, Corvallis Oregon 97331

John Y. Chen
College of Oceanic and Atmospheric Sciences, Oregon State University, Corvallis Oregon 97331

ABSTRACT

The Oregon continental shelf was subjected to subaerial and submarine erosion during the Pleistocene fluctuations in sea level ending at the close of the Pleistocene about 10,000 years ago. This erosional planation left a low-relief erosion surface and a lowstand sea cliff that we have used to investigate the nature and timing of Late Quaternary tectonism on the continental shelf. Active structures on the shelf include folds trending from NNE to WNW and associated flexural slip thrust faults; NNW to N trending right-lateral strike-slip faults; and WNW trending left-lateral strike-slip faults. Some of these structures intersect the coast and can be correlated with onshore Quaternary faults and folds, and others are suspected to be deforming the coastal region. These structures may be contributing to the coastal marsh stratigraphic record that has recorded co-seismic subsidence events in the Holocene. The likelihood of a local structures contribution to the vertical marsh record makes the use of these vertical data for location of a "zero isobase" or for elastic dislocation modeling of subduction earthquakes problematic. Three major submarine banks constitute large salients in the highly irregular seaward edge of the Oregon continental shelf. These banks differ significantly from the interbank basins between them in that they have a long term uplift history, different fold trends, and a lack of oblique folding and faulting that is common in the interbank basins. Left-lateral WNW trending strike-slip faults bound the northern and/or southern limits of the three banks, requiring clockwise rotation of these blocks about vertical axes. We interpret the localization of strike-slip faulting in the interbank basins to indicate that the banks are high-strength clockwise rotating blocks within a dextral shear couple driven by oblique subduction of the Juan de Fuca plate.

INTRODUCTION

The possibility that great earthquakes may rupture all or large parts of the Cascadia plate interface has sparked a number of studies focused on mounting evidence of co-seismic uplift, subsidence, and shaking, as well as evidence of modern elastic strain accumulation that must eventually be released by slip on the plate interface. Evidence for seismic activity on the coasts of Washington, Oregon and northern California has been found by many investigators in the form of buried marshes and coeval tsunami sand layers in coastal bays and estuaries, and drowned forests in some of the same bays (Atwater, 1987; Darienzo and Peterson, 1990; Atwater and Yamaguchi, 1991). Although some of these buried marshes probably result from non-tectonic processes (Nelson, 1992), the premise that marsh burials are evidence of co-seismic sudden subsidence remains the best explanation for the sudden lowering of upper marsh surfaces and, in some cases, forests to the intertidal zone in many of the estuaries and bays of the Pacific Northwest. Dating and correlating these geographically separated but stratigraphically similar marsh stratigraphies can potentially determine the timing of past earthquakes and extent of individual ruptures along the Cascadia margin. The limitations of ^{14}C dating techniques presently available, and the rarity of a complete tree-ring record with which to ground truth the radiocarbon dates have made this correlation problematic. The similarity of the separate marsh records makes a strong circumstantial case for major earthquakes; however, the rapid, apparently tectonic, subsidence of coastal marshes may also be the result of movement on local upper-plate faults and folds. We present evidence from the continental shelf of Oregon that active upper plate structures are widespread and most likely affect coastal areas in which the buried marshes are found. We also summarize published onshore data that suggest that many of the sites of marsh burial are adjacent to active upper plate folds and faults that could produce rapid vertical motion at the marsh sites. On a larger scale, we also present new evidence for discrete high strength blocks within the forearc that may be the nucleation sites for subduction earthquakes.

METHODS

We are studying the continental shelves of Oregon and Washington (Plate 1) using 30, 50 and 150 kHz sidescan sonar imagery, NOAA SeaBeam and BS^3 swath bathymetry, DELTA submersible observations, and a dense network of single-channel (SCS) and multichannel seismic (MCS) surveys. We are mapping the Oregon-Washington continental margin using a Computer Aided Design (CAD)/ Geographic Information System (GIS) system in which we can arrange the various datasets as layers and view any combination of raster and vector data. This system allows us to work at the best scale for each data set without the limitations of a fixed-scale base map. We have used approximately 15,000 km of seismic-reflection profiles collected by Oregon State University, University of Washington, Scripps Institution of Oceanography, U.S.G.S., N.O.A.A., and Shell, Chevron, and Exxon Corporations. (Plate 2). The profiles vary widely in quality, depth of penetration, and navigational accuracy, ranging from single-channel sparker records navigated with Loran-A, to 12 and 24-channel digital profiles navigated with TRANSIT satellite navigation.

The sidescan and bathymetric surveys were navigated with a combination of GPS and Transit satellite navigation, with Loran C tracking used between TRANSIT satellite fixes. GPS navigation during high resolution sidescan surveys and DELTA dives was continuous. Navigational accuracy for GPS navigated dives and sidescan swaths is 100 m (due to selective availability, the error introduced into the civilian use signal by the Department of Defense). Navigation accuracy for the seismic reflection profiles varies according to the systems in use at the time. Transit satellite errors range from near zero up to 200 m, Loran C errors are approximately 0-1.5 km, Loran A navigated profiles have maximum errors on the order of 1-3 kilometers. Shell Oil Company lines were navigated with a company SHORAN radio navigation system. Horizontal errors with this system are approximately 50 meters. Although these profiles were shot in 1961-62, their navigational accuracy is as good or better than the GPS navigated lines. The dense coverage of reflection profiles allowed adjustment of older lines where crossed by satellite-navigated lines. The NOAA/NOS multibeam bathymetric surveys were navigated with an ARGO shore based system; navigational accuracy is 50 m.

These bathymetry data were contoured at a 10 or 20 m interval and also rendered as shaded relief images and incorporated in the mapping as layers in the GIS system. The bathymetry is accurate to within 1% of the water depth across the swath. Where spatial misfits occur, we have adjusted the older seismic data to best fit the GPS navigated MCS lines, sidescan swaths, or the SeaBeam bathymetry where appropriate. Klein analog sidescan data were collected with a deep-towed 50 or 100 kHz system imaging an 800 m or a 400 m swath width, respectively, with spatial resolutions of 0.4 and 0.2 meters, respectively.

In 1992 and 1993 we conducted two cruises using the two-person submersible DELTA to investigate active structures at the outcrop scale. We constructed a handheld electric gyro compass and used this in conjunction with a digital level to obtain strike and dip measurements in the all steel DELTA. The submersible is equipped with still and video cameras as well as a sampling arm, and has a maximum depth capability of 1200 feet. Submersible navigation used an ORE Trackpoint system that logged range and bearing of DELTA from the ship, and these data were merged with the ships GPS position to obtain sub position accurate to about 100-150 m. Delta dives were made in daylight, while sidescan sonar surveys were done at night. Our mode of operation during sidescan surveys was to cover target areas previously located with seismic reflection profiles, then return to specific targets and conduct additional surveys and submersible dives for detailed observation and sample collection with DELTA.

AGE CONSTRAINTS ON LATE QUATERNARY STRUCTURES

The Oregon continental shelf was subjected to multiple Pleistocene transgressive/regressive cycles during the sea-level fluctuations caused by glacial advance and retreat. The last transgressive/regressive cycle left a widespread unconformity over which a thin Holocene sequence of transgressive sand was deposited on the middle to inner shelf, and a hemipelagic mud deposited on the middle to outer shelf (Kulm and others, 1975; Peterson and others, 1984). The age of the underlying strata ranges from Pleistocene (conformable in some locations on the middle to outer shelf) to Eocene and older on the southern Oregon inner shelf (Kulm and Fowler, 1974). This unconformity represents a relatively low-relief seaward-dipping surface, and thus serves as an effective strain marker for latest Pleistocene and Holocene deformation. This erosional event is time-transgressive over the shelf. The last sea-level minimum of 70-130 m below modern sea-level occurred approximately 18,000 years ago, with sea-level rising to within a few meters of present level by about 6000 years ago (Curray, 1965; Blackwelder and others, 1979; Chappel and Shackleton, 1986; Fairbanks, 1989; Matthews, 1990). Thus tectonic activity that deforms this surface has a maximum age of about 18,000 years. Deformation of the Holocene shelf sand or mud on the middle to outer shelf has a maximum age of about 6000 years. Deformation of these sediments on the inner shelf is less common, as water depths less than about 150 m are subject to active erosion and sediment transport by bottom currents and storm waves (Komar and others, 1972). In some areas of the inner shelf where sediment supply is low, recent sediments are thin and patchy or altogether absent. Deformation mapped in these older rocks is difficult to evaluate without younger sediments, however faults can be evaluated in terms of late Quaternary deformation by satisfying one of two possible criteria: 1) The fault can be traced seaward into deep enough water that a Holocene scarp in unconsolidated sand or mud is preserved along the same structure, or 2) the fault can be correlated to a known onshore fault that offsets late Quaternary deposits.

The Pleistocene-Holocene transition can easily be distinguished visually in cores and in outcrop over much of the Oregon shelf. The Holocene hemipelagic muds are olive green in color, and very poorly consolidated. A

sharp transition to more consolidated gray silty clay marks the transition into Pleistocene sediments (Barnard and McManus, 1973). The color change is due to the abrupt upsection decrease in the terrigenous sediment fraction, and thus a relative increase in organic content, at the end of the Pleistocene. This occurrence was time-transgressive, decreasing in age from the abyssal plain to the continental slope, and occurred at about 12 ka on the upper slope after application of a reservoir correction to the radiocarbon ages (Barnard and McManus, 1973). A shift from foraminiferan dominated to radiolarian dominated biostratigraphy lagged somewhat behind the color change, occurring at approximately 9-12 ka on the lower continental slope, and 8 ka on the upper slope (Barnard and McManus, 1973; Fig. 4.1).

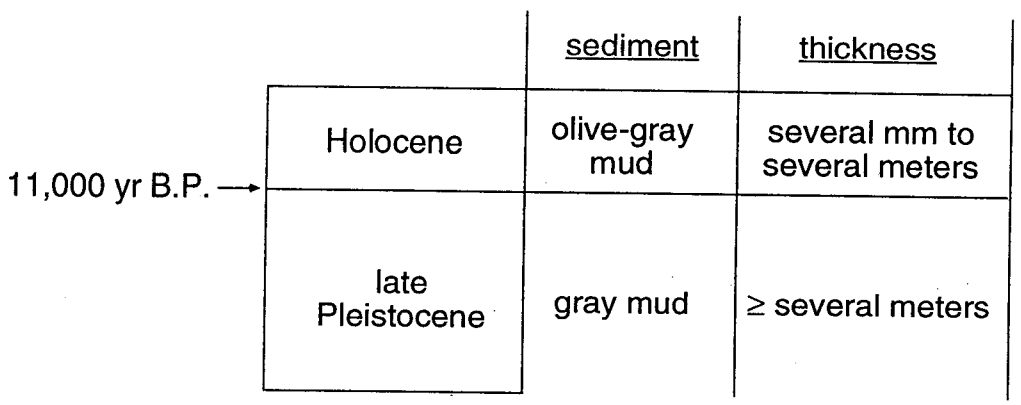

Figure 4.1. Color change across the Holocene/Pleistocene boundary. The color change was found in cores and by direct submersible observations on the Oregon-Washington continental margin. Change in color is the result of the sharp reduction in the terrigenous sediment fraction (gray) at the close of glaciation, while the organic (green-brown) fraction was relatively constant.

ACTIVE STRUCTURES ON THE OREGON CONTINENTAL SHELF

Active deformation of the Oregon continental shelf can be characterized by three structural styles: folding and associated flexural slip thrust faulting, left-lateral strike-slip faulting on WNW trending faults, and right-lateral strike-slip faulting on NNW to N trending faults.

FOLDING AND FLEXURAL-SLIP FAULTING

In numerous seismic reflection profiles on the Oregon shelf we found varying degrees of late Quaternary deformation on folds that had been truncated by the Pleistocene transgressive/regressive episodes. This post-Pleistocene deformation is most commonly expressed as warping of the seafloor and offsets of the seafloor by flexural-slip faults, or bedding plane faults (Yeats, 1986) on which dip-slip or oblique-slip motion occurs as folds grow (Fig. 4.2). These structures are common on the Oregon shelf, but are

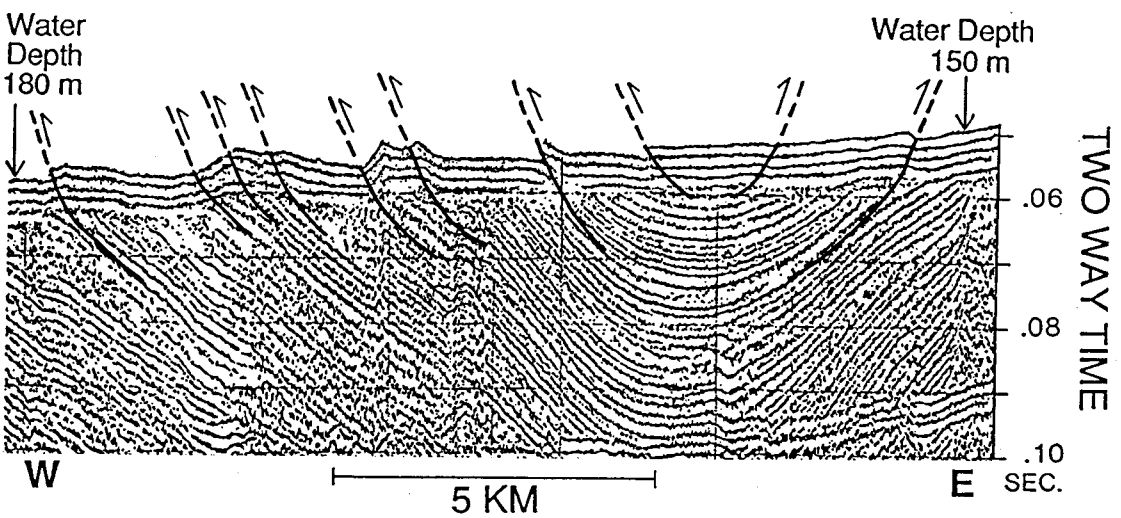

Figure 4.2. Single channel airgun seismic record (OSU line SP-118) showing an active syncline and flexural-slip faults. The flexural-slip faults offset the sea floor (latest Pleistocene abrasion platform) and Holocene cover. Location is west of Tillamook Bay, Oregon.

best expressed in areas landward of the major submarine banks discussed in more detail below (see Plate 1). In the central parts of the major banks, post-Pleistocene folding is more difficult to evaluate due to the thinning or absence of late Quaternary sediment. In seismic reflection profiles, the origin of the flexural slip faults is clear and unambiguous, since they commonly occur as outward facing pairs of scarps symmetric about the fold axis, and fault dips are parallel to the dip of the underlying beds. Individual faults in plunging folds can be traced on sidescan images along single bedding planes from one limb of the syncline, through the fold axis, to a corresponding fault on the other limb. Vertical separation at the seafloor ranges from a few centimeters to several meters, based on reflection data and corresponding observations from DELTA. The effect of this type of faulting on the seafloor topography depends on the style of the underlying fold. If the folding is gentle, growth of a set of flexural slip faults produces a topography that mimics the underlying fold, that is, the seafloor is topographically lowest at the synclinal axes, highest at the anticlinal axes. With tighter folding, an interesting topographic inversion occurs. With tighter folds, more displacement occurs on the interior bedding plane faults of the synclines, creating a topographic high that coincides with the synclinal axis. This is analogous to cutting an onion in half along the long axis, then squeezing perpendicular to the long axis. The layer-parallel slip causes the center sections to pop out. This type of topographic inversion is a temporary function of the interaction of the growing folds with the flat Pleistocene erosion surface, and would not persist through continued long term fold growth. Sidescan sonar images of these growing folds reveal that, in plan view, the flexural slip faults converge or diverge from the synclinal axes depending on the plunge direction of the fold. Submersible observations of the seafloor scarps from several localities indicate that these submarine features are better preserved than their land counterparts. We observed overhanging scarps in several locations, and mole tracks in several others, both geomorphic features that would have very short life spans on land. Both mole tracks and high-angle scarps were observed to deform both the late Pleistocene gray clay, and the overlying olive-gray Holocene unconsolidated silt, indicating movement younger than 6,000 yrs. In several cases, colonization of the fault scarps by burrowing and attaching marine organisms decreased toward the bottom of the scarp, suggesting that uplift had occurred

in multiple stages of fault movement. In several instances, the lowermost tens of centimeters were devoid of burrows, but we were unable to determine if these scarps were being kept free of marine growth by bottom currents and bottom fish that hide at the scarp bases, or if the faults had moved so recently that they were not yet colonized. As might be expected, we were unable to observe any indicators of slip direction on the exposed fault surfaces due to the lack of consolidation of the sediments. The lack of slip indicators prevented testing the hypothesis that such structures might accommodate part of the arc-parallel component of oblique convergence by oblique slip as suggested by Goldfinger and others (in press).

STRIKE-SLIP FAULTING

Detailed mapping of the Oregon continental margin (Goldfinger and others, 1992a; Plate 1) has resulted in the discovery of a number of previously unknown strike-slip faults, and improved our understanding of faults already mapped. We find that strike-slip faults on the Oregon shelf can be generally characterized as either margin-oblique faults or margin-parallel faults.

Oblique Strike-Slip faults

Oblique strike slip faulting of the submarine Cascadia margin is reported in Appelgate and others (1992), Goldfinger and others (1992b), and Goldfinger and others (in press). Further details of three left-lateral strike-slip faults and newly mapped oblique faults are given in Chapter 5. These structures strike WNW and cut both the abyssal plain sedimentary section and the underlying basaltic basement of the subducting Juan de Fuca plate as well as the margin-parallel folds and thrust faults of the accretionary wedge (Appelgate and others, 1992; Goldfinger and others, 1992b; Goldfinger and others, in press). In May 1993, a SeaMARC 1A sidescan sonar cruise was conducted with the purpose of investigating these known faults in greater detail. In addition, we investigated other similar structures along the Oregon-Washington Cascadia margin. In September 1993, another sidescan sonar

cruise, using an AMS 150 kHz system was conducted on the Oregon upper slope and shelf. A major aim of these investigations was the documentation of surface characteristics of strike-slip faults on the upper continental slope and continental shelf previously mapped with seismic reflection profiles (Goldfinger and others, 1992a). During the SeaMARC cruise, we located three oblique strike-slip faults along the Washington margin, three new faults on the Oregon margin, and gathered additional data on the three known faults in central Oregon. Three of the six Oregon faults have known left-lateral slip based on offsets of submarine channels and sediment isopachs (Goldfinger and others, in press; Chapter 5). These faults shear and offset accretionary wedge thrust faults and folds in a left-lateral sense on the continental slope (Goldfinger and others, in press; Chapter 5). The three other Oregon faults are suspected left-lateral faults, based on deformation front offsets, and sigmoidal bending and offset of accretionary wedge structures in the same style as the known left-slip faults. In September, 1993 we attempted to map the landward extent of several of these faults to determine their role in the deformation of the shelf and coastal region. The results of that cruise are presented in the following sections.

Wecoma Fault

The Wecoma fault, described in Goldfinger and others (in press), was re-surveyed in May, 1993 using SeaMARC 1A sidescan sonar (Fig 5.3). The survey was initiated at the seaward fault tip, and we followed the structure landward to the point that surface expression was no longer visible on the sidescan record. Using high resolution AMS 150 kHz sidescan sonar, we surveyed the landward projection of this fault in September, 1993, on the outer shelf and were unable to locate any surface expression of faulting landward of the 150 m contour. Transects run using DELTA show that the bottom character of the outer shelf is sandy with well developed sand waves and ripple marks in this area. This evidence of active sediment transport made the search for an active scarp along the Wecoma fault problematic. We did observe linear patterns of carbonate deposition on the seafloor sub-parallel to the projection of the Wecoma fault, which was later confirmed by submersible dives. These methane-derived carbonates have been found closely associated with active faulting both on the shelf and in the accretionary

wedge (Kulm and Suess, 1990; this study, discussed below). The venting of methane and CO_2 charged fluids occurs along most active fault zones, with the precipitation of carbonate at the seafloor. Thus, the carbonate deposits located along the projection of the Wecoma fault may be evidence of the landward continuation of the fault higher on the shelf where preservation of a scarp might not occur.

Daisy Bank Fault

The Daisy Bank fault (fault B) was also surveyed along all of its length during the May, 1993, SeaMARC 1A cruise at a 5 km swath width (see Plate 1 for location, sidescan shown on Plate 3). The upper slope and shelf portion was imaged during the September, 1993 cruise at a 1 km swath width. Sidescan sonar data from these two surveys provided a wealth of information about current faulting and the structural style of the Daisy Bank fault. Sidescan images of the this fault zone show that it has seafloor expression extending from 12 km seaward of the deformation front on the abyssal plain, to the outer continental shelf. It may terminate at the outer shelf, or on the inner shelf at Stonewall Bank. The fault is best expressed adjacent to a structural uplift called Daisy Bank, on the outer shelf (Plate 3). The bank is one of a number of uplifted structural highlands (the others are: Nehalem Bank, Heceta Bank, and Coquille Bank) located on the middle to outer Oregon shelf. Sidescan imagery shows that the Daisy Bank fault is a wide structural zone, within which Daisy bank is a large horst uplifted between two strands of the main fault. The main fault zone is 5-6 kilometers in width northwest of Daisy Bank, widening around the oblong bank, then narrowing to a single strand southeast of the bank.

Sidescan and submersible observations reveal multiple scarps, with both up to the north and up to the south strands occurring southeast of the bank. Northwest of the bank, two main strands are evident, both up the north, which is the motion sense observed in reflection profiles on the abyssal plain. Typical strike-slip morphology is evident in sidescan imagery and also at outcrop scale. The traces of the multiple strands of the fault are straight, implying a near vertical fault, and reversals of vertical separation along strike, a characteristic common only to strike-slip faults, are well imaged at many locations along the fault. Drag folding of Tertiary bedding traces, with a left-

lateral sense of motion, is visible southeast of the bank (Plate 3). Individual bedding traces are truncated across the fault and horizontally offset, although we have not determined net slip because we are unable to match piercing points across the fault. This supports the evidence for left-lateral motion inferred for this fault through stratigraphic offset on the abyssal plain (see Chapter 5, Fig. 5.4) and structural offsets mapped on the upper slope (Goldfinger and others, 1992a; Goldfinger and others, in press). In submersible observations, we found the individual scarps to range in height from tens of centimeters to 47 m. The aggregate net uplift of the southern flank of Daisy Bank by both folding and faulting is about 130 m. The main scarp is a steep (25°-50°) debris covered slope, the debris typically consisting of angular mudstone blocks on the lower slopes, and angular to tabular carbonate cemented mudstone debris on their upper parts.

The close association of carbonate deposition and active faulting (Kulm and Suess, 1990) was observed at most locations along the Daisy Bank fault. Carbonate chimneys, donuts, and slabs, deposited as a result of methane-rich fluid venting (Ritger and others, 1987; Kulm and Suess, 1990; Sample and others, 1993), are commonly within 150-100 m of the fault traces; their occurrence decreases rapidly with distance from the fault (Fig. 4.3). This association helped us locate target features from DELTA, with its limited visibility, and also enhanced the sidescan sonar returns from faulted areas. The main scarp southeast of Daisy Bank exhibited the largest concentration of carbonate deposits yet found on the Oregon shelf, with areas encompassing hundreds of square meters covered with tabular carbonate blocks. Near the top of the scarp slope, carbonate-bearing boulders up to 6 meters in the longest dimension are common. We observed that tabular bodies 10-30 cm in thickness are a common mode of carbonate occurrence over wide areas of otherwise unconsolidated Holocene sediment adjacent to faulted areas. These slabs are often broken and disrupted in a manner similar to what occurs when a parking lot is excavated by a bulldozer. The slabs were commonly tilted up at odd angles, overlapping each other, and split into pieces that could be fit back together. We presume that this pattern of disruption is tectonic in nature, since it occurs adjacent to major fault zones, and also because we are unable to find an alternative explanation. From DELTA, we directly observed breakage of carbonate bodies by bottom

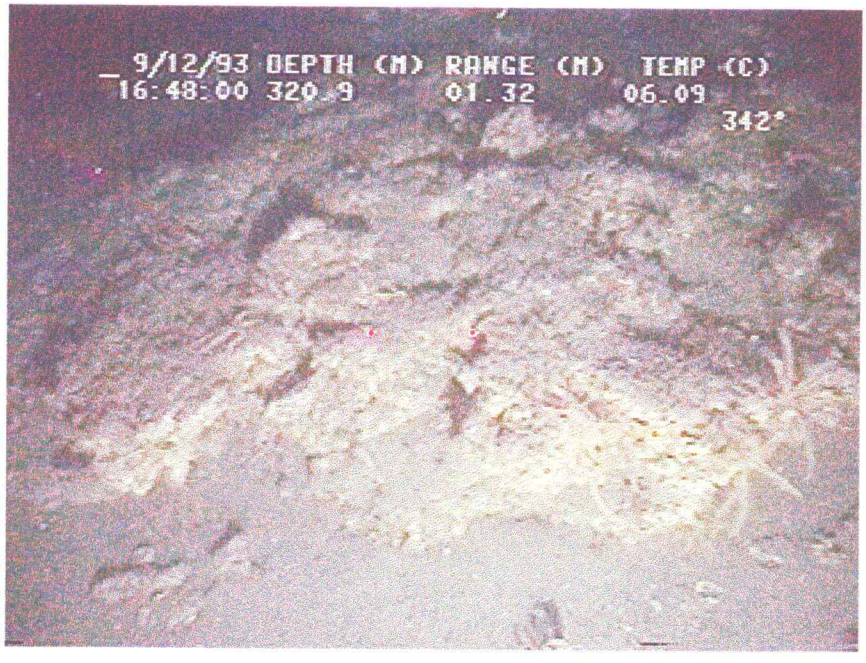

Figure 4.3. DELTA video image of encrusting methane-derived carbonate slabs along the Daisy Bank fault zone, 5 km northwest of Daisy Bank, central Oregon. Red dots are lasers 20 cm apart.

fishing trawl activity, but conclude that breakage of carbonates by this method could not be responsible for the widespread and pervasive disruption we observed. On close inspection, trawl marks could usually be distinguished from tectonic disruption by their plow-like trails, and by the marks left by dragging of carbonate slabs across the bottom. We speculate that the widespread breakage occurs during the high ground accelerations that would occur during large earthquakes. Further study of this phenomenon may lead to an estimate of the accelerations required to produce the type of disruption we have observed from the submersible.

From DELTA, we mapped one of the Daisy Bank scarps into an area of low relief and flat-lying mud deposition. In this area, we observed a fresh scarp striking 290° across the unconsolidated Holocene mud. This fresh break averages 1 m in height, dips steeply south with its south side up, and offsets gray late Pleistocene clays as well as olive-green Holocene muds (Fig. 4.4). Video images and photographs show that the scarp may represent multiple late Pleistocene events, indicated by abrupt vertical changes in oxidation color of the Pleistocene clay, and corresponding abrupt upward increases in bioturbation on the scarp face. At the outcrop scale, we observed both right and left stepping en-echelon morphology, although left-stepping was dominant. Dominant left steps suggest a compressional component of motion along the Daisy Bank fault, also suggested by the 80-90° south dip observed on this segment of the fault.

Sidescan sonar imaged the Daisy Bank fault at the surface from 12 km seaward of the deformation front on the abyssal plain, landward to about the 150 m bathymetric contour on the outer shelf. Landward of this position , the fault may continue, concealed by active shelf sedimentation and erosion, or it may die out. Stonewall Bank, which lies astride the landward projection of the Daisy Bank fault at the 80 m contour, is itself uplifted in similar fashion to Daisy Bank. The bank is divided into northern and southern halves, separated by a fault controlled channel. The entire bank also displays a pervasive WNW trending shear pattern parallel to the overall strike of the Daisy Bank fault zone, and many of the individual fractures have a minor left-lateral separation (Fig. 4.5). We speculate that the Daisy Bank fault probably extends as far landward as Stonewall Bank, which may be located at the southeastern fault

Figure 4.4. Active scarp within the Daisy Bank fault zone. Local vertical component of motion is up to the south, the fault dips steeply to the south. Olive-gray Holocene hemipelagic sediment can be seen draping horizontal surfaces. Gray Late Pleistocene clay is exposed in the scarp face. Red laser dots are 20 cm apart.

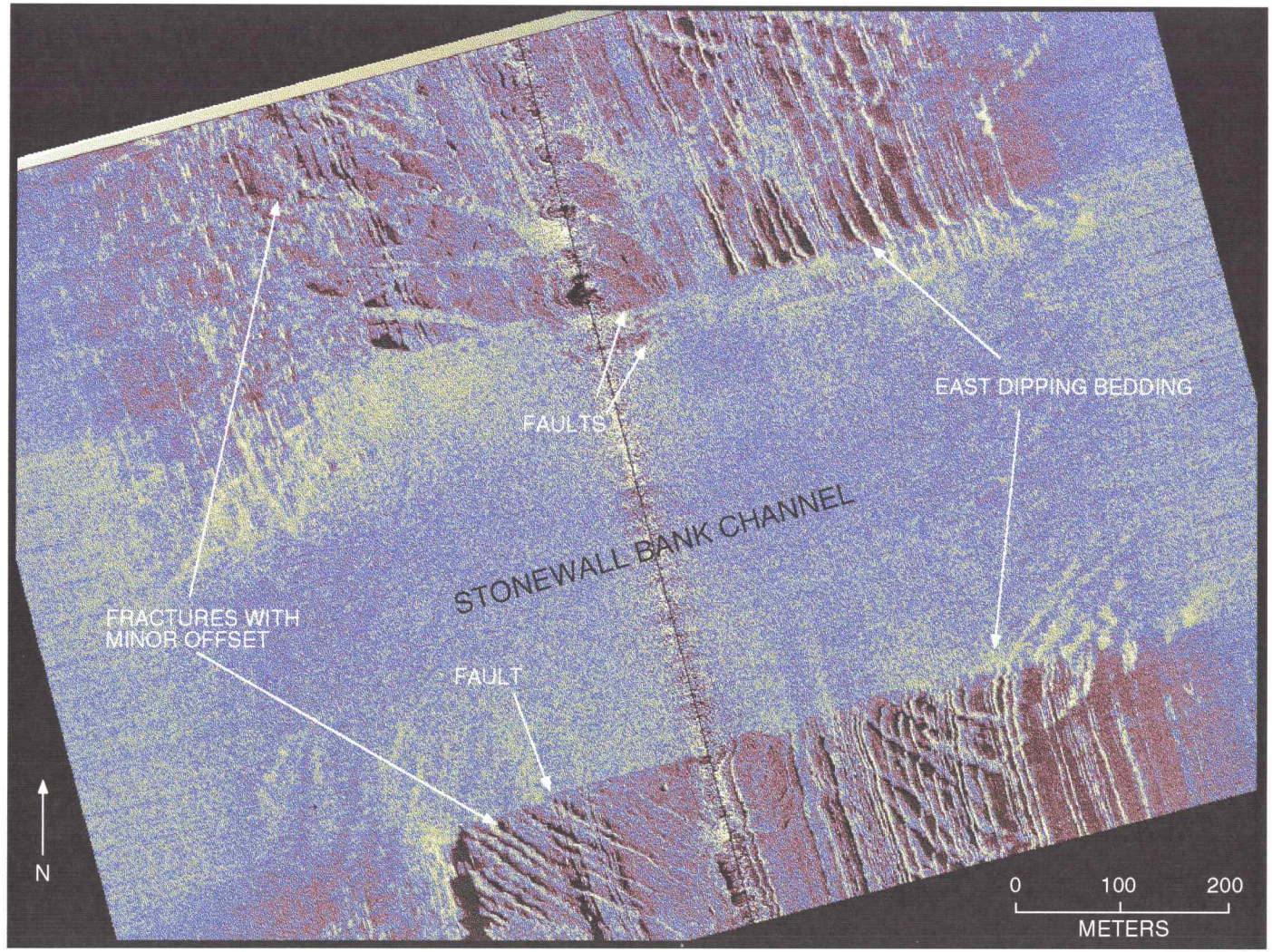

Figure 4.5. AMS 150 sonar swath over Stonewall Bank, Oregon continental shelf. Image shows fault-controlled channel and NW trending fracture set. Swath width = 1 km; resolution = 0.4 m.

tip, and that this uplifted central shelf bank may be a terminal structure of the Daisy Bank fault.

Heceta South Fault

The Heceta South fault is a WNW trending structure that truncates the southern margin of Heceta Bank (Fig. 4.6; see Plate 1 for location). This fault is blind near the bank, shown by reflection profiles, sidescan images, and submersible transects over its trace. Nevertheless, it has a large offset, down to the south, recorded by the downwarping of a Pleistocene lowstand shoreline described more fully in the next section. BS^3 swath bathymetry viewed as a perspective shaded relief image (Fig. 4.6) shows the shoreline angle and an adjacent abrasion platform located seaward of the former seacliff. The bathymetry data show that the shoreline angle at the southern end of Heceta Bank is at a depth of 210 m on the north side of the fault. Based on the bathymetry image, we infer that the shoreline angle and abrasion platform are downdropped to approximately 500 m on the south side of the fault.

We group this fault with the other oblique strike-slip faults on the basis of its similar strike, length, and morphology on the continental slope, although we do not have direct evidence of its slip direction as for the Wecoma fault and Daisy Bank fault. The large vertical offset at the south end of Heceta Bank, assuming the above interpretation of the shoreline offset is correct, could be due to pure dip-slip motion. With the available bathymetry data, which has a large noise component in that region, we are unable to resolve any horizontal offset of the shoreline angle.

Arc Parallel Strike-Slip Faults

In addition to the oblique faults mapped in this study, we investigated several known and inferred arc-parallel faults on the Oregon shelf. These faults are more difficult to investigate because they occur in areas where they are nearly parallel to other structural trends. Because of this geometry, they are less well known and may be under represented on the Oregon Neotectonic map of Goldfinger and others (1992a).

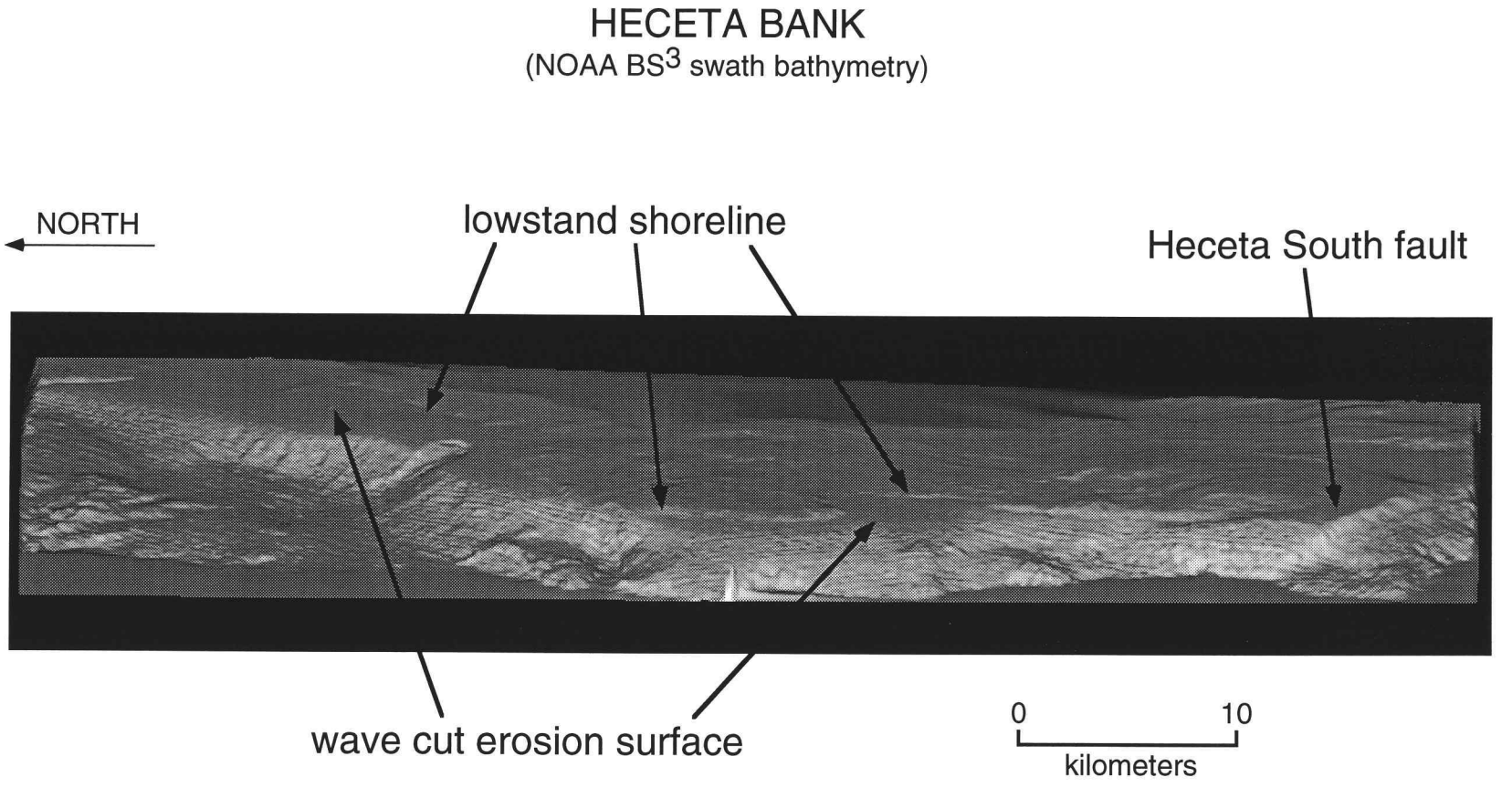

Figure 4.6. Shaded relief perspective plot of NOAA BS^3 swath bathymetry, Heceta Bank, Oregon continental shelf. Shown are the Pleistocene lowstand ersosion surface and shoreline, and the Heceta South fault. View is from the southwest; grid spacing = 100 m; no vertical exaggeration.

Nehalem Bank Fault

The Nehalem Bank fault is located 25 km west of the northern Oregon coast, on the landward side of Nehalem Bank (Plate 1). The fault trends north, gently curving southeastward toward the coast at its southern end. This fault is shown on a cross-section published by Niem and others (1990; Fault F) which we correlate with Fault C of Niem and others (1992). Using a magnetic profile and co-located industry reflection profile, Niem and others (1992) have interpreted the Nehalem Bank fault as the boundary between the Siletzia terrane, (to the east) with a basement of early to middle Eocene oceanic basalt, and Miocene and younger marine sedimentary rocks (to the west). We infer right-lateral slip on the Nehalem Bank fault, which is vertical north of Tillamook Head, flattening to moderate northeast dips as it bends southeastward toward Netarts Bay where we infer the right-lateral fault becomes a thrust. Alternatively, the fault may dip to the west (Niem and others, 1990), however we interpret the west dips from Neim and others (1990) as part of a larger flower structure associated with the Nehalem Bank fault. The southeastern projection of the Nehalem Bank fault coincides with the northern margin of Netarts Bay, where a late Quaternary WNW striking thrust fault, named the Happy Camp fault, has been mapped by Wells and others (1992). The Happy Camp fault involves southward thrusting of Miocene Columbia River Basalt over Pleistocene terrace or fluvial deposits on a northeasterly dipping thrust. Late Quaternary faulting on this structure is clear, but Holocene motion has not been demonstrated. Niem and others (1990) show a section of a high-resolution seismic profile over one strand of the Nehalem Bank fault (their fault F) showing folding and offset of Holocene strata on the inner shelf. OSU single channel reflection profiles and 50 kHz Klein sidescan records collected over the Nehalem Bank fault in 1992 show the fault zone to be a complex structural zone developed in rocks ranging in age from Holocene to Pliocene (Niem and others, 1990) at the seafloor. In addition to the seismic profile shown in Niem and others (1990), Quaternary motion on this fault is suspected because the fault zone has a seafloor expression of approximately 10-20 meters in water depths of 130-150 m, estimated from the sidescan and seismic records. We infer the present surface deformation would have been eroded during the last Pleistocene

lowstand, when the Nehalem Bank fault would have been located on the abrasion platform seaward of the Pleistocene shoreline.

Fulmar Fault

Snavely (1987) has inferred that a major arc-parallel dextral strike-slip fault, the Fulmar fault, underlies much of the Oregon shelf, and truncates the seaward edge of the Eocene Siletz River volcanics, the oceanic basalt unit that forms the basement of western Oregon (Snavely, 1987). Based upon industry test well biostratigraphy, he infers 200 km of dextral slip on this fault, mostly during the Eocene. Tréhu (in prep.), using high-quality seismic refraction and reflection data along an E-W transect at approximately 45° 48' N. latitude, has inferred the location of the western edge of the Siletz River Volcanics in central Oregon based on velocity gradients. The Siletz River basalts are apparently truncated vertically along the refraction profile, with a strong seaward decreasing velocity gradient. Overlying this location is a minor fault in the axis of a young anticline at the seafloor in Plio-Pleistocene strata. We investigated this area using existing nearby reflection profiles, and then at sea using the AMS 150 sidescan sonar and DELTA to locate this structure. We were unable to find any surface expression of this structure in sidescan records, nor in nearby industry reflection profiles. We conclude that the structure overlying the western edge of the Siletz River Volcanics is probably a bending moment normal fault developing along the axis of the active anticline, rather that the Fulmar fault. We have not found any evidence for a throughgoing arc-parallel fault in Neogene strata on the Oregon shelf, and we conclude that the Fulmar fault is not currently active in this part of the central Oregon margin.

Coquille Fault

The Coquille Fault, located on the inner southern Oregon shelf, was first mapped by Clarke and others (1985). We investigated this structure first in 1992 using an analog Klein 50 kHz sidescan sonar, then again in September, 1993 using the AMS 150 kHz digital system. We obtained spectacular records of this major structure in water depths of between 50 and 110 m, northwest of Bandon, Oregon. The rocks exposed at the surface in this area are principally a siliceous diatomaceous unit of late Miocene age,

overlain unconformably by unconsolidated Pleistocene and Holocene sand (Fowler and others, 1971). This unusual unit may be in fault contact with Jurassic-Cretaceous rocks in this area (Fowler and others, 1971), possibly across the Coquille fault, which our records and a nearby Chevron multichannel reflection record show to be a significant structure. Goldfinger and others (1992a) infer approximately 3 kilometers of dextral slip on this structure based on offsets of NE trending fold axes mapped from seismic reflection records. Sidescan records of the Coquille fault (Figure 4.7) show a structurally complex zone of primary and secondary faults and associated folding. The main fault is composed of north-south striking segments in a left-stepping pattern that has an overall NNW trend. The left steps strike E-W, and extend 1-2 km from the main segments. Tight folds, with wavelengths of 20-40 m, are also clearly visible, also striking E-W, slightly more northerly than the left-lateral faults. The folds have a seafloor expression of 2-4 m. We investigated the age of deformation in the Coquille fault zone by searching the sidescan records for signs of deformed Quaternary strata and making DELTA dives on sites of possible young deformation. However, we found in both sidescan records and submersible dives that unconsolidated sediments in this area (60-90 m water depth) are easily re-deposited and moved by even mild wave action, thus no unequivocal evidence of recent deformation of unconsolidated sediment could be found. Nevertheless, the deformation of the Miocene strata suggests that both faults and folds are currently active. The tight folds are well expressed at the seafloor and display an unusual morphology as seen from DELTA. The strata in the anticlinal hinges are separating from underlying beds by "unfolding" along the bedding planes. The upper bedding surfaces break off in tabular blocks that we observed in the bottoms of the synclines. We infer that one of two processes may be occurring: 1) a form of exfoliation of sedimentary rocks not known in subaerial settings, or 2) active folding, causing separation of the uppermost beds which have no confining boundary. As this area was subjected to extensive wave and subaerial erosion during the latest Pleistocene low-stand, we believe that the observed seafloor expression of several meters would not have survived in its present form. The seafloor folds probably are not the result of preferential weathering such as the case for hogback ridges. We observed no variations in lithology that might result in hogback ridge

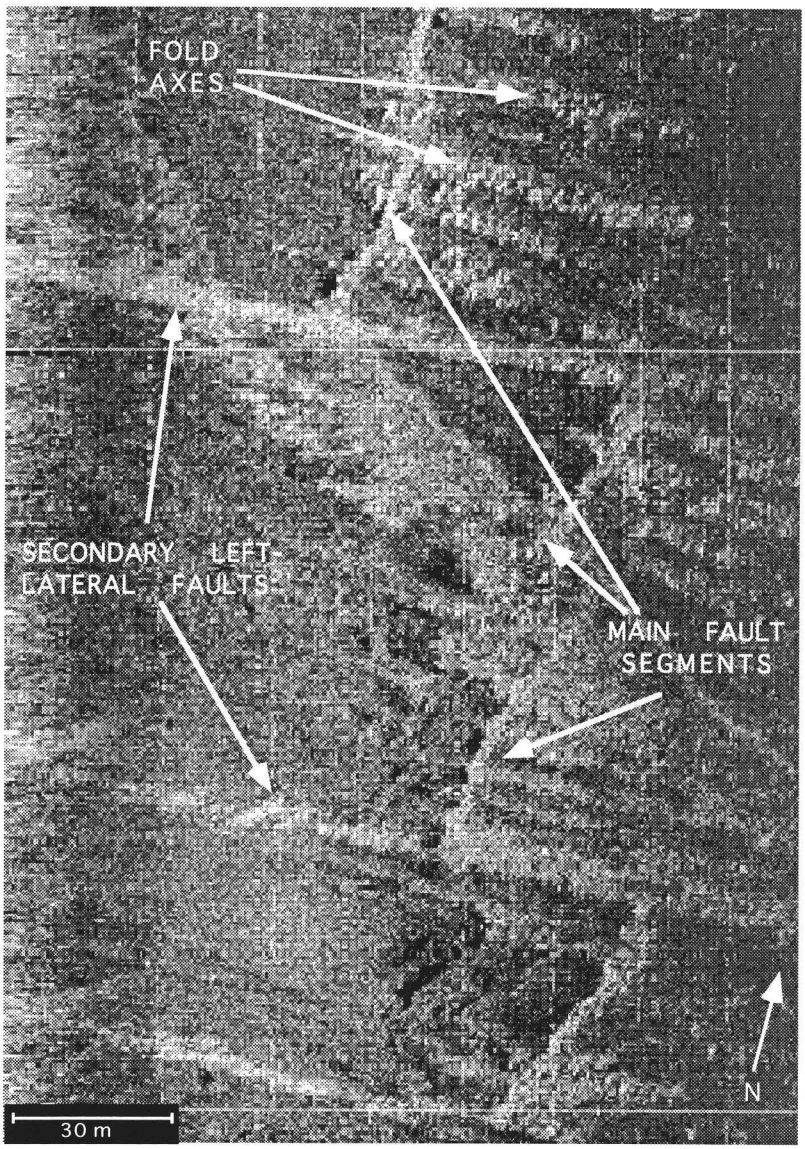

Figure 4.7. Klein 50 kHz sidescan record of the Coquille fault zone off Bandon, Oregon. En echelon main fault segments trend NNE, while fault zone as a whole trends NNW. Subsidiary WNW trending left-lateral faults are also visible, as are active folds, which establish the direction of maximum compressive stress. Water depth 85 m.

formation. We also believe that since the exfoliation observed on the anticlines would rapidly subdue the topographic expression of these features by eroding the anticlinal axes, active growth is required to maintain the observed topography. Despite the somewhat indirect nature of evidence for late Quaternary deformation associated with the Coquille fault, deformation of the marine terraces where the Coquille fault comes ashore (discussed in a later section) demonstrates clearly that this is an active structure.

OREGON'S SUBMARINE BANKS

The Oregon continental shelf includes three major submarine banks, Nehalem, Heceta, and Coquille, separated by two interbank basins, the Newport embayment and the Coos Basin (Fig. 4.8). Significant differences in structure, morphology, uplift history, and surficial geology distinguish the three banks from the interbank basins. Plate 1 illustrates the differences in fold trends between the bank and interbank areas, particularly in the Newport embayment, where fold axes strike WNW to NNW, while the northerly fold trends predominate on Nehalem and Heceta Banks. A similar relationship also occurs in Coos Basin, and the area south of Coquille Bank between Cape Blanco and Cape Sebastian, although fold trends are more variable there. The banks are also distinct from the basins in that at near surface levels they are more highly deformed than the interbank basins. Based on seismic reflection profiles, we observe that folds are tighter, and wavelengths of equivalent structures are shorter than in the two basins. This appears to be the result of greater uplift of the banks, discussed below, which has brought older, more deformed rocks to the surface. We also observe that many folds cannot be traced across the seaward boundaries of the banks, thus the bank/interbank boundary is in many locations a structural discontinuity. We also note that the major oblique strike-slip faults that cut the Oregon slope and outer shelf (Appelgate and others, 1992; Goldfinger and others, 1992b; Goldfinger and others, in press; Chapter 5) either bound the northern or southern flanks of the three banks, or are in one of the two interbank areas (Plate 1; see also Fig. 4.6).

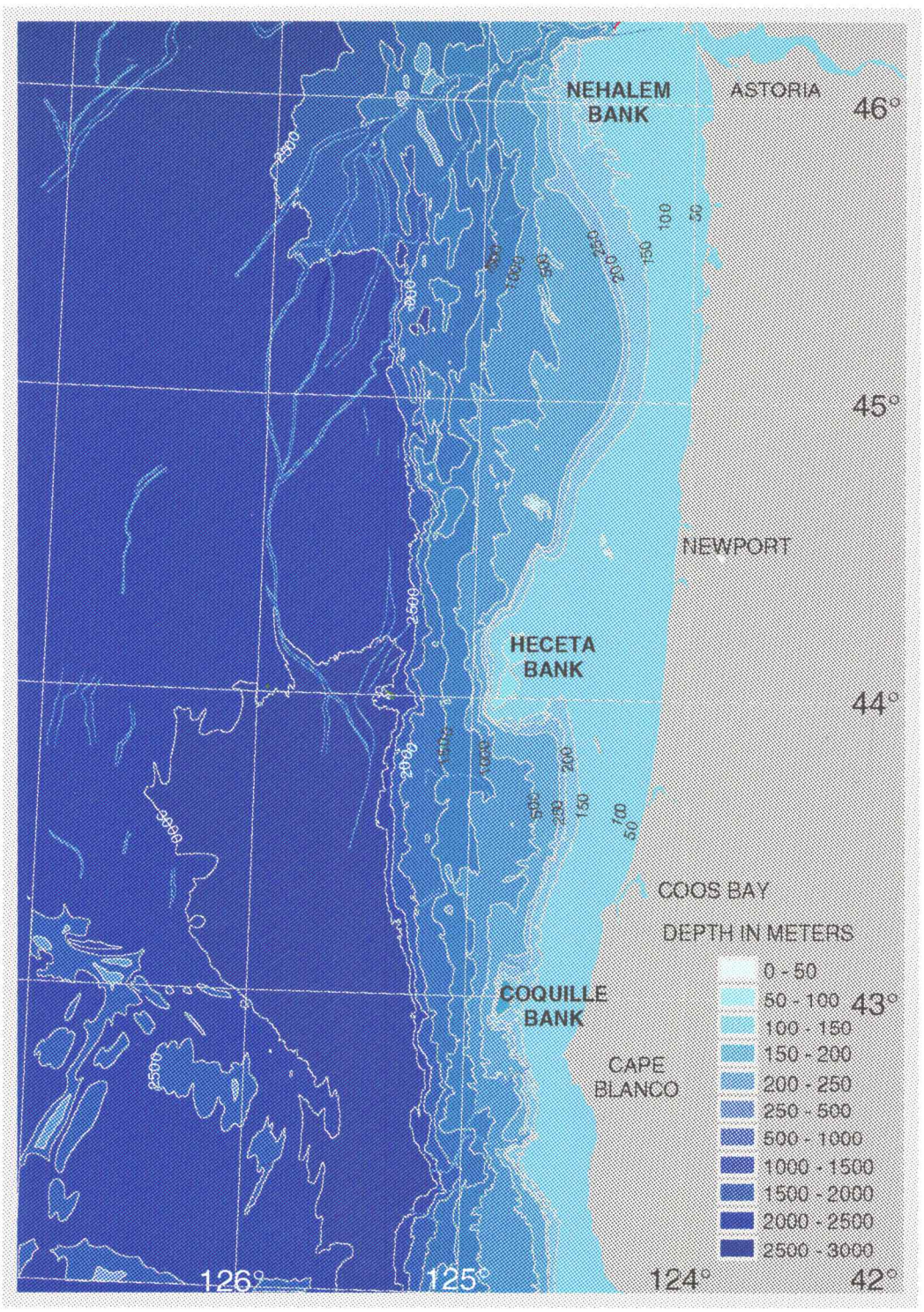

Figure 4.8. Physiography and bathymetry of the Oregon continental margin showing three major submarine banks. See text for discussion.

The morphology of the shelf break in Oregon also reflects the differences between the bank and interbank areas. The shelf break varies greatly in distance from the coast, from 22 km in the Newport embayment and 37 km in the Coos Basin, to 68 km at the seaward edge of Heceta Bank, 62 km at Nehalem Bank, and 34 km at Coquille Bank (Plate 1; Fig 4.8).

Kulm and Fowler (1974) determined the paleodepth of deposition for surficial samples from the Oregon continental shelf and upper slope. The three major submarine banks have been uplifted 200-1000 m, mostly since early Pliocene time, with 100-200 m of subsidence since the Pleistocene. During the same time period, little or no uplift has occurred in the Coos Basin and Newport embayment.

Vertical Tectonics of Heceta Bank

Heceta Bank is the largest of the three structurally uplifted banks on the Oregon shelf. The bank was surveyed by NOAA using an experimental shallow water swath bathymetry system (known as BSSS or BS^3). The data from this survey revealed a Pleistocene low-stand shoreline (Fig. 4.6) rimming the bank that is one of a very small number of lowstand sea-level indicators known from the world's continental shelves. The shoreline is expressed as a seacliff that averages 10 m in height, and a plainly visible abrasion platform seaward of the seacliff. Despite nearly one kilometer of post-Miocene uplift , the present elevation of this lowstand shoreline indicates that much of Heceta Bank has undergone late or post Pleistocene subsidence. Similar observations were made by Kulm and Fowler (1974) based on coring and drilling of Pleistocene shallow water deposits in present water depths of 150-200 m. The depth of the shoreline angle is highest at its northern end at 114 m. The depth of the shoreline angle increases to 210 m at the southern end of the bank, due to overall tilting to the south. The depth of the shoreline angle shown in Figure 4.9 also reflects numerous local faults and folds that deform the outer edge of Heceta Bank, particularly at its southern end near the Heceta South fault. The age of this shoreline is not known, however its northern end is at a depth close to 120 m, frequently reported as the depth of the 18 ka Pleistocene sea-level lowstand (Chappel

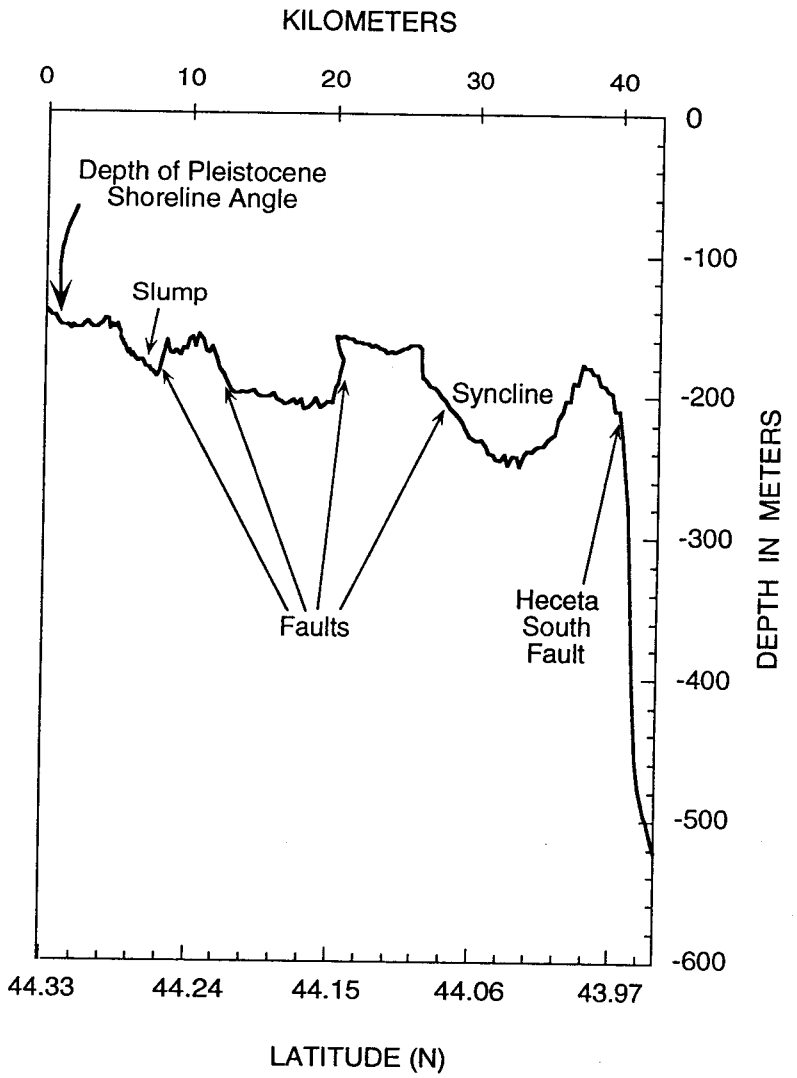

Figure 4.9. Elevation of the Pleistocene low-stand shoreline angle at Heceta Bank, Oregon. Variations in elevation are caused by deformation and tilting of Heceta Bank. Data from NOAA BS^3 swath bathymetry.

and Shackleton, 1986; Matthews, 1990; Fairbanks, 1989). Alternatively, it may be another lowstand of similar depth at approximately 135 ka (Fairbanks, 1989), or an even older event. We made several transects across the Pleistocene shoreline angle in DELTA in an attempt to recover datable material, but were unsuccessful, and found the shoreline difficult to locate from DELTA. The late Quaternary subsidence of Heceta Bank is a reversal of the long term vertical motion (uplift) of the bank as recorded in the biostratigraphy of bank sediments, and suggests that the vertical tectonics of the Oregon shelf are complex in detail.

RELATIONSHIP OF ACTIVE SHELF STRUCTURES TO COASTAL DEFORMATION

We have found abundant evidence of active deformation in the near coastal region of Oregon continental shelf, suggesting to us that deformation onshore should also be occurring on some of the shelf structures we have mapped that project to the coast. Offshore structures are difficult to correlate directly to coastal structures because seismic records in shallow water and hard sand bottoms tend to reflect seismic energy, resulting in poor seismic penetration, and numerous water bottom multiples that obscure subsurface relationships. In addition, topographic evidence of active deformation on the sea floor is continuously eroded by wave action at inner shelf water depths.

Evidence for structural deformation onshore along the Oregon coast is found primarily in the Pleistocene marine terraces which are present along most of the coast. Late Quaternary deformation of terraces in southern Oregon is well documented at Cape Blanco and the Coos Bay area (Kelsey, 1990; McInelly and Kelsey, 1990; Muhs and others, 1990). Cape Blanco is deformed by a WNW trending anticline that deforms Tertiary strata and the overlying marine terraces (Kelsey, 1990). We have mapped this anticline offshore on the same trend to the seaward edge of Coquille Bank, 34 km from the coast (Plate 1; Goldfinger and others, 1992a). Coos Bay lies in the axis of the Coos Bay syncline, which can also be traced offshore, along with several adjacent folds. Marine terraces in the Coos Bay area are offset by numerous flexural-slip reverse faults (McInelly and Kelsey, 1989) which are also observed in the reflection records NNW of Coos Bay. We believe that active folds and associated flexural slip faults also project onshore near Tillamook, Netarts, and Siletz Bays. At the mouth of the Coquille River near the town of Bandon, the Coquille fault offsets the lowest marine terrace (A.R. Niem, pers. comm. 1993). Dips exceeding 45° can be observed in the terrace deposits exposed in the seacliff. Although we were unable to find definitive evidence for late Quaternary deformation in the nearshore waters, the terrace deformation is clear evidence that this structure has been active in latest Quaternary time.

Along the central Oregon coast, we mapped Quaternary faults and or folds seaward of Alsea, Yaquina and Siletz Bays. Alsea Bay lies between the

landward projections of two normal faults that cut the seafloor 5 km offshore, although H. Kelsey did not observe these faults in his mapping of the Florence to Cape Foulweather section of the coast (H. M. Kelsey, pers. comm., 1992). The lowest marine terrace and wave cut platform between Heceta Head and Yaquina Bay is downwarped in the vicinity of Alsea Bay as noted by Kelsey and others (1992). Oblique aerial photographs clearly show this downwarping to be a long-wavelength fold, the strike of which is not known (C. Goldfinger, unpub. data). Yaquina Bay lies on the downthrown side of a fault that has offset the 125 ka terrace approximately 75 m (Plate 1; Kelsey and others, 1992). Although the lowest marine terrace appears to be continuous from the south to the north side of the bay, the lowest terraces on each side are apparently not the same terrace, based on soil chronology. Minor deformation of this terrace and wave cut platform can be seen from the beach between Jumpoff Joe and the North Jetty in Newport and may be associated with the Newport fault of Kelsey and others (1992), which has not been mapped directly.

Based on reconnaissance field mapping in 1992 by Goldfinger, and in 1993 by McNeill, the lowest marine terrace and wave cut platform are deformed near Siletz Bay. The terrace and platform dip gently north from an elevation of 12 m (wave cut platform) at Government Point to 3 m at Fishing Rock. The platform and terrace are faulted down to the north at Fishing Rock and Fogarty Creek, and the wave cut platform is faulted and warped below sea-level from Fishing Rock northward to Taft at the northern margin of Siletz Bay. A peat interval in the terrace is tilted to the vertical adjacent to the fault at Fishing Rock, which faults the terrace deposits against Miocene Depoe Bay basalt. The terrace dips northward from Fishing Rock to the southern end of the Siletz Bay spit 3.5 km to the north. North of Siletz Bay, between Taft and the D River, the terrace strata are flat lying, and the underlying wave cut platform is exposed in small creek beds just below beach level (L. McNeill and C. Goldfinger, unpub. data). The terrace units exposed on either side of the bay are apparently the same terrace (Komar and Shih, in press), unlike those at Yaquina Bay. Based on the northward dips south of the Bay, and the beach level exposure north of the bay, we estimate the wave cut platform projects to a depth of 30 m below sea level, adjacent to Siletz Bay. Goldfinger and others (1992a) mapped an active NNE trending syncline, faulted at its

northern limb that projects toward the coast at the position of the Siletz Bay entrance (Plate 1; the fold is shown as inferred, which refers to uncertainty about its strike, not its existence). The onshore deformation observed (L. McNeill and C. Goldfinger, unpub. data) is consistent with the asymmetric faulted syncline observed offshore.

Quaternary mapping is somewhat more sparse for much of the northern Oregon coast, and is made more difficult by the presence of numerous basaltic headlands of Columbia River Basalt that make correlation of the patchy intervening terraces difficult (Mulder, 1992). The Happy Camp fault of Wells and others (1992), discussed previously, is located at the northern margin of Netarts Bay. The bay lies on the downthrown side of this fault which thrusts Columbia River Basalt of middle Miocene age southward over Pleistocene marine terrace or fluvial deposits. We have tentatively correlated this fault with the Nehalem Bank fault discussed previously, which projects onshore at the northern margin of Netarts Bay. Along the northern margin of Tillamook Bay, the Tillamook Bay fault, a WNW striking high-angle fault also cuts Columbia River Basalt (Wells and others, 1992). No exposure of terrace strata with which to test for Quaternary deformation is found at the coastal location of the Tillamook Bay fault. We have tentatively correlated the Tillamook Bay fault with an unnamed fault mapped offshore (Plate 1; Goldfinger and others, 1992a) that has been active in the late Quaternary. The high-angle fault mapped from the middle shelf to the upper slope marks the southern boundary of Nehalem Bank, and projects toward the coast at the position of Tillamook Bay. This fault offsets fold axes left-laterally and has an up to the north vertical component. Onshore, the Tillamook Bay fault is also up to the north, steeply dipping, and has approximately the same strike as the offshore fault (Plate 1). The Tillamook Bay fault may offset a Columbia River Basalt contact 12 km left-laterally (R. E. Wells, pers. comm. 1992).

DISCUSSION

We find an abundance of evidence the Oregon continental shelf has been tectonically active in late Quaternary time. We have mapped active faults and folds over much of the shelf with seismic reflection records, and have investigated a number of these structures in detail using high resolution sidescan sonar and direct observations from submersibles. We find that the Oregon shelf has deformed significantly since the last Pleistocene sea-level lowstand, as evidenced by the recency of motion on submarine faults, the warped Pleistocene shoreline at Heceta Bank, and the onshore deformation of marine terraces observed by several investigators. The investigation of active structures on the Oregon shelf has relevance to the larger investigation of seismicity of the Cascadia subduction zone in three respects: (1) The importance of local deformation to the interpretation of coseismically buried coastal marshes; (2) The possible interplate tectonic role played by the structurally distinct submarine banks; and (3) The relationship of forearc deformation to the accumulation of elastic strain energy required for great earthquakes.

LOCAL STRUCTURES AND THE COASTAL MARSH RECORD

Inasmuch as the principal evidence for seismic events of any size is found in intertidal marsh deposits along the coasts of California, Oregon and Washington, a first order question when considering the significance of these marsh burial events must be what types of tectonic or non-tectonic events are capable of generating the observed marsh stratigraphy? Subsidence of hundreds of kilometers of coastline in response to elastic strain release during great earthquakes is one possibility. Our investigations of active tectonics just seaward of the marsh burial sites, combined with evidence of deformation of marine terraces in Oregon, suggests that motion on upper plate faults and folds may also be important. Marsh stratigraphy is extraordinarily sensitive to relative sea level changes, and the total thickness of the Holocene marsh sequence is very thin, 12-18 m, such that relatively minor upper plate faulting could have a large impact on the Holocene stratigraphy found in coastal bays

and estuaries. We find an apparent association between late Quaternary faults and folds mapped onshore and offshore, and bays and estuaries with buried marshes. Buried marsh sites adjacent to Quaternary upper plate structures are found at the Coquille River (Coquille fault), Coos Bay (South Slough syncline, Barview-Empire fault and other flexural slip faults), Alsea Bay (offshore normal faults), Yaquina Bay (Yaquina Bay fault), Siletz Bay (Fogarty Creek and Fishing Rock faults, Siletz Bay syncline and unnamed thrust fault), Netarts Bay (Happy Camp-Nehalem Bank fault) and Tillamook Bay (Tillamook Bay fault). Motion on all of these structures would cause relative downward motion of the adjacent coastal marshes.

An important question for the interpretation of marsh stratigraphy is whether or not the upper plate structures move in concert with, or independent of, the subduction megathrust. Low levels of seismicity are observed from the submarine forearc, possibly on some of these structures (NOAA, unpublished T-phase data; J. Nabelek, OSU, pers. comm., 1993), but at much lower rates than expected (Acharya, 1992). The Cascadia subduction zone as a whole is anomalously quiet in comparison to subduction zones worldwide by almost an order of magnitude (Acharya, 1992). This relationship holds even when comparing Cascadia seismicity to "aseismic" subduction zones and modern "seismic gaps". This can be interpreted in two ways: The subduction zone is completely locked, or some degree of aseismic slip is occurring. The anomalously low seismicity of the forearc and the subduction interface are difficult to explain only in terms of a locked plate boundary. We agree with Acharya (1992) that the seismic slip rate in Cascadia is probably much lower than the rate of plate convergence, a ratio called the seismic slip coefficient by Pacheco and others (1993), who found values much less than 1.0 for most of the 19 subduction zones studied in their investigation. Thus the quiescence of upper plate faults may not indicate that they only move during megathrust events, but simply that they have long repeat times. On the other hand, investigations of upper plate response to subduction earthquakes indicate that megathrust events often trigger upper plate faulting (see summary in Yeats and others, in prep.).

We infer that the marsh stratigraphy probably records a mixture of plate boundary relaxation (large earthquakes) and upper plate fault slip and fold growth (smaller earthquakes), regardless of the relative timing of these events.

There may also be a record of some difficult to distinguish non-tectonic events (Nelson, 1987; 1992; Nelson and Personius, in press). Discovery and detailed investigations of the Seattle fault have shown that an earthquake on an upper plate structure can and did result in a marsh stratigraphy indistinguishable from that of buried marshes on the Washington and Oregon coasts (Atwater, 1992; Bucknam and others, 1992; Yount and Holmes, 1992). An earthquake on this structure caused the rapid submergence of a high marsh located on the downthrown block about 1100 years ago, and generated a tsunami that deposited a layer of marine sand over the marsh site. It is not clear whether or not this event coincided with an interplate earthquake. It is reasonable to expect that some of the structures we and others have mapped along the Oregon coastal region have had similar earthquakes, and that the burial of marshes and generation of local tsunami resulted from some of these events, as occurred on the Seattle fault. We suggest that the evidence for such events are included in the marsh stratigraphic record throughout the Cascadia margin. If this inference is correct, vertical movements as recorded in marsh stratigraphy may be used to recognize earthquakes, but the magnitude of vertical movements should be treated with caution. Estimates of co-seismic vertical movement should be considered suspect when used either to infer the location of a zero isobase, detect trends in earthquake characteristics from bay to bay, or as input to elastic dislocation models of interplate earthquakes (Yeats and others, in prep.).

OREGON SUBMARINE BANKS AS ASPERITIES

We have briefly summarized some of the distinctive features of the three major submarine banks in Oregon from a structural perspective. A detailed analysis of the origins and significance of these prominent features is the subject of a future paper, however we speculate here on the potential importance of the banks to the investigation of interplate earthquakes on the central Cascadia margin. Kulm and Fowler (1974) note that Coquille and Heceta Banks are the centers of positive free air gravity anomalies, while the interbank areas are the centers of large negative anomalies, indicating thick

sections of low-density sedimentary rocks. Nehalem bank can be divided into two parts, in inner half floored with probable Eocene Siletz River volcanics (Niem and others, 1992), and an outer half composed of Miocene and Pliocene indurated sand and siltstones described by Niem and others (1992). The division is a structural one, occurring at the Nehalem Bank Fault. In all three cases, the banks are composed of higher strength rocks than their counterparts along the strike of the margin, and are separated from the Pliocene and younger accretionary wedge at the shelf break by a major structural and bathymetric discontinuity. Goldfinger and others (Chapter 5) have estimated the geometry of the locked plate interface on the basis of thermal considerations, aftershock data from the comparable Nankai subduction zone, and inferences drawn about the nature of the Oregon submarine banks. They have assumed that the majority of the accretionary wedge is aseismic, and that the updip limit of the seismogenic zone may occur at the lithologic and strength boundary we infer for the seaward flanks of the major submarine banks. This is in contrast to Hyndman and Wang (1993) who place most of the locked zone within the accretionary wedge (see Chapter 5 for a discussion of the two hypotheses). Between the banks, they assume that the accretionary wedge is aseismic from the deformation front 60 km landward. This assumption is based on the Washington seismicity reported in Crosson and Owens (1987) and on the aftershock area of two Nankai earthquakes in 1944 and 1946 (Chapter 5). In both cases, the seaward 60 km of the accretionary wedge is essentially aseismic with respect to background seismicity (Washington) and great earthquake aftershocks (Nankai). See Goldfinger and others (Chapter 5) for a comparison of the Nankai and Cascadia subduction zones. In Figure 5.9, which only considers Heceta Bank and Nehalem Bank due to the lack of thermal constraints south of 44° 30' N, it can be seen that if our assumptions are valid, the locked zone is either narrow or non-existent between Heceta and Nehalem Banks. The importance of the submarine banks in the context of a locked plate interface is apparent even if our chosen boundaries are shifted considerably seaward or landward. We suggest that the banks may represent asperities within the locked zone, or if our updip seismicity limit is shifted slightly landward, they may comprise the entire locked zone in central Oregon, with a 100 km gap between Nehalem and Heceta banks.

We have also noted that the major oblique left-lateral faults in Oregon either bound the major submarine banks, or are located between the banks. The Tillamook Bay fault, not included in other discussions of oblique strike-slip faulting due to its more limited length and our more limited data, is located at the southern flank of Nehalem Bank, supporting this observation. These relationships suggest a tectonic framework similar to that in the central Aleutians as described by Geist and others (1988) and by Ryan and Scholl (1993), in which the Aleutian forearc is divided by oblique structural trends that define rhomboidal rotating blocks driven by oblique subduction of the Pacific plate beneath the arc. Unlike Cascadia, the Aleutian blocks are well defined by upper plate seismicity, bathymetric trends, and rupture limits of major interplate earthquakes (Ryan and Scholl, 1993). Nevertheless, the similarities, if on a smaller scale, are apparent and warrant further investigation. If the banks do represent high strength asperities on the plate interface, they may also be the nucleation sites of past and future subduction earthquakes as is the case for the central Aleutian blocks (Geist and others, 1988; Ryan and Scholl, 1993).

CONCLUSIONS

The Oregon continental shelf is characterized by active deformation subsequent to the latest Pleistocene lowering of sea-level at 18 ka. Active folds, strike-slip faults, and flexural slip faults offset Holocene and Pleistocene sediments in numerous locations across the shelf. We find an association between the coastal bays/estuaries in which co-seismic burial of marshes has occurred, and late Quaternary faults and folds. In all studied cases where a bay/estuary system is adjacent to a mapped upper plate structure, the bay or estuary lies either on the downthrown block of a fault, or in the axis of a syncline. On this basis, we argue for the importance of upper plate structures in the vertical tectonics of the Oregon coast. We infer that the coastal marsh stratigraphy observed by many investigators is probably recording a mixture of interplate, intraplate, and possibly some non-tectonic events. Whether or not these upper plate faults move in concert with, or independent of the megathrust, the magnitude of vertical motion inferred from marsh stratigraphy cannot be directly used to model the elastic response of the forearc to subduction earthquakes. These are preliminary results and further investigation of the nature and distribution of active faults in the coastal areas of the Cascadia margin is needed to test the hypotheses presented here.

The structural contrasts between the three Oregon submarine banks and the interbank basins suggests that they may be analogs to the high-strength rotating blocks found in the Aleutian arc under similar conditions of oblique subduction. If the analogy between the segmented blocks of the Aleutian arc and the Oregon banks is valid, the banks, like the Aleutian blocks, may act as asperities on the plate interface where subduction stresses are concentrated and where nucleation of interplate earthquakes may occur.

REFERENCES CITED

Acharya, H., 1992, Comparison of seismicity parameters in different subduction zones and its implications for the Cascadia subduction zone: Journal of Geophysical Research, v. 97, p. 8831-8842.

Appelgate, B., Goldfinger, C., Kulm, L.D., MacKay, M., Fox, C.G., Embley, R.W., and Meis, P.J., 1992, A left lateral strike slip fault seaward of the central Oregon convergent margin: Tectonics, v. 11, p. 465-477.

Atwater, B.F., 1987, Evidence for great Holocene earthquakes along the outer coast of Washington State: Science, v. 236, p. 942-944.

Atwater, B.F., 1992, A Seattle tsunami 1100 years ago: Geological Society of America Abstracts with Programs, v. 24, p. 4.

Atwater, B.F., and Yamaguchi, D.K., 1991, Sudden, probably coseismic submergence of Holocene trees and grass in coastal Washington state: Geology, v. 19, p. 706-709.

Barnard, W.D., and McManus, D.A., 1973, Planktonic foraminiferan-Radiolarian stratigraphy and the Pleistocene-Holocene boundary in the northeast Pacific: Geological Society of America Bulletin, v. 84, p. 2097-2100.

Blackwelder, B.W., Pilkey, O.R., and Howard, J.D., 1979, Late Wisconsinan sealevels on the southeast U. S. Atlantic shelf based on in-place shoreline indicators: Science, v. 204, p. 618-620.

Bucknam, R.C., Hemphill-Haley, E., and Leopold, E.B., 1992, Abrupt uplift within the past 1700 years at southern Puget sound, Washington: Science, v. 258, p. 1611-1614.

Chappel, J., and Shackleton, N.J., 1986, Oxygen isotopes and sea-level: Nature, v. 324, p. 137-140.

Clarke, S.H., Field, M.E., and Hirozawa, C.A., 1985, Reconnaissance geology and geologic hazards of the offshore Coos Bay Basin, Oregon: U.S. Geological Survey Bulletin 1645, 41 p.

Crosson, R.S., and Owens, T.J., 1987, Slab geometry of the Cascadia subduction zone beneath Washington from earthquake hypocenters and teleseismic converted waves: Geophysical Research Letters, v. 14, p. 824-827.

Curray, J.R., 1965, Late Quaternary history, continental shelfs of the U. S., *in* Wright, H.E., and Frey, D.G., eds., The Quaternary of the United States: Princeton, N.J., Princeton Univ. Press, p. 723-735.

Darienzo, M.E., and Peterson, C.D., 1990, Episodic tectonic subsidence of late Holocene salt marshes, northern Oregon central Cascadia margin: Tectonics, v. 9, p. 1-22.

Fairbanks, R.G., 1989, A 17,000-year glacio-eustatic sea level record: influence of glacial melting rates on the Younger Dryas event and deep-ocean circulation: Nature, v. 342, p. 637-642.

Fowler, G.A., Orr, W.N., and Kulm, L.D., 1971, An upper Miocene diatomaceous rock unit on the Oregon continental shelf: Journal of Geology, 79, p. 603-608.

Geist, E.L., Childs, J.R., and Scholl, D.W., 1988, The origin of summit basins of the Aleutian Ridge: Implications for block rotatio of the arc massif: Tectonics, v. 7, p. 327-341.

Goldfinger, C., Kulm, L.D., and Yeats, R.S., 1992a, Neotectonic map of the Oregon continental margin and adjacent abyssal plain: Oregon Department of Geology and Mineral Industries, Open-File Report O-92-4, scale 1:500,000.

Goldfinger, C., Kulm, L.D., Yeats, R.S., Appelgate, B., MacKay, M., and Cochrane, G.R., in press, Active strike-slip faulting and folding of the Cascadia plate boundary and forearc in central and northern Oregon, *in* Rogers, A.M., Kockelman, W.J., Priest, G., and Walsh, T.J., eds., Assessing and reducing earthquake hazards in the Pacific Northwest: U.S. Geological Survey Professional Paper 1560.

Goldfinger, C., Kulm, L.D., Yeats, R.S., Appelgate, B., MacKay, M., and Moore, G.F., 1992b, Transverse structural trends along the Oregon convergent margin: implications for Cascadia earthquake potential: Geology, v. 20, p. 141-144.

Hyndman, R.D., and Wang, K., 1993, Thermal constraints on the zone of major thrust earthquake failure: the Cascadia subduction zone: Journal of Geophysical Research, v. 98, p. 2039-2060.

Kelsey, H.M., 1990, Late Quaternary deformation of marine terraces on the Cascadia subduction zone near Cape Blanco, Oregon: Tectonics, v. 9, p. 983-1014.

Kelsey, H.M., Mitchell, C.E., Weldon, R.J.II, Engebretson, D., Ticknor, R., and Bockhiem, J., 1992, Latitudinal variation in surface uplift from geodetic, wave-cut platform and topographic data, Cascadia margin: Geological Society of America Abstracts with Programs, v. 24, p. 37.

Komar, P.D., Neudeck, R.H., and Kulm, L.D., 1972, Observations and significance of deep-water oscillatory ripple marks on the Oregon continental shelf, *in* Swift, D.J.P., Duane, D.B., and Pilkey, O.H., eds., Shelf sediment transport: Stroudsburg, Pennsylvania, Dowden, Hutchinson and Ross, Inc., p. 601-619.

Komar, P.D., and Shih, S.-M., in press, Sea-cliff erosion along the Oregon Coast: Coastal Sediments.

Kulm, L.D., and Fowler, G.A., 1974, Oregon continental margin structure and stratigraphy: a test of the imbricate thrust model, *in* Burke, C.A., and Drake, C.L., eds., The geology of continental margins: New York, Springer-Verlag, p. 261-284.

Kulm, L.D., and Suess, E., 1990, Relation of carbonate deposits and fluid venting: Oregon accretionary prism: Journal of Geophysical Research, v. 95, p. 8899-8915.

Kulm, L.D., Roush, R.C., Harlett, J.C., Neudeck, R.H., Chambers, D.M., and Runge, E.J., 1975, Oregon continental shelf sedimentation: Interrelationships of facies distribution and sedimentary processes: Journal of Geology, v. 83, p. 145-175.

Matthews, R.K., 1990, Quaternary sea-level change, *in* Panel on Sea-Level Change, ed., Sea Level Change: Washington, DC, National Academy Press, p. 88-103.

McInelly, G.W., and Kelsey, H.M., 1989, Holocene and Late Pleistocene tectonic deformation of the Whiskey Run in the Cape Arago-Coos Bay area, coastal Oregon: Geological Society of America Abstracts with Programs, v. 21, p. 115.

McInelly, G.W., and Kelsey, H.M., 1990, Late Quaternary tectonic deformation in the Cape Arago-Bandon region of coastal Oregon as deduced from wave cut platforms: Journal of Geophysical Research, v. 95, p. 6699-6713.

Muhs, D.R., Kelsey, H.M., Miller, G.H., Kennedy, G.L., Whelan, G.F., and McInelly, G.W., 1990, Age estimates and uplift rates for late Pleistocene marine terraces: southern Oregon portion of the Cascadia forearc: Journal of Geophysical Research, v. 95, p. 6685-6698.

Mulder, R.A., 1992, Regional tectonic deformation of the North Oregon coast as recorded by Pleistocene marine terraces: Portland, Oregon, Portland State University, M.S. thesis, 96 p.

Nelson, A.R., 1987, Apparent gradual rise in relative sea level on the south-central Oregon coast during the late Holocene--Implications for the great Cascadia earthquake hypothesis: EOS (Transactions, American Geophysical Union), v. 68, p. 1240.

Nelson, A.R., 1992, Great subduction zone earthquakes in the Pacific Northwest? Differentiating coseismic from non-tectonic tidal marsh deposits along the Oregon Coast, *in* Proceedings, Association of Engineering Geologists 35th Annual Meeting, Los Angeles, 1992, p. 284-290.

Nelson, A.R., and Personius, S.F., in press, The potential for great earthquakes in Oregon and Washington: An overview of recent coastal geologic studies and their bearing on segmentation of Holocene ruptures, central Cascadia subduction zone, *in* Rogers, A.M., Kockelman, W.J., Priest, G., and Walsh, T.J., eds., Assessing and reducing earthquake hazards in the Pacific Northwest: U.S. Geological Survey Professional Paper 1560.

Niem, A.R., MacLeod, N.S., Snavely, P.D., Jr., Huggins, D., Fortier, J.D., Meyer, H.J., Seeling, A., and Niem, W.A., 1992, Onshore-offshore geologic cross section, northern Oregon Coast Range to continental slope: Portland, OR, State of Oregon Department of Geology and Mineral Industries, Special Paper 26, 10 p.

Niem, A.R., Snavely, P.D., Jr., and Niem, W.A., 1990, Onshore-offshore geologic cross section from the Mist gas field, northern Oregon coast range, to the northwest Oregon continental shelf: Oregon Department of Geology and Mineral Industries, Oil and Gas Investigation 17, 46 p.

Pacheco, J.F., Sykes, L.R., and Scholz, C.H., 1993, Nature of seismic coupling along simple plate boundaries of the subduction type: Journal of Geophysical Research, v. 98, p. 14,133-14,159.

Peterson, C.P., Loubere, P.W., and Kulm, L.D., 1984, Stratigraphy of the continental shelf and coastal region, *in* Kulm, L.D., and others, eds., Atlas of the Ocean Margin Drilling Program, Western North American Continental Margin and Adjacent Ocean Floor off Oregon and Washington, Region V: Joint Oceanographic Institutions, Inc., Marine Science Internations, Woods Hole, MA, sheet 30 with text.

Ritger, S., Carson, B., and Suess, E., 1987, Methane derived authigenic carbonates formed by subduction-induced pore-water expulsion along the Oregon/Washington margin: Geological Society of America Bulletin, v. 98, p. 147-156.

Ryan, H.F., and Scholl, D.W., 1993, Geologic implications of great interplate earthquakes along the Aleutian arc: Journal of Geophysical Research, v. 98, p. 22,135-22.146.

Sample, J.C., Reid, M.R., Tobin, H.J., and Moore, J.C., 1993, Carbonate cements indicate channeled fluid flow along a zone of vertical faults at the deformation front of the Cascadia accretionary wedge (northwest U.S. coast): Geology, v. 21, p. 507-510.

Snavely, P.D., Jr., 1987, Tertiary geologic framework, neotectonics, and petroleum potential of the Oregon-Washington continental margin, *in* Scholl, D.W., Grantz, A., and Vedder, J.G., eds., Geology and resource potential of the continental margin of western North America and adjacent ocean basins-Beaufort sea to Baja California: Houston, Circum-Pacific Council for Energy and Mineral Resources, p. 305-335.

Tréhu, A.M., Lin, G., Maxwell, E., Goldfinger, C., in prep., A seismic reflection profile across the Cascadia subduction zone offshore central Oregon: New constraints on the deep crustal structure and on the distribution of methane in the accretionary prism.

Wells, R.E., Snavely, P.D., Jr., and Niem, A.R., 1992, Quaternary thrust faulting at Netarts Bay, northern Oregon coast: Geological Society of America Abstracts with Programs, v. 24, p. 89.

Yeats, R.S., 1986, Active faults related to folding, *in* Wallace, R.E., ed., Active Tectonics: Washington, DC, National Academy Press, p. 63-79.

Yeats, R. S., Sieh, K.E., and Allen, C.R., in prep, Geology of Earthquakes: Oxford University Press.

Yount, J.C., and Holmes, M.L., 1992, The Seattle fault: a possible Quaternary reverse fault beneath Seattle Washington: Geological Society of America Abstracts with Programs, v. 24, p. 93.

CHAPTER 5: FOREARC DEFORMATION AND THE PROBABILITY OF GREAT EARTHQUAKES ON THE CASCADIA SUBDUCTION ZONE

Chris Goldfinger
Department of Geosciences, Oregon State University, Corvallis Oregon 97331
internet: gold@oce.orst.edu

LaVerne D. Kulm
College of Oceanic and Atmospheric Sciences, Oregon State University, Corvallis Oregon 97331

Robert S. Yeats
Department of Geosciences, Oregon State University, Corvallis Oregon 97331

Robert McCaffrey
Department of Earth and Environmental Sciences, Rensselaer Polytechnic Institute, Troy New York

Cheryl Hummon
Department of Geosciences, Oregon State University, Corvallis Oregon 97331

ABSTRACT

The occurrence of great subduction zone earthquakes has been linked to properties of the subduction system such as convergence rate, plate dip, and plate age. On the basis of comparison of subduction parameters such as plate age and convergence rate, investigators have inferred that the Cascadia subduction zone is comparable to other subduction zones where great M > 8.2 have occurred in historic times. New comparisons of subduction zone earthquakes show that forearc rheology, and convergence rate are important controls on the generation of great earthquakes in oblique subduction settings. Significant rates of arc-parallel forearc deformation are negatively correlated with M >8.2 earthquakes in subduction zones worldwide, regardless of obliquity of subduction. We present a summary of forearc deformation in the Cascadia subduction zone as mapped with seismic reflection profiles, multibeam bathymetry, and sidescan sonar. The Cascadia forearc is deformed by numerous oblique strike-slip faults and folds. We calculate that the rate of deformation on these structures is sufficient to accommodate all of the oblique component of plate convergence in Cascadia. The high rate of forearc deformation implies that the Cascadia forearc may be fully strain-partitioned, and may lack the rigidity to accumulate sufficient elastic strain energy to generate M > 8.2 earthquakes.

Another problem not yet resolved in Cascadia is the size and location of the seismogenic zone, and if and where it may be segmented. We approach this problem in two ways. First, we estimate the map pattern of the locked and seismogenic zones using published data on the thermal structure of the forearc, although with different conclusions than the original authors. We then compare our estimate of Cascadia seismogenic zone geometry to data from circum-Pacific great earthquakes of this century. We conclude that rupture length is moderately dependent on downdip width of the locked zone, that is that the aspect ratio of the seismogenic plate boundary has an upper limit. We estimate the maximum Cascadia rupture to be 500 to 600 km in length, with a 150-300 km rupture in best agreement with historical data. Lastly, we also see striking heterogeneity in the Oregon Cascadia forearc in terms of both uplift history of the submarine forearc, and the short term uplift of the coastal region recorded by re-leveling surveys. The heterogeneous

nature of strain accumulation in Cascadia is observed on the short time scale as highly variable uplift rates along the coasts of Washington, Oregon and northern California, and on a longer time scale as a highly variable uplift history in the offshore forearc. The long term uplift variations in the forearc in some cases correlate with short-term uplift rates onshore. We conclude from the patchy distribution of short term uplift that modern strain accumulation occurs in a similarly discontinuous fashion. The correlation of short and long term uplift of some areas of the forearc suggests that the observed short term variations in uplift may have occurred through many strain cycles, resulting in uplift of the submarine banks. From the apparently discontinuous nature of the plate interface, we conclude that Cascadia subduction earthquakes are likely to occur as moderate events in both rupture length (150 -300 km) and magnitude ($M<8.2$).

INTRODUCTION

The possibility of great (M > 8) earthquakes on the Cascadia subduction zone has sparked studies in many fields aimed at the questions that remain unanswered: how often?, and how big? The discovery of coseismically buried marshes in the coastal bays and estuaries of Oregon, Washington, and northern California provides direct evidence of earthquakes, but due to the presence of active upper plate structures in the forearc, the vertical deformation from the marshes cannot be used to model the forearc response to interplate strain accumulation (Yeats and others, in prep; Chapter 4). The marsh stratigraphy probably records a mixture of interplate and intraplate events, regardless of whether or not these events were simultaneous (Chapter 4). Heaton and Kanamori (1984) compared subduction zones worldwide in an attempt to characterize subduction earthquakes on the basis of plate age and convergence rate. On this basis, Cascadia was considered in the class of subduction zones capable of generating very large (M 8.3-8.5) earthquakes. However, Cascadia has the lowest seismic activity of all subduction zones by as much as an order of magnitude, when considering all plate interface events, or total arc-to-trench seismicity at M 6-7 levels (Acharya, 1992). Seismicity in Cascadia is significantly lower than in subduction zones considered to be "aseismic", and lower than modern "seismic gaps" (Acharya, 1992). Only one plate interface earthquake has occurred during recorded history, the 1991 Mw 7.1 Petrolia earthquake at the southern end of the subduction zone near Cape Mendocino (Oppenheimer and others, 1993). This event occurred near the Pacific-Gorda-North America triple junction, and may not be representative of the plate boundary elsewhere. The extremely low seismicity rates have been attributed to a combination of slow convergence, high temperature of the young slab, and a high ratio of aseismic to seismic slip on the plate interface (Acharya, 1992).

Recent work (McCaffrey, 1992; 1993) suggests that for many subduction zones, convergence rate is an important factor, but that plate age is a more complex influence. The buoyancy of a young slab, and the inferred greater interplate coupling, are countered by the high temperature profile of the young crust, which has the effect of reducing plate coupling, and shifting

the seismogenic zone seaward. McCaffrey (1993), using a larger sample of great earthquakes (40 events) than used by Heaton and Kanamori, and recent slip vector data from the world's subduction zones, finds good correlation between convergence rate and great earthquakes. In oblique subduction settings, the angular difference between earthquake slip vectors and plate convergence, termed the slip vector residual (Jarrard, 1986), is negatively correlated with the occurrence of great earthquakes. The slip vector residual has been interpreted as a measure of the internal deformation of the forearc (McCaffrey, 1993). In forearcs that are weak, much or all of the oblique component of convergence is taken up by forearc deformation, and these arcs are statistically unlikely to experience great earthquakes at better than a 1% confidence limit (McCaffrey, 1993).

We summarize evidence for arc-parallel deformation of the Cascadia forearc by strike-slip faulting in an effort to determine the degree to which the Cascadia forearc is deformed in the along arc direction, and to determine the amount of partitioning that occurs. We then compare Cascadia to other subduction zones with respect to partitioning, rupture lengths, and strain accumulation to estimate its earthquake potential.

OBLIQUE STRIKE-SLIP FAULTING IN CASCADIA

A single oblique strike-slip fault, the Wecoma fault, was discovered on the central Oregon abyssal plain in 1986 using SeaMARC 1A sidescan sonar (L. D. Kulm, unpublished data). This fault was subsequently re-surveyed in 1989 as part of the site survey for Ocean Drilling Program holes that were drilled in fall, 1993. This fault proved to be a remarkable structure, cutting both the Juan de Fuca plate and the overriding North American plate, and extending approximately 100 km from its northwestern tip 20 km west of the deformation front (abyssal plain), to the outer continental shelf (Goldfinger and others, 1992b; Goldfinger and others, in press). Detailed 144 channel seismic reflection profiles (MacKay and others, 1992) and modeling of deep towed magnetic profiles revealed that this vertical fault cut the entire sedimentary section on the abyssal plain, as well as the basaltic crust of the downgoing plate (Appelgate and others, 1992; Goldfinger and others, in press). The mechanics of plate interactions in the Cascadia thrust/strike-slip system are revealing of the nature of the locked plate interface, but are beyond the scope of this paper, in which we focus on the overall deformation of the Cascadia forearc.

Two similar strike-slip faults were also discovered in 1989, both with a left-lateral sense of motion and striking 290-295°. These two faults, the Daisy Bank fault and the Alvin Canyon fault (formerly faults B and C), also cross the plate boundary, and extend across the continental slope to the shelf edge. The Daisy Bank fault zone is the best expressed of the three faults on the upper continental slope, and was the target of high-resolution AMS 150 sidescan surveys in 1992 and 1993 as well as submersible dives which revealed the detailed structure of this fault (Chapter 4). In May of 1993, we investigated these and other suspected oblique strike-slip faults using SeaMARC 1A sidescan sonar and coincident Hydrosweep swath bathymetry. These targets were originally mapped using an extensive dataset of single and multichannel reflection profiles, NOAA swath bathymetry, U.S.G.S. GLORIA sidescan sonar (EEZ-SCAN 84 Scientific Staff, 1988; Goldfinger and others, 1992a; Goldfinger and others, unpublished data). In the following sections we present new data from this investigation of oblique faulting in Cascadia.

WASHINGTON MARGIN FAULTS

Initially we had identified 5 targets on the Washington continental slope, primarily on the basis of reflection records alone since swath bathymetry data for the Washington continental margin is still classified. Two of these targets had previously been investigated in a 1971 water gun seismic reflection survey that focused on one of the plain faults and associated abyssal plain mud volcano (L. D. Kulm, unpublished data). At that time the fault was mapped as a NNW trending feature on the basis of preliminary academic swath bathymetry and University of Washington reflection profiles. After the discovery of the Oregon oblique faults, we re-interpreted these two faults as probable WNW trending strike-slip faults similar to those mapped on the Oregon margin. Our first two targets, near a westward bend in the deformation front at Barkley submarine canyon proved inconclusive, we were unable to confirm the presence of significant oblique faults on the abyssal plain or lowermost slope at those two sites. The third and fourth targets were the above described faults first investigated in 1971, and are described below.

North Nitinat Fault

The two prominent faults first investigated in the 1971 survey are named for the Nitinat submarine fan, on whose southern flank they are located (Fig. 5.1). We surveyed the North Nitinat fault using both 5 km swath (2.4 m resolution) and 2 km swath (1 m resolution) SeaMARC 1A sidescan sonar, and simultaneously collected Hydrosweep swath bathymetry. The initial 5 km survey revealed that this fault strikes 283°, extending 20 km from the deformation front into the abyssal plain of the Juan de Fuca plate. The mud volcano targeted in the original survey lies adjacent to the fault on its south side, 1 km seaward of the deformation front. Another mud volcano straddles the fault near a right-bending section of the fault and is centered 6 km seaward of the deformation front. The 2 km swath (Plate 4) revealed detailed morphological and structural relationships which we describe below.

A late Pleistocene submarine channel paralleling the base of the continental slope on the abyssal plain is cut and offset left-laterally

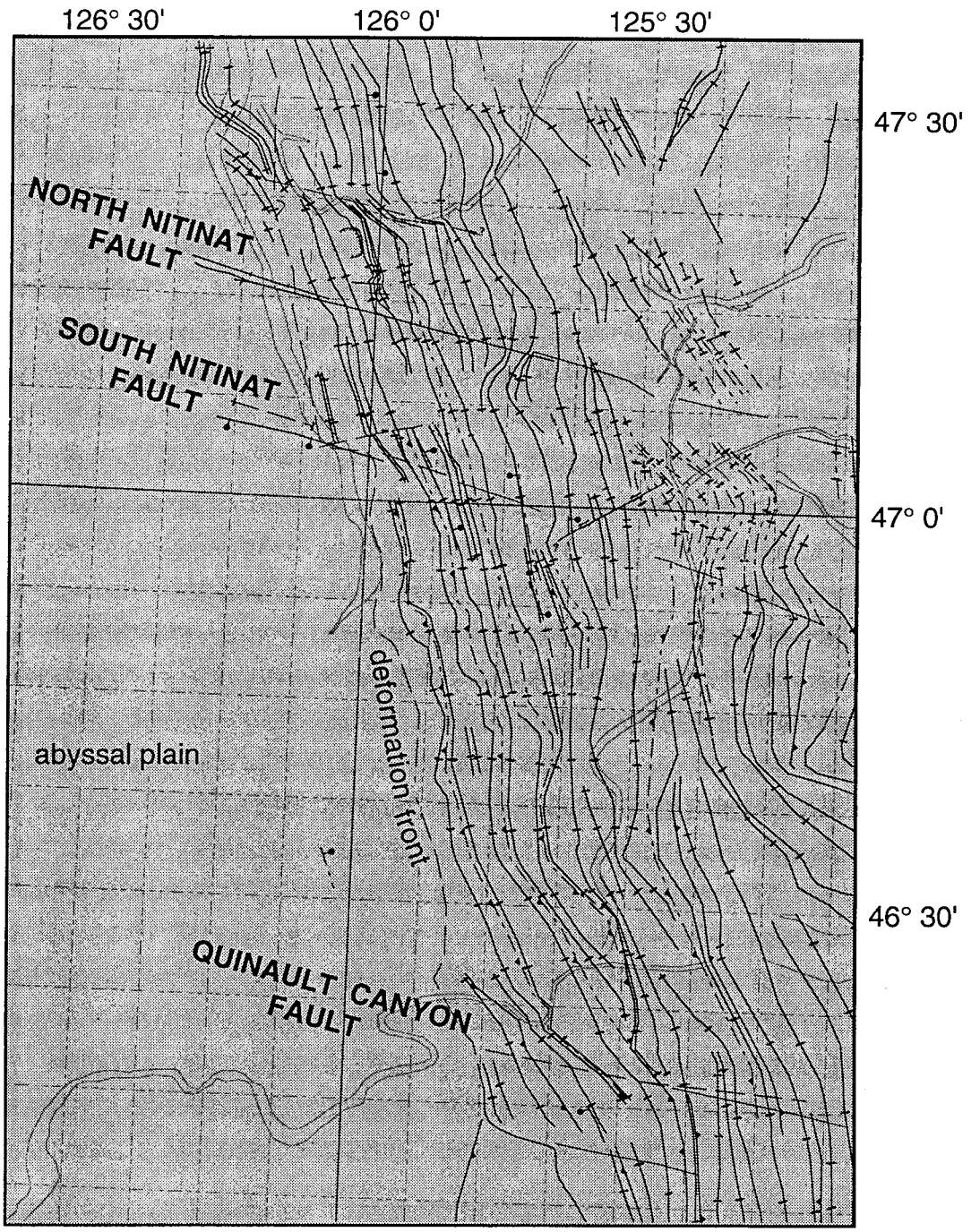

Figure 5.1. Preliminary tectonic map of central Washington continental slope and abyssal plane. The three named faults, interpreted as left-lateral strike-slip faults, are discussed in the text. Horizontal offsets of slope structures are not shown. See Plate 1 for symbol usage.

approximately 150 m by the N. Nitinat fault (Fig. 5.2). We estimate the age of the offset channel wall to be 16-20 ka, spanning the last Pleistocene lowstand at 18 ka. during which turbidite activity and channel downcutting were at a maximum (Griggs and Kulm, 1973; Nelson, 1968). This timing is consistent with other submarine channels on the Cascadia margin, although minor channel cutting continued into the Holocene at a greatly reduced rate (Nelson, 1968). The slip rate based on the observed offset and inferred age is 8.3±1.0 mm/yr, the error range reflecting uncertainty in the timing of the channel cutting episode.

The North Nitinat fault makes a gentle right-stepping bend, at which the seaward of the two mud volcanoes is located (Plate 3). Further evidence of the left-lateral sense of slip on this fault is the presence of the mud volcano at this bend, which is compressional for a left-lateral fault. We infer that the mud volcano is the result of extrusion of abyssal plain sediments caused by the compressional fault geometry.

In order to get an independent estimate of the overall net slip and slip rate on this fault, we applied the geometric technique for restoration of strike-slip faults described by Goldfinger and others (in press; Chapter 3) to the available University of Washington airgun seismic lines. This method depends on the geometry of trenchward thickening abyssal plain sediment wedges, and the availability of at least one trench-parallel and two trench-normal reflection profiles. In order to calculate the net slip on a fault nearly normal to the trench, if the geometry of the pre-faulting trenchward thickening wedges can be determined, retrodeforming the sedimentary section will result in a match of isopachs deposited prior to faulting (see Fig. 3.13). We applied this method to the 1971 water gun seismic lines in the vicinity of the North and South Nitinat faults. Using this method we derive a net left-lateral slip of 2.2±0.3 km for the N. Nitinat fault, after trigonometric correction for the 283° strike of the fault. An example of this method is shown below for the Alvin Canyon fault.

In a north-south crossing reflection line, the N. Nitinat fault is up to the north throughout the sedimentary section. Similar to the stratigraphy of the Wecoma fault (Goldfinger and others, in press; Chapter 3), the syn-faulting abyssal plain section shows growth-thickened strata on its downthrown side, a relationship that terminates downsection at the point at which syn-tectonic

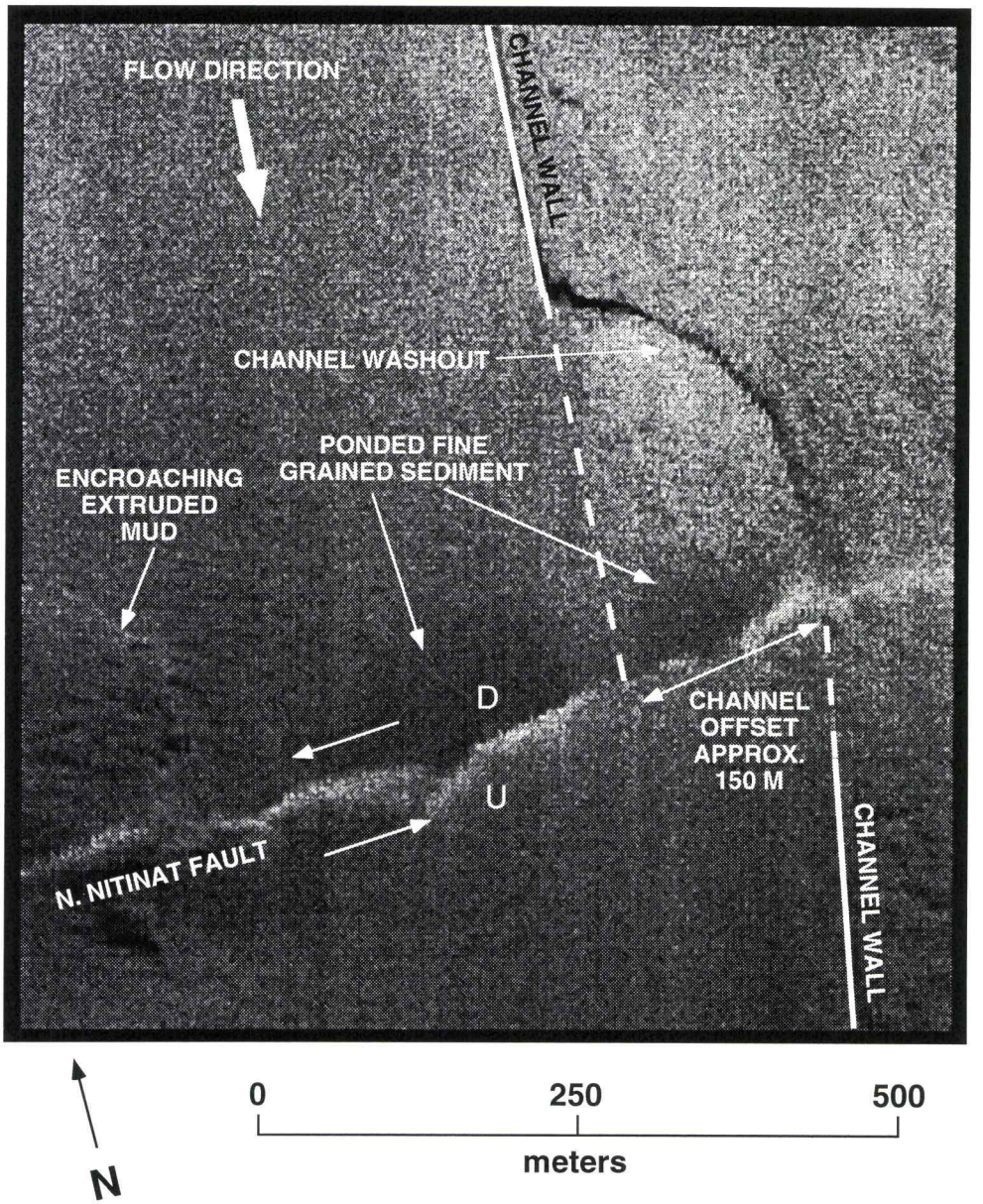

Figure 5.2. Interpretation of a part of Plate 2. N. Nitinat fault cuts a late Pleistocene abyssal plain channel. We interpret the arcuate part of the channel wall as a single event washout of the older channel wall. The light colored, rough textured area adjacent to the arcuate scarp is interpreted as a debris pile from the washout.

deposition began. We estimate the age of this point in the section by converting its depth in two-way-time to depth using an average velocity of 1680 m/s calculated for the upper 400 m of the Nitinat Fan from ODP drilling and reflection data (Bobb Carson pers. comm. 1993; Hyndman and Davis, 1992; see Appendix B for details). The age is then derived by using the net sedimentation rate of 100 cm/1000 yrs for the Nitinat Fan calculated from the 1993 ODP drill sites on the northern Nitinat Fan (Bobb Carson pers. comm. 1993). By this method we deduce that the fault first moved at 397,000±44 ka, giving a slip rate of 5.5±2 mm/yr (see Appendix B for slip rate calculations). The higher late Pleistocene slip rate is expected, since the point at which the growth strata were measured, originally located at the fault tip, is now 20 km landward of the tip. Since slip rate decreases from the center of a fault toward its tip (Bilham and Bodin, 1992), the retrodeformation method using the entire movement history includes low slip rates from the fault's early history. We assume that the onset of vertical and horizontal motion on the N. Nitinat fault (and the other strike-slip faults) were coincident.

The North Nitinat fault, like the three Oregon oblique faults, crosses the deformation front and the continental slope. Its landward tip was not observed due to conflicts with fishing vessels on the outer shelf, but was mapped from the deformation front southeastward to the shelf edge, giving a total observed length for this structure of 115 km. Like the Wecoma fault, the expression of the North Nitinat fault on the continental slope was variable. We observed regions of multiple parallel scarps, and commonly the fault was also expressed as sigmoidal bends and offsets in accretionary wedge thrust anticlines. Analysis of net slip on the continental slope portion of the fault is problematic, as we know of no datable piercing points. Based on the observation that net slip reaches a maximum at a fault's center (Bilham and Bodin, 1992, Scholz and others, 1993), we infer the maximum horizontal slip is larger than the 2.2 km slip observed near the seaward tip. Much of the data is not yet processed however, and further analysis of the processed data may result in better estimates of slip from the continental slope.

South Nitinat Fault

The South Nitinat fault (Fig. 5.1) is located nineteen kilometers south of the North Nitinat fault, was also first discovered in the 1971 seismic survey by the University of Washington (TT 063, line 32, 1971). The South Nitinat fault strikes 283°, extends 19 km seaward of the deformation front on the abyssal plain, and intersects the base of slope at a left step in the deformation front. The base of slope channel that is offset by the North Nitinat fault also is crossed by the S. Nitinat fault where its eastern bank is the seaward flank of the first thrust ridge at the base of the slope. We were initially unable to determine the offset of this channel by the South Nitinat fault, but further processing of the sidescan sonar data may reveal this relationship. In seismic section, the S. Nitinat fault is virtually identical to the N. Nitinat fault, showing an overall down to the south vertical separation, and thickened growth strata on the downthrown block in the syn-faulting part of the section. In the pre-faulting abyssal plain section, the eastward thickening abyssal plain units thin across the fault, indicating left-lateral slip on the S. Nitinat fault using the same reasoning describe above. Using the above retrodeformation method, we obtain a net slip for the South Nitinat fault of 2.0$\pm$0.8 km, the greater uncertainty due to the somewhat poorer seismic record for that fault. The point in the Nitinat fan section at which growth strata appear on the dowthrown side of the fault is 302 mbsf, thus using the Nitinat Fan sedimentation rate of 100 cm/1000 yrs, the age of the fault is 302$\pm$40 ka. From this we derive a slip rate of 6.7$\pm$3 mm/yr. for the S. Nitinat fault (see Appendix B for slip rate calculations).

Quinault Canyon Fault

The Quinault Canyon fault intersects the deformation front at 46° 18' N, 8 km south of the outlet of Quinault submarine canyon onto the abyssal plain (Fig. 5.1). This fault is one of 4 oblique faults mapped in this study that cut the accretionary wedge but do not extend into the abyssal plain as detectable surface faults. The seaward projection of the Quinault Canyon fault is crossed 4.7 km west of the deformation front by University of Washington reflection line

TT 79-1, and shows no disruption of the abyssal plain section, confirming the lack of lower plate involvement west of the plate boundary. On the accretionary wedge, the Quinault Canyon fault is poorly expressed over much of its length, but well expressed near its center, where it offsets left-laterally a northwest trending slope channel approximately 900 m. The overall strike of the fault is 280°. No age information is available for the channel, thus we are unable to determine a net slip, slip rate, or age for this fault.

OREGON MARGIN FAULTS

One of the primary objectives of the May 1993 SeaMARC sidescan cruise was to survey the full length of the Wecoma fault and Daisy Bank fault in order to determine their length, continuity, net slip, and possibly improve our estimates of slip rate derived from the western tips of these two faults on the abyssal plain.

Wecoma Fault

The Wecoma fault is described in detail elsewhere (Goldfinger and others, in press; Appelgate and others, 1992: Goldfinger and others, 1992b). We surveyed the entire length of the Wecoma fault using SeaMARC 1A at a 5 km swath width, covering the continental slope and outer shelf sections of the fault that had not previously been investigated with sidescan sonar. The new survey confirmed the continuity of the Wecoma fault on the slope as inferred by Goldfinger and others (in press), and we were able to follow this fault to its apparent eastern tip over a total length of 95 km. Figure 5.3 shows a portion of the Wecoma fault zone on the upper continental slope. The location of the eastern end of this fault is mapped where the surface trace died out on the sidescan records. This area of the outermost shelf was covered with ripple marks in unconsolidated sand, confirmed by DELTA submersible dives in 1992 and 1993. We also observed linear patterns of carbonate deposition along the eastern projection of the fault landward of the last observed surface trace. These carbonates were found on several DELTA dives to be similar to

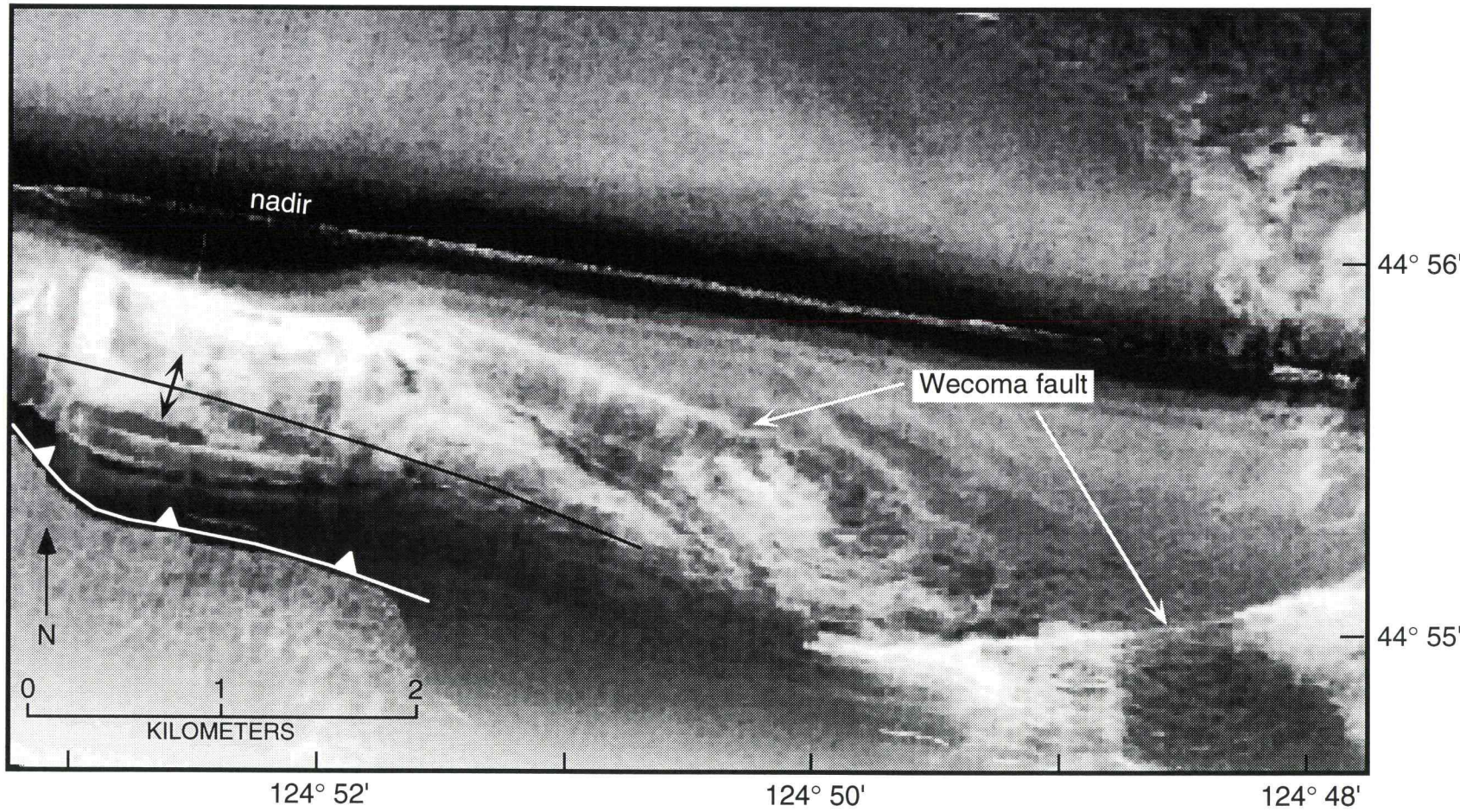

Figure 5.3. Portion of SeaMARC 5 km swath showing the Wecoma fault zone on the upper continental slope. Nadir area (no data) is the dark band across the image center. Oblong feature at left center is a fault-bend fold developed over a compresional segment of the fault. See Figure 3.22 for a seismic reflection profile over this structure.

those associated with other active fault zones on the Oregon shelf. The association between vent-derived carbonate deposition and active faulting is strong on the shelf (Chapter 4). Thus we speculate that the Wecoma fault may extend somewhat farther eastward than the mapping of its surface trace indicates.

We initially could not locate any new piercing points to improve our earlier slip rate calculations (Goldfinger and others, in press), although further analysis of these data may yield more information about the net slip on this fault on the continental slope.

Daisy Bank and Alvin Canyon Faults

We surveyed the entire length of the Daisy Bank fault (formerly Fault B) using both SeaMARC 1A and AMS 150 sidescan sonars (Chapter 4). As with the Wecoma fault, we confirmed the continuity of this fault over the continental slope from the abyssal plain to the shelf edge. The eastern tip of the fault may be near the shelf edge, or at Stonewall Bank, 10-12 km further southeast. We did not observe any surface faulting between Stonewall Bank and the shelf edge, however Stonewall Bank is highly sheared by NW trending fractures, some of which have minor left separation. If the eastern tip of the Daisy Bank fault is near Stonewall Bank on the inner shelf, the overall length of the fault is 98 km, similar to the length of the Wecoma fault.

We applied the retrodeformation technique for determination of age, slip sense, net slip, and slip rate of Goldfinger and others (in press) to the Daisy Bank fault and Alvin Canyon fault (formerly fault C). We determined the geometry of pre-faulting eastward thickening abyssal plain sediment wedges using OSU MCS line 08 for the Daisy Bank and Alvin Canyon faults (Fig. 5.4). We then calculated whole sedimentation rates for the Astoria Fan at the two faults using the sedimentation rate of 110 cm/1000 yrs (Goldfinger and others, in press), scaled to the slightly thinner fan sections at the two faults. The Alvin Canyon fault is 60 km south of the Wecoma fault along the deformation front, thus some age error due to time transgression of the base of the Astoria Fan is inherent in the age calculations below (the age of the base of the fan should decrease southward, away from its source to the north). Using the wedge

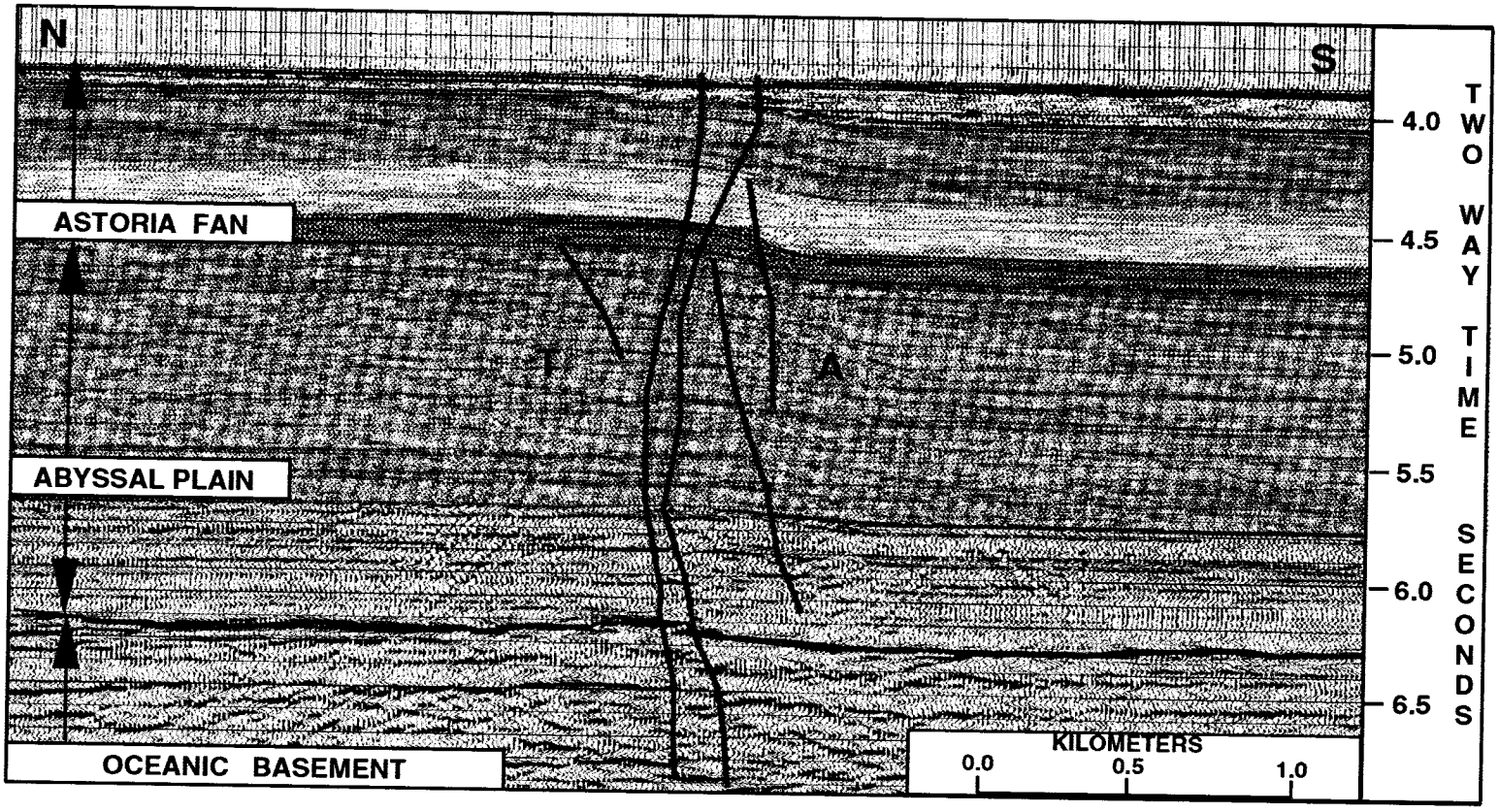

Figure 5.4. Alvin Canyon fault, shown cutting the sdimentary section and basaltic basement of the Juan de Fuca plate. The seismic line shown is OSU MCS line 37, located 3 km seaward of and parallel to the deformation front off central Oregon. Uppermost two subunits of the Astoria Fan (pink and gray) show growth thickening on the downthrown side of the Alvin Canyon fault, but the lower two subunits (yellow and green) do not thicken on the downthrown side. Therefore, faulting began at this boundary, between the gray and yellow units. Abyssal plain section (red) thins across the fault due to left-lateral strike slip motion. T = toward viewer; A = away from viewer.

geometry determined from line 08, we calculate a net slip of 2.2±0.5 and 2.6±0.6 km respectively for the Daisy Bank and Alvin Canyon faults. We determined the ages of these faults using the method described above for the Washington faults. The position in the sedimentary section at which fault related growth strata appears is determined from OSU MCS line 37. This depth in two-way time is converted to depth using scaled sedimentation rates and the Astoria fan velocity (assumed here to be the same as that of the Nitinat Fan, see Appendix B) of 1680 m/sec. By this method we obtain ages of 384 ka and 392 ka respectively for the Daisy Bank and Alvin Canyon faults. These values result in slip rates of 5.7±2 mm/yr and 6.6±2 mm/yr, respectively, for the two faults (see Appendix B for slip rate calculations).

Heceta South, Coos Basin, and Thompson Ridge Faults

Three oblique strike slip faults in southern Oregon mapped by Goldfinger and others (1992a) were also investigated with SeaMARC 1A in May, 1993. From north to south, these are the Heceta South, Coos Basin, and Thompson Ridge faults (Plate 1; Fig. 5.5). The Heceta South fault is observed in sidescan records on the abyssal plain, while the Coos Basin and Thompson Ridge faults appear to be limited to the North American plate. The Heceta South fault intersects the deformation front at 44° 02' N, along the north wall of a large slump. The slump scar is cut by numerous lineations parallel to the main fault; we speculate that the slump failure was induced by weakening of the slope in the Heceta South fault zone. Based on sidescan images, the fault extends 11 km into the Juan de Fuca plate, cutting the debris pile deposited on the abyssal plain by the large slump. The Heceta South fault is poorly expressed as a surficial feature over much of the continental slope, but is observable as a scattering of parallel small scarps. Left steps or bends of north to northwest trending accretionary wedge thrust ridges are apparent in the swath bathymetry data along the trace of the Heceta South fault. At the shelf break, the Heceta South fault sharply truncates the southwestern corner of Heceta Bank, downdropping a Pleistocene low stand shoreline of unknown age more than 200 meters (Chapter 4), down to the south (Fig. 4.6). The structural details of the Heceta

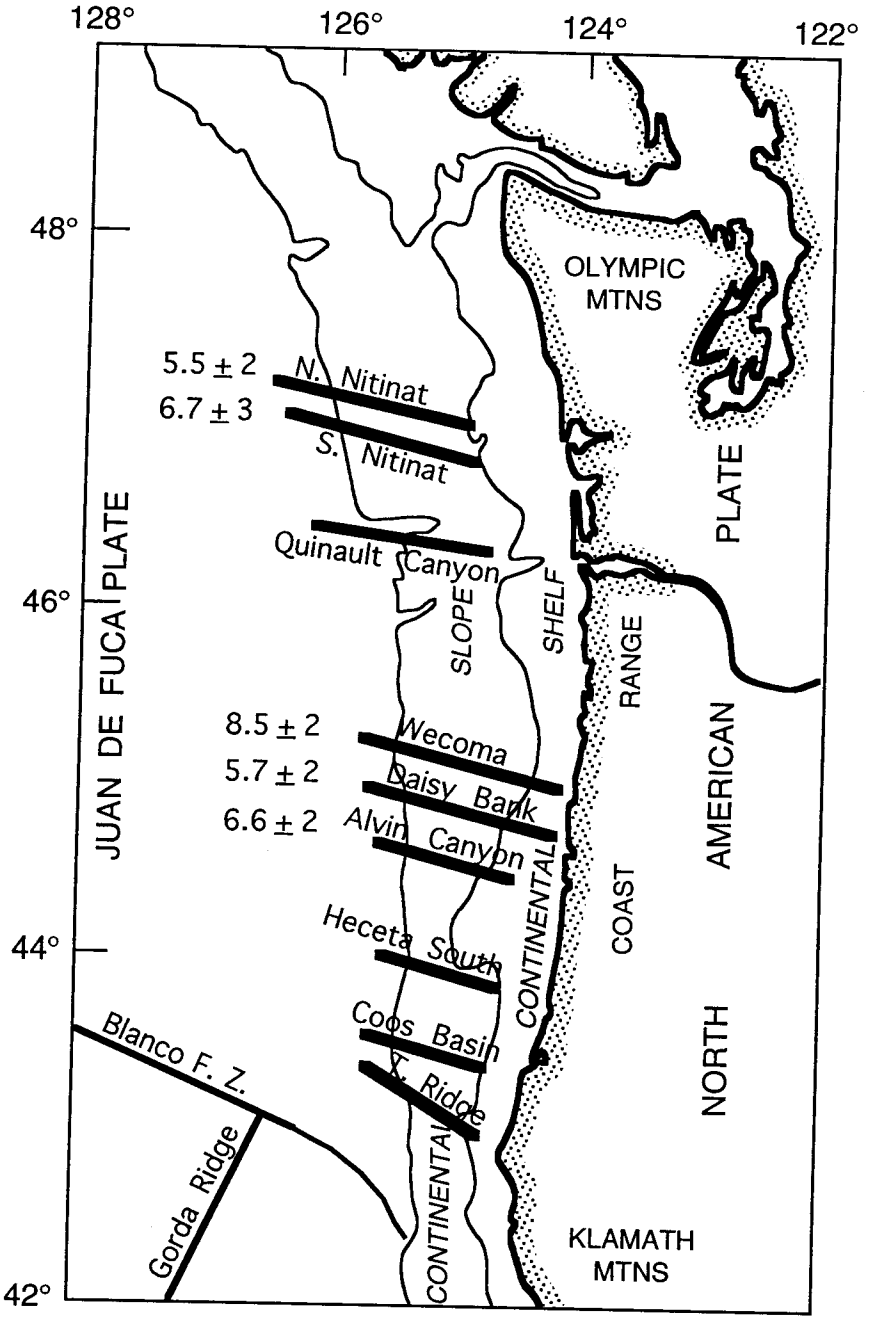

Figure 5.5. Locations of nine strike-slip faults mapped on the Oregon and Washington continental margin. Previously mapped faults are the Wecoma, Daisy Bank, and Alvin Canyon faults. Newly discovered faults are the N. Nitinat, S. Nitinat, Quinault Canyon, Heceta South, Coos Basin, and Thompson Ridge (T. Ridge) faults. Heavy lines represent approximate SeaMARC 1A swath coverage. Numbers to the left of some faults are slip rates, in mm/yr.

South, Coos Basin, and Thompson Ridge faults are not well known since they are crossed by few seismic reflection profiles. In one multichannel profile, U.S.G.S. line WO 77-05, the Heceta South fault is blind in the upper 2 seconds (twt) of data, and although the fault is down to the south, some stratigraphic units also thin to the south, indicating a complex history of vertical motion.

The Coos Basin fault intersects the base of slope at a 3 km left step in the deformation front at 44° 04' N (Plate 1; Fig. 5.5). No abyssal plain extension of this fault was observed in sidescan records, although near-surface faulting along the seaward extension of both the Coos Basin fault and Thompson Ridge faults is observed on 2 channel seismic reflection records on the abyssal plain (EEZ-SCAN 84 Scientific Staff, 1988; these faults are shown on Plate 1 as inferred faults on the abyssal plain, since their strikes are not well constrained). The Coos Basin fault at the surface is an approximately 7 km wide zone of deformation, the major elements of which are visible in the GLORIA sidescan atlas (EEZ-SCAN 84 Scientific Staff, 1988). Multiple surficial scarps offset anticlinal ridges on the lower slope left-laterally, and the broad zone is expressed bathymetrically as linear trends striking 288°-293°.

The Thompson Ridge fault intersects the base of slope at a 5 km left step in the deformation front, and, like the Coos Basin fault, does not extend into the abyssal plain as a surficial feature based on SeaMARC 1A images. The Thompson Ridge fault is the best expressed bathymetrically of any of the nine Cascadia strike-slip faults mapped to date (Fig. 5.6). It is clearly observed as a pattern of disruption of accretionary wedge thrust ridges in even low resolution bathymetry. Figure 5.6 shows a perspective shaded relief image of NOAA SeaBeam swath bathymetry data in the Thompson Ridge fault area gridded to a100 m point spacing. In map view, a pattern of left steps and sigmoidal bending of crossing folds suggests left-lateral shear (Plate 1). Other folds occur sub-parallel to the strike of the fault zone. Crossing thrust ridges

Figure 5.6. Shaded relief plot of NOAA SeaBeam swath bathymetric data in the vicinity of the Thompson Ridge fault. Figure on next page. Grid spacing 100 m. Plot shows the bathymetric trend of the Thompson Ridge fault across the lower to middle continental slope, viewed from the southwest.

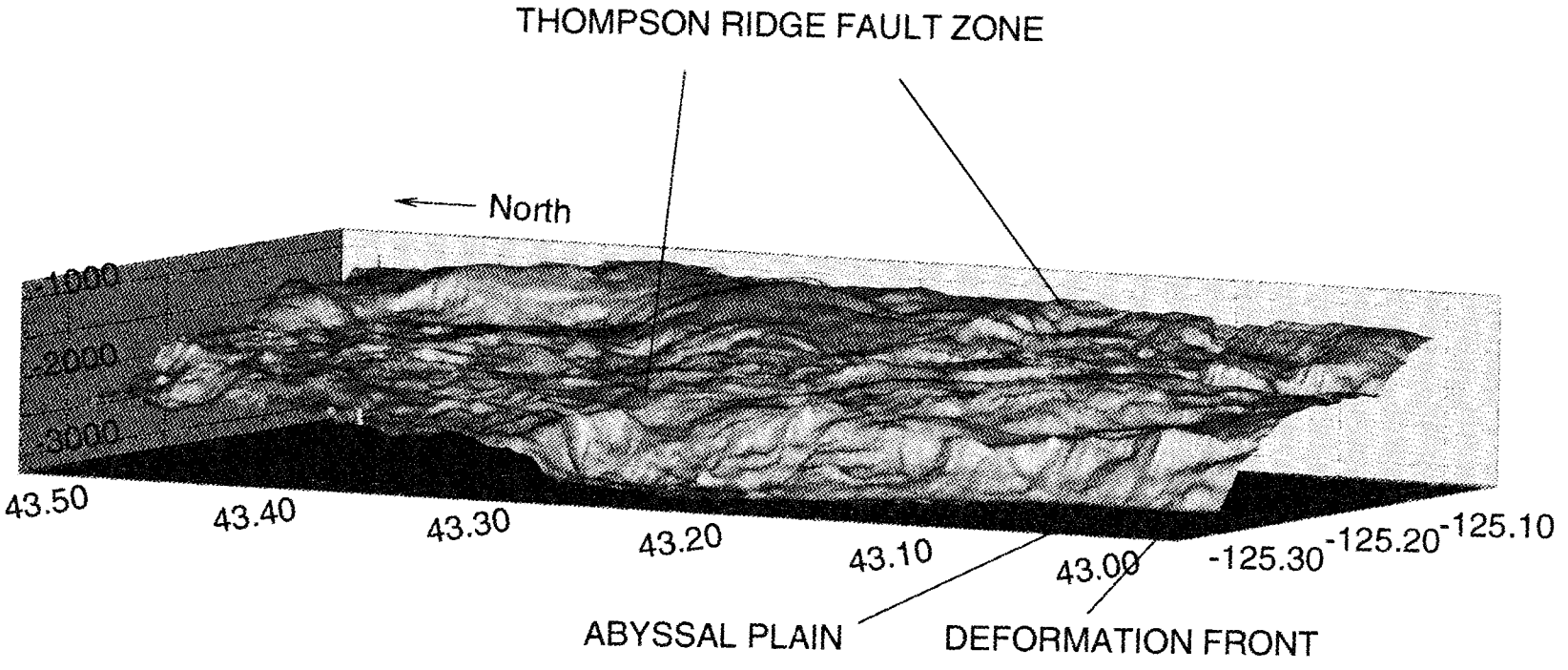

Figure 5.6, Continued.

are also elevated over the fault zone, a distinctive morphology observed on some of the other oblique faults. This elevation difference, in the case of the Wecoma fault, is the result of a compressional flower structure composed of fault splays with a small reverse component of motion based on seismic reflection records. We infer that much of the bathymetric expression of the strike-slip faults observed on the slope is due to the superimposition of flower structures on the coeval or older thrust ridges.

DISCUSSION

FOREARC DEFORMATION AND GREAT EARTHQUAKES

The presence of numerous oblique faults, and associated folds of late Quaternary rocks on the Oregon continental slope and shelf indicates that deformation of the Oregon and Washington Cascadia forearc is significant. The oblique orientation of many of these structures implies that a component of this deformation is parallel to the continental margin and the arc. Detailed mapping of the Oregon (Goldfinger and others, 1992a; Chapter 4) and Washington (Goldfinger and others, unpublished data) margins, shows this deformation is non-uniform in both rate and distribution of active structures. This is true of both the outer forearc (continental slope) and of the inner submarine forearc (continental shelf).

What does this distributed deformation tell us about the subduction process and the question of great earthquakes in Cascadia? Our general conclusion that the Cascadia forearc is deformed by strike-slip faulting, and possible clockwise rotation (Goldfinger and others, 1992b) is important because the capacity of a subduction zone to generate great earthquakes must depend, at least in part, in the capacity of the forearc to store the necessary elastic strain energy (McCaffrey, 1993). Several studies have related earthquake magnitude to such factors as plate age, plate dip, and convergence rate. However, these studies have considered forearcs to be uniformly elastic, and do not account for internal deformation of the forearc.

McCaffrey (1993) has studied the relationship between forearc deformation and great earthquakes from the perspective of plate motion and earthquake focal mechanisms. A discrepancy between the calculated motion of plate pairs and the slip vectors for recorded plate interface earthquakes has been observed in many oblique subduction zones (DeMets and others, 1990; Jarrard, 1986; McCaffrey, 1993). This discrepancy, termed the slip vector residual (Jarrard, 1986), has been attributed to deformation of the forearc in oblique subduction settings. Deformation of forearcs has been observed in the form of arc-parallel strike slip faults (Fitch, 1972; Beck, 1983; Jarrard, 1986), and rotating blocks bounded by oblique strike-slip faults (Geist and

others, 1988; Ryan and Scholl, 1993). These mechanisms are favored in oblique subduction because the high angle faults concentrate horizontal shear more effectively than the dipping subduction interface (Fitch, 1972). McCaffrey (1993) has found a negative correlation between highly deformed forearcs (as indicated by a large slip vector residual) and great earthquakes. He found that among oblique subduction zones worldwide, few if any earthquakes of Ms > 8 occurred this century in those oblique subduction zones with large (> 23°) slip-vector residuals. He also found no significant relationship between great earthquakes and plate age, plate dip, or obliquity of subduction. The study did show a moderately strong relationship between great earthquakes and convergence rate, with few Ms > 8 events occurring where subduction rates are slower than 40 mm/yr. McCaffrey (1993) concluded that the larger the slip vector residual, the more the forearc must be deforming in the along-arc direction to accommodate the oblique component of subduction. If correct, the inverse relationship between forearc deformation and large magnitude earthquakes suggests that forearcs that deform significantly in the arc-parallel direction are limited in their capacity to accumulate elastic strain energy by their inherent heterogeneity.

Cascadia has had only one interplate thrust earthquake (1991 Petrolia earthquake; Oppenheimer and others, 1993) from which to derive a slip vector, thus we cannot simply relate Cascadia to McCaffrey's work directly. However, we now have a growing body of evidence that the Cascadia forearc is deforming in the along-arc direction. The set of left-lateral strike-slip faults we have mapped implies clockwise tectonic rotation of the forearc (Fig. 2.3). Paleomagnetically determined clockwise rotations in coastal basalts in Oregon and Washington suggest that similar processes have operated throughout the Tertiary, with Miocene Columbia River Basalts in western Oregon rotated 10-30° clockwise (Wells and England, 1991; Wells and Heller, 1988). These diverse data sets all indicate significant deformation of the central Cascadia forearc that we attribute to the arc-parallel component of oblique convergence. With the slip rates we have determined, we can estimate total rates of forearc deformation in the arc-parallel direction, and by inverting those results, estimate the slip vector and slip vector residual for a plate interface event in Oregon and Washington. In the following sections, we estimate the net arc-parallel rate of deformation, and invert for the slip vector

in order to compare the slip vector residual of a hypothetical Cascadia interplate earthquake to the historical data on magnitude vs. slip vector residual of McCaffrey (1993).

In Figure 5.5, we summarize the slip data from the above discussion, and add the slip rate determined for the Wecoma fault from Goldfinger and others (Chapter 3). Each left-slip fault has a component of extension between the two blocks as a result of left-lateral motion. We calculate the net extension of the forearc due to the slip on the set of 9 faults, using the measured strikes from Goldfinger and others (1992a) for the Oregon faults, and this study for the Washington faults. For the four faults with no data we assign a value of 5.5 mm/yr, the slip rate of the Alvin Canyon fault, the lowest of the calculated rates among the other faults. The slip on each fault produces a component of extension of the forearc between each pair of blocks parallel to the arc (see Appendix B). The sum of these arc-parallel extension values is 17.4 mm/yr. This represents the net extension in this region of the forearc due to the clockwise rotation of the fault-bounded blocks (see Appendix B for calculations). This value is comparable to the total along arc component of plate convergence of 18.8 mm/yr calculated from the rotation poles of DeMets and others (1990) at 45° N along the deformation front (plate boundary). A full analysis of the kinematics of the forearc deformation due to these faults is beyond the scope of this paper, and will require a more detailed kinematic model using the newly collected, but not yet processed sidescan sonar data from the 1993 cruises. Nevertheless, even a simplistic calculation such as this suggests that all of the oblique component of Cascadia-North America convergence can be accounted for by oblique strike-slip faulting of the forearc.

In order to estimate the expected slip vector of interplate earthquakes in Oregon, we invert the fault slip data by simply subtracting the forearc extension vector (North, 17.4 mm/yr) from the JDF-NAM vector (062°, 40 mm/yr). The resultant expected slip vector is nearly perpendicular to the arc and plate boundary for the Oregon margin. This suggests that the Cascadia forearc may be fully strain partitioned; the slip vector of a subduction earthquake will be close to perpendicular to the deformation front, and thus the slip vector residual (SVR) will be equal to the obliquity, or 28 degrees in Oregon. In Figure 5.7 we add our predicted slip vector residual to the plot of other subduction zones from McCaffrey (1993). The SVR of 28 degrees is

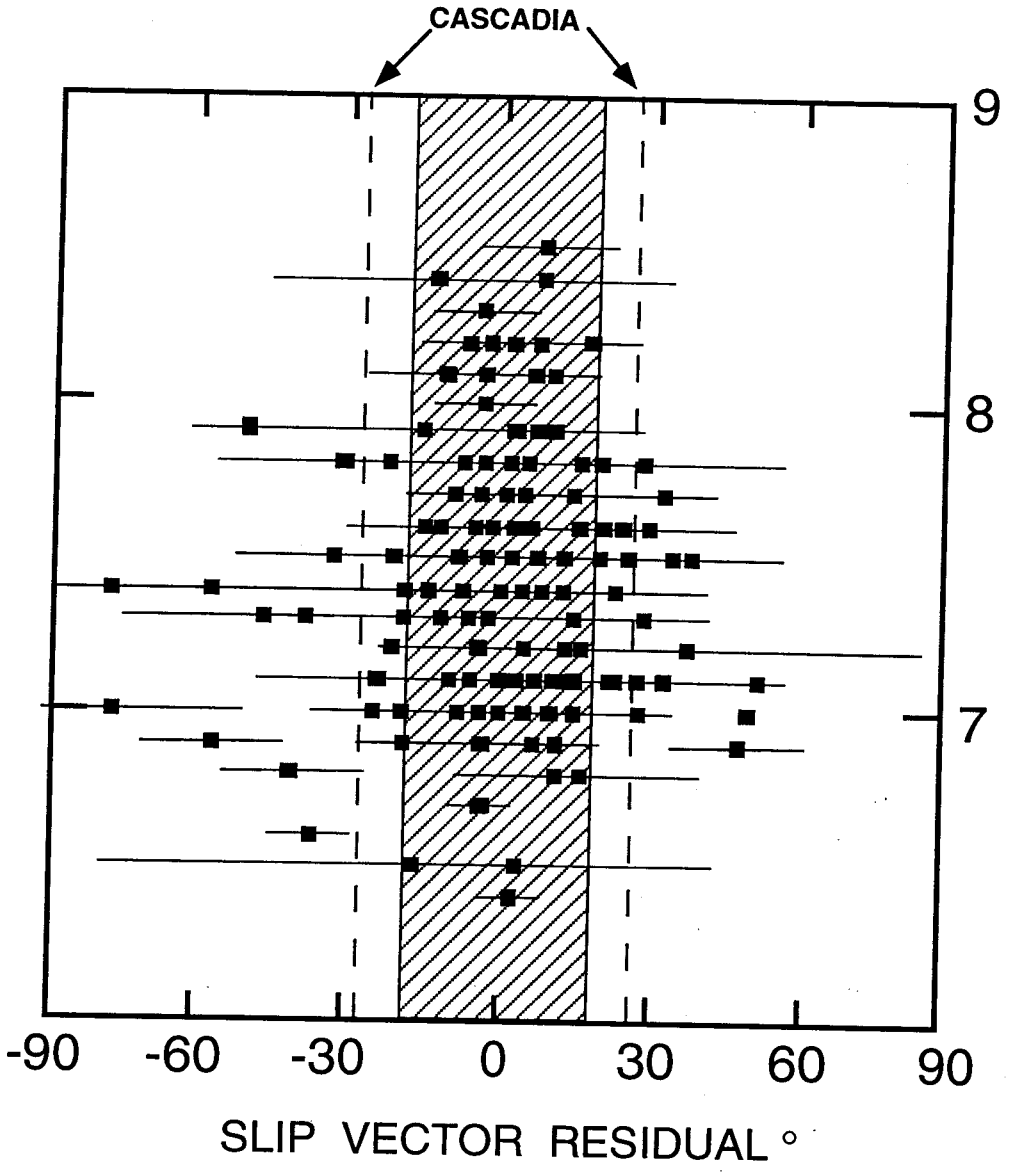

Figure 5.7. Plot of slip vector residual vs. Ms magnitude of major earthquakes this century, from the data of McCaffrey (1993). Hatched area represents maximum slip vector residual envelope for earthquakes larger than Ms 8.0. Cascadia slip vector residual, if forearc is fully partitioned, falls outside of the hatched area.

well outside the envelope of SVR values observed for other subduction zones having historic great earthquakes larger than Ms 8.0. On this basis we postulate that the Oregon Cascadia margin is an unlikely candidate for earthquakes greater than this magnitude. An additional inhibiting factor is the slow convergence rate in Cascadia, which, at 40 mm/yr, is at the lower limit of the population of worldwide subduction zones that have generated historic Ms > 8.0 earthquakes (McCaffrey, 1993).

These two arguments suggest that due to the slow convergence rate, and the incompetent nature of the forearc, Cascadia earthquakes may occur in limited rupture segments, possibly controlled or influenced by forearc structures. The comparison of subduction seismicity by Acharya (1992) suggests that if the very low seismicity in Cascadia is due in part to a very low seismic coupling coefficient (Pacheco and others, 1993), the repeat times of these events will be quite long, consistent with the 500-1000 year intervals suggested by the coastal marsh records (Atwater, 1987; Darienzo and Peterson, 1990) and analysis of abyssal plain turbidites (Adams, 1990).

HETEROGENEITY OF MODERN AND LATE QUATERNARY FOREARC DEFORMATION

In addition to the now abundant evidence summarized above for along-arc deformation of the forearc, additional evidence for the heterogeneous nature of forearc deformation is available in the published literature. Geodetic leveling surveys of the coastal areas of California, Oregon, and Washington have shed some light on the short term vertical deformation occurring over the last 70 years. This work is presented in Mitchell and others (submitted) as a contour plot of absolute rate of tectonic uplift (see Plate 1 and Fig. 5.8; the contours differ slightly due to the inclusion of data from the Willamette Valley in the plot shown in Fig. 5.8). This was accomplished by tying leveling measurements to tide gauges at several points along the coast and removing the effects of the eustatic sea level rise. The contours show that short term uplift rates along the Cascadia margin are highly variable. Rapid uplift is occurring in southern Oregon, up to 4 mm/yr centered near Cape Blanco, more moderate uplift of 2 mm/yr in northern Oregon and northern Washington,

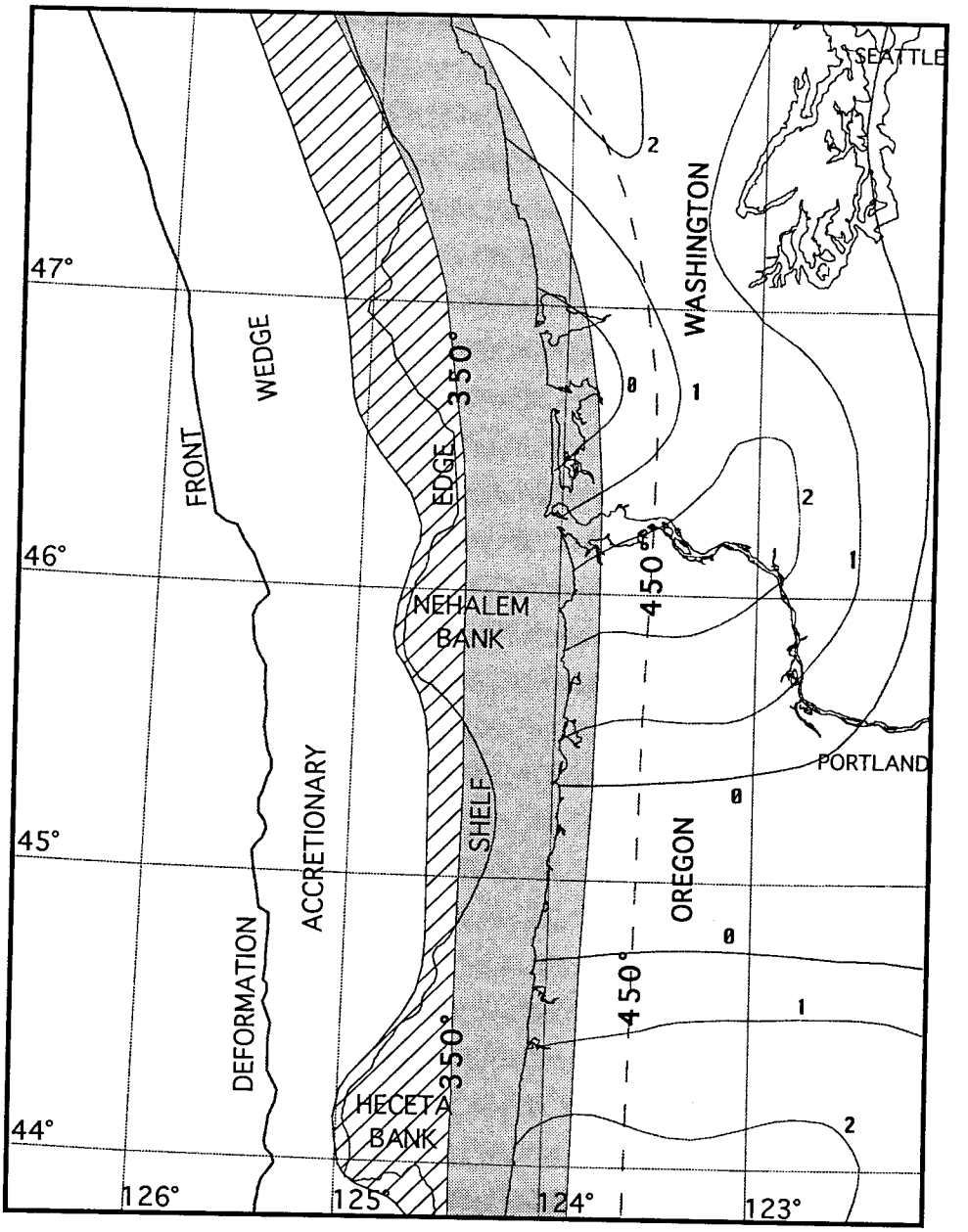

Figure 5.8. Map showing locked (hatched) and transition (shaded) zones on the Cascadia plate interface, projected to the surface. The boundary between the locked and transitional zones occurs at the 350° isotherm of Hyndman and Wang (1993). Dashed line landward of the transition zone is the 450° isotherm from Hyndman and Wang (1993). Onshore contours are absolute tectonic uplift rates in mm/yr, from Mitchell and others (submitted). Onshore contours differ somewhat from those shown on Plate 1 due to the inclusion (on this figure) of data from the Willamette valley, from Mitchell and others (submitted).

and two regions of near zero tectonic uplift are found in central Oregon centered near the Lincoln City/Siletz Bay area, and in Washington, centered in the Willapa Bay area. The short-term rates of uplift determined from leveling in southern and northern Oregon and northern Washington are significantly greater than the long term rates of uplift determined from coastal marine terrace heights (McInelly and Kelsey, 1990). This discrepancy has been attributed to the difference between interseismic strain accumulation (recorded by the re-leveling surveys) and permanent deformation (recorded by the marine terraces; Mitchell and others, submitted). Assuming that the geodetic rates are representative of the interseismic period, there is no known alternative to this explanation, and we accept it as direct evidence of interseismic strain accumulation that will be released in an earthquake or a number of earthquakes. However, the non-uniformity of the uplift pattern shown in Figure 5.8 suggests that the accumulation of elastic strain energy is also non-uniform. The contours intersect the coast at high angles in most locations, suggesting a highly heterogeneous upper plate response to subduction stresses.

Goldfinger and others (Chapter 4) discuss the nature of the three submarine banks in Oregon and the structural differences between the banks and interbank basins. They conclude that the banks represent structurally distinct domains that can be defined by bathymetry, structural trends, and to a lesser degree, gravity data. They suggest that the uplifted rocks of the banks represent structurally distinct embedded zones within the forearc that may act as asperities on the subduction interface. The banks also are bounded in some cases by the oblique left-lateral strike-slip faults discussed in Chapters 2 through 5. We postulate that this configuration is similar to, but on a smaller scale than, the structurally segmented Aleutian forearc in which clockwise rotating blocks have been defined by seismicity, bathymetry, and reflection profiles (Geist and others, 1988; Ryan and Scholl, 1993). The strong contrasts between the banks and interbank basins indicates that the overall deformation of the Oregon forearc is highly heterogeneous; like the strong variations in tectonic uplift rates, we suggest that the contrasting styles of forearc deformation represent contrasts in the upper plate response to subduction.

COMPARISON OF RUPTURE ZONE GEOMETRY FOR RECENT GREAT EARTHQUAKES TO POSSIBLE CASCADIA EARTHQUAKES

Data on earthquake rupture area are available for a number of subduction zones in which great earthquakes have occurred in historic times. We can use the known rupture geometries for these events to evaluate possible rupture scenarios in Cascadia. We first estimate the width of the Cascadia locked zone from published thermal constraints and dislocation modeling of interseismic uplift, using the Nankai subduction zone as a model.

Estimate of the Extent of the Locked Zone in Cascadia

Although interplate seismicity is virtually unknown in Cascadia, estimates of the extent of the locked zone have been made on the basis of thermal data, supplemented by dislocation modeling based on the pattern of uplift and subsidence derived from re-leveling surveys (Hyndman and Wang, 1993; Dragert and others, 1994; Mitchell and others, submitted). These studies place much of the locked zone in the young accretionary wedge, contrary to observed aseismicity of the accretionary wedges in other subduction zones (Byrne and others, 1988). We modify the geodetic and thermal models using the model of Byrne and others (1988), and the Nankai subduction zone as an analog, to estimate the dimensions of the locked zone and possible rupture zones in Cascadia.

Hyndman and Wang (1993) used seafloor heat flow measurements to define the 350° and 450° isotherms (Fig. 5.8), considered to be the downdip limits of the unstable sliding (seismogenic) zone and the transition (to stable sliding) zone, respectively, below which only stable sliding occurs. Hyndman and Wang (1993) argue that unlike most subduction zones where the subducted slab is cooler than the overriding plate, the youth of the hot subducted slab and thick (2-3.5 km) insulating sedimentary cover in Cascadia result in a reversal of the usual temperature distribution. This is supported by measured high heat flow at the sediment surface (Hyndman and Wang, 1993), and by downhole measurements in ODP site 888 on Nitinat Fan, which yield a geothermal gradient of 68°/km (Bobb Carson pers. comm. 1993). The updip

(seaward) limit of seismicity in many subduction zones corresponds to the rear of the accretionary wedge (Byrne and others, 1988). The wedge itself is too weak to deform elastically and the plate boundary strength contrast is too great to nucleate earthquakes. Hyndman and Wang (1993) argue that the high temperature of the slab at the sediment/basalt contact (250° C) causes rapid dewatering of the accreted sediments, indurating and increasing the competency of these sediments to the point where the wedge is capable of nucleating earthquakes. On this basis they position the updip limit of seismicity approximately 5 km landward of the deformation front off Vancouver Island, Washington, and Oregon. However, this argument should also apply to the Nankai subduction zone, where heat flow at the trench is similar to that in Cascadia, 130-150 Mw/m^2 (Shiono, 1988; Hyndman and Wang, 1993). In the 1944 and 1946 Nankai earthquakes, the seaward edge of the rupture zone was 60-90 km landward of the deformation front, consistent with many studies showing accretionary wedges to be largely aseismic (e.g. Byrne and others, 1988). A similar updip cutoff of background seismicity occurs in Washington (Crosson and Owens, 1987) at about 60 km from the trench, although without a great earthquake, it is unclear if this would also apply to rupture of the plate boundary.

Based on the known rupture characteristics of the Nankai subduction zone, a good Cascadia analog (see below), we reject the argument of Hyndman and Wang (1993) which places most of the locked zone within the seawardmost accretionary wedge. We adopt a distance of 60 km, from the deformation front as the seaward rupture limit for Cascadia earthquakes for purposes of comparison in the following section. 60 km is the distance from the trench to the seawardmost aftershocks recorded in the 1944 and 1946 Nankai earthquakes. The reasoning for this lies in Cascadia's similarity to Nankai with respect to most subduction parameters. The Philippine Sea Plate being subducted at the Nankai trough has a thick sediment section insulating the young (15-30 Ma), shallowly dipping (10-15°) slab (Shiono, 1988), has a similar convergence rate (45 mm/yr; Seno and others, 1993), and similar obliquity 15-30 degrees (Seno and others, 1993). Where the continental shelf edge extends closer to the deformation front, we use the shelf edge as the seaward edge of the locked zone. In these areas, at the seaward boundaries of the three major Oregon submarine banks, the shelf break represents a

strength and velocity boundary between the young accretionary wedge and older rocks of the banks which are underlain by older accreted sediments or oceanic crust of the Siletz River Volcanics (Chapter 4; Tréhu and others, 1992). We adopt as the downdip limit of the rupture zone the 420° isotherm interpolated from Hyndman and Wang (1993). The transition zone between the 350° and 450° isotherms is thought to be capable of sustaining some brittle rupture, but not capable of nucleating interplate slip. We estimate the downdip rupture limit by examining the characteristics of upper plate seismicity from Crosson and Owens (1987). Their trench-normal profile of seismicity in central Washington shows that upper plate seismicity does not occur below 25 km, and that this cutoff shallows westward. The lower boundary of upper plate seismicity is temperature related, and thus is a good indicator of the depth of rupture that might be expected on the subduction interface (Dragert and others, 1994). We infer that the downdip edge of the rupture zone will probably coincide with the point at which the subducting slab reaches 25 km. This depth roughly corresponds to the 420° isotherm of Hyndman and Wang (1993), and is in good agreement with the slab geometry modeled by Tréhu and others (1992) based on velocity modeling of a recent reflection refraction experiment in central Oregon.

The maximum width of the potential seismogenic (locked plus transition) zone thus determined varies from 60 km in central Oregon to 100 km at its widest in Washington. The 350° isotherm (Figure 5.8) shows the landward estimate of the locked zone of Hyndman and Wang (1993). Figure 5.8 shows that the width of the locked zone varies considerably, from only 13 km for an area from 44° 37' N to 45° 37' N latitude in central Oregon, to a maximum of 42 km in Washington, due to the shallower plate dip there. These results have large errors due to the assumptions built into the thermal models (see Hyndman and Wang, 1993, for discussion), and the low rates of seismicity used to determine the updip and downdip limits of seismogenic behavior. Nevertheless, the resulting estimate of the size of the seismogenic zone is within an acceptable range in comparison to the rupture widths of other subduction zones shown in Figure 5.9. We note that the maximum rupture width implied by Hyndman and Wang (1993) is 180 km, some 40 km wider than the Chile 1960 event, the largest earthquake ever recorded. This, and the above discussion of the aseismic nature of accretionary wedges,

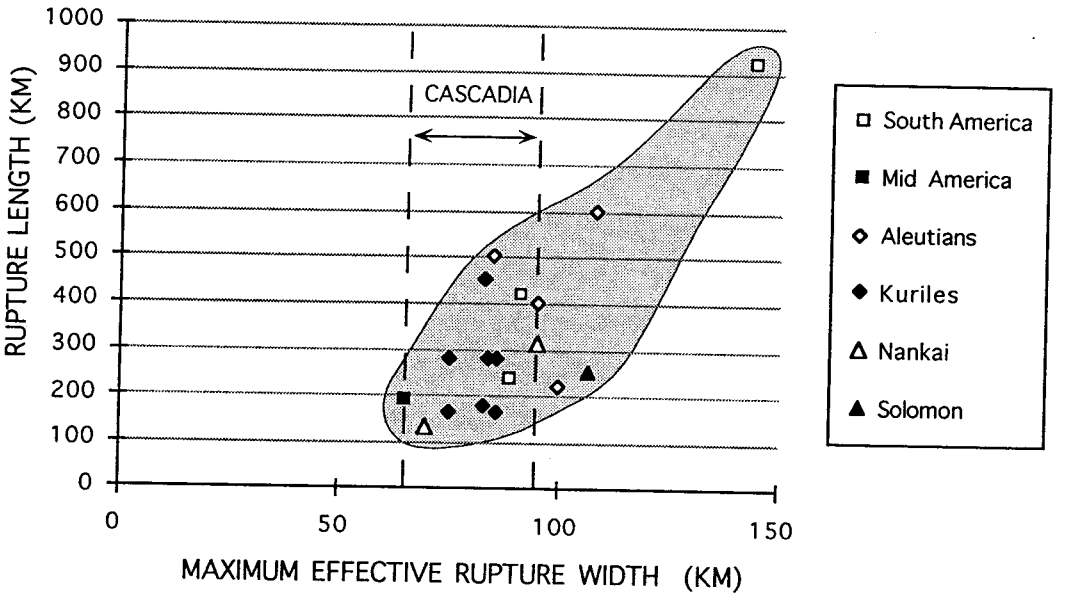

Figure 5.9. Effective rupture width vs. rupture length for great circum-Pacific earthquakes this century. See Table 5.1 for data and sources.

implies to us that Hyndman and Wang's thermal analysis overestimates the width of the seismogenic zone in Cascadia.

The inferred locked zone shown in Figure 5.8 has two significant implications. First, if correct, the locked zone and the potential centroid of moment release are closer to the coast than many previous models have suggested (Hyndman and Wang, 1993; Dragert and others, 1994; Mitchell and others, submitted), and second, the width of the locked zone is very narrow, perhaps absent in two locations. In the following section we use the estimated width of the potential rupture zone in Cascadia as a basis for estimating rupture length based on a comparison to other subduction zones that have had historic great earthquakes.

Potential Rupture Length of Cascadia Interplate Earthquakes

Kelleher and others (1974) found a general relationship between the downdip width of the seismogenic plate boundary at subduction zones and the rupture length for large subduction zone earthquakes. We update this concept using new data on the rupture geometry of great earthquakes from seven circum Pacific subduction zones. Our purpose is to first determine if the relationship inferred by Kelleher remains robust in light of the newer data, and then to compare these results to Cascadia. Kelleher and others (1974) plotted rupture length vs. width for a number of subduction zones based on aftershock distribution. We use more recent data from Pacheco and others (1993) on the downdip extent of the seismogenic plate interface, with a variety of sources for rupture lengths for great subduction earthquakes in this century. The compiled data and sources are summarized in Table 5.1. Figure 5.9 shows the plot of this data, which is similar to the result of Kelleher and others (1974). Our results differ in that the downdip widths are significantly less than the earlier study, and a significant outlier, the 1957 Andreanof earthquake, now plots with many of the other events after revision of the rupture length of this event. The narrower widths obtained by Pacheco and others (1993) are due to the use of a more limited set of aftershocks that excludes all but shallow thrust events on the plate interface. The 1200 km rupture length for the 1957 Andreanof event used by Kelleher and others (1974) was based on a 22 day aftershock distribution as reported in Sykes (1971). Ruff and others (1985) calculate that virtually all of the resolvable seismic moment was released on a 600 km rupture, and the large aftershock area is explained by either extremely low moment release on the rest of the fault, or slow stress diffusion into the rest of the aftershock area over a period of weeks to one year.

We derived the effective rupture widths from data on downdip width mostly from Pacheco and others (1993), with other sources noted in Table 5.1. We use slip vector residuals from McCaffrey (1993) to correct from downdip width to the width in the slip direction, since this is the relevant value when considering the development of forearc decoupling structures discussed below.

Figure 5.9, shows considerable scatter, but the envelope of aspect ratios of known rupture geometries has well defined limits. The scatter is due

trench*	date	Mw/Ms	latitude °	longitude °	dip °	downdip width (km)	SVR °	obliquity °	effective width (km)	rupture length (km)	width reference	length reference
South America												
27	22-May-60	9.5/8.5	-38.01	-74.79	12	140	8.7	21.9	144	920	1	1
19	6-Apr-43	8.2/7.9	-30.13	-72.41	24	88	9.5	17.3	88.8	240	2	3
9	11-Nov-22	8.3/8.1	-27.47	-71.75	24	88	12	26.7	91	420	2	3
Mid-America												
13	3-Jun-32	8.2/8.0	18.35	-104.71	21	65	2.6	1.3	65	190	2	4
Aleutians												
15	10-Nov-38	8.2/8.3	54.26	-156	25	95	2.6	1.3	95	400	2	2
40	7-May-86	8.0/7.7	50.52	-174.5	25	95	9.1	27.1	100	220	2	
24	9-Mar-57	9.1/8.1	50.29	-176.68	25	95, 83	7.9	36.5	108	600	2, 5	3
30	4-Feb-65	8.7/8.2	50.33	-162.98	18	75	22.3	49.9	85	500	2	6
Kuriles												
10	3-Feb-23	8.3/8.3	53.34	162.72	32	75	3.3	4.7	75	280	2	3
26	4-May-59	8.2/7.7	52.59	161.86	32	75	1.9	5	75	165	2	3
23	4-Nov-52	9.0/8.2	51.81	161.08	32	82	2.2	9	83	450	2	3
28	13-Dec-63	8.5/8.1	43.94	150.41	22	82	6.1	23	86	280	2	3
25	11-Nov-58	8.3/8.1	43.37	149.41	22	82	10.6	20.9	83	180	2	3
33	11-Aug-69	8.2/7.8	42.78	148.42	22	82	5.8	23	86	165	2	3
22	4-Mar-52	8.2/8.3	40.84	144.93	22	82	1.8	15.6	84	280	2	3
Nankai												
20	7-Dec-44	8.2/8.1	32.44	136.27		70	1.6	***45.3	70	130	7	7
21	20-Dec-46	8.5/8.1	31.73	134.29		**95	6.2	14.7	95	310	7	7
Solomon												
14	18-Jul-34	??/8.1	-12.56	165.8	32	107	10.9	8.5	107	250	2	3

* Numbers used by McCaffrey (1993), shown for cross referencing.

** Average over two segments of different widths.

*** Probable error in McCaffrey (1993).

Table 5.1. Earthquake and subduction parameter data used in Figure 5.9. Mw/Ms = moment magnitude/surface wave magnitude; SVR = slip vector residual (in degrees). Effective rupture width is the downdip width across the seismogenic zone, in the slip direction. References: 1= Cifuentes (1989); 2 = Pacheco and Sykes (1993); 3 = Kelleher (1972); 4 = Kelleher (1973); 5 = Boyd and Nabelek (1986); 6 = Wu and Kanamori (1973); 7 = Ando (1975).

to errors in earthquake locations and depths, as well as variability of the natural systems. Considering that many of the subduction zones represented have gone through one or more complete earthquake cycles, we find Figure 5.9 to be reasonably representative of rupture geometries for great subduction earthquakes, although we cannot assign error statistics to these data. The data define a range of known rupture area geometries with which we may evaluate possible rupture scenarios in Cascadia.

Using the maximum effective rupture width for Cascadia of 98 km derived above, we infer that the maximum rupture length based on historical evidence would be 500-600 km, with a range of 150-600 km. The total length of the Cascadia subduction zone, and thus the maximum possible rupture length, is 1400 km. However, faults of all types seldom rupture the entire fault length, instead they rupture in segments or patches, the individual offsets of which make up the observed net offset (Bilham and Bodin, 1992, and references therein). Sequential rupture of a number of segments over a span of a few years, days, or even hours is also possible and has been observed in other subduction zones (Yeats and others, in prep.). It is apparent that a scenario involving a single rupture of the Cascadia plate boundary along its 1400 km length would be unprecedented based on the available data. The only earthquake that has approached that length of rupture is the 1960 Chile event (960 km), which has a much wider (140 km) downdip extent than postulated for Cascadia.

The two very narrow or non-existent zones of locking in central Oregon and southern Washington indicate that at least for the present strain cycle, the Oregon and Washington Cascadia margin may effectively divided into several segments. If the locking width is dependent on the configuration of the outer edge of the backstop as we have suggested, this may be a long term feature of this part of the margin. The longest segment in the present strain cycle is approximately 280 km, from the projection of the subducting Blanco Fracture Zone to the low uplift zone in central Oregon (Fig. 5.8).

From this comparison to known rupture geometries, we conclude that the range of rupture lengths in Cascadia is on the order of 150-600 km. If the present segmentation of uplift shown in Figure 5.8 is represents a typical pattern of strain accumulation in Cascadia, rupture segments may be limited to a 300 km maximum. Many investigators have reported marsh burial events

at about 300 years before present from Vancouver Island to Cape Mendocino, a much greater distance. If these reported events are from a single event, the rupture length and aspect ratio of the rupture area of that event would have been well outside the bounds of available data on subduction earthquakes elsewhere as shown in Figure 5.9. The correlation of radiocarbon dated marsh burials however have at best decades of unresolvable error unless they are correlated with dendrochronology (tree ring matching). This leaves two possibilities for the explanation of a widespread 300 year event: A very long rupture (apparently unlikely), or a sequential rupture of several or many segments spanning the required length over a few years or decades. A sequential rupture of several segments over a period of a few years or decades can satisfy the marsh data without requiring individual ruptures to have unprecedented rupture lengths with respect to historical data. This type of rupture has occurred at many subduction zones, and is a commonly observed mechanism by which seismic gaps are filled (Thatcher, 1989).

CONCLUSIONS

The Oregon and Washington Cascadia forearc is undergoing a significant degree of along arc deformation in the form of oblique strike-slip faulting and folding. The cumulative extension of the forearc by the nine strike-slip faults we have mapped is similar to the total arc parallel component of plate convergence, and thus the Cascadia forearc may be fully strain partitioned. By comparison to other oblique subduction zones, using the data of McCaffrey (1993), we conclude that Cascadia is unlikely to generate earthquakes greater than magnitude 8.2 because the forearc is not capable of storing the required elastic strain energy.

Using published data on the seismicity, velocity structure, geodetics, and thermal signature of the Cascadia margin, we estimate that the width of the seismogenic (locked plus transition) plate interface varies in width from 60 to 100 km in the central Oregon-Washington part of the margin. Furthermore, the pattern of modern strain accumulation along the coast is heterogeneous; a large area in central Oregon and another in southwestern Washington are apparently accumulating little or no elastic strain energy. This suggests a locked zone consisting of a number of asperities, and two areas of poor coupling in the current strain cycle.

Finally, comparison of rupture geometry for historic great subduction earthquakes shows that the maximum rupture lengths are dependent on the downdip width of the locked plate interface. Historical data suggest that the maximum rupture possible in Cascadia is 500-600 km, far greater than the length over which an event has been reported to have occurred 300 years ago. A sequential rupture of the segmented plate boundary over several years or decades is a common mechanism for seismic gap filling, and can account for the observed similarity in marsh burial ages along the margin, without requiring unprecedented rupture lengths and earthquake magnitudes.

REFERENCES CITED

Acharya, H., 1992, Comparison of seismicity parameters in different subduction zones and its implications for the Cascadia subduction zone: Journal of Geophysical Research, v. 97, p. 8831-8842.

Adams, J., 1990, Paleoseismicity of the Cascadia subduction zone: Evidence from turbidites off the Oregon-Washington Margin: Tectonics, v. 9, p. 569-584.

Ando, M., 1975, Source mechanisms and tectonic significance of historical earthquakes along the Nankai trough, Japan: Journal of Geophysical Research, v. 27, p. 119-140.

Appelgate, T.B., Goldfinger, C., Kulm, L.D., MacKay, M., Fox, C.G., Embley, R.W., and Meis, P.J., 1992, A left lateral strike slip fault seaward of the central Oregon convergent margin: Tectonics, v. 11, p. 465-477.

Atwater, B.F., 1987, Evidence for great Holocene earthquakes along the outer coast of Washington State: Science, v. 236, p. 942-944.

Beck, M.E., Jr., 1983, On the mechanism of tectonic transport in zones of oblique subduction: Tectonophysics, v. 93, p. 1-11.

Bilham, R., and Bodin, P., 1992, Fault zone connectivity: slip rates on faults in the San Francisco Bay Area, California: Science, v. 258, p. 281-284.

Boyd, T.M., and Nabelek, J.L., 1988, Rupture Process of the Andreanof Islands Earthquake of May 7, 1986: Bulletin of the Seismological Society of America, v. 78, p. 1653-1673.

Byrne, D.E., Davis, D.M., and Sykes, L.R., 1988, Loci and maximum size of thrust earthquakes and the mechanics of the shallow region of subduction zones: Tectonics, v. 7, p. 833-857.

Cifuentes, I., 1989, The 1960 Chilean earthquakes: Journal of Geophysical Research, v. 94, p. 665-680.

Crosson, R.S., and Owens, T.J., 1987, Slab geometry of the Cascadia subduction zone beneath Washington from earthquake hypocenters and teleseismic converted waves: Geophysical Research Letters, v. 14, p. 824-827.

Darienzo, M.E., and Peterson, C.D., 1990, Episodic tectonic subsidence of late Holocene salt marshes, northern Oregon central Cascadia margin: Tectonics, v. 9, p. 1-22.

DeMets, C., Gordon, R.G., Argus, D.F., and Stein, S., 1990, Current plate motions: Geophysical Journal International, v. 101, p. 425-478.

Dragert, H., Hyndman, R. D., Rogers, G.C., and Wang, K., 1994, Current deformation and the width of the seismogenic zone of the northern Cascadia subduction thrust: Journal of Geophysical Research, v. 99, p. 653-688.

EEZ-SCAN 84 Scientific Staff, 1988, Physiography of the western United States Exclusive Economic Zone: Geology, v. 16, p. 131-134.

Fitch, T.J., 1972, Plate convergence, transcurrent faults, and internal deformation adjacent to southeast Asia and the western Pacific: Journal of Geophysical Research, v. 77, p. 4432-4460.

Geist, E.L., Childs, J.R., and Scholl, D.W., 1988, The origin of summit basins of the Aleutian Ridge: Implications for block rotation of the arc massif: Tectonics, v. 7, p. 327-341.

Goldfinger, C., Kulm, L.D., and Yeats, R.S., 1992a, Neotectonic map of the Oregon continental margin and adjacent abyssal plain: Oregon Department of Geology and Mineral Industries, Open-File Report O-92-4, scale 1:500,000.

Goldfinger, C., Kulm, L.D., Yeats, R.S., Appelgate, B., MacKay, M., and Cochrane, G.R., in press, Active strike-slip faulting and folding of the Cascadia plate boundary and forearc in central and northern Oregon, *in* Rogers, A.M., Kockelman, W.J., Priest, G., and Walsh, T.J., eds., Assessing and reducing earthquake hazards in the Pacific Northwest: U.S. Geological Survey Professional Paper 1560.

Goldfinger, C., Kulm, L.D., Yeats, R.S., Appelgate, B., MacKay, M., and Moore, G.F., 1992b, Transverse structural trends along the Oregon convergent margin: implications for Cascadia earthquake potential: Geology, v. 20, p. 141-144.

Griggs, G.B., and Kulm, L.D., 1973, Origin and development of Cascadia deep-sea channel: Journal of Geophysical Research, v. 78, p. 6325-6339.

Heaton, T.H., and Kanamori, H., 1984, Seismic potential associated with subduction in the northwestern United States: Bulletin of the Seismological Society of America, v. 74, p. 993-941.

Hyndman, R.D., and Davis, E.E., 1992, A mechanism for the formation of methane hydrate and seafloor bottom simulating reflectors by vertical fluid expulsion: Journal of Geophysical Research, 97, p. 7025-7041.

Hyndman, R.D., and Wang, K., 1993, Thermal constraints on the zone of major thrust earthquake failure: the Cascadia subduction zone: Journal of Geophysical Research, v. 98, p. 2039-2060.

Jarrard, R.D., 1986, Terrane motion by strike-slip faulting of forearc slivers: Geology, v. 14, p. 780-783.

Kelleher, J., 1972, Rupture zones of large South American earthquakes and some predictions: Journal of Geophysical Research, v. 77, p. 2087-2103.

Kelleher, J., Savino, J., Rowlett, H., and McCann, W., 1974, Why and where great thrust earthquakes occur along island arcs: Journal of Geophysical Research, v. 79, p. 4889-4899.

Kelleher, J., Sykes, L., and Oliver, J., 1973, Possible criteria for predicting earthquake locations and their application to major plate boundaries of the Pacific and the Caribbean: Journal of Geophysical Research, v. 78, p. 2547-2585.

MacKay, M.E., Moore, G.F., Cochrane, G.R., Moore, J.C., and Kulm, L.D., 1992, Landward vergence and oblique structural trends in the Oregon margin accretionary prism: Implications and effect on fluid flow: Earth and Planetary Science Letters, v. 109, p. 477-491.

McCaffrey, R., 1992, Oblique plate convergence, slip vectors, and forearc deformation: Journal of Geophysical Research, v. 97, p. 8905-8915.

McCaffrey, R., 1993, On the role of the upper plate in great subduction zone earthquakes: Journal of Geophysical Research, v. 98, p. 11,953-11,966.

McInelly, G.W., and Kelsey, H.M., 1990, Late Quaternary tectonic deformation in the Cape Arago-Bandon region of coastal Oregon as deduced from wave cut platforms: Journal of Geophysical Research, v. 95, p. 6699-6713.

Mitchell, C.E., Vincent, P., Weldon, R.J.I., and Richards, M.A., in press, Present-day vertical deformation of the Cascadia margin, Pacific Northwest, U.S.A.: submitted to: Journal of Geophysical Research.

Nelson, C.H., 1968, Marine geology of the Astoria deep-sea fan, Corvallis, Oregon State University, Ph.D. dissertation, 287 p.

Oppenheimer, D., Beroza, G., Carver, G., Dengler, L., Eaton, J., Gee, L., Gonzalez, F., Jayko, A., Li, W. H., Lisowski, M., Magee, M., Marshall, G., Murray, M., McPhereson, R., Romanowicz, B., Satake, K., Simpson, R., Somerville, P., Stein, R., and Valentine, D., 1993, The Cape Mendocino, California, earthquakes of April 1992: Subduction at the triple junction: Science, v. 261, p. 433-438.

Pacheco, J.F., Sykes, L.R., and Scholz, C.H., 1993, Nature of seismic coupling along simple plate boundaries of the subduction type: Journal of Geophysical Research, v. 98, p. 14,133-14,159.

Ruff, L., Kanamori, H., and Sykes, L., 1985, The great 1957 Andreanof earthquake: EOS (Transactions, American Geophysical Union), v. 66, p. 298.

Ryan, H.F., and Scholl, D.W., 1993, Geologic implications of great interplate earthquakes along the Aleutian arc: Journal of Geophysical Research, v. 98, p. 22,135-22,146.

Scholz, C.H., Dawers, N.H., Yu, J.-Z., and Anders, M.H., 1993, Fault growth and fault scaling laws: Preliminary results: Journal of Geophysical Research, v. 98, p. 21,951-21,961.

Seno, T., Stein, S., and Gripp, A.E., 1993, A model for the motion of the Philippine Sea plate consistent with NUVEL-1 and geologic data: Journal of Geophysical Research, v. 98, p. 17,941-17,948.

Shiono, K., 1988, Seismicity of the SW Japan Arc - Subduction of the Young Shikoku Basin: Modern Geology, v. 12, p. 449-464.

Sykes, L.R., 1971, Aftershock Zones of Great Earthquakes, Seismicity Gaps, and Earthquake Prediction for Alaska and the Aleutians: Journal of Geophysical Research, 76, p. 8021-8041.

Thatcher, W., 1989, Earthquake recurrence and risk assessment in circum-Pacific seismic gaps: Nature, v. 341, p. 432-434.

Tréhu, A.M., Nabelek, J.N., Azevedo, S., Broecher, T.M., Mooney, W.D., Leutgert, J., Asudeh, I. , Clowes, R., Nakamura, Y., Smithson, S., Miller K., 1992, A crustal cross-section across the Cascadia subduction in central Oregon: EOS (Transactions, American Geophysical Union), v. 73, p. 391.

Wells, R.E., and England, P., 1991, Neogene rotations and quasicontinuous deformation of the Pacific Northwest continental margin: Geology, v. 19, p. 978-981.

Wells, R.E., and Heller, P.L., 1988, The relative contribution of accretion, shear, and extension to Cenozoic tectonic rotation in the Pacific Northwest: Geological Society of America Bulletin, v. 100, p. 325-338.

Wu, F.T., and Kanamori, H., 1973, Source mechanism of February 4, 1965, Rat Island earthquake: Journal of Geophysical Research, v. 78, p. 6082-6092.

Yeats, R. S., Sieh, K.E., and Allen, C.R., in prep, Geology of Earthquakes: Oxford University Press.

ACKNOWLEDGMENTS

We would like to thank the following people who were members of the Scientific Party on cruises from 1992-1993: Kevin Redman, David Wilson, Tim McGiness, Wolf Krieger, Chris Center, Kirk O'Donnell from Williamson and Associates of Seattle Washington, our sidescan contractors; Lisa McNeill, Craig Schneider, Margaret Mumford, Gary Huftile, Hiroyuki Tsutsumi, Alan Neim, and John Chen, all from Oregon State University; DELTA pilots Rich and Dave Slater, Chris Ijames, and Don Tondrow; Stacey Moore, Bruce Dougan, and Wayne Bloechl; the masters and crews of the research vessels Thomas Thompson (University of Washington); Jolly Roger, and Cavalier, (DELTA support vessels chartered to DELTA Oceanographics).

This research supported by the NOAA National Undersea Research Program (NURP), by the U.S.G.S. National Earthquake Hazards Reduction Program (NEHRP), and by the National Science Foundation (NSF).

BIBLIOGRAPHY

Acharya, H., 1992, Comparison of seismicity parameters in different subduction zones and its implications for the Cascadia subduction zone: Journal of Geophysical Research, v. 97, p. 8831-8842.

Adams, J., 1990, Paleoseismicity of the Cascadia subduction zone-- Evidence from turbidites off the Oregon-Washington margin: Tectonics, v. 9, p. 569-583.

Ando, M., 1975, Source mechanisms and tectonic significance of historical earthquakes along the Nankai trough, Japan: Journal of Geophysical Research, v. 27, p. 119-140.

Ando, M., and Balazs, E.I., 1979, Geodetic evidence for aseismic subduction of the Juan de Fuca plate: Journal of Geophysical Research, v. 84, p. 3023-3027.

Appelgate, T.B., 1988, Tectonic and volcanic structures of the southern flank of Axial volcano, Juan de Fuca Ridge-- Results from a SeaMARC 1 sidescan sonar survey: Corvallis, Oregon State University, M.S. thesis, 161 p.

Appelgate, T.B., Goldfinger, C., Kulm, L.D., MacKay, M., Fox, C.G., Embley, R.W., and Meis, P.J., 1992, A left-lateral strike-slip fault seaward of the central Oregon convergent margin: Tectonics, v. 11, p. 465-477.

Atwater, B.F., 1987, Evidence for great Holocene earthquakes along the outer coast of Washington State: Science, v. 236, p. 942-944.

Atwater, B.F., 1992, A Seattle tsunami 1100 years ago: Geological Society of America Abstracts with Programs, v. 24, p. 4.

Atwater, B.F., and Yamaguchi, D.K., 1991, Sudden, probably coseismic submergence of Holocene trees and grass in coastal Washington State: Geology, v. 19, p. 706-709.

Barnard, W.D., and McManus, D.A., 1973, Planktonic foraminiferan-Radiolarian stratigraphy and the Pleistocene-Holocene boundary in the northeast Pacific: Geological Society of America Bulletin, v. 84, p. 2097-2100.

Beck, M.E., Jr., 1983, On the mechanism of tectonic transport in zones of oblique subduction: Tectonophysics, v. 93, p. 1-11.

Bilham, R., and Bodin, P., 1992, Fault zone connectivity: slip rates on faults in the San Francisco Bay Area, California: Science, v. 258, p. 281-284.

Blackwelder, B.W., Pilkey, O.R., and Howard, J.D., 1979, Late Wisconsinan sea levels on the southeast U. S. Atlantic shelf based on in-place shoreline indicators: Science, v. 204, p. 618-620.

Boyd, T.M., and Nabelek, J.L., 1988, Rupture Process of the Andreanof Islands Earthquake of May 7, 1986: Bulletin of the Seismological Society of America, v. 78, p. 1653-1673.

Bucknam, R.C., Hemphill-Haley, E., and Leopold, E.B., 1992, Abrupt uplift within the past 1700 years at southern Puget sound, Washington: Science, v. 258, p. 1611-1614.

Byrne, D.E., Davis, D.M., and Sykes, L.R., 1988, Loci and maximum size of thrust earthquakes and the mechanics of the shallow region of subduction zones: Tectonics, v. 7, p. 833-857.

Carlson, P.R., 1967, Marine geology of the Astoria submarine canyon: Corvallis, Oregon State University, Ph.D. dissertation, 259 p.

Carlson, P.R., and Nelson, H.C., 1987, Marine geology and resource potential of Cascadia Basin, *in* Scholl, D. W., Grantz, A., and Vedder, J.G., eds., Geology and resource potential of the continental margin of western North America and adjacent ocean basins-Beaufort sea to Baja California: Houston, Circum-Pacific Council for Energy and Mineral Resources, p. 523-535.

Carson, B., 1971, Stratigraphy and depositional history of Quaternary sediments in northern Cascadia Basin and Juan de Fuca abyssal plain, northeast Pacific Ocean: Seattle, University of Washington, Ph.D. dissertation, 249 p.

Carson, B., 1977, Tectonically induced deformation of deep-sea sediments off Washington and northern Oregon: Marine Geology, v. 24, p. 289-307.

Carver, G.A., Vick, G.S., and Burke, R.M., 1989, Late Holocene paleoseismicity of the Gorda segment of the Cascadia subduction zone: Geological Society of America Abstracts with Programs, v. 21, p. 64.

Chappel, J., and Shackleton, N.J., 1986, Oxygen isotopes and sea-level: Nature, v. 324, p. 137-140.

Cifuentes, I., 1989, The 1960 Chilean earthquakes: Journal of Geophysical Research, v. 94, p. 665-680.

Clarke, S.H., Jr., 1990, Map showing geologic structures of the northern California continental margin: U.S. Geological Survey, Map MF-2130, scale 1:250,000.

Clarke, S.H., Jr., 1992, Geology of the Eel River Basin and adjacent region: Implications for late Cenozoic tectonics of the southern Cascadia subduction zone and Mendocino triple junction: American Association of Petroleum Geologists Bulletin, v. 76, p. 199-224.

Clarke, S.H., Jr., and Carver, G.A., 1989, Late Cenozoic structure and seismic potential of the southern Cascadia subduction zone: EOS (Transactions, American Geophysical Union), v. 70, p. 1331-1332.

Clarke, S.H., Jr., Field, M.E., and Hirozawa, C.A., 1985, Reconnaissance geology and geologic hazards of the offshore Coos Bay Basin, Oregon: U.S. Geological Survey Bulletin 1645, 41 p.

Cochrane, G.R., and Lewis, B.T.R., 1988, Deep-tow seismic reflection records from the Oregon lower slope: EOS (Transactions, American Geophysical Union), v. 69, p. 1442-1443.

Crosson, R.S., and Owens, T.J., 1987, Slab geometry of the Cascadia subduction zone beneath Washington from earthquake hypocenters and teleseismic converted waves: Geophysical Research Letters, v. 14, p. 824-827.

Couch, R.W., and Braman, D., 1979, Geology of the continental margin near Florence, Oregon: Oregon Geology, v. 41, p. 171-179.

Curray, J.R., 1965, Late Quaternary history, continental shelfs of the U. S., *in* Wright, H.E., and Frey, D.G., eds., The Quaternary of the United States: Princeton, N.J., Princeton Univ. Press, p. 723-735.

Darienzo, M.E., and Peterson, C.D., 1990, Episodic tectonic subsidence of late Holocene salt marshes, northern Oregon central Cascadia margin: Tectonics, v. 9, p. 1-22.

DeMets, C., Gordon, R.G., Argus, D.F., and Stein, S., 1990, Current plate motions: Geophysical Journal International, v. 101, p. 425-478.

Dragert, H., Hyndman, R. D., Rogers, G.C., and Wang, K., 1994, Current deformation and the width of the seismogenic zone of the northern Cascadia subduction thrust: Journal of Geophysical Research, v. 99, p. 653-688.

Duncan, J.R., 1968, Late Pleistocene and postglacial sedimentation and stratigraphy of deep-sea environments off Oregon: Corvallis, Oregon State University, Ph.D. dissertation, 222 p.

Duncan, J.R., Fowler, G.A., and Kulm, L.D., 1970, Planktonic Foraminiferan-Radiolarian ratios and Holocene-Late Pleistocene deep-sea stratigraphy off Oregon: Geological Society of America Bulletin, v. 81, p. 561-566.

Duncan, R.A., and Kulm, L.D., 1989, Plate tectonic evolution of the Cascades arc-subduction complex, *in* Winterer, E.L., Hussong, D.M., and Decker, R.W., eds., The Eastern Pacific Ocean and Hawaii: Boulder, Colorado, Geological Society of America, The Geology of North America, p. 413-438.

EEZ-SCAN 84 Scientific Staff, 1986, Atlas of the Exclusive Economic Zone, Western Conterminous United States: U.S. Geological Survey Miscellaneous Investigations Series I-1792, 152 p., scale 1:500,000.

EEZ-SCAN 84 Scientific Staff, 1988, Physiography of the western United States Exclusive Economic Zone: Geology, v. 16, p. 131-134.

Fairbanks, R.G., 1989, A 17,000-year glacio-eustatic sea level record: influence of glacial melting rates on the Younger Dryas event and deep-ocean circulation: Nature, v. 342, p. 637-642.

Fitch, T.J., 1972, Plate convergence, transcurrent faults, and internal deformation adjacent to southeast Asia and the western Pacific: Journal of Geophysical Research, v. 77, p. 4432-4460.

Fowler, G.A., Orr, W.N., and Kulm, L.D., 1971, An upper Miocene diatomaceous rock unit on the Oregon continental shelf: Journal of Geology, 79, p. 603-608.

Freund, R., 1974, Kinematics of transform and transcurrent faults: Tectonophysics, v. 21, p. 93-134.

Gardner, J.V., Field, M.E., Lee, H., Edwards, B.E., Masson, D.G., Kenyon, N., and Kidd, R.B., 1991, Ground-truthing 6.5 kHz side scan sonographs: what are we really imaging?: Journal of Geophysical Research, v. 96, p. 5955-5974.

Geist, E.L., Childs, J.R., and Scholl, D.W., 1988, The origin of summit basins of the Aleutian Ridge: Implications for block rotation of an arc massif: Tectonics, v. 7, p. 327-341.

Goldfinger, C., Kulm, L.D., and Yeats, R.S., 1992a, Neotectonic map of the Oregon continental margin and adjacent abyssal plain: Oregon Department of Geology and Mineral Industries, Open-File Report O-92-4, scale 1:500,000.

Goldfinger, C., Kulm, L.D., Yeats, R.S., Appelgate, T.B., MacKay, M.E., and Cochrane, G., in press, Active strike-slip faulting and folding of the Cascadia plate boundary and forearc in central and northern Oregon, *in* Rogers, A.M., Kockelman, W.J., Priest, G., and Walsh, T.J., eds., Assessing and reducing earthquake hazards in the Pacific Northwest, U.S. Geological Survey Professional Paper 1560.

Goldfinger, C., Kulm, L.D., Yeats, R.S., Appelgate, T.B., MacKay, M.E., and Moore, G.F., 1992b, Transverse structural trends along the Oregon convergent margin: implications for Cascadia earthquake potential: Geology, v. 20, p. 141-144.

Griggs, G.B., and Kulm, L.D., 1970, Sedimentation in Cascadia deep-sea channel: Geological Society of America Bulletin, v. 81, p. 1361-1384.

Griggs, G.B., and Kulm, L.D., 1973, Origin and development of Cascadia deep-sea channel: Journal of Geophysical Research, v. 78, p. 6325-6339.

Griggs, G.B., Kulm, L.D., Waters, A.C., and Fowler, G.A., 1970, Deep-sea gravel from Cascadia Channel: Journal of Geology, v. 78, p. 611-619.

Hampton, M.A., Karl, H.A., and Kenyon, N.H., 1989, Sea-floor drainage features of Cascadia Basin and the adjacent continental slope, northeast Pacific Ocean: Marine Geology, 87, p. 249-272.

Harding, T.P., 1985, Seismic characteristics and identification of negative flower structures, positive flower structures, and positive structural inversion: American Association of Petroleum Geologists Bulletin, v. 69, p. 582-600.

Heaton, T.H., and Hartzell, S.H., 1987, Earthquake hazards on the Cascadia subduction zone: Nature, v. 236, p. 162-168.

Heaton, T.H., and Kanamori, H., 1984, Seismic potential associated with subduction in the northwestern United States: Seismological Society of America Bulletin, v. 74, p. 933-941.

Hyndman, R.D., and Davis, E.E., 1992, A mechanism for the formation of methane hydrate and seafloor bottom simulating reflectors by vertical fluid expulsion: Journal of Geophysical Research, 97, p. 7025-7041.

Hyndman, R.D., and Wang, K., 1993, Thermal constraints on the zone of major thrust earthquake failure: the Cascadia subduction zone: Journal of Geophysical Research, v. 98, p. 2039-2060.

Ingle, J.C., 1973, Neogene foraminifera from the northeastern Pacific ocean, Leg 18, Deep Sea Drilling Project: Initial Reports of the Deep Sea Drilling Project, v. XVIII, p. 517-567.

Jackson, J., and Molnar, P., 1990, Active faulting and block rotations in the western Transverse Ranges, California: Journal of Geophysical Research, v. 95, p. 22,073-22,087.

Jarrard, R.D., 1986, Terrane motion by strike-slip faulting of forearc slivers: Geology, v. 14, p. 780-783.

Johnson, H.P., and Helferty, M., 1990, The geological interpretation of side-scan sonar: Reviews of Geophysics, v. 28, p. 357-380.

Jones, G.A., Jull, A.J.T., Linick, T.W., and Donahue, D.J., 1989, Radiocarbon dating of deep-sea sediments: a comparison of accelerator mass spectrometer and beta decay methods: Radiocarbon, v. 31, p. 105-116.

Karig, D.E., Sarewitz, D.R., and Haeck, G.D., 1986, Role of strike-slip faulting in the evolution of allochthonous terranes in the Philippines: Geology, v. 14, p. 852-855.

Kelleher, J., 1972, Rupture zones of large South American earthquakes and some predictions: Journal of Geophysical Research, v. 77, p. 2087-2103.

Kelleher, J., Savino, J., Rowlett, H., and McCann, W., 1974, Why and where great thrust earthquakes occur along island arcs: Journal of Geophysical Research, v. 79, p. 4889-4899.

Kelleher, J., Sykes, L., and Oliver, J., 1973, Possible criteria for predicting earthquake locations and their application to major plate boundaries of the Pacific and the Caribbean: Journal of Geophysical Research, v. 78, p. 2547-2585.

Kelsey, H.M., 1990, Late Quaternary deformation of marine terraces on the Cascadia subduction zone near Cape Blanco, Oregon: Tectonics, v. 9, p. 983-1014.

Kelsey, H.M., Mitchell, C.E., Weldon, R.J.I., Engebretson, D., Ticknor, R., and Bockhiem, J., 1992, Latitudinal variation in surface uplift from geodetic, wave-cut platform and topographic data, Cascadia margin: Geological Society of America Abstracts with Programs, v. 24, p. 37.

Komar, P.D., Neudeck, R.H., and Kulm, L.D., 1972, Observations and significance of deep-water oscillatory ripple marks on the Oregon continental shelf, *in* Swift, D.J.P., Duane, D.B., and Pilkey, O.H., eds., Shelf sediment transport: Stroudsburg, Pennsylvania, Dowden, Hutchinson and Ross, Inc., p. 601-619.

Komar, P.D., and Shih, S.-M., in press, Sea-cliff erosion along the Oregon Coast: Coastal Sediments.

Kulm, L.D., and Fowler, G.A., 1974, Oregon continental margin structure and stratigraphy: a test of the imbricate thrust model, *in* Burke, C. A., and Drake, C. L., eds., The geology of continental margins: New York, Springer-Verlag, p. 261-284.

Kulm, L.D., Prince, R.A., and Snavely, P.D., Jr., 1973a, Site survey of the northern Oregon continental margin and Astoria Fan: Initial Reports of the Deep Sea Drilling Project, v. XVIII, p. 979-987.

Kulm, L.D., Roush, R.C., Harlett, J.C., Neudeck, R.H., Chambers, D.M., and Runge, E.J., 1975, Oregon continental shelf sedimentation: Interrelationships of facies distribution and sedimentary processes: Journal of Geology, v. 83, p. 145-175.

Kulm, L.D., and Scheidegger, K.F., 1979, Quaternary sedimentation on the tectonically active Oregon continental slope: Society of Economic Paleontologists and Mineralogists Special Publication 27, p. 247-263.

Kulm, L.D., and Suess, E., 1990, The relation of carbonate deposits to fluid venting processes: Oregon accretionary prism: Journal of Geophysical Research, v. 95, p. 8899-8915.

Kulm, L.D., Von Huene, R., and scientific party, 1973b, Initial reports of the Deep Sea Drilling Project, Volume 18: Washington, D.C., U. S. Government Printing Office, p. 97-168.

Lewis, S.D., Ladd, J.W., and Bruns, T.R., 1988, Structural development of an accretionary prism by thrust and strike-slip faulting-- Shumagin region, Aleutian Trench: Geological Society of America Bulletin, v. 100, p. 767-782.

Ludwin, R.S., Weaver, C.S., and Crosson, R.S.,1991, Seismicity of Washington and Oregon, *in* Slemmons, D.B., Engdahl, E.R., Blackwell, D., and Schwartz, D., eds., Neotectonics of North America: Decade of North American Geology CSMV-1, p. 77-98.

MacKay, M. E., Moore, G.F., Cochrane, G.R., Moore, J.C., and Kulm, L.D., 1992, Landward vergence, oblique structural trends, and tectonic segmentation in the Oregon margin accretionary prism: Earth and Planetary Science Letters, v. 109, p. 477-491.

Matthews, R.K., 1990, Quaternary sea-level change, *in* Panel on Sea-Level Change, ed., Sea Level Change: Washington, DC, National Academy Press, p. 88-103.

McCaffrey, R., 1992, Oblique plate convergence, slip vectors, and forearc deformation: Journal of Geophysical Research, v. 97, p. 8905-8915.

McCaffrey, R., 1993, On the role of the upper plate in great subduction zone earthquakes: Journal of Geophysical Research, v. 98, p. 11,953-11,966.

McInelly, G.W., and Kelsey, H.M., 1989, Holocene and Late Pleistocene tectonic deformation of the Whiskey Run in the Cape Arago-Coos Bay area, coastal Oregon: Geological Society of America Abstracts with Programs, v. 21, p. 115.

McInelly, G.W., and Kelsey, H.M., 1990, Late Quaternary tectonic deformation in the Cape Arago-Bandon region of coastal Oregon as deduced from wave cut platforms: Journal of Geophysical Research, v. 95, p. 6699-6713.

Mitchell, C.E., Vincent, P., Weldon, R.J.I., and Richards, M.A., in press, Present-day vertical deformation of the Cascadia margin, Pacific northwest, U.S.A.: Journal of Geophysical Research.

Muhs, D.R., Kelsey, H.M., Miller, G.H., Kennedy, G.L., Whelan, G.F., and McInelly, G.W., 1990, Age estimates and uplift rates for late Pleistocene marine terraces: southern Oregon portion of the Cascadia forearc: Journal of Geophysical Research, v. 95, p. 6685-6698.

Mulder, R.A., 1992, Regional tectonic deformation of the North Oregon coast as recorded by Pleistocene marine terraces: Portland, Oregon, Portland State University, M.S. thesis, 96 p.

Nelson, C.H., 1968, Marine geology of the Astoria deep-sea fan: Corvallis, Oregon State University, Ph.D. dissertation, 287 p.

Nelson, C.H., 1976, Late Pleistocene and Holocene depositional trends, processes and history of Astoria Deep-sea Fan: Marine Geology, v. 20, p. 129-173.

Nelson, C.H., Kulm, L.D., Carlson, P.R., and Duncan, J.R., 1968, Mazama ash in the northeastern Pacific: Science, v. 161, p. 47-49.

Nelson, A.R., 1987, Apparent gradual rise in relative sea level on the south-central Oregon coast during the late Holocene--Implications for the great Cascadia earthquake hypothesis: EOS (Transactions, American Geophysical Union), v. 68, p. 1240.

Nelson, A.R., 1992, Great subduction zone earthquakes in the Pacific Northwest? Differentiating coseismic from non-tectonic tidal marsh deposits along the Oregon Coast, *in* Proceedings, Association of Engineering Geologists 35th Annual Meeting, Los Angeles, 1992, p. 284-290.

Nelson, A.R., and Personius, S.F., in press, The potential for great earthquakes in Oregon and Washington: An overview of recent coastal geologic studies and their bearing on segmentation of Holocene ruptures, central Cascadia subduction zone, *in* Rogers, A.M., Kockelman, W.J., Priest, G., and Walsh, T.J., eds., Assessing and reducing earthquake hazards in the Pacific Northwest: U.S. Geological Survey Professional Paper 1560.

Niem, A.R., MacLeod, N.S., Snavely, P.D., Jr., Huggins, D., Fortier, J.D., Meyer, H.J., Seeling, A., and Niem, W.A., 1992, Onshore-offshore geologic cross section, northern Oregon Coast Range to continental slope: Portland, OR, State of Oregon Department of Geology and Mineral Industries, Special Paper 26, 10 p.

Niem, A.R., and Niem, W.A., 1985, Oil and gas investigations of the Astoria Basin, Clatsop and northernmost Tillamook Counties, northwestern Oregon: Oregon Department of Geology and Mineral Industries, Oil and Gas Investigation 14, scale 1:250,000.

Niem, A.R., Snavely, P.D., Jr., and Niem, W.A., 1990, Onshore-offshore geologic cross section from the Mist gas field, northern Oregon coast range, to the northwest Oregon continental shelf: Oregon Department of Geology and Mineral Industries, Oil and Gas Investigation 17, 46 p.

Oppenheimer, D., Beroza, G., Carver, G., Dengler, L., Eaton, J., Gee, L., Gonzalez, F., Jayko, A., Li, W. H., Lisowski, M., Magee, M., Marshall, G., Murray, M., McPhereson, R., Romanowicz, B., Satake, K., Simpson, R., Somerville, P., Stein, R., and Valentine, D., 1993, The Cape Mendocino, California, earthquakes of April 1992: Subduction at the triple junction: Science, v. 261, p. 433-438.

Pacheco, J.F., Sykes, L.R., and Scholz, C.H., 1993, Nature of seismic coupling along simple plate boundaries of the subduction type: Journal of Geophysical Research, v. 98, p. 14,133-14,159.

Parker, M.J., 1990, Oligocene and Miocene geology of the Tillamook embayment, Tillamook County, northwest Oregon []: Corvallis, Oregon State University, M.S. thesis, 524 p.

Peterson, C.P., Kulm, L.D., and Gray, J.J., 1986, Geologic map of the ocean floor off Oregon and the adjacent continental margin: Oregon Department of Geology and Mineral Industries, Map GMS-42, scale 1:500,000.

Peterson, C.P., Loubere, P.W., and Kulm, L.D., 1984, Stratigraphy of the continental shelf and coastal region, *in* Kulm, L.D., and others, eds., Atlas of the Ocean Margin Drilling Program, Western North American Continental Margin and Adjacent Ocean Floor off Oregon and Washington, Region V: Joint Oceanographic Institutions, Inc., Marine Science International, Woods Hole, MA, sheet 30 with text.

Plafker, G., 1972, Alaskan earthquake of 1964 and Chilean earthquake of 1960: implications for arc tectonics: Journal of Geophysical Research, v. 77, p. 901-925.

Riddihough, R., 1984, Recent movements of the Juan de Fuca plate system: Journal of Geophysical Research, v. 89, p. 6980-6994.

Ritger, S., Carson, B., and Suess, E., 1987, Methane derived authigenic carbonates formed by subduction-induced pore-water expulsion along the Oregon/Washington margin: Geological Society of America Bulletin, v. 98, p. 147-156.

Ron, H., Freund, R., Garfunkel, Z., and Nur, A., 1984, Block rotation by strike-slip faulting-- Structural and paleomagnetic evidence: Journal of Geophysical Research, v. 89, p. 6256-6270.

Ruff, L., Kanamori, H., Sykes, L., 1985, The 1957 great Aleutian earthquake: EOS (Transactions, American Geophysical Union), v. 66, p. 298.

Ryan, H.F., and Scholl, D.W., 1993, Geologic implications of great interplate earthquakes along the Aleutian arc: Journal of Geophysical Research, v. 98, p. 22,135-22,146.

Sample, J.C., Reid, M.R., Tobin, H.J., and Moore, J.C., 1993, Carbonate cements indicate channeled fluid flow along a zone of vertical faults at the deformation front of the Cascadia accretionary wedge (northwest U.S. coast): Geology, v. 21, p. 507-510.

Scholz, C.H., Dawers, N.H., Yu, J.-Z., and Anders, M.H., 1993, Fault growth and fault scaling laws: Preliminary results: Journal of Geophysical Research, v. 98, p. 21,951-21,961.

Scotti, O., Nur, A., and Estevez, R., 1991, Distributed deformation and block rotation in 3D: Journal of Geophysical Research, v. 96, p. 12,225-12,243.

Seno, T., Stein, S., and Gripp, A.E., 1993, A model for the motion of the Philippine Sea plate consistent with NUVEL-1 and geologic data: Journal of Geophysical Research, v. 98, p. 17,941-17,948.

Shiono, K., 1988, Seismicity of the SW Japan Arc - subduction of the young Shikoku Basin: Modern Geology, v. 12, p. 449-464.

Silver, E.A., 1972, Pleistocene tectonic accretion of the continental slope off Washington: Marine Geology, v. 13, p. 239-249.

Snavely, P.D., Jr., 1987, Tertiary geologic framework, neotectonics, and petroleum potential of the Oregon-Washington continental margin, *in* Scholl, D.W., Grantz, A., and Vedder, J.G., eds., Geology and resource potential of the continental margin of western North America and adjacent ocean basins--Beaufort Sea to Baja California: Houston, Tex., Circum-Pacific Council for Energy and Mineral Resources, p. 305-335.

Snavely, P.D., Jr., and McClellan, P.H., 1987, Seismic data collected in June, 1976, off the Washington/Oregon coast: U.S. Geological Survey Open-File Report 87-607.

Snavely, P.D., Jr., Pearl, J.E., and Lander, D.L., 1977, Interim report on petroleum resources potential and geologic hazards in the outer continental shelf-Oregon and Washington Tertiary province, U.S. Geological Survey Open-File Report 77-282, 64 p.

Snavely, P.D. Jr., and Wagner, H.C., 1982, Geologic cross section across the continental margin of southwestern Washington: U.S. Geological Survey Open-File Report 82-459.

Snavely, P.D., Jr., Wagner, H.C., and Lander, D.L., 1980, Interpretation of the Cenozoic geologic history, central Oregon continental margin: cross-section summary: Geological Society of America Bulletin, v. 91, p. 143-146.

Snavely, P.D., Jr., Wagner, H.C., and Lander, D.L., 1985, Land-sea geologic cross section of the southern Oregon continental margin: U.S. Geological Survey Miscellaneous Investigations Series Map I-1463, scale 1:125,000.

Snavely, P.D., Jr., and Wells, R.E., in press, Cenozoic evolution of the continental margin of Oregon and Washington, *in* Rogers, A. M., Kockelman, W. J., Priest, G., and Walsh, T. J., eds., Assessing and Reducing Seismic Hazards in the Pacific Northwest: U.S. Geological Survey Professional Paper 1560.

Spence, W., 1989, Stress origins and earthquake potential in Cascadia: Journal of Geophysical Research, v. 94, p. 3076-3088.

Stoddard, P.R., 1987, A kinematic model for the evolution of the Gorda Plate: Journal of Geophysical Research, v. 92, p. 11524-11532.

Sykes, L.R., 1971, Aftershock zones of great earthquakes, seismicity gaps, and earthquake prediction for Alaska and the Aleutians: Journal of Geophysical Research, 76, p. 8021-8041.

Sykes, L.R., 1989, Great earthquakes of 1855 and 1931 in New Zealand: evidence for seismic slip along downgoing plate boundary and implications for seismic potential of Cascadia subduction zone: EOS (Transactions, American Geophysical Union), v. 70, p. 1331.

Sylvester, A.G., 1988, Strike-slip faults: Geological Society of America Bulletin, v. 100, p. 1666-1703.

Thatcher, W., 1989, Earthquake recurrence and risk assessment in circum-Pacific seismic gaps: Nature, v. 341, p. 432-434.

Tobin, H.J., Moore, J.C., MacKay, M.E., Cochrane, G.R., Orange, D.L., Moore, G.F., and Kulm, L.D., 1991, Generation of fracture permeability along a vertical fault at the Oregon accretionary margin and implications for wedge thrust vergence: Geological Society America Abstracts with Programs, v. 23, p. A366.

Tobin, H.J., Moore, J.C., MacKay, M.E., Moore, G.F., and Orange, D.L., 1991, Alvin observations at the central Oregon accretionary prism: evidence for fault control of fluid seepage: Geological Society of America Abstracts with Programs, v. 23, p.103.

Tobin, H.J., Moore, J.C., MacKay, M.E., Orange, D.L., and Kulm, L.D., 1993, Fluid flow along a strike-slip fault at the toe of the Oregon accretionary prism-- Implications for the geometry of frontal accretion: Geological Society America Bulletin, v. 105, p. 569-582.

Tréhu, A.M., Lin, G., Maxwell, E., Goldfinger, C., in prep., A seismic reflection profile across the Cascadia subduction zone offshore central Oregon: New constraints on the deep crustal structure and on the distribution of methane in the accretionary prism.

Tréhu, A.M., Nabelek, J.N., Azevedo, S., Broecher, T.M., Mooney, W.D., Leutgert, J., Asudeh, I. , Clowes, R., Nakamura, Y., Smithson, S., Miller K., 1992, A crustal cross-section across the Cascadia subduction in central Oregon: EOS (Transactions, American Geophysical Union), v. 73, p. 391.

Vick, G.S., 1988, Late Holocene paleoseismicity and relative sea level changes of the Mad River slough, northern Humboldt Bay, California: Arcata, California, Humboldt State University, M.S. thesis, 87 p.

Wells, R.E., and Coe, R.S., 1985, Paleomagnetism and geology of Eocene volcanic rocks of southwest Washington, implications for mechanisms of tectonic rotation: Journal of Geophysical Research, v. 90, p. 1925-1947.

Wells, R.E., and England, P., 1991, Neogene rotations and quasicontinuous deformation of the Pacific Northwest continental margin: Geology, v. 19, p. 978-981.

Wells, R.E., and Heller, P., 1988, The relative contribution of accretion, shear, and extension to Cenozoic tectonic rotation in the Pacific Northwest: Geological Society of America Bulletin, v. 100, p. 325-338.

Wells, R.E., Niem, A.R., MacLeod, N.S., Snavely, P.D., Jr., Niem, W.A.,1983, Preliminary Geologic map of the west half of the Vancouver (WA-OR) 1° x 2° quadrangle, Oregon: U.S. Geological Survey Open File Report 83-591.

Wells, R.E., Snavely, P.D., Jr., and Niem, A.R., 1992, Quaternary thrust faulting at Netarts Bay, northern Oregon coast: Geological Society of America Abstracts with Programs, v. 24, p. 89.

West, D.O., and McCrumb, D.R., 1988, Coastline uplift in Oregon and Washington and the nature of Cascadia subduction zone tectonics: Geology, v. 16, p. 169-172.

Wilcox, R.E., Harding, T.P., and Seely, D.R., 1973, Basic wrench tectonics: American Association of Petroleum Geologists Bulletin, v. 57, p. 74-96.

Wilson, D.S., Hey, R.N., and Nishimura, C., 1984, Propagation as a mechanism of reorientation of the Juan de Fuca Ridge: Journal of Geophysical Research, v. 89, p. 9215-9225.

Wu, F.T., and Kanamori, H., 1973, Source mechanism of February 4, 1965, Rat Island earthquake: Journal of Geophysical Research, v. 78, p. 6082-6092.

Yeats, R.S., 1986, Active faults related to folding, *in* Wallace, R.E., ed., Active Tectonics: Washington, DC, National Academy Press, p. 63-79.

Yeats, R. S., Sieh, K.E., and Allen, C.R., in prep, Geology of Earthquakes: Oxford University Press.

Yount, J.C., and Holmes, M.L., 1992, The Seattle fault: a possible Quaternary reverse fault beneath Seattle Washington: Geological Society of America Abstracts with Programs, v. 24, p. 93.

APPENDICES

APPENDIX A: TEXT ACCOMPANYING OREGON NEOTECTONIC MAP

STATE OF OREGON
DEPARTMENT OF GEOLOGY AND MINERAL INDUSTRIES
800 N.E. Oregon Street # 28, Suite 965
Portland, Oregon 97232

OPEN-FILE REPORT 0-92-4

NEOTECTONIC MAP OF THE OREGON CONTINENTAL MARGIN AND ADJACENT ABYSSAL PLAIN

By

Chris Goldfinger, Department of Geosciences, LaVerne D. Kulm, College of Oceanography, and Robert S. Yeats, Department of Geosciences, Oregon State University, Corvallis, OR 97331;

Clifton Mitchell and Ray Weldon II, Geological Sciences Department, University of Oregon, Eugene, OR 97403;

Curt Peterson and Mark Darienzo, Department of Geology, Portland State University, Portland, OR 97207;

Wendy Grant, U.S. Geological Survey, University of Washington, Seattle, WA 98195;

and

George R. Priest, Oregon Department of Geology and Mineral Industries, Portland, OR 97232

1992

Publication and compilation of this map was supported by Geological Survey Cooperative Agreement Number 14-08-0001-A0512 under the auspices of the National Earthquake Hazards Reduction Program

DETAILED EXPLANATION OF MAP SYMBOLS ON PLATE 1

CONTOURS OF GEODETIC UPLIFT RATE

Absolute coastal uplift rates are in mm per year and are relative to an unchanging far field reference surface, approximately equivalent to the geoid. Data are from Clifton E. Mitchell and Ray Weldon II of the University of Oregon and are a modification of very similar contours presented by Mitchell and others (1991), based on analysis of benchmarks resurveyed over a 70-year time span and on changes in the monthly mean records of sea level from tide gauges. Note that eustatic (global) sea level rise is approximately 1.8 mm per year, so these uplift rates provide a guide to coastal areas that are rising or falling relative to global sea level rise. The uplift rates are additional evidence of ongoing strain in the North American Plate that may be related to a locked interface on the Cascadia subduction zone. The uplift contours were contributed by Ray Weldon Ii and Clifton Mitchell of the University of Oregon.

STRATIGRAPHIC COLUMNS SHOWING SALT MARSH BURIAL EVENTS

Stratigraphic columns from representative sample sites at salt marshes in each bay show dark stripes that are believed to represent the depths to the tops of peaty layers that are buried salt marshes These peats are overlain by muds typical of salt water bays and indicate episodic, virtually instantaneous inundation of the marshes by sea water, the inundation persisting for tens or hundreds of years after each submergence. Some peat layers are overlain by sandy sediment (sediment capping layer) possibly deposited by a seismic sea wave (tsunami) arriving shortly after submergence. Those peats with a sediment capping layer have a symbolic wave symbol on top of the stripe. Peats buried by bay mud are considered good physical evidence that the coast may have experienced great (M 8-9) subduction zone earthquakes that are commonly associated with instantaneous coseismic subsidence or uplift of coastal areas. Data sources and other details are given in the footnotes Where available, some representative radiocarbon ages (in radiocarbon

years) for uppermost and lowermost buried peat layers are listed. The salt marsh subsidence data were contributed by Curt Peterson and Mark Darienzo of Portland State University and Wendy Grant of the U.S. Geological Survey.

DESCRIPTION OF NEOTECTONIC MAP

DATA COLLECTION AND SOURCES

The neotectonic map of the Oregon continental margin represents the compilation and interpretation of about 30,000 km of seismic reflection profiles, SeaBeam swath bathymetry, and side-scan sonar mosaics of the seafloor morphology. The primary data sets used in constructing the map include: (1) single-channel sparker and airgun reflection profiles shot by Oregon State University and the University of Washington; (2) single and multi-channel airgun profiles shot by the U. S. Geological Survey; (3) migrated multi-channel airgun reflection profiles shot by Digicon for Oregon State University; (4) single-channel sparker profiles made by Shell Oil Corporation; (5) single and multi-channel profiles acquired by Chevron Oil Co (mostly shot by Gulf Oil); (6) SeaBeam swath bathymetry obtained by NOAA/National Ocean Survey and Oregon State University; (7) GLORIA long range side-scan sonar acquired by the U.S. Geological Survey; (8) 50 kHz Klein sidescan sonar and associated DELTA submersible observations; and (9) SeaMARC 1A high-resolution side-scan sonar acquired by Oregon State University. Several of these data sets were used in conjunction with one another to identify and map the active structures of the continental margin (shelf and slope) and adjacent abyssal plain. Table A.1 lists the sources and navigation methods for the various data sets (see also discussion below). Plate 2 shows the locations of ships tracks for the data used in this study.

Seismic reflection profiles made on the Oregon margin and abyssal plain were acquired using a variety of sources, including various sized air gun and sparker arrays, and a variety of digital and analog recording systems. The single- and multi-channel seismic reflection data vary widely in type of source signal, record quality, depth of penetration, and navigational accuracy. They include unmigrated single-channel sparker records navigated with Loran-A and Loran-C, as well as migrated 144-channel digital profiles navigated with GPS (Global Positioning System). Some multi-channel reflection profiles were navigated with GPS, and the position information from these lines is used as the datum for mapping that portion of the study area.

Navigational accuracy was more variable with older single-channel seismic profiles. Loran-A navigated profiles have maximum errors about 1-3 kilometers, Loran-C errors are approximately 0-1.5 km, and Transit satellite errors range from near zero up to several hundred meters. An exception is the Shell Oil Company lines. Although these profiles were shot in 1961-62, their navigational accuracy rivals the TRANSIT navigated lines due to the use of a company SHORAN radio navigation system. Horizontal errors with this system are approximately 50 meters. The dense coverage of reflection profiles allowed readjustment of older lines where crossed by satellite-navigated lines.

Data Source	Navigation System	Approx. Nav. Error
U.S.G.S MCS/GLORIA	Transit/Loran C	0-500m
OSU-U/W Sparker SCS	Loran A	1000-3000M
OSU/Digicon MCS	GPS	100m
NOAA/NOS Multibeam	ARGO	50 m
OSU Multibeam	TRANSIT/GPS/Loran C	100 m
OSU 50 kHz sidescan	GPS	100 m
OSU SeaMarc 1A	TRANSIT/GPS/Loran C	100 m
Chevron Oil MCS	Transit/Loran C	0-500m
Shell Oil Sparker SCS	SHORAN	50 m

Table A.1. Data sources used in this study and approximate navigational accuracy. MCS = multichannel seismic profiles, SCS = single channel seismic profiles, Multibeam = SeaBeam swath bathymetry.

The SeaBeam bathymetric survey system is a 12 kHz multibeam echo sounder developed by the General Instrument Corporation to produce near-real-time high-resolution contoured swath charts of the sea floor morphology. Full coverage digital SeaBeam swath bathymetry was acquired on the abyssal plain and continental slope from water depths extending from about 3,000 m to about 200 m on the upper continental slope by NOAA/NOS. These bathymetry data were contoured at a 20 m interval and used as a base map for the Oregon neotectonic map. The bathymetry is accurate to within 1% of the water depth across the swath. The NOAA/NOS multibeam surveys were navigated with an ARGO system which was placed in towers positioned along

the shoreline; navigational accuracy is 50 m. The partial coverage academic SeaBeam surveys completed in 1987 and 1988 were utilized initially in this study before the NOAA/NOS data were declassified by the U. S. Navy in 1991. The academic SeaBeam surveys were generally navigated with a combination of GPS and Transit satellite navigation, with Loran-C tracking used between satellite fixes.

The regional seafloor morphology of the abyssal plain and continental slope was imaged with the GLORIA system, a side-scan sonar instrument that uses a frequency of 6.8 kHz on the port side array and 6.2 kHz on the starboard side array. It images a 45 km swath width (i.e., 22.5 km either side of the ship's track), with spatial resolution of about 50 m in the across-track direction and 125 m in the along-track direction (see EEZ-SCAN 84 Staff, 1986 for details). This relatively low-resolution GLORIA system is designed to image the relatively large-scale features of the seafloor, such as mid-ocean ridges, fracture zones, abyssal hills and ridges, deep-sea channels, and lineaments. Higher resolution side-scan sonar data were collected with a SeaMARC 1A deep-towed vehicle, which uses a frequency of 27 kHz on the port array and 30 kHz on the starboard array. It is capable of imaging a 2 km or a 5 km swath width (i.e., 1 km and 2.5 km on either side of the ship's track, respectively), with spatial resolutions of 1 and 2.5 meters, respectively (see Appelgate, 1988 for details). The side-scan sonar surveys were navigated with a combination of GPS and Transit satellite navigation, with Loran-C tracking used between satellite fixes. Navigation of the deep-towed SeaMARC-IA side-scan fish was done by the method described by Appelgate (1988). Where spatial misfits occur, we have adjusted the side-scan and single-channel seismic reflection data to best fit the TRANSIT and GPS navigated multi-channel seismic reflection lines or the SeaBeam bathymetry where appropriate. The highest resolution side-scan sonar data were collected with a Klein 50 kHz sidescan sonar unit on the Oregon Shelf in July/August 1992. This system imaged details of shelf faults with 30 cm resolution. Ten areas of particular interest were surveyed, and dives were made with the submersible DELTA on active shelf faults to ground truth the sonar data.

MAPPING PROCEDURES

The Neotectonic map of the Oregon continental margin was constructed in a Geographical Information System (GIS) fashion with several layers consisting of the different data sets. The GLORIA side-scan sonar mosaics were used as a base layer at a scale of 1:500,000. Large features such as the major submarine channels, the Blanco Fracture Zone and the deformation front were mapped primarily from this data set. The GLORIA side-scan mosaics were selected for the base map because of its wide coverage of the Exclusive Economic Zone (EEZ) off the Pacific Northwest. At the time this mapping project was initiated in 1990, full SeaBeam coverage was not yet available for the Oregon margin from NOAA/NOS. (SeaBeam bathymetry coverage remains classified for the entire Washington margin and abyssal plain, where a new neotectonic map is being compiled by us in the same manner as described here.) Preliminary copies of the SeaBeam swath bathymetry charts were provided by NOAA/NOS as soon as they became available, and were scaled to 1:500,000 on transparent media. Together, these contour charts and GLORIA mosaics were used to map faults and fold axes between seismic reflection profiles, allowing nearly continuous mapping of individual structures from the abyssal plain to the outer continental shelf. The accurately navigated SeaBeam bathymetry provided another means of correcting position information from older Loran-A navigated seismic profiles, structural information from which was shifted to match the high-resolution bathymetry as needed. In the Coos Bay area, our mapping is modified from Clarke and others (1985), who mapped the structures of Coos Bay basin using closely spaced and well navigated single channel reflection profiles. We incorporated and modified this earlier mapping using SeaBeam bathymetry and industry reflection profiles. As a convention used in this map, we show offsets across faults only where they can be demonstrated with existing data. Other offsets that might be expected, but have not been demonstrated, are not shown. This may cause some ambiguity where seafloor features are most probably offset by a fault, but do not appear so on this map. We considered this preferable to the greater ambiguity caused by inferring offsets where insufficient data exist.

We emphasize young structures (i.e., those that offset and/or deform the seafloor) on the neotectonic map in order to evaluate regional structural trends under the present oblique subduction environment. Young structures are also the easiest to map as they generally deform the seafloor or appear in the more easily interpretable uppermost portion of seismic reflection profiles. We used a color coding scheme to represent the estimated age of youngest demonstrated activity on folds and faults. Structures active in the latest Pleistocene and Holocene are shown in red, structures active in the Pliocene-Pleistocene are shown in purple, all older structures are shown in blue. The youngest estimated age of continuous structures may vary along strike, this is represented on the map by along-strike color changes. A color change on the map could indicate either an actual along-strike change in the motion history of a structure, or it could be an artifact created by the variability in quality or distribution of the seismic data. In some areas, younger structures can be seen to overlap older (usually NE trending) structures. This occurs where erosional unconformities vertically juxtapose structures of widely differing ages. In some cases the older structural trends have remained active despite unfavorable orientation in the present stress field. In a few cases, coeval structures cross each other. These occurrences are associated with active strike-slip faults cutting other, sometimes active structures. Some of these faults have associated flower structures and fault-parallel folding that is active while other folds of different orientations also remain active. This can occur because both sets of structures are compatible with a single greatest principal stress orientation. Age determinations for structures other than active structures that cut or deform the present sea floor generally have a large and undefined error bar, and should be considered relative ages for general use. Active structures are difficult to confirm in areas of older surface exposure, thus some active fault have probably been missed in these areas (i.e. inshore areas of southern Oregon south of Coos Bay and inshore areas between Cape Falcon and Cape Foulweather). Structures in these areas that are shown as active have generally been confirmed as active by sidescan sonar imaging or submersible dives. A number of other suspected active structures have been ground truthed in this manner. Ages are constrained by biostratigraphy in industry drill holes, Deep-Sea Drilling Program (DSDP) drill

holes, dart cores and dredges from sedimentary rock outcrops on the seafloor, and piston and gravity cores from unconsolidated sediments.

DISCUSSION OF MAP FEATURES AND SYMBOLS

The physiography of the Oregon margin and abyssal plain is shown in Figure 4.8 to show the relationship of the structures to the main physiographic features of the region. The continental shelf extends from the shoreline to the shelf break (i.e., a significant increase in bottom slope), at a water depth from 180 to 200 m. The shelf break is highly sinuous in Oregon and its distance from the coast varies from 25 to 75 km. The widest shelf areas correspond to Nehalem, Heceta, and Coquille submarine banks. The continental slope extends from the shelf break to a water depth of about 3,000 m, seaward of which is the relatively flat abyssal plain of the Juan de Fuca Plate. In northern and central Oregon, the slope is further subdivided morphologically into an upper and lower slope based upon the occurrence of upper and lower structural terraces, respectively (see below). Various named and unnamed submarine channels are indicated on the continental slope and abyssal plain. On the abyssal plain, most of these channels are distributary channels of the Astoria submarine fan, the apex of which is at the mouth of Astoria canyon in the northwestern quadrant of the map. The Blanco Fracture Zone, a transform fault, connects the southern end of the spreading Juan de Fuca Ridge with the northern end of the spreading Gorda Ridge. The Juan de Fuca plate is converging with the North American plate off central Oregon along a vector oriented at 062° and at a rate of 40 mm/yr (calculated from the poles of DeMets and others (1990) at 45° 00' N latitude along the deformation front).

The neotectonic structures of the Oregon margin, abyssal plain and Blanco Fracture Zone are shown on the accompanying map. A brief description of the structure is presented here to acquaint the reader with the main structural elements. The reader is referred to the following publications for a detailed description of these structures: Appelgate and others (1992); Goldfinger and others (1992b, in press); and MacKay and others (1992). Additional background information on the structural and tectonic setting of this portion of the NE Pacific Ocean is given in Cited and Related References.

The primary structural feature is the North American-Juan de Fuca plate boundary at about 3,000 m water depth. The deformation front is characterized by a seaward-vergent thrust fault from the Gorda plate off northern California north to 44° 51' N latitude off southern and south-central Oregon. North of 44° 51' N latitude into Washington, the basal thrust is landward-vergent, with one minor exception (Goldfinger and others, in press). The plate boundary is complex in detail, highly sinuous in many seaward-vergent areas, offset by oblique structures, and commonly distributed over many splay thrusts. Many small and several large slumps are mapped on the lowermost slope and abyssal plain, notably a very large debris pile and arcuate scarp at 44° 00' N and a smaller one at 45° 21' N latitude.

In central and northern Oregon, the continental slope is characterized by upper and lower terraces separated by a major landward-dipping thrust and a coincident break in slope (labeled SB for slope break on the map) at about 1,000 meters water depth. Seaward of this fault, thrusts and folds of the accretionary wedge trend north-south, sub-parallel to the continental margin. Landward of the fault, folds of the upper slope and shelf trend mostly north-northwest to west-northwest, oblique to the margin. In southern Oregon, the terraces become one steep escarpment and this boundary becomes indistinguishable as a bathymetric feature, but the two domains of structural orientations remain distinct south into California (Clarke and Carver, 1992). Thrust faulting within the accretionary wedge occurs in both landward and seaward vergent styles, with landward vergence common off northern Oregon and rare off southern Oregon. Out of sequence thrusting follows a similar pattern, being common, if not typical, in the north and less so in the south.

Many second order features of particular tectonic significance are also apparent on the map. On the continental slope and abyssal plain of northern and central Oregon, detailed investigations using sidescan sonar surveys, SeaBeam bathymetry and single/multichannel seismic records show three confirmed and three probable WNW- trending left-lateral strike-slip faults between 43° 20' N and 45° 12' N latitude. The three northernmost structures (Wecoma fault, faults B, and C) between 44° 40' N and 45° 12' N latitude offset the basaltic crust and overlying sedimentary section (Goldfinger and others, 1992b, in press; Appelgate and others, 1992). The best known fault (Wecoma fault) extends 18 km seaward of the deformation front, offsets sub-

bottom reflectors and basaltic basement approximately 100 m (NE block up). Late Pleistocene to Holocene seafloor channels are offset 150-400 m in a left-lateral sense. Strike-slip faulting is also indicated by flower structures, mismatched stratigraphy, and reversals of vertical separation along trend. These structures are inferred to be active from direct ALVIN submersible observation of bedding attitudes, fresh scarps and fluid venting (Tobin and others, 1991). Faults B and C are associated with left offsets of the deformation front and/or left offsets of fold axes on the continental slope. Fault B intersects the base of the continental slope at 44° 51' N latitude, the point at which regional thrust vergence reverses, being seaward-vergent to the south and landward-vergent to the north. On the continental slope, these structures are characterized by deformation zones composed of WNW-trending linear scarps, en-echelon NW- to WNW-trending folds, and left-stepping and sigmoidally bent folds. Oblique folds are commonly fault-propagation and fault-bend folds developed above high-angle faults. Some of these active NNW to WNW striking faults and folds are re-folding somewhat older or coeval north- and NNE-trending folds. Deformation in these zones is consistent with a left-lateral sense of shear (see Goldfinger and others, 1992b, in press; and Appelgate and others, 1992, for a detailed discussion of these structures). Detailed mapping and submersible observations of fault B in the area of Daisy Bank confirmed the presence of the active left-lateral fault there, and suggest that Daisy Bank itself may be a pressure ridge uplift across a compressional step in fault B. We have added selected Quaternary and suspected Quaternary structures mapped onshore by other investigators that are probable correlatives of offshore structures, including the following: South slough syncline and other Coos Bay area structures from McInelly and Kelsey, (1990) and references therein; Cape Blanco anticline and Port Orford area faults from Kelsey (1990); Yaquina Bay fault from Kelsey and others (1992); Happy Camp fault and other Netarts Bay area structures from Parker (1990) and Wells and others (1992); Tillamook Bay fault from Wells and others (1983).

ACKNOWLEDGMENTS

We thank Richard Perry and Steve Matula, National Ocean Service, National Ocean & Atmospheric Administration, Rockville, MD for preliminary copies of the Oregon multibeam swath bathymetry used in mapping the continental margin structures. Chris Fox, NOAA Marine Resources Research Division, Hatfield Marine Science Center, Newport, OR, produced several colored contour maps of the multibeam bathymetry from the Oregon State University and NOAA/NOS digital databases. He also supplied digital data multibeam bathymetry data for computer analysis and visualization at Oregon State University. His collective efforts in this project are greatly appreciated. Bruce Appelgate, also at NOAA Newport (now at School of Earth Sciences and Technology, University of Hawaii, Honolulu, HI) processed the SeaMarc sidescan data and produced spectacular mosaics of the plate boundary near 45° N. Mary MacKay and Guy Cochrane processed a large set of 144 channel seismic profiles used in this study at University of Hawaii under the direction of Greg Moore. We thank Sam Clarke, Parke Snavely Jr., and Monty Hampton, U.S. Geological Survey Branch of Pacific Marine Geology Menlo Park, CA for providing U.S.G.S. seismic records. We had fruitful discussions on the geology of the Oregon margin with many investigators interested in Cascadia, including Sam Clarke, Parke Snavely Jr., Ray Wells, Ray Weldon, Paul Komar, Harvey Kelsey, Curt Peterson, Brian Atwater, Dan Orange, Bruce Appelgate, Mary MacKay, Guy Cochrane, Casey Moore, Harold Tobin, and Greg Moore. Thanks also to Nathan Potter, OSU, for showing us how to deal with digital SeaBeam data, and to Margaret Mumford, OSU, for carefully digitizing the many structures on the map. Special thanks go to the crews of the research vessels R.V. Atlantis II, DSV ALVIN, Digicon M.V. Geotide, R.V. Wecoma, R.V. Jolly Roger, and DELTA, and to the sidescan techs at Williamson and Associates of Seattle, WA. This research was supported by NSF grants OCE-8812731 (OSU) and OCE-8821577 (UH), by the National Earthquake Hazards Reduction Program, U.S. Geological Survey, Department of Interior, under award 14-08-001-G1800 (OSU), and by the National Undersea Research Program, National Oceanic and Atmospheric Administration. Publication and compilation of this map was supported by United States Geological Survey Cooperative Agreement Number 14-08-

0001-A0512 under the auspices of the National Earthquake Hazards Reduction Program.

CITED AND RELATED REFERENCES

Appelgate, T.B., 1988, Tectonic and volcanic structures of the southern flank of Axial volcano, Juan de Fuca Ridge: results from a SeaMARC 1 side-scan sonar survey: Corvallis, Oregon State University, M.S. thesis, 161 p.

Appelgate, T.B., Goldfinger, C., Kulm, L. D., MacKay, M., Fox, C.G., Embley, R.W., and Meis, P.J., 1992, A left-lateral strike-slip fault seaward of the central Oregon convergent margin: Tectonics, v. 11, p. 465-477.

Carlson, P.R., 1967, Marine geology of the Astoria submarine canyon: Corvallis, Oregon State University, Ph.D. dissertation, 259 p.

Carlson, P.R., and Nelson, H.C., 1987, Marine geology and resource potential of Cascadia Basin, *in* Scholl, D. W., Grantz, A., and Vedder, J.G., eds., Geology and resource potential of the continental margin of western North America and adjacent ocean basins-Beaufort sea to Baja California: Houston, Circum-Pacific Council for Energy and Mineral Resources, p. 523-535.

Carson, B., 1971, Stratigraphy and depositional history of Quaternary sediments in northern Cascadia Basin and Juan de Fuca abyssal plain, northeast Pacific Ocean: Seattle, University of Washington, Ph.D. dissertation, 249 p.

Carson, B., 1977, Tectonically induced deformation of deep-sea sediments off Washington and northern Oregon: Marine Geology, v. 24, p. 289-307.

Clarke, S.H., Jr., 1990, Map showing geologic structures of the northern California continental margin: U.S. Geological Survey, Map MF-2130, scale 1:250,000.

Clarke, S.H., Jr., 1992, Geology of the Eel River Basin and adjacent region: Implications for late Cenozoic tectonics of the southern Cascadia subduction zone and Mendocino triple junction: American Association of Petroleum Geologists Bulletin, v. 76, p. 199-224.

Clarke, S.H., Jr., Field, M.E., and Hirozawa, C.A., 1985, Reconnaissance geology and geologic hazards of the offshore Coos Bay Basin, Oregon: U.S. Geological Survey Bulletin 1645, 41 p.

Cochrane, G.R., and Lewis, B.T.R., 1988, Deep-tow seismic reflection records from the Oregon lower slope: EOS, (Transactions, American Geophysical Union), v. 69, p. 1442-1443.

Couch, R.W., and Braman, D., 1979, Geology of the continental margin near Florence, Oregon: Oregon Geology, v. 41, p. 171-179.

DeMets, C., Gordon, R.G., Argus, D.F., and Stein, S., 1990, Current plate motions: Geophysical Journal International, v. 101, p. 425-478.

Duncan, J.R., 1968, Late Pleistocene and postglacial sedimentation and stratigraphy of deep-sea environments off Oregon: Corvallis, Oregon State University, Ph.D. dissertation, 222 p.

Duncan, J.R., Fowler, G.A., and Kulm, L.D., 1970, Planktonic Foraminiferan-Radiolarian ratios and Holocene-Late Pleistocene deep-sea stratigraphy off Oregon: Geological Society of America Bulletin, v. 81, p. 561-566.

Duncan, R.A., and Kulm, L.D., 1989, Plate tectonic evolution of the Cascades arc-subduction complex, *in* Winterer, E.L., Hussong, D.M., and Decker, R.W., eds., The Eastern Pacific Ocean and Hawaii: Boulder, Colorado, Geological Society of America, The Geology of North America, p. 413-438.

EEZ-SCAN 84 Scientific Staff, 1986, Atlas of the Exclusive Economic Zone, Western Conterminous United States: U.S. Geological Survey Miscellaneous Investigations Series I-1792, 152 p., scale 1:500,000.

Gardner, J.V., Field, M.E., Lee, H., Edwards, B.E., Masson, D.G., Kenyon, N., and Kidd, R.B., 1991, Ground-truthing 6.5 kHz side scan sonographs: what are we really imaging?: Journal of Geophysical Research, v. 96, p. 5955-5974.

Goldfinger, C., Kulm, L.D., Yeats, R.S., Appelgate, B., MacKay, M., and Cochrane, G.R., in press, Active strike-slip faulting and folding of the Cascadia plate boundary and forearc in central and northern Oregon, *in* Rogers, A. M., Kockelman, W. J., Priest, G., and Walsh, T. J., eds., Assessing and reducing earthquake hazards in the Pacific Northwest: U.S. Geological Survey Professional Paper 1560.

Goldfinger, C., Kulm, L.D., Yeats, R.S., Appelgate, B., MacKay, M., and Moore, G.F., 1992b, Transverse structural trends along the Oregon convergent margin: implications for Cascadia earthquake potential: Geology, v. 20, p. 141-144.

Griggs, G.B., and Kulm, L.D., 1970, Sedimentation in Cascadia deep-sea channel: Geological Society of America Bulletin, v. 81, p. 1361-1384.

Griggs, G.B., and Kulm, L.D., 1973, Origin and development of Cascadia deep-sea channel: Journal of Geophysical Research, v. 78, p. 6325-6339.

Hampton, M.A., Karl, H.A., and Kenyon, N.H., 1989, Sea-floor drainage features of Cascadia Basin and the adjacent continental slope, northeast Pacific Ocean: Marine Geology, 87, p. 249-272.

Ingle, J.C., 1973, Neogene foraminifera from the northeastern Pacific ocean, leg 18, deep Sea Drilling Project: Initial Reports of the Deep Sea Drilling Project, v. XVIII, p. 517-567.

Johnson, H.P., and Helferty, M., 1990, The geological interpretation of side-scan sonar: Reviews of Geophysics, v. 28, p. 357-380.

Jones, G.A., Jull, A.J.T., Linick, T.W., and Donahue, D.J., 1989, Radiocarbon dating of deep-sea sediments: a comparison of accelerator mass spectrometer and beta decay methods: Radiocarbon, v. 31, p. 105-116.

Kelsey, H.M., 1990, Late Quaternary deformation of marine terraces on the Cascadia subduction zone near Cape Blanco, Oregon: Tectonics, v. 9, p. 983-1014.

Kelsey, H.M., Mitchell, C.E., Weldon, R.J. II, Engebretson, D., Ticknor, R., and Bockhiem, J., 1992, Latitudinal variation in surface uplift from geodetic, wave-cut platform and topographic data, Cascadia margin: Geological Society of America Abstracts with Programs, v. 24, p. 37.

Kulm, L.D., and Fowler, G.A., 1974, Oregon continental margin structure and stratigraphy: a test of the imbricate thrust model, *in* Burke, C.A., and Drake, C.L., eds., The geology of continental margins: New York, Springer-Verlag, p. 261-284.

Kulm, L.D., Prince, R.A., and Snavely, P.D., Jr., 1973a, Site Survey of the northern Oregon continental margin and Astoria Fan: Initial Reports of the Deep Sea Drilling Project, v. XVIII, p. 979-987.

Kulm, L.D., Roush, R.C., Harlett, J.C., Neudeck, R.H., Chambers, D.M., and Runge, E.J., 1975, Oregon continental shelf sedimentation: Interrelationships of facies distribution and sedimentary processes: Journal of Geology, v. 83, p. 145-175.

Kulm, L.D., and Scheidegger, K.F., 1979, Quaternary sedimentation on the tectonically active Oregon continental slope: Society of Economic Paleontologists and Mineralogists Special Publication 27, p. 247-263.

Kulm, L.D., Von Huene, R., and scientific party, 1973b, Initial Reports of the Deep Sea Drilling Project: Washington, D.C., U.S. Government Printing Office, v. 18, p. 97-168.

MacKay, M.E., Moore, G.F., Cochrane, G.R., Moore, J.C., and Kulm, L.D., 1992, Landward vergence, oblique structural trends, and tectonic segmentation in the Oregon margin accretionary prism: Earth and Planetary Science Letters, v. 109, p. 477-491.

McInelly, G.W., and Kelsey, H.M., 1990, Late Quaternary tectonic deformation in the Cape Arago-Bandon region of coastal Oregon as deduced from wave cut platforms, Journal of Geophysical Research, v. 95, p. 6699-6713.

Nelson, C.H., 1968, Marine geology of the Astoria deep-sea fan: Corvallis, Oregon State University, Corvallis, Ph.D. dissertation, 287 p.

Nelson, C.H., Kulm, L.D., Carlson, P.R., and Duncan, J.R., 1968, Mazama ash in the northeastern Pacific: Science, v. 161, p. 47-49.

Niem, A.R., Snavely, P.D., Jr., and Niem, W.A., 1990, Onshore-offshore geologic cross section from the Mist gas field, northern Oregon coast range, to the northwest Oregon continental shelf: Oregon Department of Geology and Mineral Industries, Oil and Gas Investigation 17, 46 p.

Parker, M.J., 1990, Oligocene and Miocene geology of the Tillamook embayment, Tillamook County, northwest Oregon: Corvallis, Oregon State University, M.S. thesis, 524 p.

Peterson, C.P., Kulm, L.D., and Gray, J.J., 1986, Geologic map of the ocean floor off Oregon and the adjacent continental margin: Oregon Department of Geology and Mineral Industries, Map GMS-42, scale 1:500,000.

Riddihough, R.P., 1984, Recent movements of the Juan de Fuca plate system: Journal of Geophysical Research, v. 89, p. 6980-6994.

Silver, E.A., 1972, Pleistocene tectonic accretion of the continental slope off Washington: Marine Geology, v. 13, p. 239-249.

Snavely, P.D., Jr., 1987, Tertiary geologic framework, neotectonics, and petroleum potential of the Oregon-Washington continental margin, *in* Scholl, D. W., Grantz, A., and Vedder, J.G., eds., Geology and resource potential of the continental margin of western North America and adjacent ocean basins-Beaufort sea to Baja California: Houston, Circum-Pacific Council for Energy and Mineral Resources, p. 305-335.

Snavely, P.D., Jr., Pearl, J.E., and Lander, D.L., 1977, Interim report on petroleum resources potential and geologic hazards in the outer continental shelf-Oregon and Washington Tertiary province, U.S. Geological Survey Open-File Report 77-282, 64 p.

Snavely, P.D. Jr., and Wagner, H.C., 1982, Geologic cross section across the continental margin of southwestern Washington: U.S. Geological Survey Open-File Report 82-459.

Snavely, P.D., Jr., Wagner, H.C., and Lander, D.L., 1980, Interpretation of the Cenozoic geologic history, central Oregon continental margin: cross-section summary: Geological Society of America Bulletin, v. 91, p. 143-146.

Snavely, P.D., Jr., and Wells, R.E., in press, Cenozoic evolution of the continental margin of Oregon and Washington, *in* Rogers, A. M., Kockelman, W. J., Priest, G., and Walsh, T. J., eds., Assessing and Reducing Seismic Hazards in the Pacific Northwest: U.S. Geological Survey Professional Paper 1560.

Spence, W., 1989, Stress origins and earthquake potential in Cascadia: Journal of Geophysical Research, v. 94, p. 3076-3088.

Stoddard, P.R., 1987, A kinematic model for the evolution of the Gorda Plate: Journal of Geophysical Research, v. 92, p. 11524-11532.

Tobin, H.J., Moore, J.C., MacKay, M.E., Moore, G.F., and Orange, D.L., 1991, Alvin observations at the central Oregon accretionary prism: evidence for fault control of fluid seepage: Geological Society of America Abstracts with Programs, v. 23, p.103.

Wells, R.E., Niem, A.R., MacLeod, N.S., Snavely, P.D., Jr., Niem, W.A.,1983, Preliminary Geologic map of the west half of the Vancouver (WA-OR) 1° x 2° quadrangle, Oregon: U.S. Geological Survey Open File Report 83-591.

Wells, R.E., Snavely, P.D., Jr., Niem, A.R., 1992, Quaternary thrust faulting at Netarts Bay, northern Oregon coast: Geological Society of America Abstracts with Programs, v. 24, p. 89.

APPENDIX B: SLIP-RATE CALCULATIONS FOR OREGON AND WASHINGTON MARGIN STRIKE-SLIP FAULTS

The slip rate calculations presented here are dependent sedimentation rates and velocity structure of the Astoria and Nitinat Fans. These values are derived from Ocean Drilling Program logging and previous coring studies of sedimentation rates. For both Washington and Oregon faults we use a velocity of 1680 m/s. This is derived by integrating an average of multiple velocity curves derived from sonic logs and seismic interval velocities from ODP site 888 on the Nitinat Fan and empirical modeling. Integration for an average velocity for the upper 400 m in site 888 results in a velocity of 1680 m/s. The sedimentation rate for the Nitinat Fan is from Bobb Carson (pers. comm.) and the Astoria fan rate is from Goldfinger and others (in press; and references therein).

WASHINGTON FAULTS

North Nitinat Fault

Age:
Depth of disappearance of growth strata: 0.44 sec below sea floor twt.
Fan thickness: 0.63 sec twt.
Velocity used: 1680 m/s
Depth of disappearance growth strata: 397 mbsf.
Sedimentation rate for Nitinat Fan at from ODP site 888: 100 cm/1000 yrs.
Age of disappearance of growth strata: (397 m/1.0 m/1000 yrs) = 397 ka.

Net Slip:
Eastward thickening abyssal plain sedimentary unit is expressed as a percent per kilometer of total section thickness.
Lower abyssal plain wedge angle = 3.9%/km
Observed thinning across fault: 8.6%
Net Slip: 2.20 km.

Slip Rate:
Slip Rate = 2200 m/397 ka = 5.5 mm/yr

South Nitinat Fault

Age:
Depth of disappearance of growth strata: 0.36 sec below sea floor twt.
Fan thickness: 0.74 sec twt.
Velocity used: 1680 m/s
Depth of disappearance of growth strata: 302 mbsf.
Sedimentation rate for Nitinat Fan at from ODP site 888: 100 cm/1000 yrs.
Age of disappearance of growth strata: (302 m/1.0 m/1000 yrs) = 302 ka.

Net Slip:
Eastward thickening abyssal plain sedimentary unit is expressed as a percent per kilometer of total section thickness.
Lower abyssal plain wedge angle = 3.9%/km
Observed thinning across fault: 8.0%
Net Slip: 2.05 km.

Slip Rate:
Slip Rate = 2050 m/302 ka = 6.7 mm/yr

OREGON FAULTS

Wecoma Fault

Age:
Depth of disappearance of growth strata: 0.85 sec below sea floor twt.
Velocity used: 1680 m/s
Depth of disappearance of growth strata: 714 mbsf.
Sedimentation rate for Astoria Fan from Goldfinger and others (in press):
110 cm/1000 yrs.
Age of disappearance of growth strata: (714 m/1.0 m/1000 yrs) = 649 ka.

Net Slip:
From Goldfinger and others (in press):
Net Slip: 5.5 km.

Slip Rate:
Slip Rate = 5500 m/649 ka = 8.5 mm/yr

Daisy Bank Fault

Age:
Depth of disappearance of growth strata: 0.43 sec below sea floor twt.
Fan thickness: 0.90 sec twt.
Velocity used: 1680 m/s
Depth of disappearance of growth strata: 361 mbsf.
Scaled sedimentation rate inferred for the Astoria Fan at Alvin Canyon fault:
94 cm/1000 yrs.
Age of disappearance of growth strata: (361 m/.94 m/1000 yrs) = 384 ka.

Net Slip:
Eastward thickening abyssal plain sedimentary unit is expressed as a percent per kilometer of total section thickness.
Lower abyssal plain wedge angle = 2.3%/km
Observed thinning across fault: 5.0%
Net Slip: 2.2 km.

Slip Rate:
Slip Rate = 2200 m/384 ka = 5.7 mm/yr

Alvin Canyon Fault

Age:
Depth of disappearance of growth strata: 0.37 sec below sea floor twt.
Fan thickness: 0.75 sec twt.
Velocity used: 1680 m/s
Depth of disappearance of growth strata: 310 mbsf.
Scaled sedimentation rate inferred for the Astoria Fan at Alvin Canyon fault: 79 cm/1000 yrs.
Age of disappearance of growth strata: (310 m/.79 m/1000 yrs) = 392 ka.

Net Slip:
Eastward thickening abyssal plain sedimentary unit is expressed as a percent per kilometer of total section thickness.
Lower abyssal plain wedge angle = 2.3%/km
Observed thinning across fault: 6%
Net Slip: 2.6 km.

Slip Rate:
Slip Rate = 2600 m/392 ka = 6.6 mm/yr

Sedimentation rates for these three faults are scaled from the value of 110 cm/1000 years determined in Goldfinger and others (in press: Chapter 2) because the fan thins to the south (called scaled sedimentation rates below). Some unknown amount error due to time transgression of the Astoria fan base is not accounted for.

SUM OF ARC PARALLEL COMPONENT OF SLIP FROM STRIKE-SLIP FAULTING, OREGON AND WASHINGTON

FAULT	STRIKE	SLIP-RATE	ARC-PARALLEL SLIP
N. Nitinat	283°	5.5	1.24 mm/yr
S. Nitinat	283°	6.7	1.51 mm/yr
Quinault Canyon	280°	5.5*	0.96 mm/yr
Wecoma	292°	8.5	3.18 mm/yr
Daisy Bank	292°	5.7	2.13 mm/yr
Alvin Canyon	292°	6.6	2.47 mm/yr
Heceta South	292°	5.5*	2.06 mm/yr
Coos Basin	282°	5.5*	1.14 mm/yr
Cecile	300°	5.5*	2.75 mm/yr
TOTAL			**17.4 mm/yr**

* No data; value assigned from low value among calculated rates.

Table B.1. Sum of arc-parallel slip rates calculated from strike and slip rate of individual strike-slip faults. Strike of margin in Oregon averages N-S. Washington coast and shelf strike 348°, while deformation front strikes 338° due to northward widening of accretionary wedge. The volcanic arc maintains a northerly strike almost to the Canadian border. If we use 348° as the strike of the Washington margin for slip calculations on the N. Nitinat, S. Nitinat and Quinault Canyon faults, the arc-parallel component increases to a total of 20.9 mm/yr.